MULTIDISCIPLINARY CENTER FOR EARTHQUAKE ENGINEERING RESEARCH
A National Center of Excellence in Advanced Technology Applications

ISSN 1520-295X

3D-BASIS-ME-MB: Computer Program for Nonlinear Dynamic Analysis of Seismically Isolated Structures

by

P.C. Tsopelas, P.C. Roussis, M.C. Constantinou, R. Buchanan and A.M. Reinhorn
University at Buffalo, State University of New York
Department of Civil, Structural and Environmental Engineering
Buffalo, New York 14260

Technical Report MCEER-05-0009

October 3, 2005

This research was conducted at the University at Buffalo, State University of New York and was supported primarily by the Earthquake Engineering Research Centers Program of the National Science Foundation under award number EEC-9701471.

Report Documentation Page 50272-101	1. Report No. MCEER-05-0009	2.	3. Recipient's Accession No.
4. Title and Subtitle 3D-BASIS-ME-MB: Computer Program for Nonlinear Dynamic Analysis of Seismically Isolated Structures			5. Report Date 10/3/2005 6.
7. Authors P.C. Tsopelas, P.C. Roussis, M.C. Constantinou, R. Buchanan, A.M. Reinhorn			8. Perfoming Organization Report No. 10. Project / Task / Work Unit No 8.2.1
9. Performing Organization Name and Address Department of Civil, Structural and Environmental Engineering State University of New York at Buffalo Buffalo, NY 14260			11.Contract (C) or Grant (G) No. (C) EEC-9701471 (G)
12. Sponsoring Organization Name and Address Multidisciplinary Center for Earthquake Engineering Research State University of New York at Buffalo Red Jacket Quadrangle Buffalo, NY 14261			13. Type of Report / Period Covered Technical Report 14.

15. Supplementary Notes

This research was conducted at the University at Buffalo, State University of New York and was supported primarily by the Earthquake Engineering Research Centers Program of the National Science Foundation.

16. Abstract (limit 200 Words)

This report introduces 3D-BASIS-ME-MB, a new computer program for the dynamic response-history analysis of seismically isolated structures. Improvements over its predecessor include: (a) capability to analyze multiple superstructures on multiple isolation-system levels; (b) addition of a new element for modeling the uplift-restraining XY-FP isolator; (c) improvement modeling of viscous damper element; (d) capability to capture overturning moment effects on axial bearing loads, including bearing uplift; and (e) streamlined program output. Two examples of seismically isolated structures are used for verifying 3D-BASIS-ME-MB and to demonstrate its capabilities, where each is excited under conditions of bearing uplift. The software program user's guide, figures and tables are also provided.

17. Document Analysis a. Descriptors

Earthquake Engineering. Computer programs. Nonlinear dynamic analyses. Response-history analyses. Seismic isolation. 3-D-BASIS-ME-MB. Superstructures. Models. Multiple isolation-system levels. Viscous dampers. Axial bearing loads. Multistory structures. Bearing uplift. Software. Overturning moment effects.

b. Identifiers/Open-Ended Terms

c. COSATI Field/Group

18. Availability Statement	19. Security Class (This Report)	21. No. of Pages
Release Unlimited.	Unclassified	196
	20. Security Class (This Page)	22. Price
	Unclassified	35.00

MULTIDISCIPLINARY CENTER FOR EARTHQUAKE ENGINEERING RESEARCH
A National Center of Excellence in Advanced Technology Applications

3D-BASIS-ME-MB:
Computer Program for Nonlinear Dynamic Analysis of Seismically Isolated Structures

by

P.C. Tsopelas,[1] P.C. Roussis,[2] M.C. Constantinou,[3]
R. Buchanan,[4] and A.M. Reinhorn[5]

Publication Date: October 3, 2005
Submittal Date: May 13, 2005

Technical Report MCEER-05-0009

Task Number 8.2.1

NSF Master Contract Number EEC 9701471

1 Associate Professor, Department of Civil Engineering, The Catholic University of America
2 Postdoctoral Associate, Department of Civil, Structural and Environmental Engineering, University at Buffalo, State University of New York
3 Professor, Department of Civil, Structural and Environmental Engineering, University at Buffalo, State University of New York
4 Lead Engineer, AMEC Oil & Gas, Aberdeen, United Kingdom
5 Furnas Eminent Professor, Department of Civil, Structural and Environmental Engineering, University at Buffalo, State University of New York

MULTIDISCIPLINARY CENTER FOR EARTHQUAKE ENGINEERING RESEARCH
University at Buffalo, State University of New York
Red Jacket Quadrangle, Buffalo, NY 14261

Preface

The Multidisciplinary Center for Earthquake Engineering Research (MCEER) is a national center of excellence in advanced technology applications that is dedicated to the reduction of earthquake losses nationwide. Headquartered at the University at Buffalo, State University of New York, the Center was originally established by the National Science Foundation in 1986, as the National Center for Earthquake Engineering Research (NCEER).

Comprising a consortium of researchers from numerous disciplines and institutions throughout the United States, the Center's mission is to reduce earthquake losses through research and the application of advanced technologies that improve engineering, pre-earthquake planning and post-earthquake recovery strategies. Toward this end, the Center coordinates a nationwide program of multidisciplinary team research, education and outreach activities.

MCEER's research is conducted under the sponsorship of two major federal agencies: the National Science Foundation (NSF) and the Federal Highway Administration (FHWA), and the State of New York. Significant support is derived from the Federal Emergency Management Agency (FEMA), other state governments, academic institutions, foreign governments and private industry.

MCEER's NSF-sponsored research objectives are twofold: to increase resilience by developing seismic evaluation and rehabilitation strategies for the post-disaster facilities and systems (hospitals, electrical and water lifelines, and bridges and highways) that society expects to be operational following an earthquake; and to further enhance resilience by developing improved emergency management capabilities to ensure an effective response and recovery following the earthquake (see the figure below).

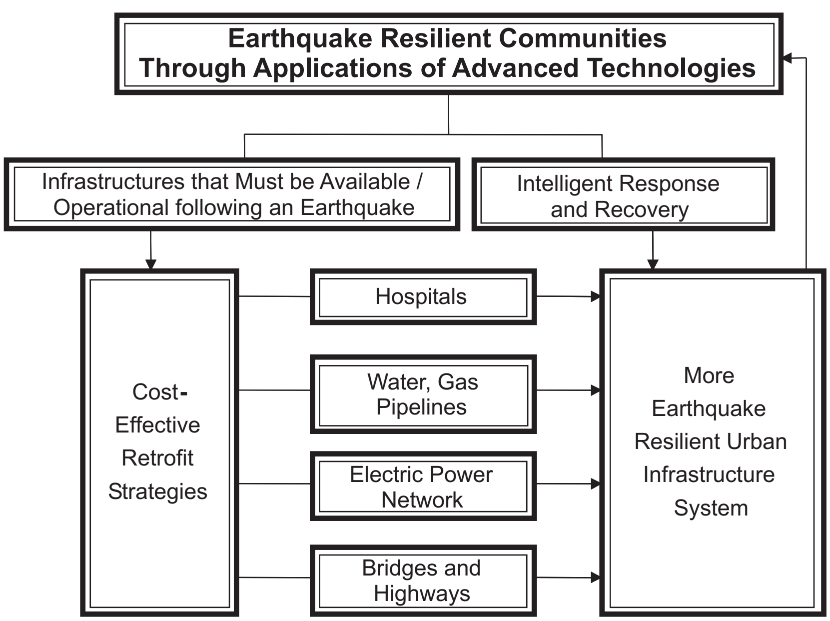

A cross-program activity focuses on the establishment of an effective experimental and analytical network to facilitate the exchange of information between researchers located in various institutions across the country. These are complemented by, and integrated with, other MCEER activities in education, outreach, technology transfer, and industry partnerships.

The suite of 3D-BASIS computer programs is widely accepted by the engineering and academic communities for use in the nonlinear dynamic analysis of three-dimensional seismically isolated structures. This report introduces 3D-BASIS-ME-MB, which offers a new capability to analyze multiple superstructures on multiple bases, hence the extension MB. The enhanced 3D-BASIS-ME-MB program is primarily useful in (a) performing analyses for schematic designs where speed in both modeling of the isolated structure and performing multiple dynamic analyses is desired, and (b) verifying the validity of modeling assumptions and the accuracy of solutions of more complex analysis programs such as SAP2000 and ETABS. The authors provide two examples of seismically isolated structures to verify 3D-BASIS-ME-MB and demonstrate its capabilities. The first example is a 7-story model structure that was tested on the earthquake simulator of the University at Buffalo and was also used as a verification example for program SAP2000. The second example is a two-tower, multi-story structure with a split-level seismic isolation system, which was analyzed in computer code ABAQUS using the most advanced analysis tools available. The results from both examples attest to the validity and accuracy of 3D-BASIS-ME-MB.

ABSTRACT

Program 3D-BASIS-ME-MB is a computer program for the dynamic response-history analysis of seismically isolated structures. The new program offers the following improvements over its predecessor: capability to analyze multiple superstructures on multiple isolation-system levels; (b) addition of a new element for modeling the uplift-restraining XY-FP isolator; (c) improvement modeling of viscous damper element; (d) capability to capture overturning moment effects on axial bearing loads, including bearing uplift; and (e) streamlined program output. Two examples of seismically isolated structures are used for verifying 3D-BASIS-ME-MB and demonstrating its capabilities. The first example is a 7-story model structure that was tested on the earthquake simulator of the University at Buffalo (Al-Hussaini et al, 1994) and was also used as a verification example for program SAP2000 (Scheller and Constantinou, 1999 and Computers and Structures Inc., 2004). The second example is a two-tower, multi-story structure with a split-level seismic isolation system. In both examples the analyzed structure is excited under conditions of bearing uplift, thus yielding a case of much interest in verifying the capabilities of analysis software.

ACKNOWLEDGEMENTS

Financial support for this project was provided by the Multidisciplinary Center for Earthquake Engineering Research (Project 8.2.1) and by Mills-Peninsula Health Services of Burlingame, CA. Dr. Charles Kircher of C. Kircher and Associates, Palo Alto, CA and Mr. William Holmes, Mr. Tom Lauck, Ms. Leticia Duenas and Mr. Francisco Parisi of Rutherford and Chekene, Oakland, CA provided assistance in the development of the verification examples.

TABLE OF CONTENTS

TABLE OF CONTENTS

TABLE OF CONTENTS

LIST OF FIGURES

FIGURE **TITLE** **PAGE**

LIST OF FIGURES

FIGURE **TITLE** **PAGE**

SECTION 1
INTRODUCTION

Used by the engineering and academic communities, the 3D-BASIS class of computer programs is widely accepted for the nonlinear dynamic analysis of three-dimensional seismically isolated structures. The program contributed to the verification and development of new standards for the design of seismically isolated structures and contributed to the advancement of seismic isolation.

Built on the core philosophy of its predecessors, program 3D-BASIS-ME-MB represents an enhanced version of program 3D-BASIS-ME (Tsopelas et al, 1994), which is a further extension of the original program 3D-BASIS (Nagarajaiah et al, 1989).

An overview of features offered by the current version, 3D-BASIS-ME, is given below:

1. Analyzes an isolated structure consisting of a rigid base with several superstructures connected on top of the common base (Figure 1-1). Each superstructure consists of several rigid floors.
2. The degrees of freedom consist of three displacements (2 translations and one rotation about the vertical axis) of each of the floors and the base.
3. The isolation system is explicitly modeled with each isolator or damper described in terms of a constitutive relation and location beneath the base.
4. Vertical ground acceleration effects are considered in modeling the behavior of sliding isolators. The modeling simply increases or decreases the instantaneous axial load on the bearings by use of $N = \left(1 + a_{\mathrm{V}}\right)P$, where N is the instantaneous axial load, P is the gravity load and a_{V} is the vertical ground acceleration. In case the vertical flexibility of the structure affects the axial load on the bearings, a separate pre-analysis can be performed (given that the modeling assumes independency between the vertical and lateral degrees of freedom) and an effective vertical acceleration history is calculated first and then used in the dynamic analysis.
5. The overturning moment effects on the axial load of bearings are calculated at each time step by a user defined subroutine. This routine calculates the axial load on each

bearing on the basis of the overturning moments along the two principal directions. This modeling cannot properly handle bearing uplift. However, the program does not calculate the amount of uplift displacement at individual isolators.

6. Each superstructure is described either in terms of a shear type representation or in terms of mode shapes, masses, moments of inertia, eccentricities and locations of center of mass. The mode shapes are derived from a detailed model of each superstructure in another computer program like SAP2000 (Computers and Structures, 1998) or ETABS (Computers and Structures, 1995).

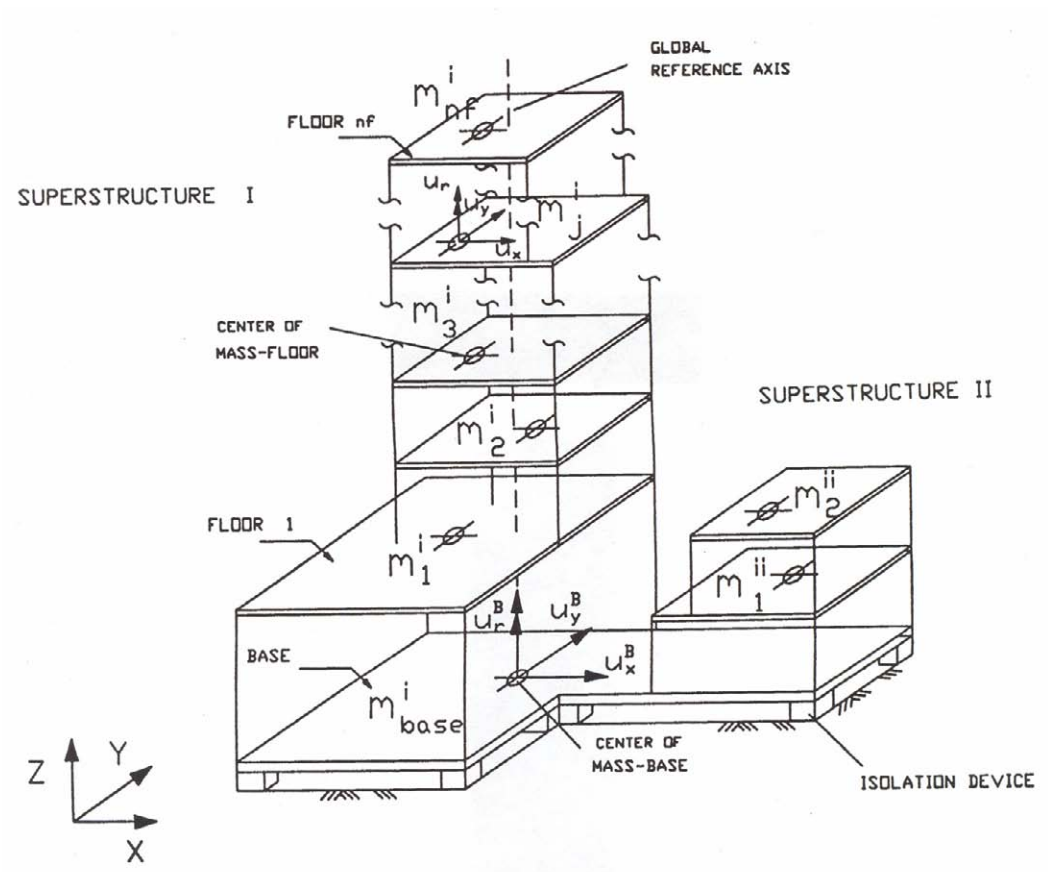

Figure 1-1: Model that can be analyzed in program 3D-BASIS-ME.

The new program 3D-BASIS-ME-MB offers the following additional features:

1. Analyzes a more complex configuration as illustrated in Figure 1-2. In this configuration the structure consists of three parts:

   - Superstructure, consisting of up to 5 separate superstructures. Each superstructure is modeled as having rigid floors with three degrees of freedom each (two translations and one rotation). The input data consists of the floor mass, moment of inertia and location of centers of mass, and shear stiffness, torsional stiffness and center of resistance per story. Alternatively, the input data for representing the stiffness of each part of the superstructure are in terms of mode shapes and frequencies obtained from analysis of a detailed model in another program like SAP2000 or ETABS.

- Substructure consisting of up to 5 bases above the lowest isolation interface. Isolators are located at each of the 5 bases. Each base is represented as a rigid floor with 3 degrees of freedom. The mass, moment of inertia and location of center of mass of each floor is input. The stiffness characteristics of the substructure are input in a manner similar to that of each part of the superstructure.

- Isolators and dampers may be located at each base of the substructure. Each isolator and damper is explicitly modeled in terms of its location, orientation and constitutive relation.

2. The isolation system has the following new elements:

   - The new XY-FP bearing capable of sustaining tension is represented (Roussis and Constantinou, 2005). The orientation of the bearing may be in any arbitrary direction with the respect to the global reference frame.

   - The existing viscous damper element is modified to have a more general constitutive relation and to have capability for placement at an arbitrary direction with respect to the global reference frame.

3. Overturning moment effects are captured in a more complex and accurate way. The axial load on each isolator is calculated at each time step through a procedure that relates the instantaneous floor inertia forces to the axial load on the bearings. This relation can be exactly derived in a static analysis model of the complete structural system (say in a program SAP2000 or ETABS) including cases in which uplift occurs. When bearing uplift occurs, the program returns zero axial bearing force for

the bearings which uplift and redistributes axial forces to the other bearings so that equilibrium in the vertical direction is satisfied.

4. Program output is streamlined for easy assessment of performance of the structural system. Specifically, floor response spectra are calculated and exported to excel files for viewing.

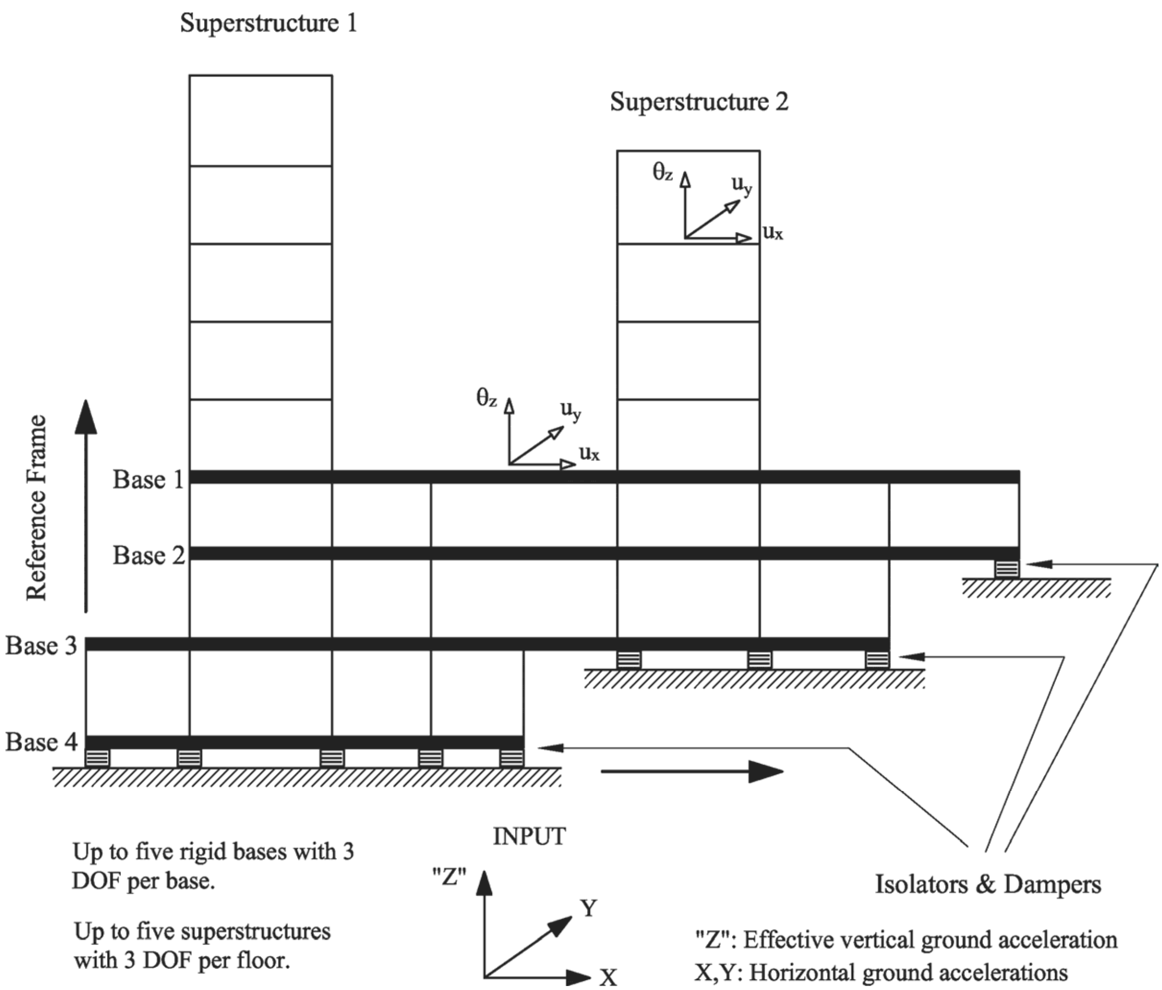

Figure 1-2: Model that can be analyzed in program 3D-BASIS-ME-MB.

The enhanced 3D-BASIS-ME-MB program is primarily useful in (a) performing analyses for schematic designs where speed in modeling of the isolated structure and speed in performing multiple dynamic analyses is desired, and (b) verifying the validity of modeling assumptions and verifying the accuracy of solutions of more complex analysis programs such as SAP2000 and ETABS. Program 3D-BASIS-ME-MB is not intended to replace or compete with commercial programs for the analysis of seismically isolated structures. Rather, it is intended to be a public domain analysis program that is complementary to commercially available analysis programs.

SECTION 2
DESCRIPTION OF PROGRAM 3D-BASIS-ME-MB

2.1 Superstructure and Isolation System Configuration

Program 3D-BASIS-ME-MB offers the capability to analyze multiple superstructures on Multiple Bases, hence the extension MB over its predecessor program 3D-BASIS-ME (Tsopelas et al, 1994). Figure 2-1 and 2-2 illustrate what the program can analyze: a number of superstructures (here shown as three superstructures) supported by a number of bases (here shown as three bases). The bases are inter-connected with linear elastic and viscous elements (representing structural elements such as columns, braces, walls, etc.). The bases are also connecting to the ground through elements that represent seismic isolation hardware. Each base is considered rigid in its own plane and described by its mass, the moment of inertia about the center of mass and the location of the center of mass. The motion of each base is calculated with respect to the position of the ground, which is described with respect to a fixed reference frame. The motion of each base is described by two displacements in the horizontal direction and a rotation about the vertical axis at the center of mass, all with respect the instantaneous position of the ground. The ground motion consists of translational three-dimensional components along the global axes. Each superstructure consists of floors that are rigid, with motion described with respect to the superstructure reference frame that parallels the fixed reference frame and is attached to the center of mass of the first (top) base. The superstructure reference frame serves as the global reference system with respect to which all coordinates are measured.

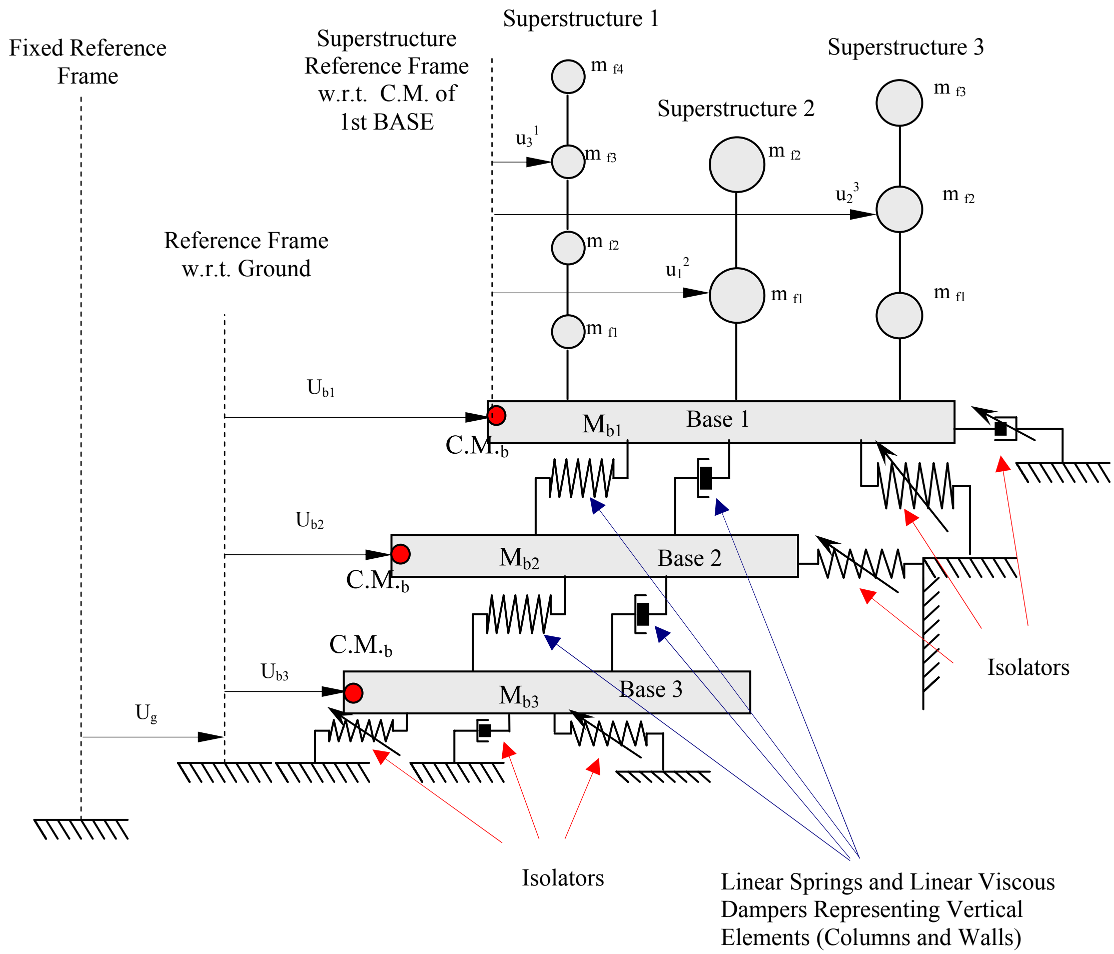

Figure 2-1: Degrees of freedom and reference frames in 3D-BASIS-ME-MB.

2.2 Superstructure Configuration

Assumed to remain elastic at all times, each superstructure in 3D-BASIS-ME-MB can be modeled using:

(i) A shear-building representation, or

(ii) A full three-dimensional representation.

In the shear-building representation, the stiffness matrix of the superstructure is internally constructed by the program, based on input story translational and rotational stiffnesses, and eccentricities of center of stiffness (or resistance) with respect to the center of mass for each floor. In the shear-type representation, it is assumed that the centers of mass (C.M.) of each floor in each superstructure lie on a common vertical axis. The reader

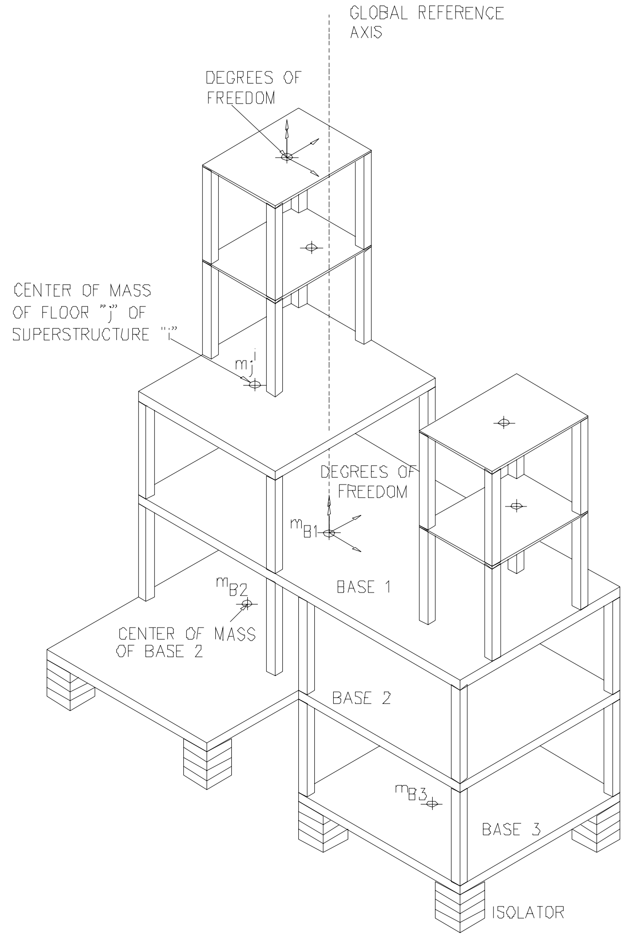

Figure 2-2: Three-dimensional rendering of isolated multiple superstructures on several bases.

should note that this assumption introduces an error with respect to the rotational degrees of freedom in the case that the centers of mass of each floor in a superstructure do not satisfy this constraint. In addition it is assumed that the floors are rigid, and all vertical story elements (walls and columns) are inextensible.

In the full three-dimensional representation, the dynamic characteristics of the superstructure in terms of frequencies and mode shapes are determined externally by other software and imported into program 3D-BASIS-ME-MB. In this way, the extensibility of the vertical elements, joint rotations, arbitrary location of the centers of mass, and floor flexibility may be implicitly accounted for.

Three degrees of freedom (DOF) per floor are required in the three-dimensional representation of the superstructure. Thus, the number of modes required for modal reduction of the differential equation of motion of each superstructure is a multiple of three. The minimum number of modes required is three.

The degrees of freedom of the floors and bases and the configuration of a multiple-building isolated structure are presented in Figure 2-2 in a three-dimensional illustration. The coordinates of the center of mass of each floor of every superstructure are measured with respect to the global reference system, which is attached to the C.M. of the first (top) base. The center of stiffness (or resistance) of each floor is located at distances e_{xj} and e_{yj} (eccentricities) with respect to the center of mass of the floor (Figure 2-3).

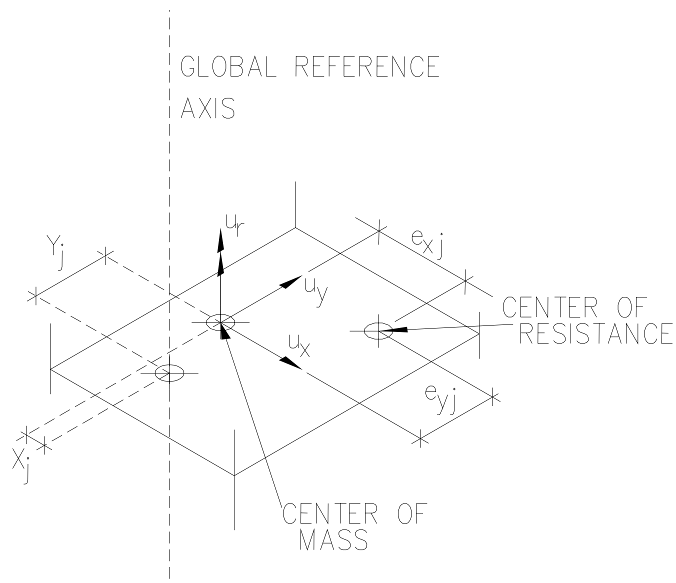

Figure 2-3: Degrees of freedom of one floor of one superstructure.

In both the shear-building and the full three-dimensional representation, floor masses are considered lumped at the center of mass of the floor. Three degrees of freedom are used to describe the motion of the C.M. of each floor; two translational (in the horizontal global X and Y directions) and one rotational about the vertical global axis.

2.3 Isolation System Configuration

The isolation system is modeled with spatial distribution and explicit nonlinear force-displacement relation for each isolator. The isolators are considered rigid in the vertical direction and to have negligible resistance to torsion. Program 3D-BASIS-ME-MB has the following elements for modeling the behavior of isolators:

(i) Linear elastic element.

(ii) Linear and nonlinear viscous elements for fluid viscous dampers or other devices displaying viscous behavior.

(iii) Hysteretic element for elastomeric bearings and steel dampers.

(iv) Stiffening (biaxial) hysteretic element for elastomeric bearings.

(v) Hysteretic element for flat sliding bearings.

(vi) Hysteretic element for spherical sliding (Friction Pendulum) bearings.

(vii) Hysteretic element for the uplift-restraining FP (XY-FP) bearings.

Isolator elements can be placed below each base of the structure (see Figures 1-1 and 2-1).

2.4 Modeling of Structural System between Bases

In program 3D-BASIS-ME-MB, a base is a rigid slab below which isolators are placed (see Figure 2-1). The part below the first base is the called substructure, whereas the part above the first base consists of a number of superstructures. In-between bases, structural elements such as columns and walls extend vertically. The behavior of these vertical elements between bases is modeled using linear springs and linear viscous dampers. Program 3D-BASIS-ME-MB requires as input the constants of springs and dampers and the location of the center of resistance of these elements.

Figure 2-4 shows two consecutive bases, designated as Top and Bottom, interconnected by columns and walls which are represented by two translational springs and one rotational spring (about axes X, Y and Z, respectively), all located at the center of stiffness of the story (or space) between the two bases.

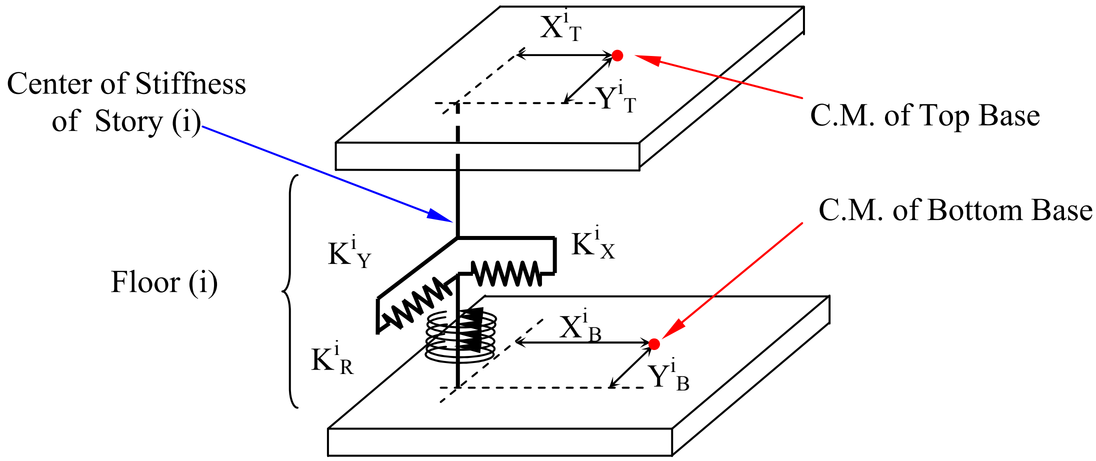

Figure 2-4: Linear springs representing vertical elements of story (i) connecting top and bottom bases

The following matrix equation relates forces and displacements at the center of mass (C.M.) of the top and bottom bases (3 degrees of freedom for each base; X and Y translational displacements and one rotation about the vertical axis):

$$\begin{Bmatrix} F^{Top} \\ F^{Bot} \end{Bmatrix} = \begin{pmatrix} K_{Bi}^{TopTop} & K_{Bi}^{TopBot} \\ K_{Bi}^{BotTop} & K_{Bi}^{BotBot} \end{pmatrix} \begin{Bmatrix} u^{Top} \\ u^{Bot} \end{Bmatrix} \tag{2-1}$$

where the sub-matrices in the above equation are expanded as follows:

$$\begin{Bmatrix} F_X^{Top} \\ F_Y^{Top} \\ M^{top} \\ F_X^{Bot} \\ F_Y^{Bot} \\ M^{Bot} \end{Bmatrix} = \begin{pmatrix} K_X & 0 & -K_X Y_{Top} & -K_X & 0 & K_X Y_{Bot} \\ 0 & K_Y & K_Y X_{Top} & 0 & -K_Y & -K_Y X_{Bot} \\ -K_X Y_{Top} & K_Y X_{Top} & K_R + K_X Y_{Top}^2 + K_Y X_{Top}^2 & K_X Y_{Top} & -K_Y X_{Top} & -K_R - K_X Y_{Top} Y_{Bot} - K_Y X_{Top} X_{Bot} \\ -K_X & 0 & K_X Y_{Top} & K_X & 0 & -K_X Y_{Bot} \\ 0 & -K_Y & -K_Y X_{Top} & 0 & K_Y & K_Y X_{Bot} \\ K_X Y_{Bot} & -K_Y X_{Bot} & -K_R - K_X Y_{Top} Y_{Bot} - K_Y X_{Top} X_{Bot} & -K_X Y_{Bot} & K_Y X_{Bot} & K_R + K_X Y_{Bot}^2 + K_Y X_{Bot}^2 \end{pmatrix} \begin{Bmatrix} u_X^{Top} \\ u_Y^{Top} \\ \phi^{top} \\ u_X^{Bot} \\ u_Y^{Bot} \\ \phi^{Bot} \end{Bmatrix} \tag{2-2}$$

It should be noted that in this formulation of the stiffness matrix, the centers of mass of the bases do not have to fall on the same vertical axis as in the shear type representation of the superstructures.

An identical formulation is applied for the linear viscous elements used to represent the energy dissipation capability of the vertical elements between two consecutive bases. In general, the location of the center of resistance or center of stiffness of the vertical elements between two bases should be the same as the location of the center of damping of the same elements.

2.5 Story Stiffness, Center of Stiffness and Center of Damping

The story stiffness and location of the center of stiffness and center of damping may be calculated if the lateral (horizontal) stiffness of each vertical element is known. Referring to Figure 2-5, the story horizontal stiffness is described by

$$K_X^i = \sum_j^N k_x^j, \quad K_Y^i = \sum_j^N k_y^j \tag{2-3}$$

where K^i_X and K^i_Y are the resultant stiffness constants along the X and Y directions in story (i), and k^j_x , k^j_y are the lateral (horizontal) stiffness constants along X and Y directions of the vertical element (j). The location of the center of stiffness of the floor is described by:

$$X_{CS}^i = \frac{\sum_j^N k_y^j x_j}{\sum_j^N k_y^j}, \quad Y_{CS}^i = \frac{\sum_j^N k_x^j y_j}{\sum_j^N k_x^j} \tag{2-4}$$

where X^i_{CS} and Y^i_{CS} are the coordinates of the center of stiffness of story (i) with respect to the coordinate system xOy as shown in Figure 2-5. Moreover, x_j and y_j are the coordinates of vertical element (j) with respect to coordinate system xOy.

The resultant rotational stiffness constant of the story, K^i_R, is given by:

$$K_R^i = \sum_j^N \left(k_x^j (y_j - Y_{CS}^i)^2 + k_y^j (x_j - X_{CS}^i)^2 + k_r^j \right) \tag{2-5}$$

The resultant damping constants and the location of the center of damping of each story of the substructure can be calculated in a similar manner by use of equations (2-3) to (2-5) and replacing the stiffness constants with the damping constants. However, in general the location of the center of damping is assumed to be the same as the location of the center of stiffness.

The resultant stiffness and the location of the center of stiffness of each story of the substructure may be most conveniently calculated by static analysis in computer programs like ETABS and STAAD. One example of such calculation is presented in

Appendix A.

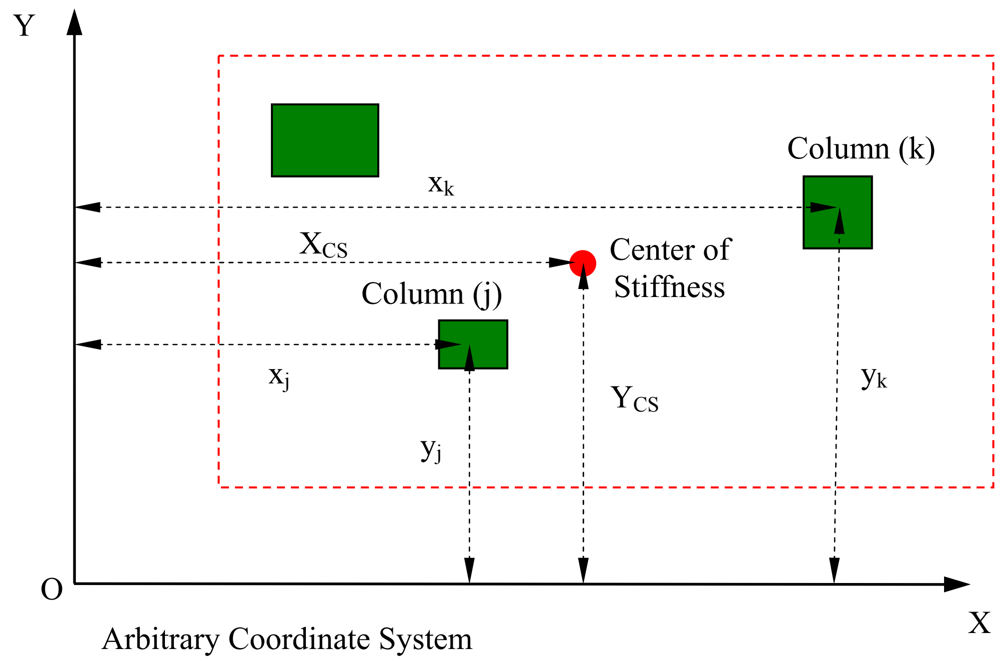

Figure 2-5: Plan view of story (i) and vertical elements connecting two bases.

2.6 Analytical Model and Equations of Motion

The equations of motion of the superstructures (structures above first base) are given by the following matrix expression:

$$M_{N_b\times N_b}\ddot{u}_{N_b\times 1}+C_{N_b\times N_b}\dot{u}_{N_b\times 1}+K_{N_b\times N_b}u_{N_b\times 1}=-M_{N_b\times N_b}R_{N_b\times 3}\left\{\ddot{u}_{B1}+\ddot{u}_g\right\}_{3\times 1} \qquad (2\text{-}6)$$

In the above equation, *M, C*, and *K* are the combined mass, damping and stiffness matrices of the superstructure buildings, *u* is the combined displacement vector of the superstructure buildings relative to the first base, and *R* is a transformation matrix which transfers the first base and ground acceleration vectors from the center of mass of the first base to the center of mass of each floor of each superstructure. The subscripts in the equation indicate matrix sizes. N_b is the total number of degrees of freedom of the superstructures above the first base and is equal to 3 times the number of floors of all superstructures. The interested reader can find the description of matrix R in Tsopelas et al. (1994).

The equations of dynamic equilibrium of the isolated structure are given by the following matrix equation:

$$\begin{bmatrix} M & MR & 0 \\ R^T M & R^T MR + M_{B1} & 0 \\ 0 & 0 & M_{Bk} \end{bmatrix} \left\{ \begin{matrix} \ddot{u} \\ \ddot{u}_{B1} \\ \ddot{u}_{Bk} \end{matrix} \right. + \begin{bmatrix} 0 \\ I \\ I \end{bmatrix} \{\ddot{u}_g\} \left. \vphantom{\begin{matrix} \ddot{u} \\ \ddot{u}_{B1} \\ \ddot{u}_{Bk} \end{matrix}} \right\} + \begin{bmatrix} K & & \\ & K_{B1}^{11} & K_{B1}^{1k} \\ & K_{B1}^{k1} & K_{B1}^{kk} + K_{Bk}^{kk} \end{bmatrix} \begin{Bmatrix} u \\ u_{B1} \\ u_{Bk} \end{Bmatrix} + \tag{2-7}$$
$$+ \begin{bmatrix} C & & \\ & C_{B1}^{11} & C_{B1}^{1k} \\ & C_{B1}^{k1} & C_{B1}^{kk} + C_{Bk}^{kk} \end{bmatrix} \begin{Bmatrix} \dot{u} \\ \dot{u}_{B1} \\ \dot{u}_{Bk} \end{Bmatrix} + \begin{Bmatrix} 0 \\ f_{NB1} \\ f_{NBk} \end{Bmatrix} = 0$$

The second (middle) of the three sub-matrix equations in (2-7) is the equation of equilibrium of the first base, which acts as the interface between the superstructures and the lower bases. The modified mass matrix in (2-7) is a product of the mass matrix and the transformation matrices involving R in the following expression:

$$\begin{bmatrix} I & 0 & 0 \\ R^T & I & 0 \\ 0 & 0 & I \end{bmatrix} \begin{bmatrix} M & 0 & 0 \\ 0 & M_{B1} & 0 \\ 0 & 0 & M_{Bk} \end{bmatrix} \begin{bmatrix} I & R & 0 \\ 0 & I & 0 \\ 0 & 0 & I \end{bmatrix} \tag{2-8}$$

where, M_{B1} is a 3x3 diagonal mass matrix of the first base, M_{Bk} is a $(N_{bs}-3)$x$(N_{bs}-3)$ mass matrix which contains the masses and moments of inertia of the rest of the bases of the substructure (excluding the first base), and N_{bs} is the total number of degrees of freedom of the bases (equal to three times the number of bases). Sub-matrices $K^{11}{}_{B1}$, $K^{1k}{}_{B1}$, $K^{k1}{}_{B1}$, $K^{11}{}_{B1}$, $K^{kk}{}_{Bk}$, $C^{11}{}_{B1}$, $C^{1k}{}_{B1}$, $C^{k1}{}_{B1}$, $C^{11}{}_{B1}$, $C^{kk}{}_{Bk}$ are stiffness and damping matrices of the vertical elements (represented as linear elastic and linear viscous elements) between bases. Matrices $K^{kk}{}_{Bk}$ and $C^{kk}{}_{Bk}$ also include contributions from linear-elastic and linear-viscous elements of the isolation system located below at the lowest base (connected between the lowest base and the ground). Moreover, f_N is a vector containing the forces in elements of the isolation system.

Modal reduction for the equations of equilibrium of the superstructure is employed in accordance with the following equation:

$$u^i_{3nf^i} = \Phi^i_{3nf^i \times ne^i} Y^i_{ne^i \times 1} \tag{2-9}$$

where, Φ^i is the ortho-normal modal matrix relative to the mass matrix of superstructure (i), Y^i is the modal displacement vector of superstructure (i) relative to the first base and ne^i is the number of eigenvectors of superstructure (i) used in the analysis.

Combining equations (2-6) to (2-9), the following equation is derived. Note that this equation is written for the case of three bases.

$$\begin{pmatrix} I & \Phi^T MR & & \\ R^T M\Phi & R^T MR + M_{B1} & & \\ & & M_{B2} & \\ & & & M_{B3} \end{pmatrix}_{(M_b+N_{bs})\times(M_b+N_{bs})} \begin{Bmatrix} \ddot{Y} \\ \ddot{u}_{B1} \\ \ddot{u}_{B2} \\ \ddot{u}_{B3} \end{Bmatrix}_{(M_b+N_{bs})\times 1} +$$

$$+\begin{pmatrix} 2\xi\omega & & & \\ & C^{11}_{B1} & C^{12}_{B1} & \\ & C^{21}_{B1} & C^{22}_{B1}+C^{11}_{B2} & C^{12}_{B2} \\ & & C^{21}_{B2} & C^{22}_{B2}+C^{11}_{B3} \end{pmatrix}_{(M_b+N_{bs})\times(M_b+N_{bs})} \begin{Bmatrix} \dot{Y} \\ \dot{u}_{B1} \\ \dot{u}_{B2} \\ \dot{u}_{B3} \end{Bmatrix}_{(M_b+N_{bs})\times 1} +$$

$$+\begin{pmatrix} \omega^2 & & & \\ & K^{11}_{B1} & K^{12}_{B1} & \\ & K^{21}_{B1} & K^{22}_{B1}+K^{11}_{B2} & K^{12}_{B2} \\ & & K^{21}_{B2} & K^{22}_{B2}+K^{11}_{B3} \end{pmatrix}_{(M_b+N_{bs})\times(M_b+N_{bs})} \begin{Bmatrix} Y \\ u_{B1} \\ u_{B2} \\ u_{B3} \end{Bmatrix}_{(M_b+N_{bs})\times 1} +$$

$$+\begin{Bmatrix} 0 \\ f_{NB1} \\ f_{NB2} \\ f_{NB3} \end{Bmatrix}_{(M_b+N_{bs})\times 1} = -\begin{Bmatrix} \Phi^T MR \\ R^T MR + M_{B1} \\ M_{B2} \\ M_{B3} \end{Bmatrix}_{(M_b+N_{bs})\times 3} \{\ddot{u}_g\}_{3\times 1} \tag{2-10}$$

Equation (2-10) may be written as

$$\tilde{\mathbf{M}}\,\ddot{\tilde{\mathbf{u}}}_{\mathbf{t}} + \tilde{\mathbf{C}}\,\dot{\tilde{\mathbf{u}}}_{\mathbf{t}} + \tilde{\mathbf{K}}\,\tilde{\mathbf{u}}_{\mathbf{t}} + \mathbf{f}_{\mathbf{t}} = \tilde{\mathbf{P}}_{\mathbf{t}} \tag{2-11}$$

in which subscript t denotes that the equation is valid at time t. Extending Equation (2-11) to time (t + Δt), where Δt is the time step, we have

$$\tilde{\mathbf{M}}\,\ddot{\tilde{\mathbf{u}}}_{\mathbf{t+\Delta t}} + \tilde{\mathbf{C}}\,\dot{\tilde{\mathbf{u}}}_{\mathbf{t+\Delta t}} + \tilde{\mathbf{K}}\,\tilde{\mathbf{u}}_{\mathbf{t+\Delta t}} + \mathbf{f}_{\mathbf{t+\Delta t}} = \tilde{\mathbf{P}}_{\mathbf{t+\Delta t}} \tag{2-12}$$

The difference between Equations (2-11) and (2-12) gives the incremental equation of equilibrium

$$\tilde{\mathbf{M}}\,\Delta\ddot{\tilde{\mathbf{u}}}_{\mathbf{t+\Delta t}} + \tilde{\mathbf{C}}\,\Delta\dot{\tilde{\mathbf{u}}}_{\mathbf{t+\Delta t}} + \tilde{\mathbf{K}}\,\Delta\tilde{\mathbf{u}}_{\mathbf{t+\Delta t}} + \Delta\mathbf{f}_{\mathbf{t+\Delta t}} = \tilde{\mathbf{P}}_{\mathbf{t+\Delta t}} - \tilde{\mathbf{M}}\,\ddot{\tilde{\mathbf{u}}}_{\mathbf{t}} - \tilde{\mathbf{C}}\,\dot{\tilde{\mathbf{u}}}_{\mathbf{t}} - \tilde{\mathbf{K}}\,\tilde{\mathbf{u}}_{\mathbf{t}} - \mathbf{f}_{\mathbf{t}} \tag{2-13}$$

Accordingly, the response of the multiple building superstructure and bases is represented by the mixed vectors consisting of modal coordinates for the superstructures and vectors $\ddot{\tilde{\mathbf{u}}}_{\mathbf{t}}$, $\dot{\tilde{\mathbf{u}}}_{t}$, and $\tilde{\mathbf{u}}_{\mathbf{t}}$.

2.7 Solution Method

The pseudo-force method is used in the present study as originally adopted in the program 3D-BASIS by Nagarajaiah et al. (1989). This method has been used for nonlinear dynamic analysis of shells by Stricklin et al. (1971) and by Darbre and Wolf (1988) for soil-structure interaction problems. More details and the advantages of this method in the analysis of seismically isolated structures have been presented by Nagarajaiah et al. (1989, 1990, 1991a, and 1991b). In the pseudo-force method, the incremental nonlinear force vector $\Delta f_{t+\Delta t}$ in Equation (2-13) is unknown. It is, thus, brought on the right hand side of Equation (2-13) and treated as pseudo-force vector.

2.8 Solution Algorithm

The differential equations of motion are integrated in the incremental form of Equations 2-13. The solution involves two stages:

(i) Solution of the dynamic equations of motion (second-order ordinary differential equations) using the unconditionally stable (for both positive and negative tangent stiffness—Cheng, 1988) Newmark's constant-average-acceleration method (Newmark, 1959).

(ii) Solution of the first-order ordinary differential equations governing the nonlinear behavior of the isolation elements using an unconditionally stable semi-implicit Runge-Kutta method suitable for stiff differential equations (Rosenbrock, 1964). The solution algorithm of the pseudo force method with iteration is presented in Table 2-1.

2.8.1 Varying Time Step for Accuracy

The solution algorithm has the option of using a constant time step or variable time step. For the variable time step option, the time step is reduced from Δt_{slip} (time step at high velocities) to a fraction of its value at low velocities to maintain accuracy in sliding isolated structures. The time step is reduced based on the magnitude of the resultant velocity at the center of mass of the lower isolation level:

$$\Delta t_{stick} = \Delta t_{slip} \left[1 - \exp\left(-\frac{\dot{u}^2}{B} \right) \right] \tag{2-14}$$

in which $\dot{u}$ is the resultant velocity at the center of mass of the lowest base, Δt_{stick} is the reduced time step when the base velocity is low ($\Delta t_{slip} > \Delta t_{stick} > \Delta t_{slip}/nl$; nl is an integer to introduce the desired reduction), and B is a constant to define the range of velocity over which the reduction takes place. It is important to note that the reduction in the time step is not continuous as indicated by Equation (2-14), but rather at discrete intervals of velocity. This procedure is adopted for computational efficiency. Equation (2-14) has been a feature in the 3D-BASIS series of programs (Nagarajaiah et al, 1989, 1990, 1991a, and 1991b).

Table 2-1: Solution algorithm

A. Initial Conditions:

1. Form stiffness $\tilde{\mathbf{K}}$, mass $\tilde{\mathbf{M}}$, and damping matrices $\tilde{\mathbf{C}}$. Initialize $\tilde{\mathbf{u}}_0$, $\dot{\tilde{\mathbf{u}}}_0$, and $\ddot{\tilde{\mathbf{u}}}_0$.
2. Select time step Δt, set parameters $\delta = 0.25$ and $\theta = 0.5$, and calculate the integration constants:

$$a_1 = \frac{1}{\delta \cdot \Delta t^2}; \quad a_2 = \frac{1}{\delta \cdot \Delta t}; \quad a_3 = \frac{1}{2\delta}; \quad a_4 = \frac{\theta}{\delta \cdot \Delta t}; \quad a_5 = \frac{\theta}{\delta}; \quad a_6 = \Delta t \cdot \left(\frac{\theta}{2\delta} - 1\right)$$

3. Form the effective stiffness matrix $\mathbf{K}^* = a_1 \cdot \tilde{\mathbf{M}} + a_4 \cdot \tilde{\mathbf{C}} + \tilde{\mathbf{K}}$
4. Triangularize $\mathbf{K}^*$ using Gaussian elimination (only if the time step is different from the previous step).

B. Iteration at each time step:

1. Assume the pseudo-force $\Delta \mathbf{f}^i_{t+\Delta t} = 0$ in iteration i = 1.
2. Calculate the effective load vector at time $t + \Delta t$:

$$\mathbf{P}^*_{t+\Delta t} = \Delta \tilde{\mathbf{P}}_{t+\Delta t} - \Delta \mathbf{f}^i_{t+\Delta t} + \tilde{\mathbf{M}} \cdot \left(a_2 \cdot \dot{\tilde{\mathbf{u}}}_t + a_3 \cdot \ddot{\tilde{\mathbf{u}}}_t\right) + \tilde{\mathbf{C}}\left(a_5 \cdot \dot{\tilde{\mathbf{u}}}_t + a_6 \cdot \ddot{\tilde{\mathbf{u}}}_t\right)$$

$$\Delta \tilde{\mathbf{P}}_{t+\Delta t} = \tilde{\mathbf{P}}_{t+\Delta t} - \left(\tilde{\mathbf{M}} \cdot \ddot{\tilde{\mathbf{u}}}_\mathbf{t} + \tilde{\mathbf{C}} \cdot \dot{\tilde{\mathbf{u}}}_t + \tilde{\mathbf{K}} \cdot \tilde{\mathbf{u}}_\mathbf{t} + \mathbf{f}_t\right)$$

3. Solve for displacements at time $t+\Delta t$: $\mathbf{K}^* \cdot \Delta \mathbf{u}^i_{t+\Delta t} = \mathbf{P}^*_{t+\Delta t}$
4. Update the state of motion at time $t+\Delta t$:

$$\ddot{\tilde{\mathbf{u}}}_{t+\Delta t} = \ddot{\tilde{\mathbf{u}}}_t + a_1 \cdot \Delta \tilde{\mathbf{u}}^i_{t+\Delta t} - a_2 \cdot \dot{\tilde{\mathbf{u}}}_t - a_3 \cdot \ddot{\tilde{\mathbf{u}}}_t$$

$$\dot{\tilde{\mathbf{u}}}_{t+\Delta t} = \dot{\tilde{\mathbf{u}}}_t + a_4 \cdot \Delta \tilde{\mathbf{u}}^i_{t+\Delta t} - a_5 \cdot \dot{\tilde{\mathbf{u}}}_t - a_6 \cdot \ddot{\tilde{\mathbf{u}}}_t$$

$$\tilde{\mathbf{u}}_{t+\Delta t} = \tilde{\mathbf{u}}_t + \Delta \tilde{\mathbf{u}}^i_{t+\Delta t}$$

5. Compute the forces mobilized in each isolation element following the steps:
   5a. Calculate bearing axial forces at iteration (i) using acceleration distribution at time (t). [Axial forces are calculated using an iterative process. First, the isolators which undergo uplift are identified using the method described in Section 3.4. Then, axial loads in each isolator are updated and if there are additional isolators that uplift then an iteration process takes place until it converges.]
   5b. Compute the state of motion at each bearing.
   5c. Solve the first-order ODEs, using semi-implicit Runge-Kutta method, to evaluate the variable $Z^i_{t+\Delta t}$ used in the nonlinear force equations at each bearing. [For the calculation of the $Z^i_{t+\Delta t}$ the average velocity between the previous and current time steps are used $(V_t + V^i_{t+\Delta t})/2$].
6. Compute the resultant nonlinear force vector of the isolation system, $\Delta \mathbf{f}^{i+1}_{t+\Delta t}$. [The nonlinear forces are with respect to the C.M. of the base that the isolators are located.]
7. Compute : $Error = \dfrac{\left\|\Delta \mathbf{f}^{i+1}_{t+\Delta t} - \Delta \mathbf{f}^i_{t+\Delta t}\right\|}{ref.\,Max.\,Moment}$, where ||.|| is the Euclidean norm
8. If Error ≥ Tolerance, further iteration is needed, iterate starting form step B-1 and use $\Delta \mathbf{f}^{i+1}_{t+\Delta t}$ as the pseudo-force and the state of motion at time t, $\tilde{\mathbf{u}}_t$, $\dot{\tilde{\mathbf{u}}}_t$, and $\ddot{\tilde{\mathbf{u}}}_t$.
9. If Error ≤ Tolerance, no further iteration is needed, update the nonlinear force vector:

$$\mathbf{f}_{t+\Delta t} = \mathbf{f}_t + \Delta\mathbf{f}_{t+\Delta t}^{i+1}$$

10. Reset time step if necessary (the velocity of the lowest isolation base is used in the criteria of Section 2.4.1)
11. **GoTo Step B-1** if the time step is not reset or **GoTo A-2** if the time step is reset.

SECTION 3
ENHANCEMENTS INTRODUCED IN 3D-BASIS-ME-MB

3.1 Introduction

Program 3D-BASIS-ME-MB offers the following new features:

1. Analyzes a more complex configuration as illustrated in Figure 1-2. In this configuration the structure consists of three parts:

    - Superstructure, consisting of up to 5 separate superstructures. Each is modeled as having rigid floors with three degrees of freedom each (two translations and one rotation). The input data consists of the floor mass, moment of inertia and location of centers of mass, and shear stiffness, torsional stiffness and center of resistance per story. Alternatively, the input data for representing the stiffness of each part of the superstructure are in terms of mode shapes and frequencies obtained from analysis of a detailed model in another program like SAP2000 or ETABS.

    - Substructure consisting of up to 5 bases above the lowest isolation interface. Isolators are located at each of the 5 bases. Each base is represented as a rigid floor with 3 degrees of freedom. The mass, moment of inertia and location of center of mass of each floor is input. The stiffness characteristics of the substructure are input in a manner similar to that of each part of the superstructure.

    - Isolators and dampers that may be located at each base of the substructure. Each isolator and damper is explicitly modeled in terms of its location, orientation and constitutive relation.

2. The isolation system has the following new elements:

    - The new XY-FP bearing capable of sustaining tension is represented (Roussis and Constantinou, 2005). The orientation of the bearing may be in any arbitrary direction with the respect to the global reference frame.

    - The existing viscous damper element is modified to have a more general constitutive relation and to have capability for placement at an arbitrary direction with respect to the global reference frame.

3. Overturning moment effects are captured in a more complex and accurate way. The axial load on each isolator is calculated at each time step through a procedure described below in Section 3.4 that relates the instantaneous floor inertia forces to the axial load on the bearings. This relation can be exactly derived in a static analysis model of the complete structural system (say in a program like SAP2000 or ETABS) including cases in which uplift occurs. When bearing uplift occurs, the program returns zero axial bearing force for the bearings which uplift and redistributes axial forces to the other bearings so that equilibrium in the vertical direction is satisfied.
4. Program output is streamlined for easy assessment of performance of the structural system. Specifically, floor response spectra are calculated and exported to excel files for viewing.

3.2 Element for the Uplift-Restraining XY-FP Isolator

Force-displacement constitutive relationship

The principles of operation and mathematical model of the newly introduced XY-FP isolator have been established by Roussis and Constantinou (2005).

Based on the Friction-Pendulum principle (Zayas et al., 1987; Mokha et al., 1988), the XY-FP isolator consists of two orthogonal concave stainless steel-faced beams interconnected through a sliding mechanism that permits tension to develop in the bearing, thereby preventing potential uplift (Figure 3-1). Under the imposed constraint to remain mutually perpendicular (except for small rotation about the vertical axis), the two opposing beams can move independently relative to each other to form a bi-directional (XY) motion mechanism. For a detailed description of the XY-FP isolator, the reader is referred to Roussis and Constantinou (2005).

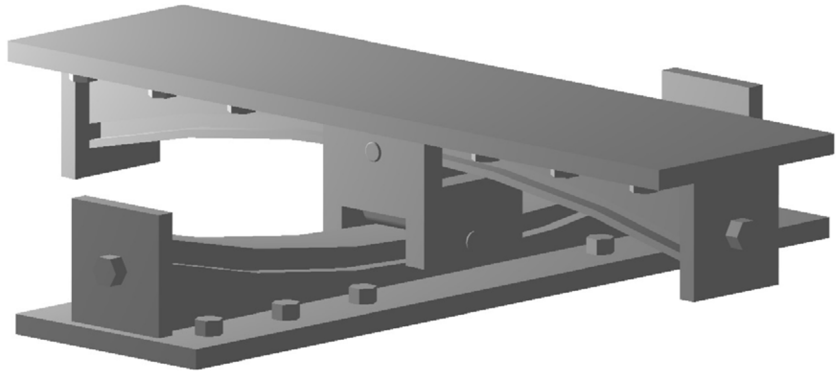

Figure 3-1: Three-dimensional view of the uplift-restraining XY-FP isolator.

Neglecting the effect of lateral force on friction force, the force-displacement constitutive relationship in the local co-ordinate system is given collectively by

$$\begin{Bmatrix} F_1 \\ F_2 \end{Bmatrix} = \begin{bmatrix} N/R_1 & 0 \\ 0 & N/R_2 \end{bmatrix} \begin{Bmatrix} U_1 \\ U_2 \end{Bmatrix} + \begin{bmatrix} \mu_1 |N| & 0 \\ 0 & \mu_2 |N| \end{bmatrix} \begin{Bmatrix} \operatorname{sgn}(\dot{U}_1) \\ \operatorname{sgn}(\dot{U}_2) \end{Bmatrix} \tag{3-1}$$

where R_1 and R_2 are the radii of curvature of the lower and upper concave beams, respectively (minus the small height of the pivot point to the concave surface of the beam); μ_1 and μ_2 are the associated sliding friction coefficients; U_1 and U_2 are the displacements in local axis 1 and 2, respectively; N is the normal force on the bearing, positive when compressive; and $\operatorname{sgn}(\dot{U}_i)$ is the signum function operating on the sliding velocities.

Equation (3-1) describes the resisting force of the isolator along the i-direction assuming small angles of rotation φ (linearized form). The resisting force is synthesized by two components, one representing the pendulum effect associated with a restoring force (in the case of compressive normal load), and the other representing the contribution of friction developed at the sliding interface.

Having defined the constitutive relation of the bearing with respect to the local co-ordinate system, the corresponding force-displacement relationship in the global co-ordinate system can be readily derived as

$$\begin{Bmatrix} F_x \\ F_y \end{Bmatrix} = \begin{bmatrix} \cos\theta & \sin\theta \\ -\sin\theta & \cos\theta \end{bmatrix}^T \begin{Bmatrix} F_1 \\ F_2 \end{Bmatrix} \tag{3-2}$$

Isolator normal force

In general, the normal force on the isolation bearing is a fast-varying function of time due to the effect of vertical earthquake motion and global overturning moment. For a vertically rigid superstructure, the normal force on the bearing at any given time is synthesized by

$$N = W\left(1 + \frac{\ddot{u}_{gv}}{g} + \frac{N_{OM}}{W}\right) \tag{3-3}$$

where W is the weight acting on the isolator; $\ddot{u}_{gv}$ is the vertical ground acceleration (positive when the direction is upwards); and N_{OM} is the additional axial force due to overturning moment effects (positive when compressive).

Evaluation of the bearing normal force according to Equation (3-3) is of utmost importance for the accuracy of the XY-FP model. The fluctuation in the bearing axial force caused by the vertical component of ground motion and overturning moments can be large enough to cause reversal of the axial force from compression to tension.

Coefficient of sliding friction

The coefficient of sliding friction mobilized on a typical sliding bearing interface is modeled by the following equation (Constantinou et al., 1990):

$$\mu_s = f_{\max} - (f_{\max} - f_{\min})e^{-a|\dot{u}|} \tag{3-4}$$

where the coefficient of sliding friction μ_s ranges from $f_{\min}$, at very low velocities of sliding, to $f_{\max}$, at large velocities; $\dot{u}$ is the velocity of sliding; and a is a constant, having units of time per unit length, that controls the variation of the coefficient of friction with velocity. The dependency of the coefficient of friction on velocity is illustrated in Figure 3-2(a).

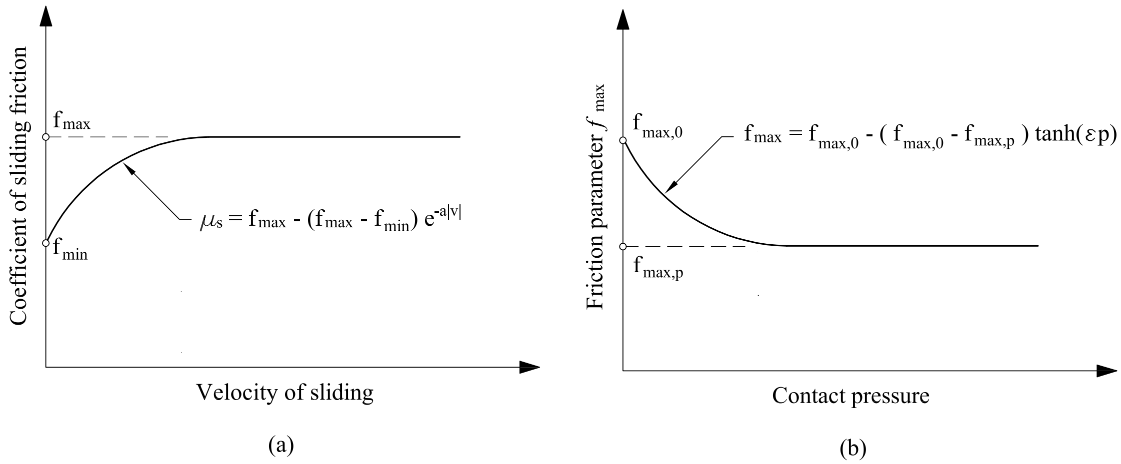

Figure 3-2: Variation of coefficient of friction with (a) velocity of sliding; and (b) bearing contact pressure.

In general, parameters $f_{\max}$, $f_{\min}$, and a are functions of bearing pressure and temperature. However, the dependency of $f_{\min}$ and a on pressure is insignificant (compared with that of $f_{\max}$) and can be neglected (Tsopelas et al., 1994). A representative expression describing the variation of parameter $f_{\max}$ with pressure is given by

$$f_{\max} = f_{\max 0} - (f_{\max 0} - f_{\max \mathrm{p}})\tanh(\varepsilon p) \tag{3-5}$$

where parameter $f_{\max}$ ranges from $f_{\max 0}$, at almost zero pressure, to $f_{\max \mathrm{p}}$, at very high pressure; p is the bearing contact pressure; and ε is a constant that controls the variation of $f_{\max}$ between very low and very high pressures. Figure 3-2(b) presents the assumed variation of friction parameter $f_{\max}$ with pressure, which is typical of the behavior of sliding bearings (Soong and Constantinou, 1994).

Model for XY-FP isolator in 3D-BASIS-ME-MB

To accommodate the mechanical behavior of the new XY-FP isolator, a new hysteretic element was incorporated into 3D-BASIS-ME-MB. The new element is synthesized by two independent uniaxial hysteretic elements allowing different frictional interface properties along the principal isolator directions (Roussis and Constantinou, 2005). It should be emphasized that, contrary to the element representing the conventional FP isolator, the new element is capable of accommodating the uplift-restraint property of the

XY-FP isolator by allowing continuous transition of the bearing axial force from compression to tension and vice versa. Moreover, the new element can assume different frictional interface properties under compressive and tensile isolator normal force.

The force-displacement relationship utilized in modeling the XY-FP element in 3D-BASIS-ME-MB is given by

$$\begin{Bmatrix} F_1 \\ F_2 \end{Bmatrix} = \begin{bmatrix} N/R_1 & 0 \\ 0 & N/R_2 \end{bmatrix} \begin{Bmatrix} U_1 \\ U_2 \end{Bmatrix} + \begin{bmatrix} \mu_1 |N| & 0 \\ 0 & \mu_2 |N| \end{bmatrix} \begin{Bmatrix} Z_1 \\ Z_2 \end{Bmatrix} \tag{3-6}$$

where R_1 and R_2 are the radii of curvature of the lower and upper concave beams, respectively; μ_1 and μ_2 are the associated sliding friction coefficients; U_1 and U_2 are the displacements in bearing local axis 1 and 2, respectively; N is the normal force on the bearing, positive when compressive; and Z_1 and Z_2 are hysteretic dimensionless quantities governed by the following differential equations:

$$\begin{Bmatrix} \dot{Z}_1 Y_1 \\ \dot{Z}_2 Y_2 \end{Bmatrix} = A \begin{bmatrix} 1 & 0 \\ 0 & 1 \end{bmatrix} \begin{Bmatrix} \dot{U}_1 \\ \dot{U}_2 \end{Bmatrix} - \begin{bmatrix} |Z_1|^{\eta} (\gamma \operatorname{sgn}(\dot{U}_1 Z_1) + \beta) & 0 \\ 0 & |Z_2|^{\eta} (\gamma \operatorname{sgn}(\dot{U}_2 Z_2) + \beta) \end{bmatrix} \begin{Bmatrix} \dot{U}_1 \\ \dot{U}_2 \end{Bmatrix} \tag{3-7}$$

where $\dot{U}_1$ and $\dot{U}_2$ are the velocities in local axis 1 and 2, respectively; A, β, γ, and η are dimensionless quantities that control the shape of the hysteresis loop; and Y_1 and Y_2 represent displacement quantities.

Constantinou et al. (1990) have shown that when $A = 1$ and $\beta + \gamma = 1$, the model of Equation (3-7) reduces to a model of viscoplasticity that was proposed by Ozdemir

(1976). In this case, Y_1 and Y_2 represent the yield displacements, while parameter η controls the mode of transition into the inelastic range. The model exhibits rate dependency, which reduces with increasing values of the exponent, η, and/or increasing values of the ductility ratio (maximum value of U/Y).

The conditions of separation and reattachment (stick-slip) are accounted for by variables Z_1 and Z_2 in Equation (3-7). In this respect, quantity Z_i may be regarded as a continuous approximation to the unit step function, $\operatorname{sgn}(\dot{U}_i)$ in Equation (3-1). It should be noted that

$Z_i = \pm 1$ during the sliding phase, whereas $|Z_i| < 1$ during the sticking phase (elastic behavior with very high stiffness).

A limitation of the employed plasticity model is its inability to reproduce truly rigid-plastic behavior. However, since Teflon-steel interfaces undergo very small elastic displacement before sliding, a small value of yield displacement Y, in the range of 0.13 to 0.50 mm (0.005 to 0.02 in.), can be reasonably assumed (larger values can also be justified on the basis of actual bearing behavior), and hence the viscoplasticity model can be used (Constantinou et al., 1990). The model exhibits insignificant rate dependency for such low yield displacement and resulting ductility ratio, and for parameter values of $\eta = 2$, $\beta = 0.1$, and $\gamma = 0.9$ suggested by Constantinou et al. (1990).

It should be emphasized that Equation (3-7) is uncoupled, representing two independent uniaxial hysteretic elements along the principal directions of the isolator. Accordingly, the biaxial interaction between forces in the two orthogonal directions is nonexistent, rendering the interaction surface to be square, as opposed to the circular interaction surface for the biaxial behavior of the spherical FP isolator (Figure 3-3).

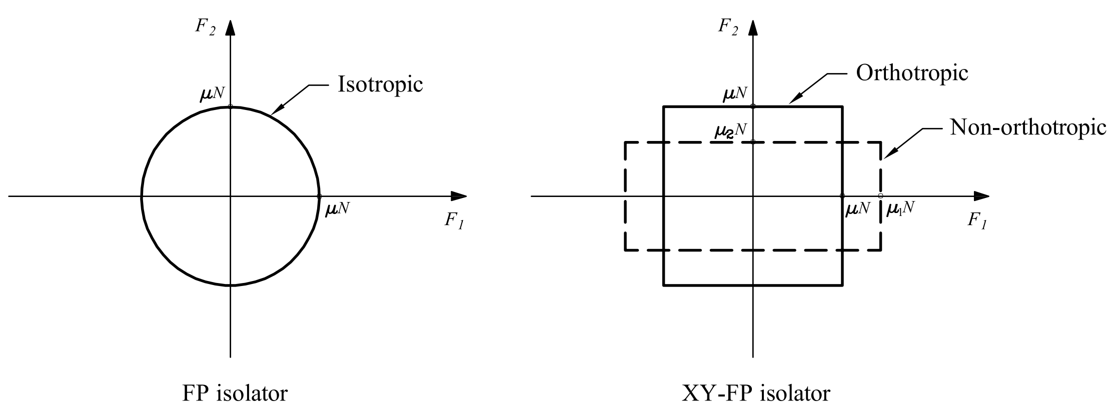

Figure 3-3: Force interaction curves for XY-FP and FP isolators.

The model in 3D-BASIS-ME-MB accounts for the variability of the normal force through Equation (3-3). The additional axial force due to overturning moment effects, N_{OM}, in Equation (3-3) is calculated through the procedure presented in Section 3.4.1. Moreover, the dependency of the coefficient of friction on sliding velocity and bearing pressure is explicitly modeled according to Equations (3-4) and (3-5), respectively.

3.3 Element for Viscous Damper

Program 3D-BASIS-ME-MB has two elements for modeling viscous damper behavior. Both are uni-axial elements that can be placed in an arbitrary direction with respect to the global co-ordinate system.

Linear/nonlinear viscous element

This element has the following constitutive relation:

$$F = C\left|\dot{U}\right|^{\alpha}\operatorname{sgn}(\dot{U}) \tag{3-8}$$

Where F is the force along the axis of the damper, $\dot{U}$ is the relative velocity of the one end of the damper with respect to the other end along the axis of the damper, C is the damper constant, and α is the power constant. For $\alpha = 1$, linear viscous behavior is obtained.

General nonlinear viscous element

This element has the following constitutive relation:

$$F = \begin{cases} \left(F_{01} + C_1\left|\dot{U}\right|^{\alpha_1}\right)\operatorname{sgn}(\dot{U}) & \text{for } \left|\dot{U}\right| \le V_{12} \\ \left(F_{02} + C_2\left|\dot{U}\right|^{\alpha_2}\right)\operatorname{sgn}(\dot{U}) \le F_{\max} & \text{for } \left|\dot{U}\right| > V_{12} \end{cases} \tag{3-9}$$

which is portrayed in Figure 3-4. This relation distinguishes between two ranges of velocity, separated by velocity V_{12}, in each of which a different constitutive relation applies. This relation is the linear or nonlinear viscous relation with an added friction force (F_{01} and F_{02}) that simulates friction in the seals of viscous dampers. Moreover, the force output of the element is bound by force limit $F_{\max}$. Equation (3-9) represents the novelty introduced in 3D-BASIS-ME-MB. It allows for a more realistic representation of viscous damper behavior.

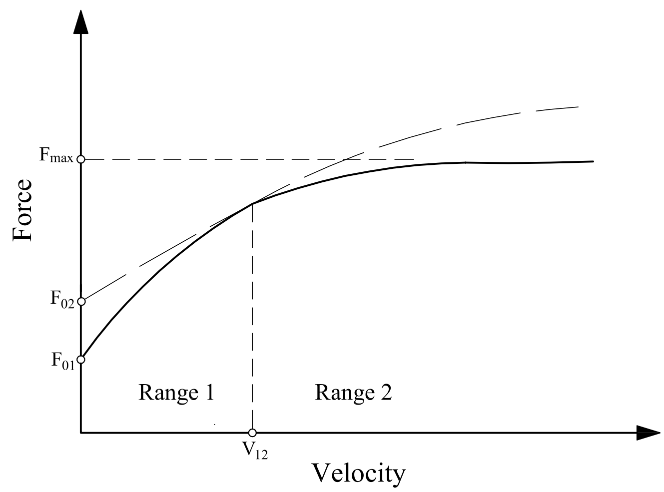

Figure 3-4: Graphical representation of the constitutive relation for the general nonlinear viscous element.

3.4 Construction of Relation between Inertial Forces and Axial Bearing Loads

3.4.1 Case of No Isolator Uplift

In order to account for the variability of axial forces in the isolation bearings due to overturning moment effects, 3D-BASIS-ME was modified to include a direct relationship between floor inertia forces and additional axial load on bearings (Roussis and Constantinou, 2005). At each time step of integration (beginning of time step), the horizontal inertia forces, $\{F_I\}$, are calculated from the floor accelerations and multiplied by a coefficient matrix, $[T]$, to obtain the corresponding change of vertical loads on the bearings due to overturning moment effects, $\{N_{OM}\}$. The additional vertical load can be expressed as

$$\{N_{OM}\} = [T]\{F_I\} \tag{3-10}$$

where $\{N_{OM}\}_{n\times 1} = \begin{bmatrix} N_{OM,1} & N_{OM,2} & \dots & N_{OM,n} \end{bmatrix}^T$ is the vector of bearing axial forces; $[T]_{n\times 2i}$ is a coefficient matrix relating additional bearing axial forces to floor inertia forces; $\{F_I\}_{2i\times 1} = \begin{bmatrix} F_{I,ix} & F_{I,iy} & \dots & F_{I,1x} & F_{I,1y} \end{bmatrix}^T$ is the vector of inertia forces at every floor level and isolated-base level; n is the number of bearings; and i is three times the total number of floors plus the number of isolated bases (model might have more than one superstructure/building), or in other words i is equal to the total number of dynamic degrees of freedom considered in the structural model (X and Y translation and Rotation at the C.M. of every slab in the structural model).

The coefficient matrix, $[T]$, is evaluated externally by other computer programs (e.g., SAP2000 or ETABS) and imported into program 3D-BASIS-ME-MB. It shall be calculated from linear static analyses of the structure supported on hinge supports and subjected to horizontally acting unit loads at the C.M. of the different floor levels. For example, the i-th column of matrix $[T]$ is calculated as the local frame column loads upon application of a unit lateral force at the center of mass of the i-th floor, with the lateral forces of the remaining floors being zero. It should be noted that construction of matrix $[T]$ is not sufficient to describe the distribution of axial force on the bearings when uplift occurs.

In the case of a multi-story structure on five isolators as shown in Figure 3-5, and assuming that no uplift occurs, matrix $[T]$, supplied in file TMATRIX.DAT, is calculated by static analysis (e.g., SAP2000; ETABS; or STAAD, Research Engineers International, 2002) using a model in which the bearings are modeled as pins or as a combinations of pins and rollers. Care should be exercised in modeling the isolators so that the horizontal component of reactions does not incorrectly affect the balance of moments. For example, in cases in which all isolators are at the same level (as in the case illustrated in Figure 3-5), the bearings can be arbitrarily represented as pins or rollers since the resultant horizontal reaction is always the same. However, in the case of split level isolation system, the horizontal reaction distribution to the various levels needs to be properly considered. This will become apparent in one of the two examples in this manual.

The unit horizontal load is applied at the i^{th} degree of freedom and the reactions at isolator locations constitute the i^{th} column of the matrix $[T]$.

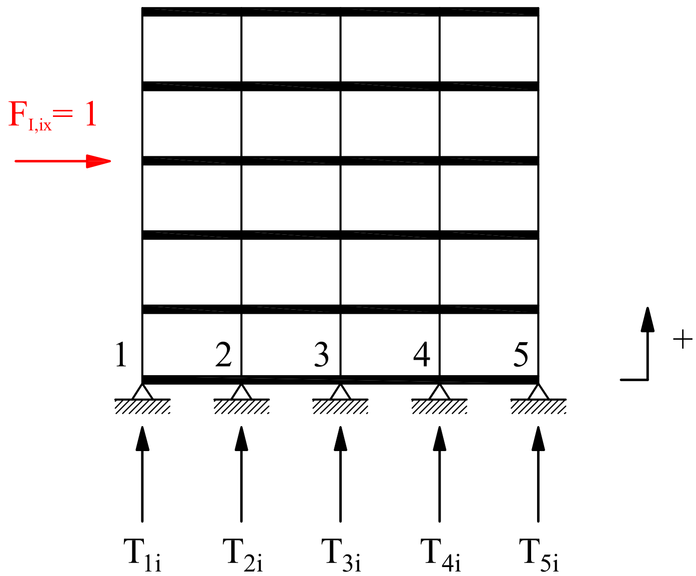

Figure 3-5: Schematic of model used to calculate matrix $[T]$.

The full matrix is shown below. It should be noted that matrix $[T]$ is a rectangular matrix with dimensions n by $3\times(nf+nb)$ (n = total number of isolators, nf = number of floors above the bases, and nb = number of bases). The matrix coefficient T_{ij} can be interpreted as the reaction at isolator location i for unit horizontal load (positive in the positive horizontal direction) applied at the location of the j dynamic degree of freedom. Positive forces at the isolators are considered when pointing upwards (see schematic above).

$$[T]=\begin{bmatrix} T_{11} & T_{12} & T_{13} & .. & T_{1i} & .. & .. & .. & T_{1,3(nf+nb)} \\ T_{21} & T_{22} & T_{23} & .. & T_{2i} & .. & .. & .. & T_{2,3(nf+nb)} \\ T_{31} & T_{32} & T_{33} & .. & T_{3i} & .. & .. & .. & T_{3,3(nf+nb)} \\ .. & .. & .. & .. & .. & .. & .. & .. & .. \\ T_{n1} & T_{n2} & T_{n3} & .. & T_{ni} & .. & .. & .. & T_{n,3(nf+nb)} \end{bmatrix}. \tag{3-11}$$

3.4.2 Case of Isolator Uplift

When isolator uplift occurs, the redistribution of the axial forces on the isolators, which are not uplifting, is accomplished using the coefficient matrix $[A]$, which is supplied by the user.

The coefficient matrix, $[A]$, is evaluated externally by other computer programs (e.g., SAP2000, ETABS or STAAD) and imported into program 3D-BASIS-ME-MB. It is calculated by linear static analyses of the structure loaded with unit vertical loads at the location of an isolator (which is removed for the analysis). The calculated reactions at each location of the remaining isolators constitute the coefficients of a column of matrix $[A]$. The non-uplifting isolators must be modeled as pins or rollers using the same concepts as for the case of construction of the $[T]$ matrix. However, in this case the errors introduced by incorrect distribution of horizontal reactions in split level isolation systems are less important and all isolators could be modeled as pins for simplicity. The analysis needs to be repeated for each isolator. For example, the i^{th} column of matrix $[A]$ is calculated as shown in the schematic below:

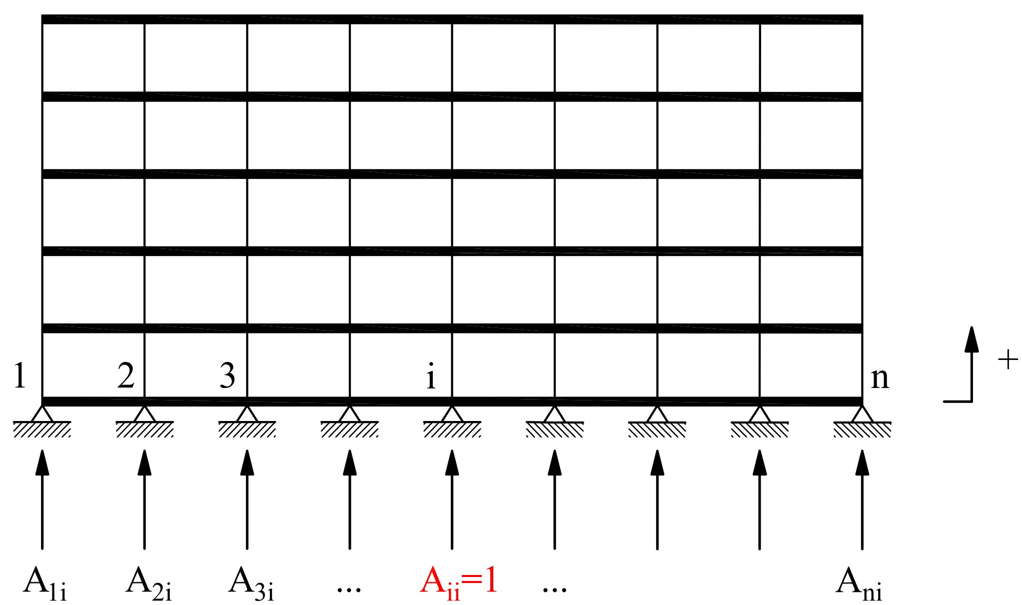

Figure 3-6: Schematic of model used to calculate matrix $[A]$.

The full matrix $[A]$ is presented in (3-12). It should be noted that matrix $[A]$ is square, with a unit diagonal, non-symmetric matrix with dimensions n by n (n = total number of isolators). The matrix coefficient A_{ij} can be interpreted as the reaction at isolator location i for unit vertical load applied at the isolator location j (where isolator j has been removed).

$$[A]=\begin{bmatrix} 1 & A_{12} & A_{13} & .. & A_{1i} & .. & A_{1n} \\ A_{21} & 1 & A_{23} & .. & A_{2i} & .. & A_{2n} \\ A_{31} & A_{32} & 1 & .. & A_{3i} & .. & A_{3n} \\ .. & .. & .. & .. & .. & .. & .. \\ A_{i1} & A_{i2} & A_{i3} & .. & 1 & .. & A_{in} \\ .. & .. & .. & .. & .. & .. & .. \\ A_{n1} & A_{n2} & A_{n3} & .. & A_{ni} & .. & A_{nn} \end{bmatrix} \tag{3-12}$$

The axial loads on the isolators when *a* number of them uplift (*a* = number of isolators which uplift) is given by equation (3-13).

$$\begin{Bmatrix} 0 \\ N_{uplf}^{b} \end{Bmatrix} = \begin{Bmatrix} N_{OM}^{a} \\ N_{OM}^{b} \end{Bmatrix} + \begin{bmatrix} A^{aa} & A^{ab} \\ A^{ba} & A^{bb} \end{bmatrix} \begin{Bmatrix} X^{a} \\ 0 \end{Bmatrix} \tag{3-13}$$

where, N_{uplf}^{b} contains the axial loads on the isolators which do not uplift, $\{N_{OM}\}=\begin{bmatrix} N_{OM}^{a} & N_{OM}^{b} \end{bmatrix}^{T}$ is the vector containing the normal loads on the bearings as calculated by equation (3-10) rearranged in such a way that the terms corresponding to isolators that uplift are located in the first a positions of the vector, matrix $[A]$ is the coefficient matrix obtained as described above rearranged in such a way that the columns and rows corresponding to isolators that uplift and those that do not uplift, and $\{X^{a}\}$ is a vector, which is evaluated by solving the system of linear algebraic equations in equation (3-14).

$$\{-N_{OM}^{a}\}=[A^{aa}]\{X^{a}\} \tag{3-14}$$

3.4.3 User Supplied Information

In the case where it is desired to account for overturning moment effects, the user needs to provide the following information in program 3D-BASIS-ME-MB:

- For the uplift-restraining XY-FP isolators (C.7.8 in Section 5): matrix $[T]$

supplied in file TMATRIX.DAT.

- For flat sliding and FPS isolators (C.7.5 and C.7.8 in Section 5): matrix $[T]$ supplied in file TMATRIX.DAT and matrix $[A]$ supplied in file TMATRIXUPLF.DAT.

All other calculations are internally done in the program.

It should be noted that when the user supplies a zero matrix [T] and a unit matrix [A], the result is constant axial load on all bearings due to overturning moment effects.

SECTION 4
VERIFICATION EXAMPLES

4.1 Introduction

Two examples are used in the verification of program 3D-BASIS-ME-MB. In both cases the analyzed structure is seismically isolated with Friction Pendulum bearings and is excited under conditions of bearing uplift. This represents the most extreme condition that bearings are subjected to and is a case of much interest in verifying the capabilities of analysis software. It may be mentioned in passing that the verification examples include a great deal of information on how to use the program and provide further clarifications on practical topics that are inherently difficult to explain in the abstract.

The first example is a 7-story model structure that was tested on the shake table at the University at Buffalo (Al-Hussaini et al, 1994). This example is of much interest since it was studied in verification examples of program SAP2000 (Scheller and Constantinou, 1999; and Computers and Structures, 2003). Results of analysis by program 3D-BASIS-ME-MB and by program ABAQUS (ABAQUS, 2004) are compared to experimental results.

The second example is a two-tower multi-story structure with a split seismic-isolation-system level. The isolation system again consists of Friction Pendulum bearings and the structure is excited under conditions of bearing uplift. Results of analysis by program 3D-BASIS-ME-MB are compared to results produced by program ABAQUS.

4.2 Verification Example 1: Seven-Story Isolated Model

Figure 4-1 illustrates the 7-story model of this verification study. It was tested by Al-Hussaini et al (1994). Additional information on this model may be found in Scheller and Constantinou (1999), where experimental results in electronic format are available, and in Computers and Structures (2004).

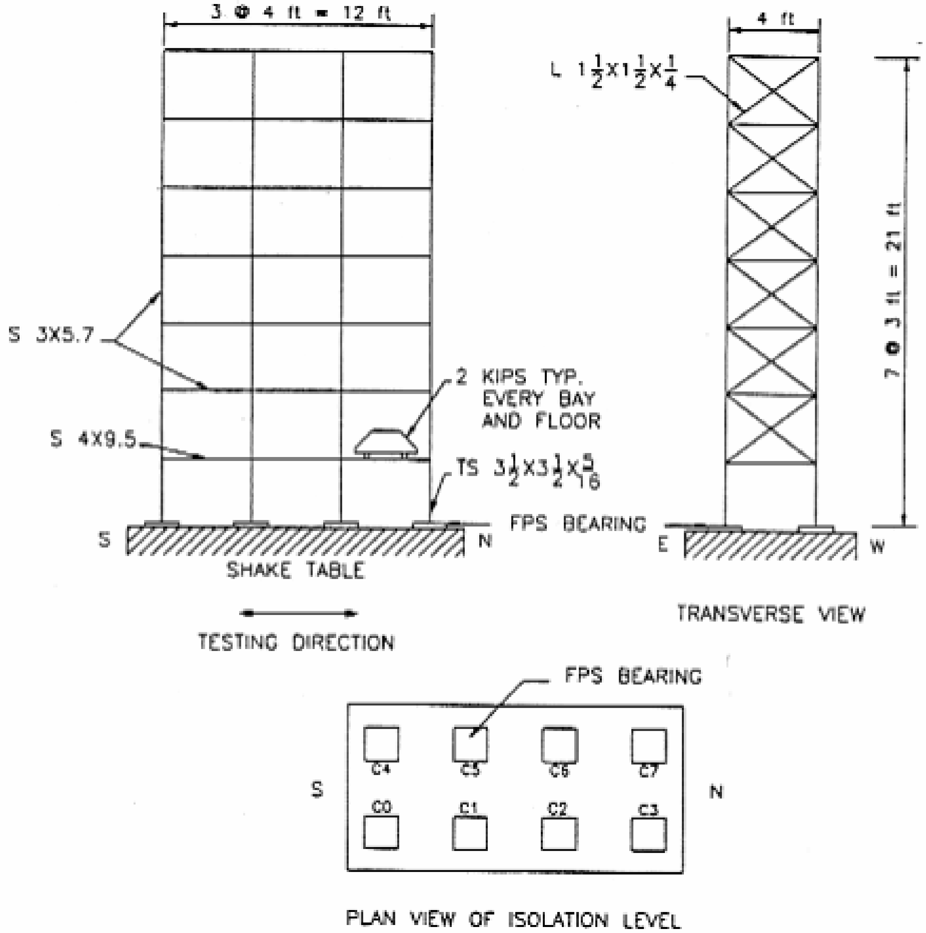

Figure 4-1: Schematic of 7-story model tested on shake table (Al Hussaini et al, 1994).

The isolation system of this model structure consisted of eight Friction Pendulum bearings with radius of curvature equal to 9.75 in. and coefficient of friction in high-velocity motion equal to 0.06. Total weight on the eight bearings was 47.5 kip. In one test in configuration MFUIS with El Centro motion, component S00E, scaled to peak acceleration of 0.58g, the model experienced uplift. This case is modeled in programs 3D-BASIS-ME-MB and ABAQUS and compared to experimental results.

The input file in program 3D-BASIS-ME-MB is presented in Appendix B. Moreover, Appendix C describes the construction of matrices [T] and [A].

The Friction Pendulum bearings were modeled in program ABAQUS by modeling coincident nodes at the position of each isolator. One node was defined as part of the superstructure, whilst the other was used in the definition of the substructure or foundations. The bearing was then modeled using a contact feature known as an analytical rigid surface that creates master/slave sliding contact between the coincident nodes, as shown in Figure 4-2. This feature allowed each component of the bearing to be explicitly modeled. One node was selected as the master and the concave sliding surface of the bearing was created at this node by defining an axis of revolution that sets up a local coordinate cylindrical coordinate system, in (r,z) space. The sliding surface was then created by defining the coordinates of three points in this local coordinate system, one at the center of curvature of the sliding surface, one on the axis of revolution, at the surface of the bearing and one at an arbitrary point on the sliding surface, at or beyond the displacement capacity of the bearing. The convex slider was defined simply as the slave node. The articulation of the slider in the housing plate socket, in effect a pinned connection was defined implicitly, since the analytical surface feature activates only translational degrees of freedom at nodes connected to it. The concave sliding surface is a smooth, continuous surface, which is important for contact since it avoids the inherent discontinuities that arise when using a surface defined with discrete facets and was modeled with a radius of 9.75 inch. The interaction between the slider and sliding surface was defined using the same friction model described in Al-Hussaini et al (1994) and Scheller and Constantinou (1999) for this structure.

Note that the representation of the slider shown in Figure 4-2 makes no contribution to the physical response of the bearing model and is purely for visualization. By default separation of the coincident nodes and hence bearing uplift is allowed. However, additional features can be employed to allow transmittal of tension forces normal to the bearing, as well as limit the bearing displacement, e.g. due to the presence of the retaining ring on the concave surface, as required. This modeling technique could be readily adapted to model the XY-FP isolator described in Section 3.2 of this report. Further details on the modeling of structures isolated with Friction Pendulum bearings in ABAQUS may be found in Clarke et al. (2005).

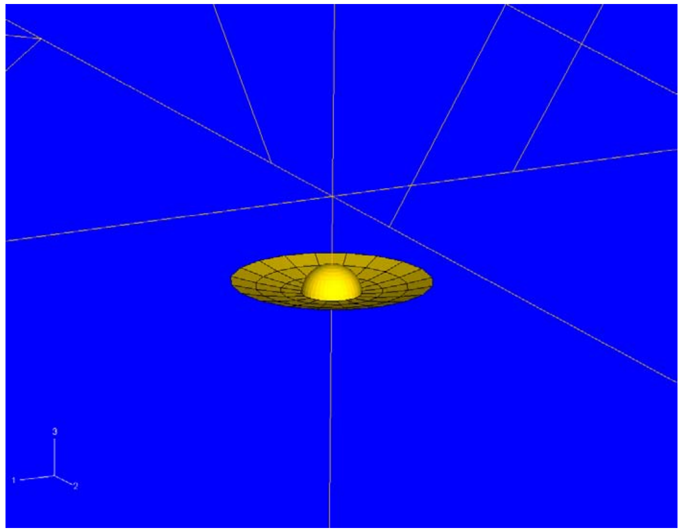

Figure 4-2: View of Friction Pendulum bearing modeled in ABAQUS.

Results of program 3D-BASIS-ME-MB plotted against experimental results are presented in Appendix D and results of program ABAQUS plotted against experimental results are presented in Appendix E.

It may be observed in the results of Appendix D that program 3D-BASIS-ME-MB predicts very well the experimental response, with the exception of the hysteretic loops for the interior bearing. However, in this case the gravity load on the bearings was not measured and it was assumed to be the one based on tributary area distribution, thus leading to differences in the calculated and measured shear forces and displacements in the bearing. Assumption of different gravity load distribution leads to different calculated response that is closer to the experimental response.

The response calculated by program ABAQUS also compares very well with the experimental response. However, it may be noted that certain predictions of program 3D-BASIS-ME-MB are slightly better than those of program ABAQUS (i.e., shear force in uplifted bearings and drift). This may be attributed to the fact that the model of the superstructure in program 3D-BASIS-ME-MB was adjusted to better fit the experimentally identified modal properties of the model.

4.3 Verification Example 2: Two-Tower, Split-Level Isolated Structure

The second example concerns a two-tower multi-story structure with a split seismic-isolation-system level. The model geometry is illustrated in the schematic of Figure 4-3. The isolation system consists of Friction Pendulum bearings with radius of curvature equal to 169 in. and coefficient of friction in high-velocity motion equal to 0.07. The frictional model used along with the associated isolator properties are depicted in Figure 4-4. Appendix F presents schematics that describe the two-tower verification model in terms of section properties, model masses, and weight on bearings.

The first two modes of the structure (with isolators represented as pins) were assumed to have damping ratio equal to 2% of critical. Damping in the remaining modes was represented by the Rayleigh approach.

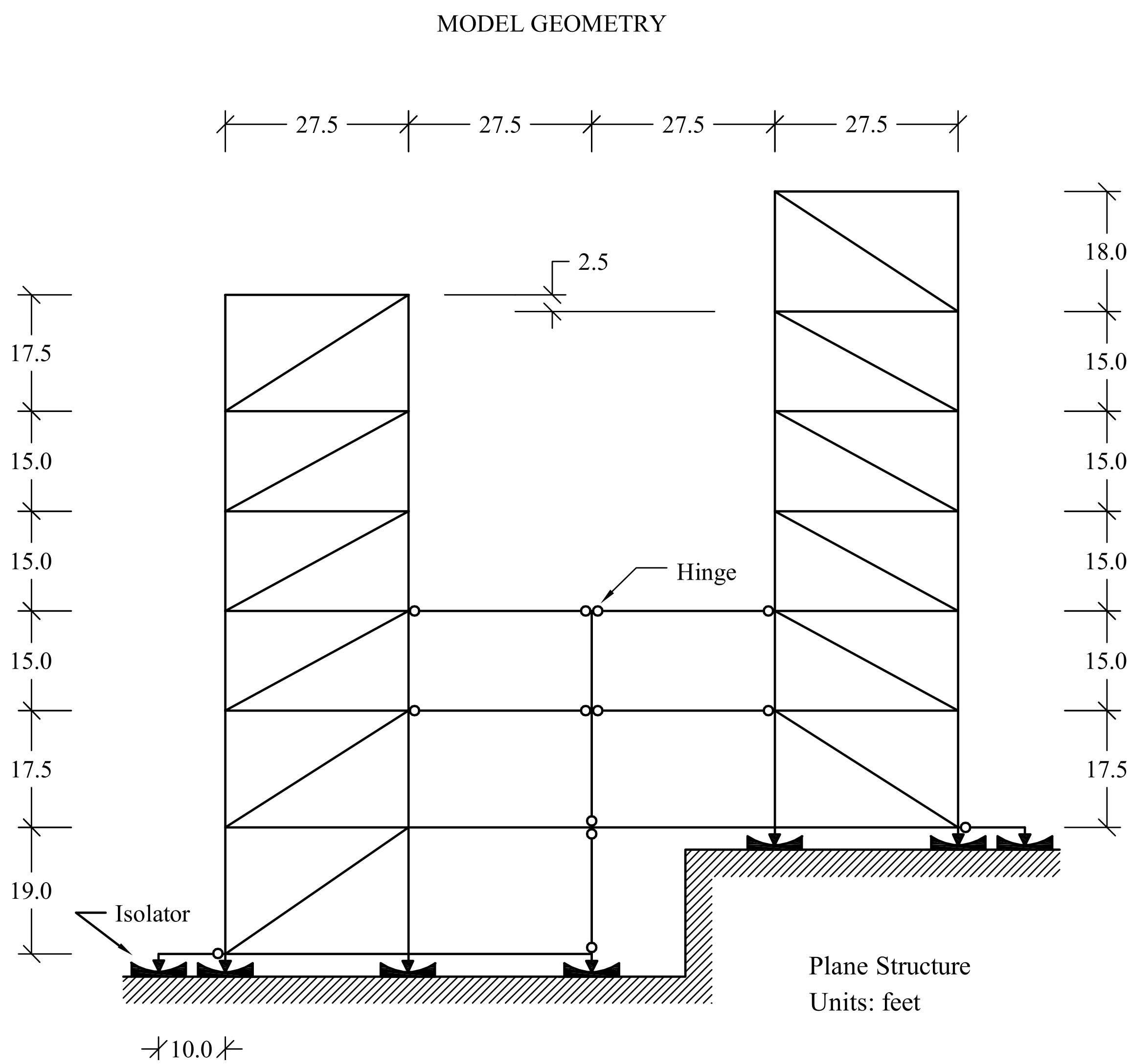

Figure 4-3: Schematic of two-tower, split-level isolated structure.

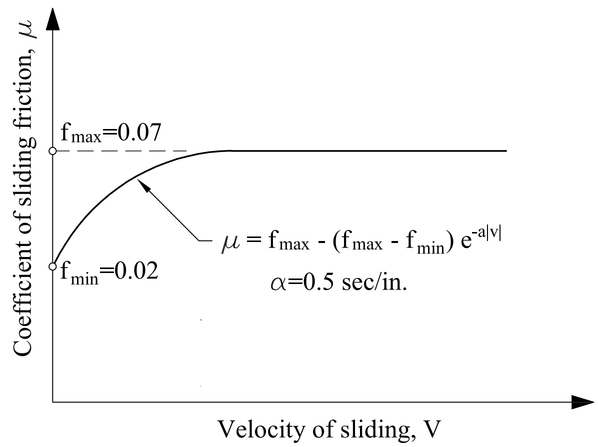

Figure 4-4: Frictional model used for FP isolators of two-tower structure.

The seismic excitation consists of the horizontal component acceleration history shown in Figure 4-5. Appendix G presents the input file in program 3D-BASIS-ME-MB and Appendix H describes the construction of matrices $[T]$ and $[A]$. Appendix I describes the analysis that resulted in the information on stiffness, etc. for input to program 3D-BASIS-ME-MB to describe the superstructure. Appendix J presents a comparison of results obtained with programs 3D-BASIS-ME-MB and ABAQUS. These results are for the case in which the coefficient of friction f_{max}=0.07 as presented in the description of the model in Appendix F.

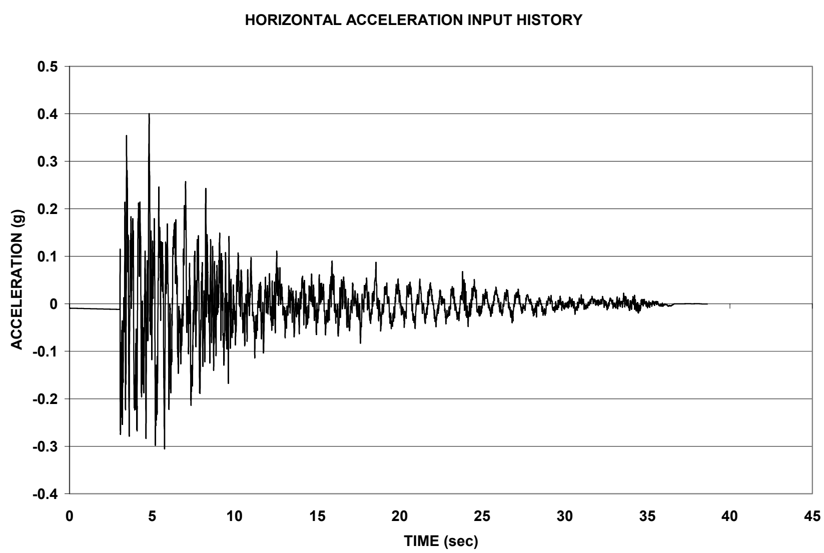

Figure 4-5: Horizontal ground acceleration history in two-tower model.

In comparing the results obtained by programs ABAQUS and 3D-BASIS-ME-MB, it is important to note that the analyzed structure experiences considerable bearing uplift. As an example, Figure 4-6 presents the uplift displacement history calculated in ABAQUS for isolator No. 2 (similar behavior was calculated for bearing 3 and to a lesser extent for bearings 5 and 6-those directly below the two towers). The maximum uplift displacement is about 0.45 inch and the duration of each uplift episode is about 0.5 second. That is, the analyzed structure is in a state of rocking mode, which can be accurately captured only in an analysis in which geometric nonlinearities are accounted for. Nevertheless, the results obtained by program 3D-BASIS-ME-MB, which does not have geometric nonlinearity capabilities, favorably compare to those obtained by program ABAQUS.

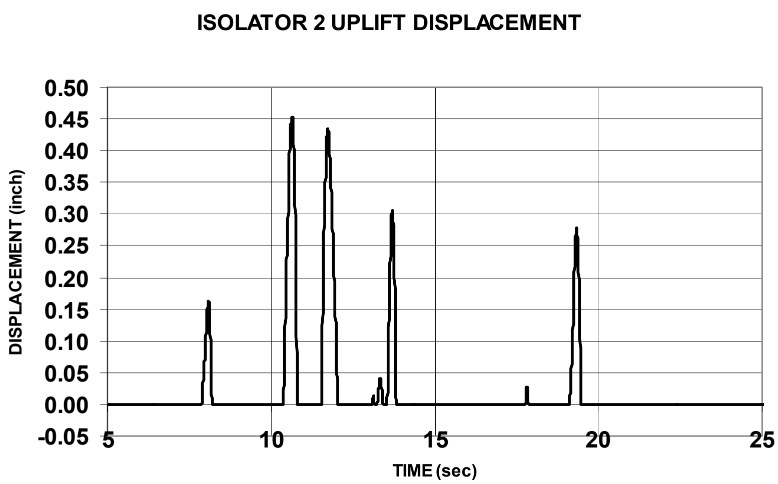

Figure 4-6: Uplift displacement history of isolator 2 as predicted in ABAQUS.

The following observations may be made in the comparison of results in Appendix J:

1. The bearing displacement histories appear different in the predictions of the two programs. The differences are attributed to the tendency of program ABAQUS to predict more permanent displacement. A likely explanation for this behavior are small differences in modeling the velocity dependence of the coefficient of friction in the two programs and differences in modeling frictional behavior (viscoplasticity-based model in 3D-BASIS-ME-MB and direct friction model in ABAQUS). While these differences in modeling are typically insignificant in high velocity motions, they are important in low velocity motions as those in this example. The bearing displacement

history compared more favorably when the input excitation was scaled up so that the predicted displacements increased substantially (however, the uplift displacements also increased to unrealistic levels).

2. Force-displacement loops of individual bearings and of the isolation system at the two levels compare well in the predictions of the two programs. Particularly interesting are the loops for isolators No.2 and 3, which indicate that the two bearings experience much more uplift than any of the other bearings. Nevertheless, the predictions of program 3D-BASIS-ME-MB favorably compares to those of the much more sophisticated program ABAQUS.

3. The drift history predicted by 3D-BASIS-ME-MB for the bottom story of the 4-story tower on the right compare very well with those of ABAQUS. However, the comparison is not as good for the drift history predicted for the bottom story of the 3-story tower on the left. This is the result of the significant uplift experienced by isolators No. 2 and 3 and the resulting rocking of the left tower. The results on drift presented for ABAQUS include the rigid body rocking effect, whereas those of 3D-BASIS-ME-MB do not. The rigid body contribution to drift (difference in displacement between top and bottom of story) is as much as 0.45x15/27.5=0.25 inch, where 0.45 inch is the maximum uplift displacement, 15 feet is the story height and 27.5 feet is the span between the uplifting bearings.

4. The predictions of the two programs for the top floor accelerations of the two towers compare well, although program 3D-BASIS-ME-MB predicts more acceleration than program ABAQUS. This appears as a paradox given that program 3D-BASIS-ME-MB does not account for the additional acceleration due to the rigid body, rocking motion effect when uplift occurs. However, program ABAQUS with its geometric nonlinearity capabilities captures the effects of rocking on reducing the inertia effects due to lengthening of the period of oscillations, resulting in a canceling of the effects.

5. Predictions of brace forces in the two programs compare well, although program 3D-BASIS-ME-MB appears to over-predict the force. There are two reasons contributing to this difference. First, program 3D-BASIS-ME-MB does not account for period lengthening and thus reduction of inertia effects as the towers undergo rocking.

Second, and likely the major contributor to the difference, is that the brace force was not directly calculated in 3D-BASIS-ME-MB but rather extracted from the history of story shear as follows (in a separate analysis following analysis in 3D-BASIS-ME-MB): the contribution to the story shear from column deformation was subtracted (assuming shear type behavior) and the remaining force was resolved along the brace axis assuming truss behavior.

Additional results for the two-tower example are presented in Appendix K where all parameters of the analyzed model are the same except that the friction coefficient f_{max} is 0.04 rather than 0.07. This situation results in larger bearing displacements and in reduction of the duration and amplitude of uplift displacements (reduced to a peak of about 0.3 inch and of duration of about 0.3 second for each uplift episode). The results of analysis by the two programs presented in Appendix K compare more favorably than those of Appendix J. Apparently, the amount and duration of bearing uplift episodes is important in the accurate prediction of response by program 3D-BASIS-ME-MB. This statement is further collaborated by the excellent comparison of results predicted by the two programs in the case of the tested 7-story model, a case in which the duration and amount of uplift were very small.

SECTION 5

USER’S GUIDE TO PROGRAM 3D-BASIS-ME-MB

A.1 INPUT FORMAT FOR 3D-BASIS-ME-MB

The program 3D-BASIS-ME-MB requires the input file with name 3DBMEMB.DAT and the earthquake excitation file names WAVEX.DAT, WAVEY.DAT and WAVEZ.DAT. The main output file is 3DBMEMB.OUT.

The program produces other output files: (i) output files for each isolated base named [ISOLBASE_No 1.OUT] containing time histories of the accelerations and displacements of the base at the C.M. of the base; (ii) output files for each superstructure/building named [1001], [1002], etc., containing time histories of the accelerations and displacements of each floor at the C.M. of the floor; (iii) output file named [BASE] containing time histories of isolators (forces, displacement, etc.), shear forces of the bases and structural shears above the top (first) base.

In the program dynamic arrays are used; also, double precision is used for accuracy. Common block size has been set to 100,000 and should be changed if the need arises. A free format is used to read all input data. Hence, conventional delimiters (commas, blanks) may be used to separate data items. Standard FORTRAN variable format is used to distinguish integers and floating-point numbers. Therefore, input data must conform to the specified variable type. All values are to be input unless mentioned otherwise. No blank lines are to be specified.

■ Note:

1. Provision is made for a line of user defined descriptive text between each set of data items (refer to variable USER_TXT in sections A.2 to A.9 and to the example data files accompanying this.

   In addition, comment lines could be used in the data file directly following the user-defined text lines (variable USER_TXT). Comment lines must begin with “:”. The following is an example of the syntax of the aforementioned variables:

   GENERAL CONTROL INFORMATION....(section header; variable USER_TXT)

   : option story eigenv isol .....………………..(comment line)

   1 6 6 22 ..………………………..(data line)

2. Equations of motion are written at the reference frame located at the C.M. of the top base for each floor of every superstructure and for the bases the equations of motion are written with respect to the C.M. of each base.

3. Figure 5-1 presents the sketch of the model of multiple structures on several bases.

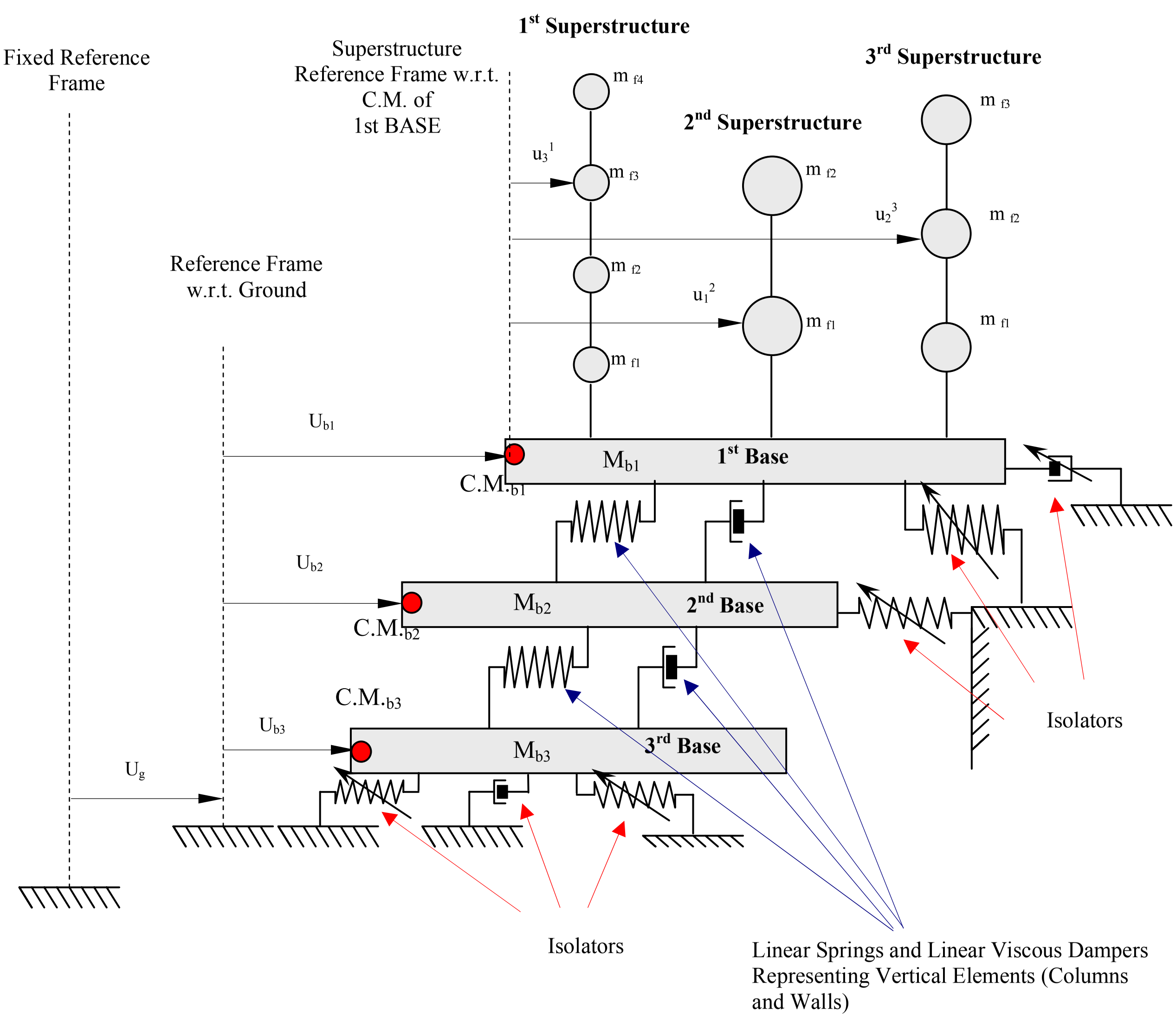

Figure 5-1: Reference frames and degrees of freedom in 3D-BASIS-ME-MB.

A.2 PROBLEM TITLE

One card

TITLE TITLE up to 80 characters

A.3 UNITS

One card

LENGTH, **MASS**, **RTIME**

LENGTH	=	Basic unit of length up to 20 characters
MASS	=	Basic unit of mass up to 20 characters
RTIME	=	Basic unit of time up to 20 characters

A.4 CONTROL PARAMETERS

A.4.1 Control Parameters: Entire structure

USER_TXT Reference information; up to 80 characters of text.

One card

ISEV, **NB**, **NBSLBS**, **NP**, **INP**, **ITMAT, ITRDAL**, **G**

ISEV = Index for superstructure stiffness input

ISEV = 1 for option 1 - Data for stiffness of the superstructures to be input.

ISEV = 2 for option 2 - Eigenvalues and eigenvectors of the superstructures (for fixed base condition) to be input.

NBSLBS = Number of “isolated” bases of the substructure

NB = Number of superstructures on the top base (first base).

NP = Number of isolation bearings.

INP = Number of bearings at which output is desired.

ITMAT = Index to account for variations of axial loads on isolators due to overturning moment effects.

ITMAT = 1 - For neglecting variation of axial bearing loads due to overturning moment effects.

ITMAT = 2 - For variation of the isolators normal loads to be accounted for using externally supplied Normal Load Distribution Matrices. Data is supplied in the files TMATRIX.DAT and TMATRIXUPLF.DAT. See Section H.

ITRDAL = Index to account for type of iterations in the isolator axial load redistribution scheme (relevant only for ITMAT=2)

ITRDAL = 1 - Iteration and redistribution until convergence.

ITRDAL = 2 - Two-Step Iteration that is fast and only slightly in error.

G = Gravitational acceleration.

■ **Note:**

1. Number of bearings is the total number of isolators under all bases.
2. If ITMAT =1 then the value of ITRDAL index does not affect the execution of the program.

A.4.2 Control Parameters: Superstructures

USER_TXT Reference information; up to 80 characters of text.
NB cards

NF(I), NE(I), I	=	1 ,NB
NF(I)	=	Number of floors of superstructure "I" excluding bases. (If NF<l then NF set = 1)
NE(I)	=	Number of eigenvalues of superstructure "I" to be retained in the analysis. (If NE<3then NE set = 3)

■ **Note:**

1. Number of eigenvectors to be retained in an analysis should be in groups of three (3); the minimum being one set of three modes.

A.4.3 Control Parameters: Integration

USER_TXT Reference information; up to 80 characters of text.
one card
TSI, **TOL**, **FMNORM**, **MAXMI**, **KVSTEP**

TSI	=	Time step of integration. Default = TSR (refer to A.4.5)
TOL	=	Tolerance for the nonlinear force vector computation. Recommended value = 0.001.
FMNORM	=	Reference moment for convergence.
MAXMI	=	Maximum number of iterations within a time step.
KVSTEP	=	Index for time step variation.
KVSTEP	=	1 for constant time step.
KVSTEP	=	2 for variable time step.

■ **Note:**

1. The time step of integration cannot exceed the time step of earthquake record.
2. If MAXMI is exceeded the program is terminated with an error message.
3. Compute an estimate of FMNORM by multiplying the expected base shear by one half of the maximum base dimension.

A.4.4 Control Parameters: Newmark's Method

USER_TXT Reference information; up to 80 characters of text.
One card
GAM, **BET**

GAM	=	Parameter which produces numerical damping within a time step. (Recommended value = 0.5)
BET	=	Parameter which controls the variation of acceleration within a time step. (Recommended value = 0.25)

A.4.5 Control Parameters: Earthquake Input

USER_TXT Reference information; up to 80 characters of text.
One card
INDGACC, **TSR**, **LOR**, **XTH**, **ULF**

INDGACC	=	Index for earthquake time history record.
INDGACC	=	1 for a single earthquake record at an angle of incidence XTH.
INDGACC	=	2 for two independent earthquake records along the X and Y Axes.
INDGACC	=	3 for two independent earthquake records along the X and Z (vertical) axes. (X axis excitation at angle of incidence XTH)
INDGACC	=	4 for three independent earthquake records along X, Y and Z (vertical) axes.
TSR	=	Time step of earthquake record(s).
LOR	=	Length of earthquake record(s). (number of data in earthquake record)
XTH	=	Angle of incidence of the earthquake with respect to the X-axis in anticlockwise direction (only for option INDGACC=l). The unit for angle is degrees.
ULF	=	Load factor (multiplies earthquake records for scaling to the desired units and amplitude).

■ Note:

1. Four options are available for the earthquake record input:

   INDGACC = 1 refers to a single earthquake record input at any angle of incidence XTH. Input only one earthquake record (read through a single file WAVEX.DAT). Refer to F.2 for wave input information.

   INDGACC = 2 refers to two independent earthquake records input in the X and Y directions, e.g. El Centro N-S along the X direction and El Centro E-W along the Y direction. Input two independent earthquake records in the X and Y directions (read through two files WAVEX.DAT and WAVEY.DAT). Refer to F.2 and F.3 for wave input information.

INDGACC = 3 refers to two independent earthquake records input in the X and Z directions, e.g. El Centro N-S along the X direction and El Centro Vertical along the Z direction. Input two independent earthquake records in the X and Z directions (read through two files WAVEX.DAT and WAVEZ.DAT). Refer to F.2 and F.4 for wave input information.

INDGACC = 4 refers to three independent earthquake records input in the X, Y and Z directions, e.g. El Centro N-S along the X direction and El Centro E- W along the Y direction and El Centro vertical along the Z direction. Input three independent earthquake records in the X, Y and Z directions (read through three files WAVEX.DAT, WAVEY.DAT and WAVEZ.DAT). Refer to F.2 to F.4 for wave input information.

2. The time step of earthquake record and the length of earthquake record has to be the same in X, Y and Z directions for INDGACC = 2 or 3 or 4.
3. Specification of angle for cases INDGACC 2, 3 and 4 other than zero is disregarded. No rotation of motions is performed.
4. Load factor is applied to the earthquake records in the X, Y and Z directions.

B.1 SUPERSTRUCTURE DATA

USER_TXT Reference information; up to 80 characters of text.

Go to B.2 for **option 1** – three-dimensional shear-building representation of superstructure.

Go to B.3 for **option 2** - full three-dimensional representation of the superstructure. Eigenvalue analysis has to be done prior to 3D-BASIS-ME-MB analysis using another computer program, e.g., ETABS.

■ **Note:**

1. The same type of group, B2 or B3, must be given for all superstructures (the same option, either 1 or 2, must be used for all superstructures).
2. The data must be supplied in the following sequence:

   B2 or B3, B4, B5, B6 and B7 for superstructure No.1, then repeat for superstructure No.2, etc. for a total of NB superstructures.

B.2 SHEAR STIFFNESS DATA FOR THREE-DIMENSIONAL SHEAR BUILDING (ISEV=1)

USER_TXT Reference information; up to 80 characters of text.

B.2.1 Shear Stiffness: X-Direction (Input only if ISEV=1)

USER_TXT Reference information; up to 80 characters of text.
NF cards
SX(I), **I=1**,**NF**

SX(I) = Shear stiffness of story **I** in the **X** direction.

■ **Note:**

1. Shear stiffness of each story in the X direction starting from the top story and progressing to the first story. One card is used for each story.

B.2.2 Shear Stiffness: Y-Direction (Input only if ISEV=1)

USER_TXT Reference information; up to 80 characters of text.
NF cards
SY(I), **I=1**,**NF**

SY(I) = Shear stiffness of story I in the Y direction.

■ **Note:**

1. Shear stiffness of each story in the Y direction starting from the top story and progressing to the first story.

B.2.3 Torsional Stiffness in θ-Direction (Input only if ISEV=1)

USER_TXT Reference information; up to 80 characters of text.
NF cards
ST(I), **I=1**,**NF**

ST(I) = Torsional stiffness of story I in the θ direction *about the Center of Mass of the* floor .

■ **Note:**

1. Torsional stiffness of each story starting from the top story and progressing to the first story.

B.2.4 Eccentricity Data: X-Direction (Input only if ISEV=1)

USER_TXT Reference information; up to 80 characters of text.
NF cards
EX(I), **I=I**,**NF**

EX(I) = Distance of Center of Resistance from the Center of Mass of floor I. Default = 0.0001.

B.2.5 Eccentricity Data: Y-Direction (Input only if ISEV=1)

USER_TXT Reference information; up to 80 characters of text.
NF cards
EY(I), I=I,NF

EY(I) = Distance of Center of Resistance from the Center of Mass of floor I. Default = 0.0001.

■ **Note:**

1. The case of zero eccentricity in both the X and Y directions cannot be solved correctly by the eigen-solver in the program; hence if both the eccentricities are zero, a default value of 0.0001 is used.

B.3 EIGENVALUES AND EIGENVECTORS FOR FULLY THREE DIMENSIONAL BUILDING (ISEV=2)

USER_TXT Reference information; up to 80 characters of text.

B.3.1 Eigenvalues (Input only if ISEV=2)

USER_TXT Reference information; up to 80 characters of text.
NE cards
W(I), I=I,NE

W(I) = Eigenvalue of I^{th} mode.

■ **Note:**

1. Input starting from the first mode and progressing to the NE mode.
2. Eigenvalues are frequencies squared (ω^2 in units of rad^2/s^2)

B.3.2 Eigenvectors (Input only if ISEV=2)

USER_TXT Reference information; up to 80 characters of text.
NE cards
(E(K,J), K=1,3*NF), J=1,NE

E(K,J) = Value corresponding to K^{th} floor of eigenvector of J^{th} mode.

■ **Note:**

1. Input starting from the first mode and progressing to the NE mode.
2. Eigenvectors must be normalized with respect to the mass matrix of superstructure ($\Phi^T M \Phi = \{1\}$).

B.4 SUPERSTRUCTURE MASS DATA

B.4.1 Translational Mass

USER_TXT Reference information; up to 80 characters of text.
NF Cards
CMX(I), I=I,NF

CMX(I) = Translational mass at floor I.

■ **Note:**

1. Input starting from the top floor and progressing to the first floor.

B.4.2 Rotational Mass (Mass Moment of Inertia)

USER_TXT Reference information; up to 80 characters of text.
NF Cards
CMT(I), I=I,NF

CMT(I) = Mass moment of inertia of floor I about the center of mass of the floor .

■ **Note:**

1. Input starting from the top floor and progressing to the first floor.

B.5 SUPERSTRUCTURE DAMPING DATA

USER_TXT Reference information; up to 80 characters of text.
NE Cards
DR(I), I=l,NE

DR(I) = Damping ratio corresponding to mode I.

■ **Note:**

1. Input starting from the first mode and progressing to the NE mode.

B.6 DISTANCE TO THE CENTER OF MASS OF THE FLOOR

USER_TXT Reference information; up to 80 characters of text.
NF cards
XN(I), YN(I), I=1,NF

XN(I) = Distance of the Center of Mass of the floor I from the Center of Mass of the top (first) base in the X direction.

YN(I) = Distance of the Center of Mass of the floor I from the Center of Mass of the top (first) base in the Y direction. (If ISEV=1 then XN(I) and YN(I) set 0)

■ **Note:**

1. Input starting from the top floor and progressing to the first floor.

B.7 HEIGHT OF THE FLOORS FROM THE GROUND

USER_TXT Reference information; up to 80 characters of text.
NF cards
H(I), **I=1**,**NF**

H(I) = Height of the floor I from the ground.

■ **Note:**

1. Input starting from the top floor and progressing to lower floor.

C.1 ISOLATION SYSTEM DATA

USER_TXT Reference information; up to 80 characters of text.

C.2 HEIGHT OF THE ISOLATED BASES/SLABS FROM THE GROUND

USER_TXT Reference information; up to 80 characters of text.
NBSLBS cards
HSLABS(I), **I=1**,**NBSLBS**

HSLABS(I) = Height of base I from the ground.

■ **Note:**

1. Input starting from the top (first) base and progessing to the bottom NBSLBSst base.

C.3 STIFFNESS DATA FOR VERTICAL ELEMENTS CONNECTING TWO BASES

USER_TXT Reference information; up to 80 characters of text.
NBSLBS cards
SXE(I), **SYE(I)**, **STE(I)**,
EXETOP(I), **EYETOP(I)**, **EXEBOT(I)**, **EYEBOT(I)**, **I=1**,**NBSLBS**

SXE(I) = Resultant stiffness of vertical elements (exclusive of isolators) connecting base I to base (I+1) in the X direction.

SYE(I) = Resultant stiffness of vertical elements (exclusive of isolators) connecting base I to base (I+1) in the Y direction.

STE(I) = Resultant of Torsional stiffness of vertical elements (exclusive of isolators) connecting base I to base (I+1) in the vertical direction *about the Center of Resistance* of the vertical elements connecting base I to base I+1.

EXETOP(I) = Distance of the Center of Stiffness of the vertical elements connecting base I to base I+1 from the Center of Mass of base I in the X-direction.

EYETOP(I) = Distance of the Center of Stiffness of the vertical elements connecting base I to base I+1 from the Center of Mass of base I in the Y-direction.

EXEBOT(I) = Distance of the Center of Stiffness of the vertical elements connecting base I to the base I+1 from the Center of Mass of base I+1 in the X-direction.

EYEBOT(I) = Distance of the Center of Stiffness of the vertical elements connecting base I to the base I+1 from the Center of Mass of base I+1 in the Y-direction.

C.4 MASS DATA OF BASES

USER_TXT Reference information; up to 80 characters of text.
NBSLBS cards
CMXB(I), **CMTB(I)**, **I=1**,**NBSLBS**

CMXB = Mass of base in the translational direction.
CMTB = Mass moment of inertia of base about the center of mass of base.

C.5 DAMPING DATA FOR VERTICAL ELEMENTS CONNECTING TWO BASES

USER_TXT Reference information; up to 80 characters of text.
NBSLBS cards
CBX(I), **CBY(I)**, **CBT(I)**,
ECXTOP(I), **ECYTOP(I)**, **ECXBOT(I)**, **ECYBOT(I)**, **I=1**,**NBSLBS**

CBX(I) = Resultant Damping of vertical elements (exclusive of isolators) connecting base I to base I+1 in the X direction.

CBY(I) = Resultant Damping of vertical elements (exclusive of isolators) connecting base I to base I+1 in the Y direction.

CBT(I) = Resultant of Torsional Damping of vertical elements (exclusive of isolators) connecting base I to base I+1 in the vertical direction about the Center of Damping of the vertical elements connecting base I to base I+1.

ECXTOP(I) = Eccentricity of the Center of Damping of vertical elements connecting base I to base I+1 from the Center of Mass of base I in the X-direction.

ECYTOP(I) = Eccentricity of the Center of Damping of vertical elements connecting base I to base I+1 from the Center of Mass of base I in the Y-direction.

ECXBOT(I) = Eccentricity of the Center of Damping of vertical elements connecting base I to base I+1 from the Center of Mass of base I+1 in the X-direction.

ECYBOT(I) = Eccentricity of the Center of Damping of vertical elements connecting base I to base I+1 from the Center of Mass of base I+1 in the Y-direction.

C.6 COORDINATES OF BEARINGS

Coordinates of isolation elements with respect to the Center of Mass of the base its element belongs. One card containing the X and Y coordinates of each isolation element is used. The first card in the sequence corresponds to element No.1, the second to element No.2, etc. up to element No. NP.

USER_TXT Reference information; up to 80 characters of text.
NP Cards
XP(I), **YP(I)**, **I=1**,**NP**

XP(I) = X-Coordinate of isolation element I from the Center of Mass of the isolated base below which is placed.

YP(I) = Y-Coordinate of isolation element I from the Center of Mass of the isolated base below which is placed.

■ **Note:**

1. If NP equals zero then skip Section C.6.

C.7 ISOLATION ELEMENT DATA

USER_TXT Reference information; up to 80 characters of text.

This set of data for the isolation elements consists of two (2) cards for each isolation element.

1. The first card contains three (3) values. The first identifies the base below which the element is located, the second identifies the type of element, and the third specifies its orientation.

2. The second card contains the mechanical properties. The values in the second card vary for each type of isolator.

Two cards are used for isolation element No.1, then another two for element No.2, etc. up to No. NP. The first of the two cards for each element always contains three integer numbers. These numbers are stored in array INELEM(NP,3) which has NP rows and three columns. The card containing these three numbers is identified in the sequel as:

INELEM(K,3), INELEM(K,1), INELEM(K,2),

where K refers to the isolation element number (1 to NP), INELEM(K,3) indicates the location of the isolator, INELEM(K,1) denotes whether the element is uniaxial (unidirectional) or biaxia1 (bi-directional), and INELEM(K,2) denotes the type of element :

INELEM(K,3)	=	Base below which the isolator is located; takes values 1 or 2 or 3….or NBSLBS
INELEM(K,1)	=	1 for uni-axial e1ement in the X direction
	=	2 for uni-axial element in the Y direction
	=	3 for bi-axial element
INELEM(K,2)	=	1 for linear elastic element
	=	2 for linear/nonlinear viscous element
	=	3 for hysteretic element for elastomeric bearings/steel dampers
	=	4 for hysteretic element for flat sliding bearings (friction force and $f_{\max}$ independent of instantaneous value of normal load)
	=	5 for hysteretic element for flat sliding bearings (friction force and $f_{\max}$ depend on instantaneous value of normal load)
	=	6 for FPS bearing element
	=	7 for stiffening hysteretic element
	=	8 for uplift-restraining XY-FP baring element
	=	9 for a general nonlinear viscous element

■ **Note:**

1. Uniaxial element refers to an element in which biaxial interaction between forces in the X and Y directions is neglected. The interaction surface is square. A bi-axial element has circular interaction surface.
2. If NP equals zero then skip Section C.7.

C.7.1 Linear Elastic Element

One card
INELEM(K,3), **INELEM(K, 1)**, **INELEM(K,2)**

INELEM(K,3) = Base below which the isolator is located
INELEM(K,1) = 1 or 2 or 3
INELEM(K,2) = 1 (Refer to C.7 for further details).

One card
PS(K,1), PS(K,2)

PS(K, 1) = Shear stiffness in the X direction for biaxial element or uniaxial element in the X direction (leave blank if the uniaxial element is in the Y direction only).

PS(K,2) = Shear stiffness in the y direction for biaxial element or uniaxial element in the Y direction (leave blank if the uniaxial element is in the X direction only).

■ Note:

1. Biaxial element means elastic stiffness in both X and Y directions (no interaction between forces in X and Y direction).

■ Constitutive Equations:

This element can be used to model the behavior of helical steel springs, rubber springs or other devices that exhibit linear elastic behavior.

The forces generated in each element are

$$F_x = K_x U_x \tag{5-1}$$

$$F_y = K_y U_y \tag{5-2}$$

where K_x, K_y, and U_x, U_y are the stiffnesses and displacements of the element in X and Y directions, respectively.

C.7.2 Linear/Nonlinear Viscous Element

One card
INELEM(K,3), INELEM(K, 1), INELEM(K,2)

INELEM(K,3) = Base below which the isolator is located
INELEM(K,1) = 1 or 2 or 3
INELEM(K,2) = 2 (Refer to C.7 for further details).

One card
PC(K,1), PC(K,2), PC(K,3), PC(K,4), PC(K,5), PC(K,6)

PC(K, 1) = Damping coefficient in the A-direction for biaxial element or uniaxial element in the A-direction (leave blank if the uniaxial element is in the B-direction only).

PC(K,2) = Damping coefficient in the B-direction for biaxial element or uniaxial element in the B-direction (leave blank if the uniaxial element is in the B-direction only).

PC(K,3) = Power for the velocity (integer or fractional) of the damper in the A-direction (α in Equations (5-3) and (5-4)). Values are usually in the range of 0.5 to 1.2. If given value is 1.0 then the linear viscous element is recovered (leave blank if the uniaxial element is in the B-direction only).

PC(K,4) = Power for the velocity (integer or fractional) of the damper in the B-direction (a in the Equations (5-3) and (5-4)). Values are usually in the range of 0.5 to 1.2. If given value is 1.0, linear viscous behavior is recovered (leave blank if the uniaxial element is in the A-direction only).

PC(K,5) = Orientation Angle θ_A for damper A with respect to the X-Axis in degrees ($-180^o \leq \theta_A \leq 180^o$). (leave blank if the uniaxial element is in the B-direction only).

PC(K,6) = Orientation Angle θ_B for damper B with respect to the X-Axis in degrees ($-180^o \leq \theta_B \leq 180^o$). (leave blank if the uniaxial element is in the B-direction only).

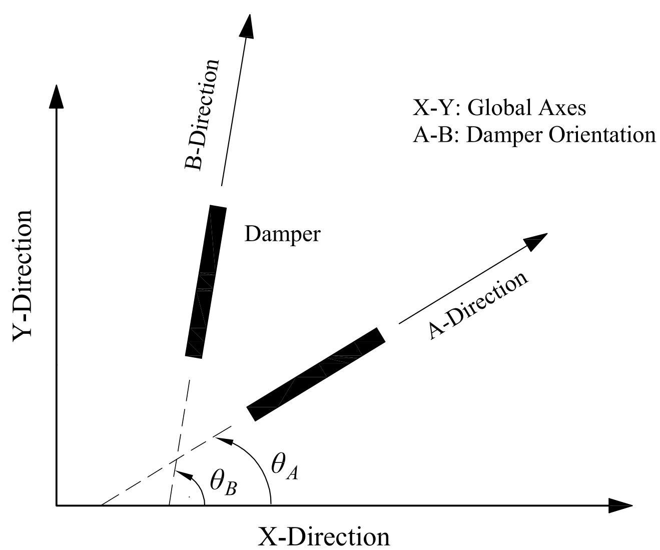

■ Note:

1. Biaxial element means that there are dampers in both A and B directions (no interaction between forces in X and Y direction).

■ Constitutive Equations:

This element is suitable for modeling the behavior of fluid viscous dampers or other devices displaying viscous behavior. Specifically, fluid dampers which operate on the principle of fluid orificing produce an output force which is proportional to the power of the velocity (Constantinou et al., 1992).

The mobilized forces on a viscous element are described by

$$F_A = C_A \left|\dot{U}_A\right|^{\alpha} \operatorname{sgn}(\dot{U}_A) \tag{5-3}$$

$$F_B = C_B \left|\dot{U}_B\right|^{\alpha} \operatorname{sgn}(\dot{U}_B) \tag{5-4}$$

where C_A, C_B and $\dot{U}_A$, $\dot{U}_B$ are damping coefficients and velocities experienced by viscous elements placed along the A and B directions respectively, and α is a coefficient taking real positive values. For $\alpha = 1$, the linear viscous element is recovered.

C.7.3 Hysteretic Element for Elastomeric Bearings/Steel Yielding Devices

One card

INELEM(K,3), **INELEM(K, 1)**, **INELEM(K,2)**

INELEM(K,3)= Base below which isolator is located
INELEM(K,1)= 1 or 2 or 3
INELEM(K,2)= 3 (Refer to C.7 for further details).

One card

(ALP(K,I), **I=1,2)**, **(YF(K,I)**, **I=1**,**2)**, **(YD(K,I)**, **I=1**,**2)**

ALP(K,l) = Post-to-pre-yielding stiffness ratio (leave blank if the uniaxial element is in the Y-direction only);

YF(K,l) = Yield Force (leave blank if the uniaxial element is in the Y direction only);

YD(K,1) = Yield Displacement; in the X-direction for biaxial element or uniaxial element in the X-direction (leave blank if the uniaxial element is in the Y direction only);

ALP(K,2) = Post-to-pre-yielding stiffness ratio (leave blank if the uniaxia1 element is in the X-direction only);

YF(K,2) = Yield force (leave blank if the uniaxial element is in the X-direction only);

YD(K,2) = Yield displacement; in the Y-direction for biaxial element or uniaxial element in the Y-direction (leave blank if the uniaxial element is in the X-direction only).

■ **Constitutive Equations:**

This element may be used in modeling the behavior of low-damping rubber bearings, high-damping rubber bearings in the range of strain prior to stiffening, and lead-rubber bearings.

The forces along the orthogonal directions which are mobilized during motion of elastomeric bearings or steel yielding devices are described by

$$F_x = \alpha \frac{F^Y}{Y} U_x + \left(1-\alpha\right) F^Y Z_x \tag{5-5}$$

$$F_y = \alpha \frac{F^Y}{Y} U_y + \left(1-\alpha\right) F^Y Z_y \tag{5-6}$$

where α is the post-yielding to pre-yielding stiffness ratio; F^Y is the yield force; Y is the yield displacement; and Z_x and Z_y are dimensionless variables governed by the following system of differential equations which was proposed by Park et al. (1986) :

$$\begin{Bmatrix} \dot{Z}_x Y \\ \dot{Z}_y Y \end{Bmatrix} = A \begin{bmatrix} 1 & 0 \\ 0 & 1 \end{bmatrix} \begin{Bmatrix} \dot{U}_x \\ \dot{U}_y \end{Bmatrix} - \begin{bmatrix} \left|Z_x\right|^2 (\gamma \mathrm{sgn}(\dot{U}_x Z_x) + \beta) & Z_x Z_y (\gamma \mathrm{sgn}(\dot{U}_y Z_y) + \beta) \\ Z_x Z_y (\gamma \mathrm{sgn}(\dot{U}_x Z_x) + \beta) & \left|Z_y\right|^2 (\gamma \mathrm{sgn}(\dot{U}_y Z_y) + \beta) \end{bmatrix} \begin{Bmatrix} \dot{U}_x \\ \dot{U}_y \end{Bmatrix} \tag{5-7}$$

in which A, γ, and β are dimensionless quantities that control the shape of the hysteresis loop. Furthermore, U_x, U_y and $\dot{U}_x$, $\dot{U}_y$ represent the displacements and velocities that occur at the isolation element.

C.7.4 Biaxial Hysteretic Element for Flat Sliding Bearings (Friction Coefficient Independent of Instantaneous Value of Normal Load)

One card

INELEM(K,3), **INELEM(K, 1)**, **INELEM(K,2)**

INELEM(K,3)= Base below which the isolator is located
INELEM(K,1)= 1 or 2 or 3
INELEM(K,2)= 4 (Refer to C.7 for further details).

One card

(FMAX(K,I), **I=1,2)**, **(FMIN(K,I)**, **I=1,2), (PA(K,I)**, **I=1,2)**, **(YD(K,I)**, **I=1,2)**, **FN(K)**

FMAX(K,1) = Maximum coefficient of sliding friction (leave blank if the uniaxial element is in the Y-direction only);

FMAX(K,2) = Maximum coefficient of sliding friction (leave blank if the uniaxial element is in the X-direction only);

FMIN(K,1) = Minimum coefficient of sliding friction (leave blank if the uniaxial element is in the Y-direction only);

FMIN(K,2) = Minimum coefficient of sliding friction (leave blank if the uniaxial element is in the X-direction only);

PA(K,I)	=	Constant which controls the transition of coefficient of sliding friction from maximum to minimum value (leave blank if the uniaxial element is in the Y-direction only);
PA(K,2)	=	Constant which controls the transition of coefficient of sliding friction from maximum to minimum value (leave blank if the uniaxial element is in the X-direction only);
YD(K, 1)	=	Yield displacement; in the X-direction for biaxial element or uniaxial element in the X-direction (leave blank if the uniaxial element is in the Y-direction only);
YD(K,2)	=	Yield displacement; in the Y-direction for biaxial element or uniaxial element in the Y-direction (leave blank if the uniaxial element is in the X-direction only).
FN(K)	=	Initial normal force at the sliding interface.

■ Constitutive Equations:

For flat sliding bearings, the mobilized forces are described by the equations (Constantinou et al., 1990; Mokha et al., 1993)

$$F_x = \mu_s N Z_x \tag{5-8}$$

$$F_y = \mu_s N Z_y \tag{5-9}$$

in which N is the vertical load carried by the bearing; and μ_s is the coefficient of sliding friction which, in general, depends on the bearing pressure, direction of motion as specified by angle $\theta = \tan^{-1}\left(\dot{U}_y / \dot{U}_x\right)$ and the instantaneous velocity of sliding $\dot{U} = \sqrt{\dot{U}_x^{\ 2} + \dot{U}_y^{\ 2}}$.

The conditions of separation and reattachment and biaxial interaction are accounted for by variables Z_x and Z_y in Equation (5-7), namely

$$\begin{Bmatrix} \dot{Z}_x Y \\ \dot{Z}_y Y \end{Bmatrix} = A \begin{bmatrix} 1 & 0 \\ 0 & 1 \end{bmatrix} \begin{Bmatrix} \dot{U}_x \\ \dot{U}_y \end{Bmatrix} - \begin{bmatrix} \left|Z_x\right|^2 (\gamma \operatorname{sgn}(\dot{U}_x Z_x) + \beta) & Z_x Z_y (\gamma \operatorname{sgn}(\dot{U}_y Z_y) + \beta) \\ Z_x Z_y (\gamma \operatorname{sgn}(\dot{U}_x Z_x) + \beta) & \left|Z_y\right|^2 (\gamma \operatorname{sgn}(\dot{U}_y Z_y) + \beta) \end{bmatrix} \begin{Bmatrix} \dot{U}_x \\ \dot{U}_y \end{Bmatrix}$$

in which U_x, U_y and $\dot{U}_x$, $\dot{U}_y$ represent the displacements and velocities respectively that occur at the isolation element; A, γ, and β are dimensionless quantities that control the shape of the hysteresis loop.

The dependency of the coefficient of friction on sliding velocity is explicitly modeled according to Equation (3-4), namely

$$\mu_s = f_{\max} - (f_{\max} - f_{\min}) e^{-a|\dot{U}|}$$

where the coefficient of sliding friction μ_s ranges from $f_{\min}$, at very low velocities of sliding, to $f_{\max}$, at large velocities; $\dot{U}$ is the velocity of sliding; and α is a constant, having units of time per unit length, that controls the variation of the coefficient of friction with velocity. The dependency of the coefficient of friction on velocity is illustrated in Figure 3-2(a).

The dependency of the maximum coefficient of friction $f_{\max}$ on bearing pressure is neglected.

C.7.5 Biaxial Hysteretic Element for Flat Sliding Bearings (Friction Coefficient Dependent on Instantaneous Value of Normal Load)

One card

INELEM(K,3), INELEM(K,1), INELEM(K,2)

INELEM(K,3)= Base below which the isolator is located
INELEM(K,1)= 1 or 2 or 3
INELEM(K,2)= 5 (Refer to C.7 for further details).

One card

(FMAX(K,I), I=1,2), (FMIN(K,I), I=1,2), (PA(K,I), I=1,2), (YD(K,I), I=1,2), FN(K)

FMAX(K, 1) = Maximum coefficient of sliding friction at almost zero pressure ($f_{\max 0}$ in Equation (3-5)) (leave blank if the uniaxial element is in the Y-direction only);

FMAX(K,2) = Maximum coefficient of sliding friction at almost zero pressure ($f_{\max 0}$ in Equation (3-5)) (leave blank if the uniaxial element is in the X-direction only);

FMIN(K,l) = Minimum coefficient of sliding friction (independent of pressure) (leave blank if the uniaxial element is in the Y-direction only);

FMIN(K,2) = Minimum coefficient of sliding friction (independent of pressure) (leave blank if the uniaxial element is in the X-direction only);

PA(K,1) = Constant which controls the transition of coefficient of sliding friction from maximum ($f_{\max}$) to minimum ($f_{\min}$) value (leave blank if the uniaxial element is in the Y-direction only);

PA(K,2) = Constant which controls the transition of coefficient of sliding friction from maximum ($f_{\max}$) to minimum ($f_{\min}$) value (leave blank if the uniaxial element is in the X-direction only);

YD(K,1)	=	Yield displacement; in the X-direction for biaxial element or uniaxial element in the X-direction (leave blank if the uniaxial element is in the Y-direction only).
YD(K,2)	=	Yield displacement; in the Y-direction for biaxial element or uniaxial element in the Y-direction (leave blank if the uniaxial element is in the X-direction only).
FN(K)	=	Initial normal force at the sliding interface (static condition).

■ Constitutive Equations:

This element for flat sliding bearings is again described by Equations (5-7) to (5-9) with the exception that N is not constant but rather described by Equation (3-3), namely

$$N = W\left(1 + \frac{\ddot{u}_{gv}}{g} + \frac{N_{OM}}{W}\right)$$

where W is the weight acting on the isolator; $\ddot{u}_{gv}$ is the vertical ground acceleration (positive when the direction is upwards); and N_{OM} is the additional axial force due to overturning moment effects (positive when compressive).

The user needs to provide matrix $[T]$ in file TMATRIX.DAT and matrix $[A]$ in file TMATRIXUPLF.DAT according to the procedure described in Section 3.4.

It should be noted that when $\ddot{u}_{gv}$ is not given and when the user-supplied routine returns zero for the additional axial load N_{OM}, the model collapses to the constant normal load ($N = W_i$) model.

The dependency of the maximum coefficient of friction $f_{\max}$ on bearing pressure is accounted for through Equation (3-5), namely

$$f_{\max} = f_{\max 0} - (f_{\max 0} - f_{\max \mathrm{p}})\tanh(\varepsilon p)$$

where parameter $f_{\max}$ ranges from $f_{\max 0}$, at almost zero pressure, to $f_{\max \mathrm{p}}$, at very high pressure; p is the bearing contact pressure; and ε is a constant that controls the variation of $f_{\max}$ between very low and very high pressures. Figure 3-2(b) presents the assumed variation of friction parameter $f_{\max}$ with pressure, which is typical of the behavior of sliding bearings.

The element requires the user-supplied subroutine FFMAX described in Section J.1.

C.7.6 Element for Friction Pendulum Bearing (FPS) (Friction Coefficient Dependent on Instantaneous Value of Normal Load)

One card

INELEM(K,3), INELEM(K,1), INELEM(K,2)

INELEM(K,3)= Base below which the isolator is located
INELEM(K,1)= 1 or 2 or 3
INELEM(K,2)= 6 (Refer to C.7 for further details).

One card

ALP(K,3), (FMAX(K,I), I= 1,2), (FMIN(K,I), 1=1,2), (PA(K,I), I= 1,2), (YD(K,I), I= 1,2), FN(K)

ALP(K,3) = Radius of curvature of the concave surface of the bearing;

FMAX(K,1) = Maximum coefficient of sliding friction at almost zero pressure ($f_{\max 0}$ in Equation (3-5)) (leave blank if the uniaxial element is in the Y-direction only);

FMAX(K,2) = Maximum coefficient of sliding friction at almost zero pressure ($f_{\max 0}$ in Equation (3-5)) (leave blank if the uniaxial element is in the X-direction only);

FMIN(K,1) = Minimum coefficient of sliding friction (independent of pressure) (leave blank if the uniaxial element is in the Y-direction only);

FMIN(K,2) = Minimum coefficient of sliding friction (independent of pressure) (leave blank if the uniaxial element is in the X-direction only);

PA(K,1) = Constant which controls the transition of coefficient of sliding friction from maximum ($f_{\max}$) to minimum ($f_{\min}$) value (leave blank if the uniaxial element is in the Y-direction only);

PA(K,2) = Constant which controls the transition of coefficient of sliding friction from maximum ($f_{\max}$) to minimum ($f_{\min}$) value (leave blank if the uniaxial element is in the X-direction only);

YD(K,1) = Yield displacement; in the X-direction for biaxial element or uniaxial element in the X-direction (leave blank if the uniaxial element is in the Y-direction only);

YD(K,2) = Yield displacement; in the Y-direction for biaxial element or uniaxial element in the Y-direction (leave blank if the uniaxial element is in the X-direction only).

FN(K) = Initial normal force at the sliding interface (static condition).

■ Constitutive Equations:

The forces in the FPS element are described by

$$F_x = \frac{N}{R}U_x + \mu_s N Z_x \tag{5-10}$$

$$F_y = \frac{N}{R}U_y + \mu_s N Z_y \tag{5-11}$$

where U_x and U_y are the displacements in global axis X and Y, respectively; μ_s is the coefficient of sliding friction; N is the normal force on the bearing; and Z_x and Z_y are hysteretic dimensionless quantities.

The dimensionless variables Z_x and Z_y are governed by Equation (5-7), namely

$$\begin{Bmatrix} \dot{Z}_x Y \\ \dot{Z}_y Y \end{Bmatrix} = A\begin{bmatrix} 1 & 0 \\ 0 & 1 \end{bmatrix}\begin{Bmatrix} \dot{U}_x \\ \dot{U}_y \end{Bmatrix} - \begin{bmatrix} |Z_x|^2(\gamma \operatorname{sgn}(\dot{U}_x Z_x)+\beta) & Z_x Z_y(\gamma \operatorname{sgn}(\dot{U}_y Z_y)+\beta) \\ Z_x Z_y(\gamma \operatorname{sgn}(\dot{U}_x Z_x)+\beta) & |Z_y|^2(\gamma \operatorname{sgn}(\dot{U}_y Z_y)+\beta) \end{bmatrix}\begin{Bmatrix} \dot{U}_x \\ \dot{U}_y \end{Bmatrix}$$

in which U_x, U_y and $\dot{U}_x$, $\dot{U}_y$ represent the displacements and velocities respectively that occur at the isolation element; A, γ, and β are dimensionless quantities that control the shape of the hysteresis loop.

The dependency of the coefficient of friction on sliding velocity is explicitly modeled according to Equation (3-4), namely

$$\mu_s = f_{\max} - (f_{\max} - f_{\min})e^{-a|\dot{U}|}$$

where the coefficient of sliding friction μ_s ranges from $f_{\min}$, at very low velocities of sliding, to $f_{\max}$, at large velocities; $\dot{U}$ is the velocity of sliding; and α is a constant, having units of time per unit length, that controls the variation of the coefficient of friction with velocity. The dependency of the coefficient of friction on velocity is illustrated in Figure 3-2(a).

The variation of the normal force on the isolation bearing due to the effect of vertical earthquake motion and global overturning moment is accounted for through Equation (3-3), namely

$$N = W\left(1 + \frac{\ddot{u}_{gv}}{g} + \frac{N_{OM}}{W}\right)$$

where W is the weight acting on the isolator; $\ddot{u}_{gv}$ is the vertical ground acceleration (positive when the direction is upwards); and N_{OM} is the additional axial force due to overturning moment effects (positive when compressive).

The user needs to provide matrix $[T]$ in file TMATRIX.DAT and matrix $[A]$ in file TMATRIXUPLF.DAT according to the procedure described in Section 3.4.

It should be noted that when $\ddot{u}_{gv}$ is not given and when the user-supplied routine returns zero for the additional axial load N_{OM}, the model collapses to the constant normal load ($N = W_i$) model.

The dependency of the maximum coefficient of friction $f_{\max}$ on bearing pressure is accounted for through Equation (3-5), namely

$$f_{\max} = f_{\max 0} - (f_{\max 0} - f_{\max \mathrm{p}})\tanh(\varepsilon p)$$

where parameter $f_{\max}$ ranges from $f_{\max 0}$, at almost zero pressure, to $f_{\max \mathrm{p}}$, at very high pressure; p is the bearing contact pressure; and ε is a constant that controls the variation of $f_{\max}$ between very low and very high pressures. Figure 3-2(b) presents the assumed variation of friction parameter $f_{\max}$ with pressure, which is typical of the behavior of sliding bearings.

The element requires the user-supplied subroutine FFMAX described in Section J.1.

C.7.7 Stiffening Biaxial Hysteretic Element for Elastomeric Bearings

One card

INELEM(K,3), INELEM(K,1), INELEM(K,2)

INELEM(K,3)= Base below which the isolator is located
INELEM(K,1)= 1 or 2 or 3
INELEM(K,2)= 7 (Refer to C.7 for further details).

One card

ALP(K,3), ALP(K,4), ALP(K,5), ALP(K,6), ALP(K,7), YD(K,1)

ALP(K,3) = Characteristic strength (Q of Equation 4.6);
ALP(K,4) = Tangent stiffness K_1 (see Equation 4.1);
ALP(K,5) = Tangent stiffness K_2 (see Equation 4.1);

ALP(K,6) = Displacement limit D_1 (see Equation 4.1);
ALP(K,7) = Displacement limit D_2 (see Equation 4.1);
YD(K,1) = Yield displacement;

■ Constitutive Equations:

The element is appropriate for modeling the behavior of high-damping rubber bearings. Typically, these bearings exhibit higher stiffness at large strains. The element is formed by combining the elastoplastic version ($\alpha = 0$) of the biaxial hysteretic element described by Equations (5-5) through (5-7) and a stiffening bilinear spring.

The complete model consists of the combination of components given by Equations (5-5) and (5-6), with $\alpha = 0$ and $F^Y = Q$, and components F_{xs} and F_{ys} of the resultant force F of the stiffening bilinear spring:

$$F_x = QZ_x + F_{xs} \tag{5-12}$$

$$F_y = QZ_y + F_{ys} \tag{5-13}$$

where

$$F_{xs} = F\cos\theta \tag{5-14}$$

$$F_{ys} = F\sin\theta \tag{5-15}$$

in which

$$F = \left\{ \begin{array}{ccc} K_1 U & , & U \le D_1 \\ \dfrac{(K_2 - K_1)}{(D_2 - D_1)} \dfrac{(U - D_1)^2}{2} \mathrm{sgn}(U) + K_1 U & , & D_1 < U \le D_2 \\ \dfrac{(K_1 - K_2)(D_1 + D_2)}{2} \mathrm{sgn}(U) + K_2 U & , & U > D_2 \end{array} \right\} \tag{5-16}$$

$$\left.\begin{array}{lll}\theta=\theta^{*} & \text{when} & U_x,\ U_y>0\\ \theta=\theta^{*}+\pi/2 & \text{when} & U_x<0,\ U_y>0\\ \theta=\theta^{*}+\pi & \text{when} & U_x,\ U_y<0\\ \theta=-\theta^{*} & \text{when} & U_x>0,\ U_y<0\\ \theta=\pi/2 \text{ and } U=U_y & \text{when} & U_x=0\\ \theta=0 \text{ and } U=U_x & \text{when} & U_y=0\end{array}\right\} \tag{5-17}$$

and

$$\theta^{*}=\tan^{-1}\left(\frac{|U_y|}{|U_x|}\right) \tag{5-18}$$

In Equation (5-16), $U=\sqrt{U_x^{\,2}+U_y^{\,2}}$ is the resultant displacement; K_1 is the tangent stiffness mobilized for displacements less than the limit D_1; and K_2 is the higher tangent stiffness mobilized for displacements larger than the limit D_2, as illustrated in the figure below.

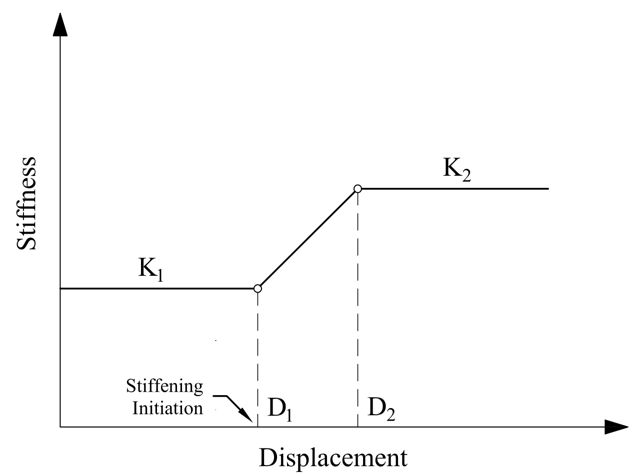

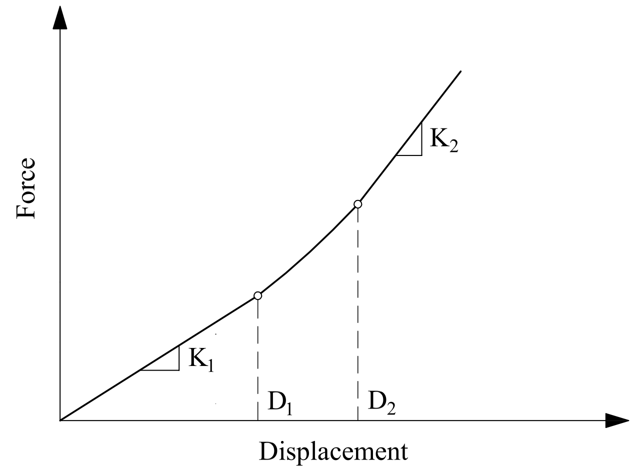

Model for stiffening bilinear spring.

C.7.8 Element for Uplift-Restraining (XY-FP) Friction Pendulum Bearing

One card

INELEM(K,3), INELEM(K,1), INELEM(K,2)

INELEM(K,3) = Base below which the isolator is located
INELEM(K,1) = 1 or 2 or 3
INELEM(K,2) = 8 (Refer to C.7 for further details).

Three Cards

ALP(K,3), ALP(K,5), FN(K), ALP(K,4)

Compression:

(FMAX(K,J), J=1,2), (FMIN(K,J), J=1,2), (PA(K,J), J=1,2), (YD(K,J), J=1,2)

Tension:

(FMAX(K,J), J=3,4), (FMIN(K,J), J=3,4), (PA(K,J), J=3,4), (YD(K,J), J=3,4)

ALP(K,3) = R_1 ; Radius of curvature of the concave surface of the bearing in direction 1;
ALP(K,5) = R_2 ; Radius of curvature of the concave surface of the bearing in direction 1;
FN(K) = Initial normal force at the sliding interface (static condition)
ALP(K,4) = Angle of orientation of the isolator with respect to global X-direction in units of degrees.

Frictional Interface Properties when Isolator in COMPRESSION

FMAX(K,1) = Maximum coefficient of sliding friction at almost zero pressure in 1-direction ($f_{\max 0}$ in Equation (3-5))

FMAX(K,2) = Maximum coefficient of sliding friction at almost zero pressure in 2-direction ($f_{\max 0}$ in Equation (3-5))

FMIN(K,1) = Minimum coefficient of sliding friction (independent of pressure) in 1-direction

FMIN(K,2) = Minimum coefficient of sliding friction (independent of pressure) in 2-direction

PA(K,1) = Constant which controls the transition of coefficient of sliding friction from maximum (f_{max}) to minimum (f_{min}) value along 1-direction.

PA(K,2) = Constant which controls the transition of coefficient of sliding friction from maximum (f_{max}) to minimum (f_{min}) value along 2-direction.

YD(K,1) = Yield displacement in the 1-direction

YD(K,2) = Yield displacement in the 2-direction

Frictional Interface Properties when Isolator in TENSION

FMAX(K,3) = Maximum coefficient of sliding friction at almost zero pressure in 1-direction ($f_{max\,0}$ in Equation (3-5))

FMAX(K,4) = Maximum coefficient of sliding friction at almost zero pressure in 2-direction ($f_{max\,0}$ in Equation (3-5))

FMIN(K,3) = Minimum coefficient of sliding friction (independent of pressure) in 1-direction

FMIN(K,4) = Minimum coefficient of sliding friction (independent of pressure) in 2-direction

PA(K,3) = Constant which controls the transition of coefficient of sliding friction from maximum (f_{max}) to minimum (f_{min}) value along 1-direction.

PA(K,4) = Constant which controls the transition of coefficient of sliding friction from maximum (f_{max}) to minimum (f_{min}) value along 2-direction.

YD(K,3) = Yield displacement in the 1-direction

YD(K,4) = Yield displacement in the 2-direction

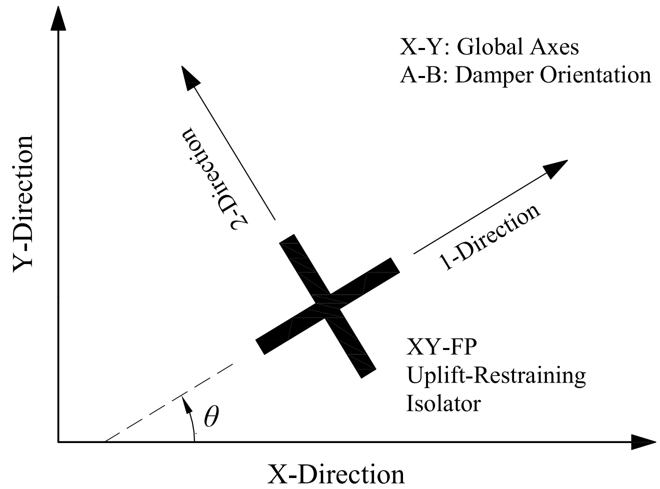

■ Constitutive Equations:

The element for the new XY-FP isolator is synthesized by two independent uniaxial hysteretic elements allowing different frictional interface properties along the principal isolator directions (Roussis and Constantinou, 2005). Contrary to the element representing the conventional FP isolator, the new element is capable of accommodating the uplift-restraint property of the XY-FP isolator by allowing continuous transition of the bearing axial force from compression to tension and vice versa. Moreover, the new element can assume different frictional interface properties under compressive and tensile isolator normal force.

The force-displacement relationship in the local co-ordinate system utilized in modeling the XY-FP element in 3D-BASIS-ME-MB is given by Equation (3-6), namely

$$\begin{Bmatrix} F_1 \\ F_2 \end{Bmatrix} = \begin{bmatrix} N/R_1 & 0 \\ 0 & N/R_2 \end{bmatrix} \begin{Bmatrix} U_1 \\ U_2 \end{Bmatrix} + \begin{bmatrix} \mu_1 |N| & 0 \\ 0 & \mu_2 |N| \end{bmatrix} \begin{Bmatrix} Z_1 \\ Z_2 \end{Bmatrix}$$

where R_1 and R_2 are the radii of curvature of the lower and upper concave beams, respectively; μ_1 and μ_2 are the associated sliding friction coefficients; U_1 and U_2 are the displacements in bearing local axis 1 and 2, respectively; N is the normal force on the bearing, positive when compressive; and Z_1 and Z_2 are hysteretic dimensionless quantities governed by the differential Equation (3-7), namely

$$\begin{Bmatrix} \dot{Z}_1 Y_1 \\ \dot{Z}_2 Y_2 \end{Bmatrix} = A \begin{bmatrix} 1 & 0 \\ 0 & 1 \end{bmatrix} \begin{Bmatrix} \dot{U}_1 \\ \dot{U}_2 \end{Bmatrix} - \begin{bmatrix} |Z_1|^{\eta} (\gamma \operatorname{sgn}(\dot{U}_1 Z_1) + \beta) & 0 \\ 0 & |Z_2|^{\eta} (\gamma \operatorname{sgn}(\dot{U}_2 Z_2) + \beta) \end{bmatrix} \begin{Bmatrix} \dot{U}_1 \\ \dot{U}_2 \end{Bmatrix}$$

where $\dot{U}_1$ and $\dot{U}_2$ are the velocities in local axis 1 and 2, respectively; A, β, γ and η are dimensionless quantities that control the shape of the hysteresis loop; and Y_1 and Y_2 represent the yield displacements.

The corresponding force-displacement relationship in the global co-ordinate system is given by Equation (3-2):

$$\begin{Bmatrix} F_x \\ F_y \end{Bmatrix} = \begin{bmatrix} \cos\theta & \sin\theta \\ -\sin\theta & \cos\theta \end{bmatrix}^T \begin{Bmatrix} F_1 \\ F_2 \end{Bmatrix}$$

The dependency of the coefficient of friction on sliding velocity is explicitly modeled according to Equation (3-4), namely

$$\mu_s = f_{\max} - (f_{\max} - f_{\min})e^{-a|\dot{U}|}$$

where the coefficient of sliding friction μ_s ranges from $f_{\min}$, at very low velocities of sliding, to $f_{\max}$, at large velocities; $\dot{U}$ is the velocity of sliding; and α is a constant, having units of time per unit length, that controls the variation of the coefficient of friction with velocity. The dependency of the coefficient of friction on velocity is illustrated in Figure 3-2(a).

The variation of the normal force on the isolation bearing due to the effect of vertical earthquake motion and global overturning moment is accounted for through Equation (3-3), namely

$$N = W\left(1 + \frac{\ddot{u}_{gv}}{g} + \frac{N_{OM}}{W}\right)$$

where W is the weight acting on the isolator; $\ddot{u}_{gv}$ is the vertical ground acceleration (positive when the direction is upwards); and N_{OM} is the additional axial force due to overturning moment effects (positive when compressive).

The user needs to provide matrix $[T]$ in file TMATRIX.DAT according to the procedure described in Section 3.4.1.

The dependency of the maximum coefficient of friction $f_{\max}$ on bearing pressure is accounted for through Equation (3-5), namely

$$f_{\max} = f_{\max 0} - (f_{\max 0} - f_{\max p})\tanh(\varepsilon p)$$

where parameter $f_{\max}$ ranges from $f_{\max 0}$, at almost zero pressure, to $f_{\max p}$, at very high pressure; p is the bearing contact pressure; and ε is a constant that controls the variation of $f_{\max}$ between very low and very high pressures. Figure 3-2(b) presents the assumed variation of friction parameter $f_{\max}$ with pressure, which is typical of the behavior of sliding bearings.

The element requires the user-supplied subroutine FFMAX described in Section J.1.

C.7.9 General Nonlinear Viscous Element

One card
INELEM(K,3), INELEM(K,1), INELEM(K,2)

INELEM(K,3)= Base below which the isolator is located
INELEM(K,1)= 1 or 2 or 3
INELEM(K,2)= 9 (Refer to C.7 for further details).

One card
(PC(K,I), I=1,14)

PC(K,1) = Force offset for dampers A or B in range 1 (F_{01} in Equation (5-19)). (leave blank if the uniaxial element is in the B-direction only).

PC(K,2) = Force offset for dampers A or B in range 2 (F_{02} in Equation (5-19)). (leave blank if the uniaxial element is in the A-direction only).

PC(K,3) = Nonlinear viscous constant for damper A in range 1 (C_{1A} in Equation (5-19)) (leave blank if the uniaxial element is in the B-direction only).

PC(K,4) = Nonlinear viscous constant for damper A in range 2 (C_{2A} in Equation (5-19)) (leave blank if the uniaxial element is in the B-direction only).

PC(K,5) = Limit velocity for transition from range 1 to 2 in A-direction $\left(V_{12}\right)_A$ (leave blank if the uniaxial element is in the B-direction only).

PC(K,6) = Nonlinear viscous constant for damper B in range 1 (C_{1B} in Equation (5-19)) (leave blank if the uniaxial element is in the A-direction only).

PC(K,7) = Nonlinear viscous constant for damper B in range 2 (C_{2B} in Equation (5-19)) (leave blank if the uniaxial element is in the A-direction only).

PC(K,8) = Limit velocity for transition from range 1 to 2 in B-direction $\left(V_{12}\right)_B$ (leave blank if the uniaxial element is in the A-direction only).

PC(K,9) = Power for the velocity (integer or fractional) in the range 1 for either dampers A or B (p_1 in Equation (5-19))

PC(K,10) = Power for the velocity (integer or fractional) in the range 2 for either dampers A or B (p_2 in Equation (5-19))

PC(K,11) = Maximum damper force for either one of the dampers A or B ($F_{\max}$ in Equation (5-19))

PC(K,12) = Displacement limit for damper operation start at low velocities and displacements for either A or B.

PC(K,13) = Orientation Angle θ_A for damper A with respect to the X-Axis in degrees ($-180^o \leq \theta_A \leq 180^o$). (leave blank if the uniaxial element is in the B-direction only).

PC(K,14) = Orientation Angle θ_B for damper B with respect to the X-Axis in degrees ($-180^o \leq \theta_B \leq 180^o$) (leave blank if the uniaxial element is in the B-direction only).

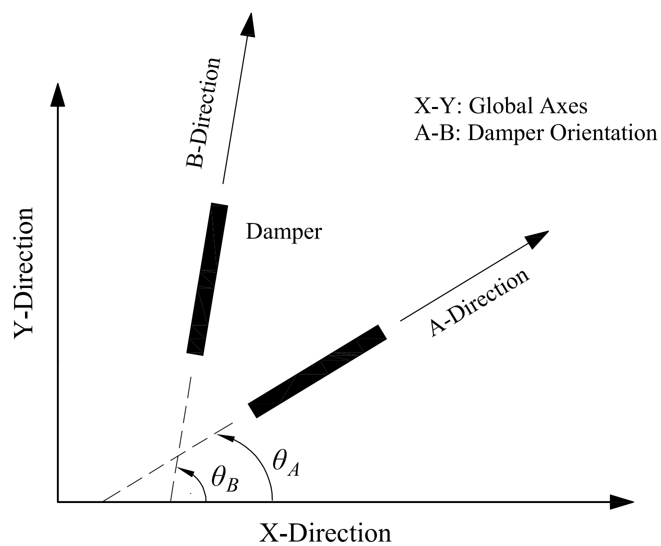

■ Note:

1. This model is suitable for a cluster of two (horizontal) damper A and B oriented at an arbitrary angle to each other and to the building. The dampers have different nonlinear properties, but same maximum and same offset constants. Biaxial element means that there are dampers in both A and B directions (no interaction between forces in X and Y direction).

■ Constitutive Equations:

The force-velocity relation of the general nonlinear viscous element is given by

$$F_D = \begin{cases} \left(F_{01} + C_1 \left|\dot{U}\right|^{p_1}\right)\mathrm{sgn}(\dot{U}) & \text{if } \left|\dot{U}\right| \le V_{12} \\ \left(F_{02} + C_2 \left|\dot{U}\right|^{p_2}\right)\mathrm{sgn}(\dot{U}) \le F_{\max} & \text{if } \left|\dot{U}\right| > V_{12} \end{cases} \quad (5\text{-}19)$$

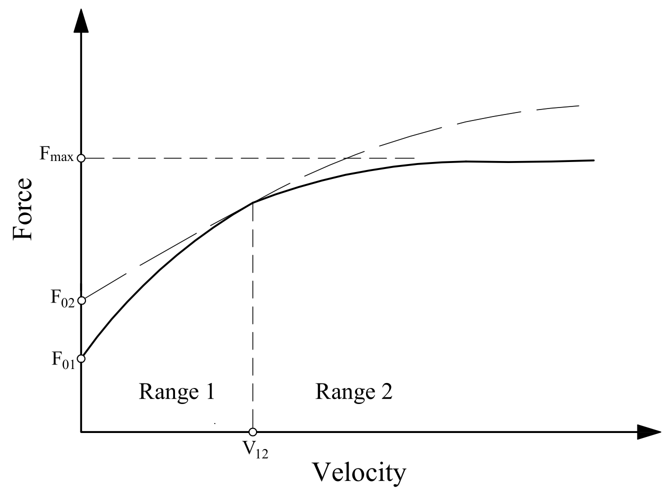

D.1 OUTPUT DATA

D.2 OUTPUT PARAMETERS

USER_TXT Reference information; up to 80 characters of text.
One card
LTMH, KPD, IPROF

LTMH:
- LTMH = 1 for both the time history and peak response output.
- LTMH = 0 for only peak response output.

KPD = No. of time steps before the next response quantity is output.

IPROF:
- IPROF = 1 for accelerations-displacements profiles output.
- IPROF = 0 for no accelerations-displacements profiles output.

D.3 ISOLATOR OUTPUT

USER_TXT Reference information; up to 80 characters of text.
INP cards
IP(I), **I=1**,**INP**

IP(I) = Bearing number of bearings I at which the force and displacement response is desired.

■ **Note:**

1. If INP equals zero then skip Section D.3.

D.4 INTERSTORY DRIFT OUTPUT

The following set of cards must be imported as many times as the number of super-structures NB.

USER_TXT Reference information; up to 80 characters of text.
One card
ICOR(I), **I=l**,**NB**

ICOR(I) = Number of column lines of superstructure I at which the interstory drift is desired.

ICOR(I) cards
CORDX(K), **CORDY(K)**, **K= 1**,**ICOR(I)**

CORDX(K) = X co-ordinate of the column line at which the interstory drift is desired.

CORDY(K) = Y co-ordinate of the column line at which the interstory drift is desired.

■ **Note:**

1. Maximum number of columns at which drift output may be requested is limited to six for each superstructure (maximum value for ICOR(I) is six)
2. The coordinates of the column lines are with respect to the reference axis at the center of mass of the top (first) base.

E.1 INITIAL CONDITIONS

USER_TXT Reference information; up to 80 characters of text.
NBSLBS cards
DN(3*(K-1)+1,1), **DN(3*(K-1)+2,1)**, **DN(3*(K-1)+3,1)**, **K=1**,**NBSLBS**

DN(3*(K-1)+1,1) = Initial displacement of the C.M. of base K along the X-direction

DN(3*(K-1)+2,1) = Initial displacement of the C.M. of base K along the Y-direction

DN(3*(K-1)+3,1) = Initial rotation of the C.M. of base K.

F.1 SEISMIC INPUT (EARTHQUAKE TIME HISTORIES)

This set of data requires separate file(s) from the set of data presented in sections A to E.

F.2 UNI-DIRECTIONAL EARTHQUAKE RECORD

File: WAVEX.DAT

USER_TXT Reference information; up to 80 characters of text.
LOR cards
X(I), **I= 1**,**LOR**

X(I) = Unidirectional acceleration component.

■ **Note:**

1. If INDGACC as specified in A.4.4 is 1 or 3, then the input will be assumed at an angle XTH specified in A.4.4. If INDGACC as specified in A.4.4 is 2 or 4, then X(LOR) is considered to be the X component of the bidirectional earthquake.

F.3 EARTHQUAKE RECORD IN THE Y-DIRECTION FOR BIDIRECTIONAL EARTHQUAKE

File: WAVEY.DAT (Input only if INDGACC = 2 or 4)

USER_TXT Reference information; up to 80 characters of text.
LOR cards
Y(I,l), **I=1**,**LOR**

Y(I,1) = Acceleration component in the Y direction.

F.4 EARTHQUAKE RECORD IN THE Z (VERTICAL) DIRECTION

File: WAVEZ.DA T (Input only if INDGACC = 3 or 4)

USER_TXT Reference information; up to 80 characters of text.
LOR cards
Y(I,2), **I=1**,**LOR**

Y(I,2) = Acceleration component in the Z direction.

G.1 NORMAL LOAD VARIATION INPUT FOR ISOLATORS

This set of data requires separate files from the set of data presented in sections A to F.

This set of data is supplied only for ITMAT =2 (in section A.4.1)

G.2 EFFECT OF INERTIAL LOADS (HORIZONTAL LOADS ON FLOORS AND BASES) ON THE NORMAL LOADS OF ISOLATORS

File: TMATRIX.DAT (Input only if ITMAT = 2)

USER_TXT Reference information; up to 80 characters of text.
NP cards
TMATRIX(I,J), **J = 1**, **3*MNF+3*NBSLBS**

TMATRIX(I,J) = Coefficients relating the normal loads on the isolators with the horizontal inertia forces.

G.3 EFFECT OF ISOLATOR UPLIFT ON THE NORMAL LOADS OF THE ISOLATORS

File: TMATRIXUPLF.DAT (Input only if ITMAT = 2)

USER_TXT Reference information; up to 80 characters of text.

NP cards

ALPHA(I,J), J = 1,NP

ALPHA(I,J) = Coefficients relating axial loads on the isolators when one isolator undergoes uplift.

H.1 OUTPUT FILES

The set of output files and their contents are presented in the table below.

FILE	DESCRIPTION / COMMENT
3DBMEMB.OUT	General output, summary results in terms of Maxima and Minima and profiles of accelerations and displacements
1001, 1002, etc.	Time histories of Superstructure quantities (Accelerations and Displacements)
BASE	Time histories of quantities related to bases (Isolator Displacement and Forces, Structural Shears and Base Shears)
ISOLBASE_No 1.OUT, ISOLBASE_No2.OUT, etc.	Time histories of Accelerations and Displacements at C.M. of each Base
ISOL8	Time histories of all Isolators of Type 8 only
The following files are printed to aid the user in plotting important results	
ACCELR.INP	Accelerations for all dynamic DOF of the model at C.M. of each level 1st col.: Time, 2nd col: Accel. in x-dir. of top floor of superstructure #1 3nd col: Accel. in y-dir. of top floor of superstructure #1 4th col: Accel. in rot-dir. of top floor of superstructure #1 5th col: Accel. in x-dir. of the second-from-the-top floor of superstructure #1 …..the dynamic DOFs of superstructure #2 follow ….. …..the dynamic DOFs of the isol. bases follow from top to bottom
DISPLR.INP	Displacements for all dynamic DOF of the model at C.M. of each level 1st col.: Time, 2nd col: Displ. in x-dir. of top floor of superstructure #1 3nd col: Displ. in y-dir. of top floor of superstructure #1 4th col: Displ. in rot-dir. of top floor of superstructure #1 5th col: Displ. in x-dir. of the second-from-the-top floor of superstructure #1 …..the Dynamic DOFs of superstructure #2 follow ….. …..the Dynamic DOFs of the isol. bases follow, from top to bottom
ISOL_NOR-FORCE.INP	Normal forces on isolators Output for (n) number of isolators requested in Section D3
ISOL_D-F_X-DIR.INP, ISOL_D-F_X-DIR.INP	Isolator Displacement and Forces in X-dir and Y-dir respectively Output for (n) number of isolators requested in Section D3 1st col.: Time, 2nd col: Displ. of Isolator #1 3nd col: Displ. of Isolator #2 ….. nth +1 col: Force of Isolator #1 ….

I.1 USER-SUPPLIED SUBROUTINES

Subroutine FFMAX for describing the dependency of friction parameter $f_{\max}$ on bearing pressure

Program 3D-BASIS-ME-MB requires a user-supplied routine for describing the variation of friction coefficient $f_{\max}$ with bearing pressure.

The variation of parameter $f_{\max}$ with pressure is given by Equation (3-5), namely

$$f_{\max} = f_{\max 0} - (f_{\max 0} - f_{\max \mathrm{p}})\tanh(\varepsilon p)$$

where the maximum coefficient of friction $f_{\max}$ ranges from $f_{\max 0}$, at almost zero pressure, to $f_{\max \mathrm{p}}$, at very high pressure; p is the bearing contact pressure; and ε is a constant that controls the variation of $f_{\max}$ between very low and very high pressures. The figure below presents the assumed variation of friction parameter $f_{\max}$ with pressure, which is typical of the behavior of sliding bearings (Soong and Constantinou, 1994).

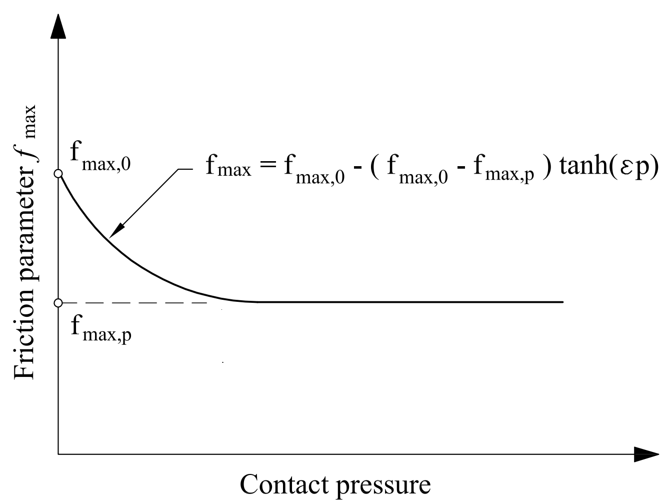

Variation of coefficient of friction with bearing contact pressure.

The user-supplied routine (function) has the form

FFMAX(FRMAX, FRMIN, FNOR, I)

in which I is the bearing number, FNOR is the normal load on bearing I, which includes the gravity, vertical ground motion and overturning moment effects, normalized by the weight W_i on the bearing. Furthermore, FRMAX and FRMIN are respectively the parameters $f_{\max 0}$ and $f_{\min 0}$ under almost zero static pressure of bearing I, supplied through the input file. Function FFMAX returns the value of $f_{\max}$ at the bearing pressure resulting from the instantaneous normal load. Note that parameter $f_{\min}$ is assumed independent of pressure, that is $f_{\min 0} = f_{\min}$.

As an example, Constantinou et al. (1993) gave the following values for the parameters of a bearing at pressure of 17.2 MPa: $f_{\max 0} = 0.12$, $f_{\max \mathrm{p}} = 0.05$, $\varepsilon = 0.012$ (p is in units of MPa). For this case function FFMAX should be of the form:

```
FUNCTION FFMAX(FRMAX, FRMIN, FNOR, I)
IMPLICIT REAL *8
COMMON / MAIN1 / NB, NP, MNF, MNE, NFE, MXF
DIMENSIQN P(500)
DATA / P(J)=17.2, J=1,../
etc.
PRES=FNOR*P(I)
FFMAX=FRMAX-0.07*DTANH(0.012*PRES)
RETURN
END
```

Note that P(J) contains the bearing pressure under static conditions of bearing J. Quantity PRES is the instantaneous bearing pressure in units of MN/m^2 or MPa.

In the case where the dependency on pressure of parameter $f_{\max}$ is neglected—as is the default in 3DBASIS-ME-MB—function FFMAX should be

```
FUNCTION FFMAX(FRMAX, FRMIN, FNOR, I)
IMPLICIT REAL *8
COMMON / MAIN1 / NB, NP, MNF, MNE, NFE, MXF
FFMAX=FRMAX
RETURN
END
```

SECTION 6
SUMMARY

Program 3D-BASIS-ME-MB represents a versatile tool for the analysis of complex seismically-isolated structures. The new program offers improvements over its predecessor (3D-BASIS-ME) including the capability to analyze multiple superstructures on multiple isolation-system levels; the addition of a new element for modeling the mechanical behavior of the uplift-restraining XY-FP isolator; an improvement of the existing viscous damper element; capability to capture the effects of lateral loads on bearing axial forces, including bearing uplift; and streamlined program output.

Two examples of seismically isolated structures have been used for verifying 3D-BASIS-ME-MB and demonstrating its capabilities. The first example is a 7-story model structure that was tested on the earthquake simulator of the University at Buffalo (Al-Hussaini et al, 1994) and was also used as a verification example for program SAP2000 (Scheller and Constantinou, 1999 and Computers and Structures, 2004). The second example is a two-tower, multi-story structure with a split seismic-isolation-system level. In both examples the analyzed structure is seismically isolated with Friction Pendulum bearings and is excited under conditions of bearing uplift. This represents the most extreme condition that bearings are subjected to and is a case of much interest in verifying the capabilities of analysis software.

In the first example, analysis results obtained from program 3D-BASIS-ME-MB are compared with both experimental results and results obtained from program ABAQUS. In the second example, results of analysis produced by program 3D-BASIS-ME-MB are compared with results obtained from program ABAQUS.

The satisfactory comparisons of results in both examples attest to the validity and accuracy of program 3D-BASIS-ME-MB.

Finally, it should be noted that program 3D-BASIS-ME-MB has inherent limitations as described below:

1) Although it is possible to detect bearing uplift from histories of isolator axial load (also from the shapes of isolator force-displacement loops and from histories of isolator shear force), the program cannot calculate the isolator uplift displacement.
2) Analysis of structures with split level isolation system is approximate in the sense that the effect on the isolator axial loads of the shear force distribution at the various isolation levels is approximate.
3) The program is not capable of capturing rigid body rocking effects that result from isolator uplift. (To capture these effects, geometrically nonlinear analysis would be required).

SECTION 7
REFERENCES

ABAQUS, Inc. (2004), "ABAQUS Analysis User's Manual," Version 6.4, Pawtucket, Rhode Island.

Al-Hussaini T. M., Zayas V. A., and Constantinou M. C. (1994), "Seismic Isolation of Multi-Story Frame Structures Using Spherical Sliding Isolation System," *Technical Report NCEER-94-0007*, National Center for Earthquake Engineering Research, State University of New York, Buffalo, NY.

Clarke, C. S. J., Buchanan, R., Efthymiou, M., and Shaw, C. (2005), "Structural Platform Solution for Seismic Arctic Environments—Sakhalin II Offshore Facilities," Paper OTC-17378-PP, *Offshore Technology Conference*, Houston, Texas.

Computers and Structures, Inc. (1998), "SAP2000 Analysis Reference Manual," Version 7.5, Berkeley, CA.

Computers and Structures Inc. (2003), "SAP2000: Integrated Finite Element Analysis and Design of Structures," Version 8.2, Berkeley, CA.

Computers and Structures Inc. (1995), "ETABS Analysis Reference Manual," Version 6.0, Berkeley, CA.

Constantinou M. C., Mokha A., and Reinhorn A. M. (1990), "Teflon Bearings in Base Isolation II: Modeling," *Journal of Structural Engineering*; 116(2): 455-474.

Constantinou, M. C. and Symans, M. D. (1992), "Experimental and analytical investigation of seismic response of structures with supplemental fluid viscous dampers," *Technical Report NCEER-92-0032*, National Center for Earthquake Engineering Research, State University of New York, Buffalo, NY.

Mokha A., Constantinou M. C., and Reinhorn A. M. (1988), "Teflon Bearings in Aseismic Base Isolation: Experimental Studies and Mathematical Modeling," *Technical Report NCEER-88-0038*, National Center for Earthquake Engineering Research, State

University of New York, Buffalo, NY.

Mokha, A. S., Constantinou, M. C., and Reinhorn, A. M. (1993), "Verification of Friction Model of Teflon Bearings under Triaxial Load," *Journal of Structural Engineering*, 119(1), 240-261.

Nagarajaiah, S., Reinhorn, A.M., and Constantinou, M.C. (1989), "Nonlinear Dynamic Analysis of Three Dimensional Base Isolated Structures (3D-BASIS)," *Technical Report NCEER-89-0019*, National Center for Earthquake Engineering Research, State University of New York, Buffalo, NY.

Nagarajaiah, S. (1990), "Nonlinear Dynamic Analysis of Three Dimensional Base Isolated Structures", Ph.D. Thesis, University at Buffalo, State University of New York, Buffalo, NY.

Nagarajaiah, S., Reinhorn, A.M., and Constantinou, M.C. (1991a), "Nonlinear Dynamic Analysis of Three Dimensional Base Isolated Structures", Journal of Structural Engineering, ASCE, Vol. 117, No. 7, 2035-2054.

Nagarajaiah, S., Reinhorn, A.M., and Constantinou, M.C. (1991b), "3D-BASIS: Nonlinear Dynamic Analysis of Three Dimensional Base Isolated Structures," *Technical Report NCEER-91-0005*, National Center for Earthquake Engineering Research, State University of New York, Buffalo, NY.

Ozdemir H. (1976), "Nonlinear Transient Dynamic Analysis of Yielding Structures," Ph.D. Thesis, Department of Civil Engineering, University of California, at Berkeley, CA.

Park, Y. J., Wen, Y. K., and Ang, A. H. S. (1986), "Random Vibration of Hysteretic Systems under Bidirectional Ground Motions," *Earthquake Engineering and Structural Dynamics*, 14(4), 543-557.

Research Engineers International (2002), "Computer Program STAAD Pro."

Roussis, P. C. and Constantinou, M. C. (2005), "Experimental and Analytical Studies of

Structures Seismically Isolated with an Uplift-Restraint Isolation System," *Technical Report MCEER-05-0001*, Multidisciplinary Center for Earthquake Engineering Research, State University of New York, Buffalo, NY.

Scheller, J. and Constantinou, M. C. (1999), "Response History Analysis of Structures with Seismic Isolation and Energy Dissipation Systems: Verification Examples for Program SAP2000," *Technical Report MCEER-99-0002*, Multidisciplinary Center for Earthquake Engineering Research, Buffalo, NY.

Soong T. T. and Constantinou M. C. (1994), *Passive and Active Structural Vibration Control in Civil Engineering*, Springer-Verlag: Wien, NY.

Tsopelas, P.C., Constantinou, M.C., and Reinhorn, A.M. (1994), "3D-BASIS-ME: Computer Program for Nonlinear Dynamic Analysis of Seismically Isolated Single and Multiple Structures and Liquid Storage Tanks," *Technical Report MCEER-94-0010*, Multidisciplinary Center for Earthquake Engineering Research, State University of New York, Buffalo, NY.

Zayas V., Low S. S., and Mahin S. A. (1987), "The FPS Earthquake Resisting System: Experimental Report," *Technical Report UBC/EERC-87/01*, Earthquake Engineering Research Center, University of California, Berkeley, CA.

APPENDIX A

EXAMPLE OF CALCULATION OF STORY STIFFNESS

AND LOCATION OF CENTER OF STIFFNESS

EXAMPLE OF CALCULATION OF STORY STIFFNESS AND LOCATION OF CENTER OF STIFFNESS

This appendix presents an example of calculating the stiffness and location of the center of stiffness of a story. A story is the part of the substructure between two bases exclusive of the isolators. The resultant stiffness in the two horizontal directions, the rotational stiffness and the location of the center of stiffness are parameters that must be input in program 3D-BASIS-ME-MB for each story of the substructure.

Consider Figure 1-2 and the story between bases 3 and 4. In determining the stiffness and location of the center of stiffness of this story, the structure needs to be modeled in a static analysis program exclusive of the isolators. Each base in this model will be modeled as a rigid diaphragm. Base 4 will be restrained against lateral movement and rotation. Horizontal loads will be applied to base 3 and the displacement and rotation of base 3 with respect to base 4 will be calculated and used to determine the stiffness and location of the center of stiffness. Two loading cases in each principal direction need to be considered. It is appropriate to include in the model of analysis the part of the structure above base 3. However, in the example this part is disregarded for simplicity and ease in the presentation of results.

Figure A-1 shows the analyzed system. Since base 4 is the lowest base (at the ground level) it modeled fixed to the ground. Also, the part above base 3 is disregarded (only for simplicity in this example). The vertical elements in this story consist of six columns of which four are rigidly connected to the bases and two (numbered 1 and 2) are pin-connected at the bottom. Figure A-1 presents the model of the story in program STAAD. Input to this program is listed in Table A-1. Analysis is performed only for loading in the transverse direction (direction Z in the STAAD model) so that only the following can be calculated: rotational stiffness, transverse stiffness (or Z direction stiffness in the STAAD model) and the location of the center of stiffness in the longitudinal direction (direction X in the STAAD model). A similar analysis for loading in the longitudinal direction (or X direction in the STAAD model) will result in the longitudinal stiffness (or X direction stiffness in the STAAD model) and the location of the center of stiffness along the transverse direction (or Z direction in the STAAD model).

Loads are applied at joints 7 and 18 in the transverse direction and the displacements and rotations are calculated. Output of program STAAD is listed in Table A-2 and Figure A-2 shows a graph of the deformed structure under action of one of the joint loads.

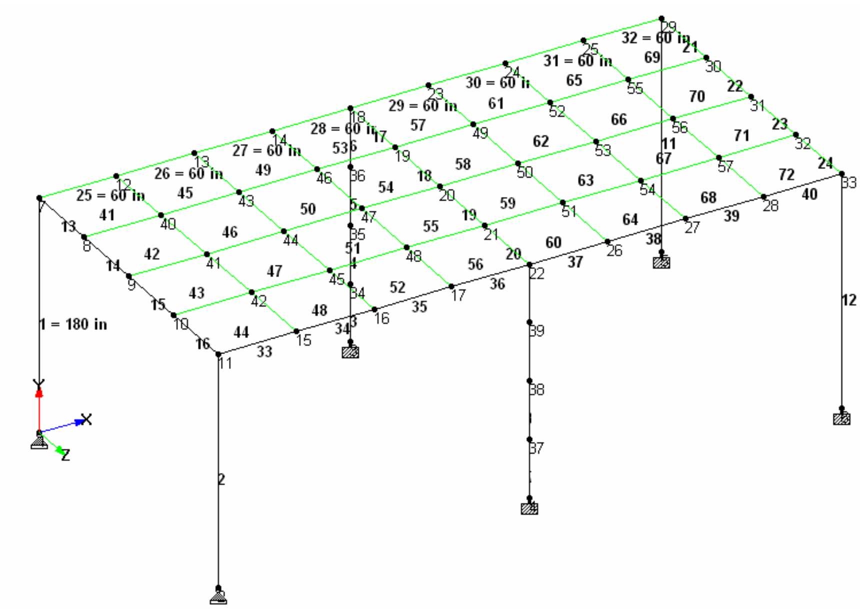

Figure A-1: Model of story between bases 3 and 4 in program STAAD.

Table A-1: Input to program STAAD

```
STAAD SPACE
* EXAMPLE PROBLEM FOR CALCULATING
*STIFFNESS AND LOCATION OF CENTER OF STIFFNESS
UNIT FEET KIP
JOINT COORD
1 0 0 0 ; 2 0 0 20
REP ALL 2 20 0 0
7 0 15 0 11 0 15 20
12 5 15 0 14 15 15 0
15 5 15 20 17 15 15 20
18 20 15 0 22 20 15 20
23 25 15 0 25 35 15 0
26 25 15 20 28 35 15 20
29 40 15 0 33 40 15 20
34 20 3.75 0 36 20 11.25 0
37 20 3.75 20 39 20 11.25 20
MEMBER INCI
*COLUMNS
1 1 7 ; 2 2 11
3 3 34 ; 4 34 35 ; 5 35 36 ; 6 36 18
7 4 37 ; 8 37 38 ; 9 38 39 ; 10 39 22
11 5 29 ; 12 6 33
*BEAMS IN Z DIRECTION AT X=0
13 7 8 16
*BEAMS IN Z DIRECTION AT X=20
17 18 19 20
*BEAMS IN Z DIRECTION AT X=40
21 29 30 24
*BEAMS IN X DIRECTION AT Z = 0
25 7 12 ; 26 12 13 ; 27 13 14 ; 28 14 18
```

```
29 18 23 ; 30 23 24 ; 31 24 25 ; 32 25 29
*BEAMS IN X DIRECTION AT Z = 20
33 11 15 ; 34 15 16 ; 35 16 17 ; 36 17 22
37 22 26 ; 38 26 27 ; 39 27 28 ; 40 28 33
DEFINE MESH
A JOINT 7
B JOINT 11
C JOINT 22
D JOINT 18
E JOINT 33
F JOINT 29
G JOINT 3
H JOINT 4
GENERATE ELEMENT
MESH ABCD 4 4
MESH DCEF 4 4
*
MEMB PROP
1 TO 40 PRIS YD 1 ZD 1
ELEM PROP
*
41 TO 72 TH 5.0
UNIT INCH
CONSTANT
E 3000 ALL
POISSON CONCRETE ALL
SUPPORT
3 TO 6 FIXED
1 2 PINNED
LOAD 1
JOINT LOAD
7 FZ 1000
LOAD 2
JOINT LOAD
18 FZ 1000
PERFORM ANALYSIS
PRINT DISPLACEMENTS LIST 7 18
FINISH
```

Table A-2: Output of program STAAD

JOINT DISPLACEMENT (INCH RADIANS)   STRUCTURE TYPE = SPACE

JOINT	LOAD	X-TRANS	Y-TRANS	Z-TRANS	X-ROTAN	Y-ROTAN	Z-ROTAN
7	1	-19.40704	0.08213	72.83197	0.00193	0.16202	0.00077
	2	-4.82303	0.05593	34.01469	0.00103	0.04003	0.00034
18	1	-19.38635	0.08121	34.01469	0.00113	0.16093	0.00016
	2	-4.82710	0.06784	24.37395	0.00089	0.04007	0.00006

************** END OF LATEST ANALYSIS RESULT **************

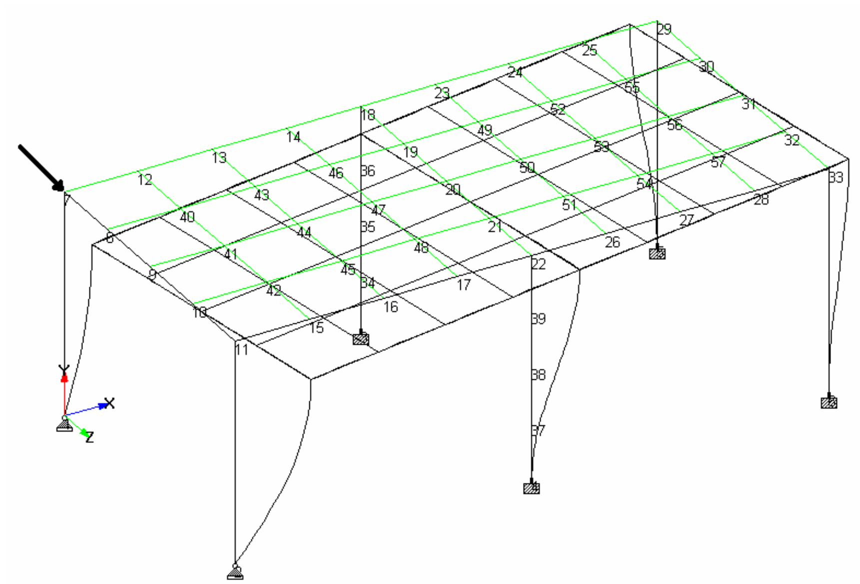

Figure A-2: Deformed story under action of load at joint 7.

Results of the analysis are used as follows to calculate the stiffness and location of the center of stiffness. The displacement of joint 7 in the direction of the applied load of 1000 kip at joint 7 can be written as:

$$u_7 = u_T + \theta_7 X_7 \qquad \text{(A-1)}$$

where u_T is the displacement of the center of stiffness, θ_7 is the rotation of the base and X_7 is the distance (along the X axis) of joint 7 to the center of stiffness. Similarly, the displacement of joint 18 in the direction of the applied load of 1000 kip at joint 18 can be written as:

$$u_{18} = u_T + \theta_{18} X_{18} \qquad \text{(A-2)}$$

where u_T is the displacement of the center of stiffness, θ_{18} is the rotation of the base and X_{18} is the distance (along the X axis) of joint 18 to the center of stiffness ($X_{18} = X_7 - 240\ in$).

From analysis (see Table A-2), $u_7 = 72.832\ in.$, $\theta_7 = 0.1615 rad$ (average of values at joints 7 and 18: 0.162 and 0.161), $u_{18} = 24.374\ in.$ and $\theta_{18} = 0.040\ rad$ (average values at joints 7 and 18). Solution of equations (A-1) and (A-2) results in values for displacement u_T and distance X_1:

$u_T = 21.18\ in., X_7 = 319.82\ in.$ The translational stiffness in the Z direction is then calculated as

$$K_z = F_7 / u_T = 1000/21.18 = 47.21 \ kip/in \quad \text{(A-3)}$$

The rotational stiffness is calculated as

$$K_R = F_7 X_7 / \theta_7 = 1000 \cdot 319.82/0.1615 = 1{,}980{,}310 \ kip-in/rad \quad \text{(A-4)}$$

The rotational stiffness can also be calculated from the data in the case of loading joint 18:

$$K_R = F_{18}(X_7 - 240)/\theta_{18} = 1000 \cdot (319.82 - 240)/0.04 = 1{,}995{,}500 \ kip-in/rad \quad \text{(A-5)}$$

The difference in the numbers calculated by equations (A-4) and (A-5) are due to rounding of numbers. It is appropriate to use the average value of the two figures in Equations (A-4) and (A-5), $K_R = 1{,}987{,}905 \ kip-in/rad$, which is within 5% of the calculated values in the two cases of loading.

APPENDIX B

INPUT TO PROGRAM 3D-BASIS-ME-MB

FOR EXAMPLE OF 7-STORY TESTED MODEL

Input consists of the following (six) files:

- File **3DBMEMB.DAT** which contains the description of the structure to be analyzed. The content of the file for this structure is printed below.

```
7-STORY BUILDING WITH 8 FPS ISOLATION SYSTEM - VARIABLE NORMAL LOAD N=T*F
in              kips/in*sec^2       sec
GENERAL CONTROL INFORMATION
: comment line
2 1 1 4 4 2 386.22
SUPERSTRUCTURE CONTROL INFORMATION
6 6
INTEGRATION CONTROL PARAMETERS
0.001 0.0001 100000 500 1
NEWMARK METHOD CONTROL PARAMETERS
:(DEFAULT VALUES: 0.50 AND 0.25)
0.5 0.25
EARTHQUAKE CONTROL PARAMETERS
1 0.01 3001 0 386.22
SUPERSTRUCTURE INFORMATION
BUILDING No#1
EIGENVALUES
142.62  1581.29384  5599.812644  13237.78684  24804.06141  37147.06764
EIGENVECTORS
3.8970  0.00  0.00  3.7247  0.00  0.00  3.4184  0.00  0.00  2.9821  0.00  0.00  2.4243  0.00  0.00  1.6753  0.00  0.00
4.0801  0.00  0.00  2.3826  0.00  0.00  -0.1510  0.00  0.00  -2.6037  0.00  0.00  -4.0066  0.00  0.00  -3.6286  0.00  0.00
-3.7532  0.00  0.00  0.6197  0.00  0.00  4.0636  0.00  0.00  2.8507  0.00  0.00  -1.6122  0.00  0.00  -4.0673  0.00  0.00
3.0145  0.00  0.00  -3.4181  0.00  0.00  -2.3582  0.00  0.00  3.6863  0.00  0.00  2.0020  0.00  0.00  -3.7517  0.00  0.00
-2.0447  0.00  0.00  4.2531  0.00  0.00  -2.7092  0.00  0.00  -1.4283  0.00  0.00  4.2003  0.00  0.00  -2.9150  0.00  0.00
-1.0061  0.00  0.00  2.8085  0.00  0.00  -4.0633  0.00  0.00  4.2654  0.00  0.00  -3.3846  0.00  0.00  1.5948  0.00  0.00
TRANSLATIONAL MASS OF FLOORS
0.016829786  0.017347626  0.017347626  0.017347626  0.017347626  0.017347626
ROTATIONAL MOMENT OF INERTIA OF FLOORS
100.0 100.0 100.0 100.0 100.0 100.0
MODAL DAMPING RATIO
0.0142 0.0204 0.0235 0.0155 0.0059 0.0086
X-Y COORDINATES OF C.M. OF FLOORS W.R.T. C.M. OF TOP/1ST BASE
0 0   0 0   0 0   0 0   0 0   0 0
HEIGHT OF FLOORS  of Building #1
216 180 144 108 72 36
HEIGHT OF BASES  FROM GROUND
0.0
STIFFNESS DATA OF THE LINEAR ELASTIC ELENMENTS CONNECTING TWO SUBSEQUENT BASES
0 0 0      0 0      0 0
TRANSLATIONAL AND ROTATIONAL MASS DATA OF THE BASES
0.01968 100.0
DAMPER DATA OF THE LINEAR VISCOUS ELENMENTS CONNECTING TWO SUBSEQUENT BASES
0 0 0      0 0      0 0
X-Y COORDINATES OF ISOLATORS
-72 0
-24 0
24 0
72 0
ISOLATOR DATA
1 3 6
9.75 0.06 0.06 0.04 0.04 1.09 1.09 0.04 0.04 7.92
1 3 6
9.75 0.06 0.06 0.04 0.04 1.09 1.09 0.04 0.04 15.84
1 3 6
```

```
9.75 0.06 0.06 0.04 0.04 1.09 1.09 0.04 0.04 15.84
1 3 6
9.75 0.06 0.06 0.04 0.04 1.09 1.09 0.04 0.04 7.92
OUTPUT CONTROL PARAMETERS
1 10 1
ISOLATOR NUMBER WHICH OUTPUT IS DESIRED
1 2 3 4
COORDINATES OF DESIRED INTERSTORY DRIFT
BUILDING No 1
4
-72 -24
-24 -24
24 -24
72 -24
INITIAL CONDITIONS OF EACH BASE
 0.0 0.0 0.0
```

- File **TMATRIX.DAT** which contains matrix [T]. The content of the file for this structure is printed below.

```
-1.7964   0.0  0.0 -1.5444  0.0  0.0 -1.2946  0.0 0.0 -1.0434 0.0 0.0  -0.7904 0.0  0.0 -0.5352  0.0 0.0 -0.2714 0.0  0.0
0.13934  0.0   0.0  0.13296  0.0  0.0  0.1338  0.0  0.0  0.13032  0.0  0.0  0.12122  0.0   0.0  0.10572  0.0  0.0  0.06442  0.0  0.0
-0.13934  0.0  0.0  -0.13296  0.0  0.0  -0.1338  0.0   0.0  -0.13032  0.0 0.0  -0.12122  0.0  0.0  -0.10572  0.0  0.0  -0.06442 0.0  0.0
1.7964  0.0  0.0  1.5444  0.0  0.0  1.2946  0.0  0.0  1.0434  0.0  0.0  0.7904  0.0  0.0  0.5352  0.0  0.0  0.2714  0.0  0.0
```

- File **TMATRIXUPLF.DAT** which contains matrix [A]. The content of the file for this structure is printed below.

```
1.0000   -0.6000    0.2000   0.4040
-1.5950   1.0000   -0.6000   0.1932
 0.1932  -0.6000    1.0000  -1.5950
 0.4040   0.2000   -0.6000   1.000
```

- Files **WAVEX.DAT, WAVEY.DAT**, and **WAVEZ.DAT** which contain the seismic input (acceleration histories in horizontal longitudinal, horizontal transverse and vertical directions). Partial contents of these files are printed below.

WAVEX.DAT	**WAVEY.DAT**	**WAVEZ.DAT**
.00019	0	0
-.00025	0	0
-.00081	0	0
-.00013	0	0
-.00031	0	0
-.00006	0	0
-.00044	0	0
etc.	etc.	etc.

APPENDIX C

CONSTRUCTION OF RELATION BETWEEN INERTIA FORCES AND AXIAL BEARING LOADS IN EXAMPLE OF TESTED 7-STORY MODEL

CONSTRUCTION OF RELATION BETWEEN INERTIA FORCES AND AXIAL BEARING LOADS IN EXAMPLE OF TESTED 7-STORY MODEL

For the 7-story model verification example described in Section 4.2, the coefficient matrices $\left[T\right]$ and $\left[A\right]$, which are required for accounting for the variation of normal loads on isolators, were constructed as follows:

- Matrix $\left[T\right]$ was calculated by static analysis in computer code SAP2000 of a model of the 7-story structure with all bearings represented as pins.
- Matrix $\left[A\right]$ was also calculated in a series of four SAP2000 static analyses in which one of the four supports was removed, an upward unit load was applied at the bearing location, and the reactions at the remaining three bearings (represented as pins) were calculated.

Figure C-1 shows the models considered in constructing matrix $\left[T\right]$. The reactions in this case, where a unit force is applied at the 7th floor, correspond to the 1st column of matrix $\left[T\right]$. The complete matrix is obtained in an analogous way by applying the unit force at each floor level.

Matrix $\left[T\right]$ is presented below:

$$\begin{bmatrix} -1.7964 & 0 & 0 & -1.5444 & 0 & 0 & -1.2946 & 0 & 0 & -1.0434 & 0 & 0 & -0.7904 & 0 & 0 & -0.5352 & 0 & 0 & -0.2714 & 0 & 0 \\ 0.1393 & 0 & 0 & 0.1329 & 0 & 0 & 0.1338 & 0 & 0 & 0.1303 & 0 & 0 & 0.1212 & 0 & 0 & 0.1057 & 0 & 0 & 0.0644 & 0 & 0 \\ -0.1393 & 0 & 0 & -0.1329 & 0 & 0 & -0.1338 & 0 & 0 & -0.1303 & 0 & 0 & -0.1212 & 0 & 0 & -0.1057 & 0 & 0 & -0.0644 & 0 & 0 \\ 1.7964 & 0 & 0 & 1.5444 & 0 & 0 & 1.2946 & 0 & 0 & 1.0434 & 0 & 0 & 0.7904 & 0 & 0 & 0.5352 & 0 & 0 & 0.2714 & 0 & 0 \end{bmatrix}$$

Note that several columns in matrix $\left[T\right]$ have zero values. The zero elements in the matrix represent reactions at the four supports due to inertia forces acting in the transverse (z) direction and in the rotational direction (moment about vertical axis). This is necessary since the model in 3D-BASIS-ME-MB is three-dimensional, wheres the analysis performed herein is two-dimensional. Note that in a three-dimensional analysis of the structure (by including excitation in the transverse direction or by providing torsional coupling), these elements would not be zero.

Matrix $\left[A\right]$ was calculated by the procedure described in Section 3.2, which is illustrated in the schematic of Figure C-2.

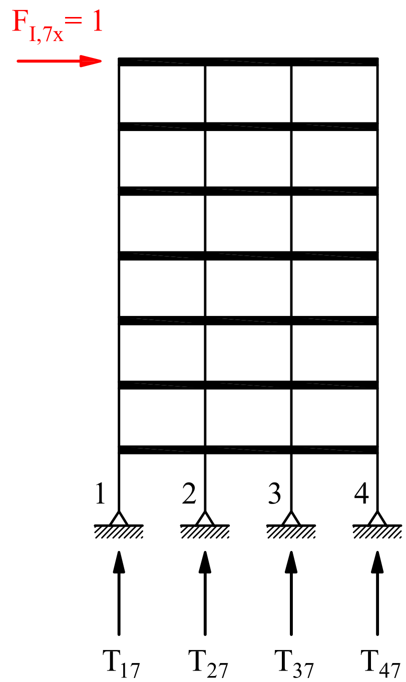

Figure C-1: Structural model used in constructing matrix $[T]$. (The reaction forces shown constitute the first column of matrix $[T]$)

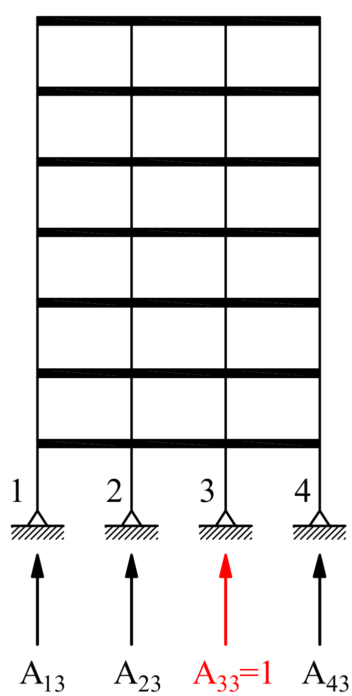

Figure C-2: Illustration of procedure used to construct matrix $[A]$.

The resulting matrix $[A]$ is presented below.

$$A = \begin{bmatrix} 1 & -0.6 & 0.2 & 0.404 \\ -1.595 & 1 & -0.6 & 0.1932 \\ 0.1932 & -0.6 & 1 & -1.595 \\ 0.404 & 0.2 & -0.6 & 1 \end{bmatrix}$$

Matrices $[T]$ and $[A]$ are supplied to program 3D-BASIS-ME-MB in input files **TMATRIX.DAT** and **TMATRIXUPLF.DAT**, respectively. Program 3D-BASIS-ME-MB performs calculations at each time step and determines the axial loads on each bearing using the procedure described in Section 3. The calculation is done in subroutine **INERVSAXLOADTRNSMTRX**.

APPENDIX D

COMPARISON OF RESULTS OF PROGRAM 3D-BASIS-ME-MB TO EXPERIMENTAL RESULTS FOR TESTED 7-STORY MODEL

Superstructure Response: El Centro S00E 200%

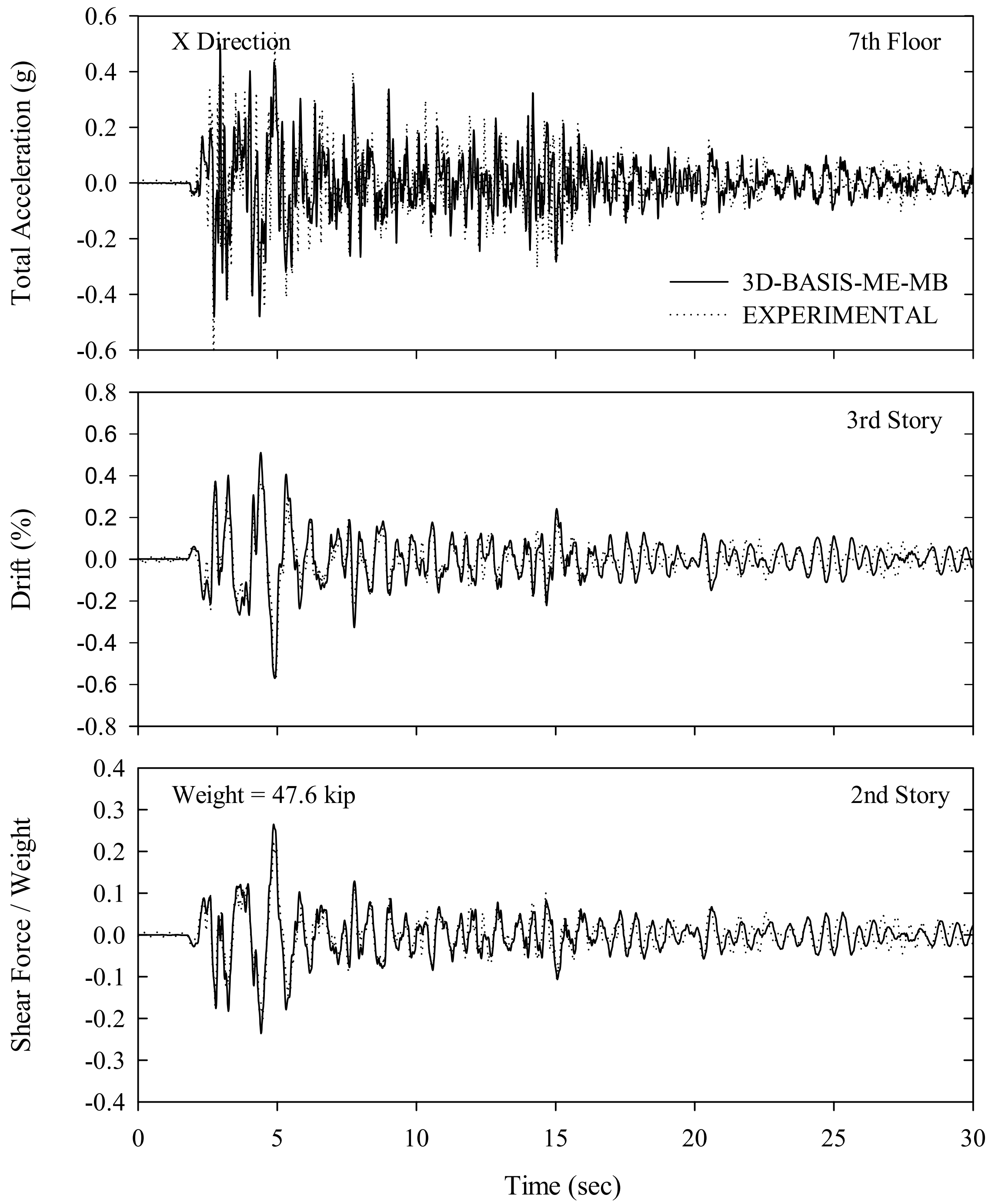

Isolation System Response: El Centro S00E 200%

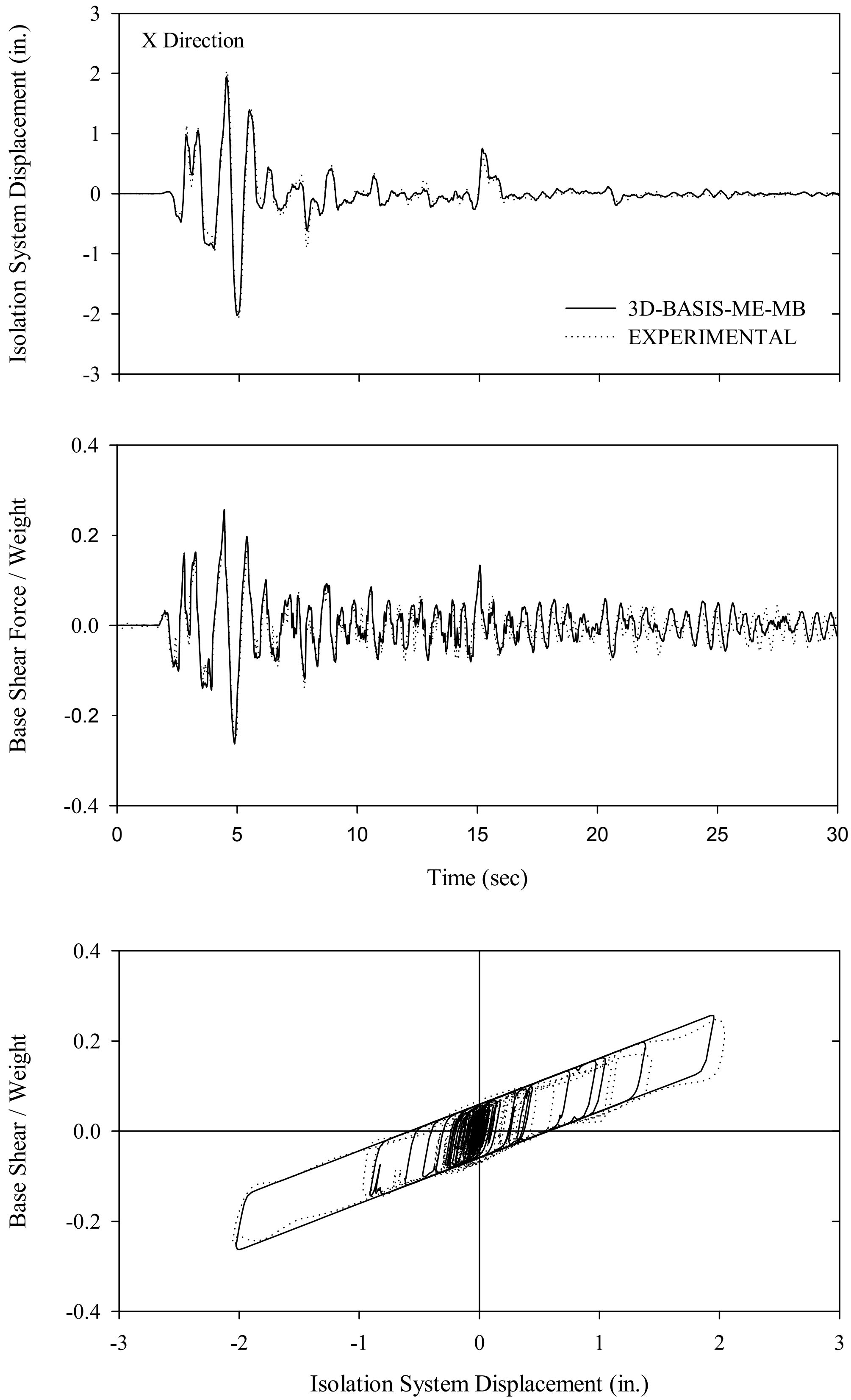

Individual Bearing Response: El Centro S00E 200%

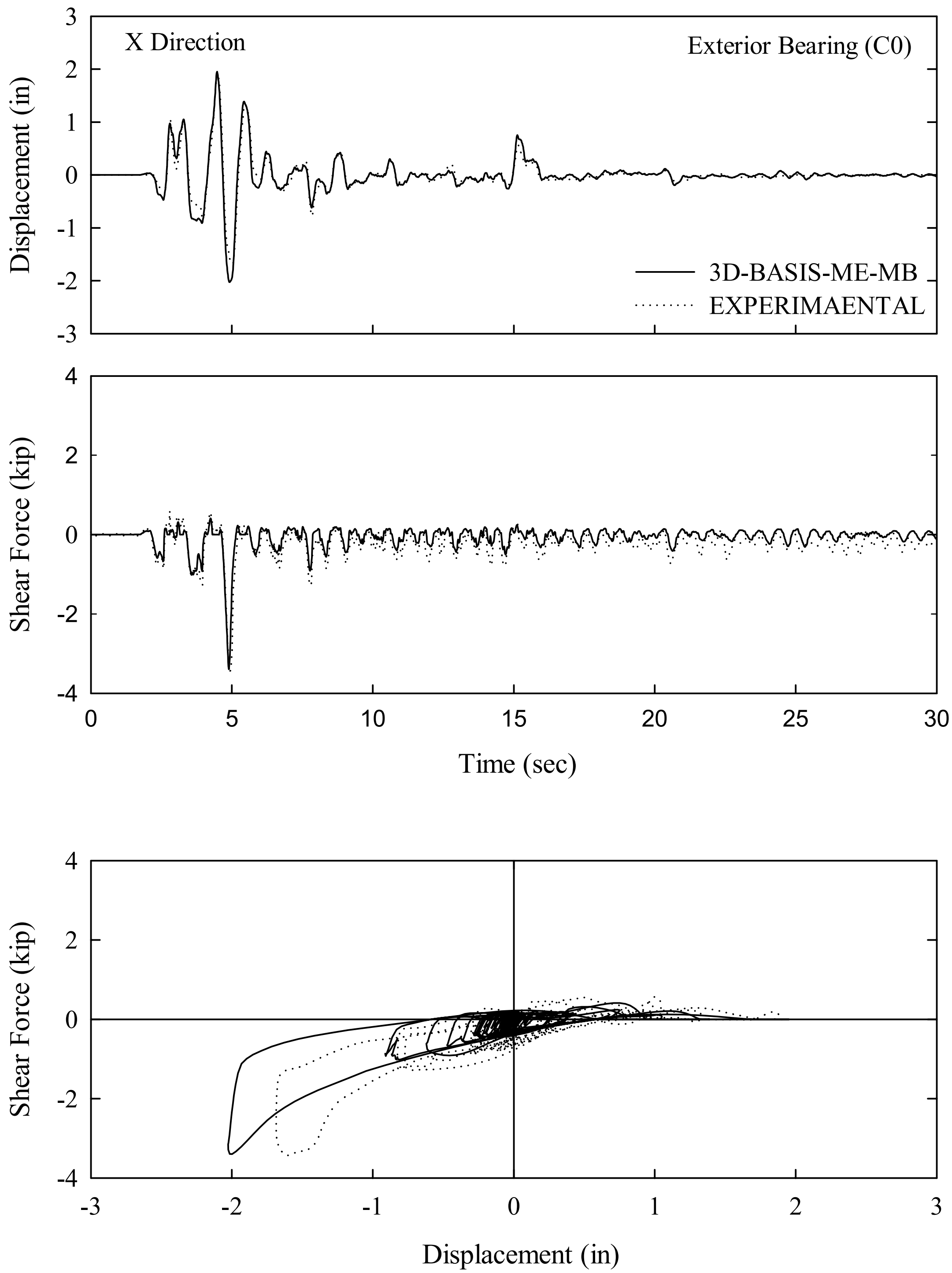

Individual Bearing Response: El Centro S00E 200%

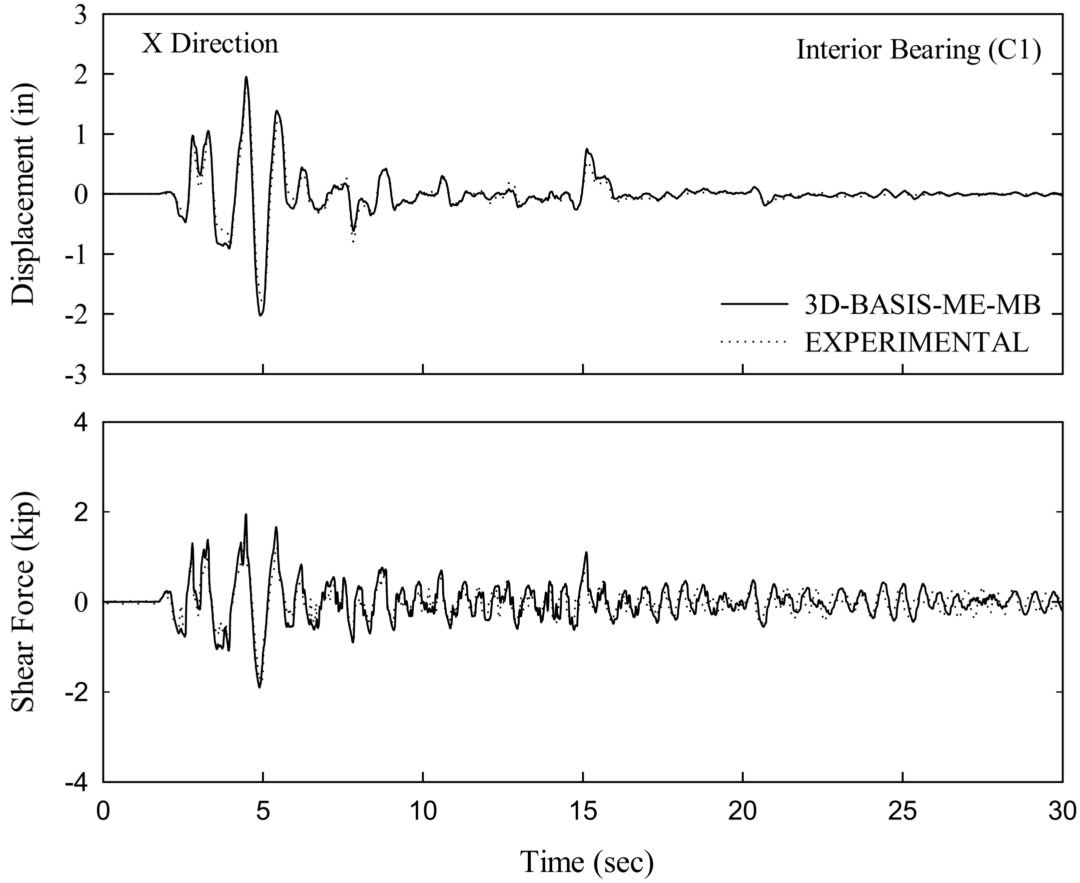

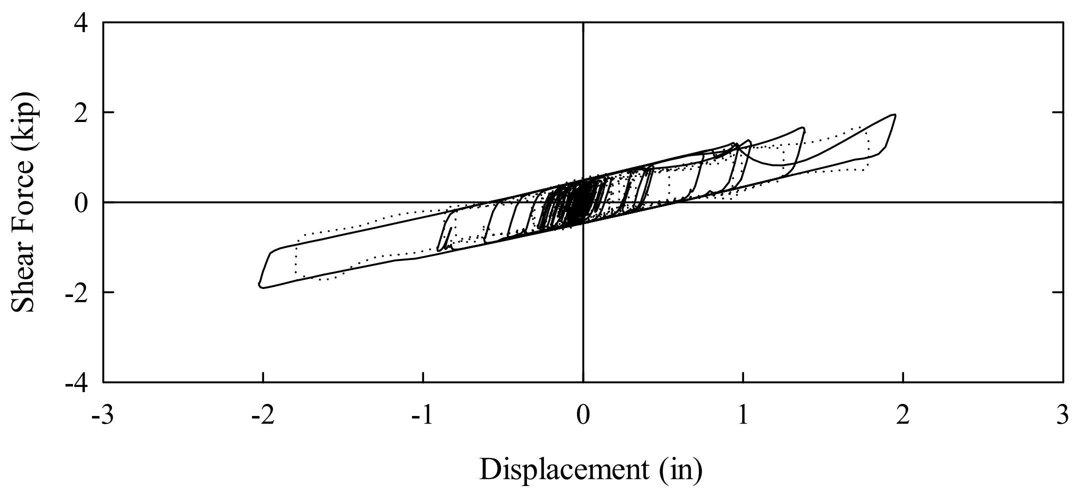

APPENDIX E

COMPARISON OF RESULTS OF PROGRAM ABAQUS TO EXPERIMENTAL RESULTS FOR TESTED 7-STORY MODEL

Superstructure Response: El Centro S00E 200%

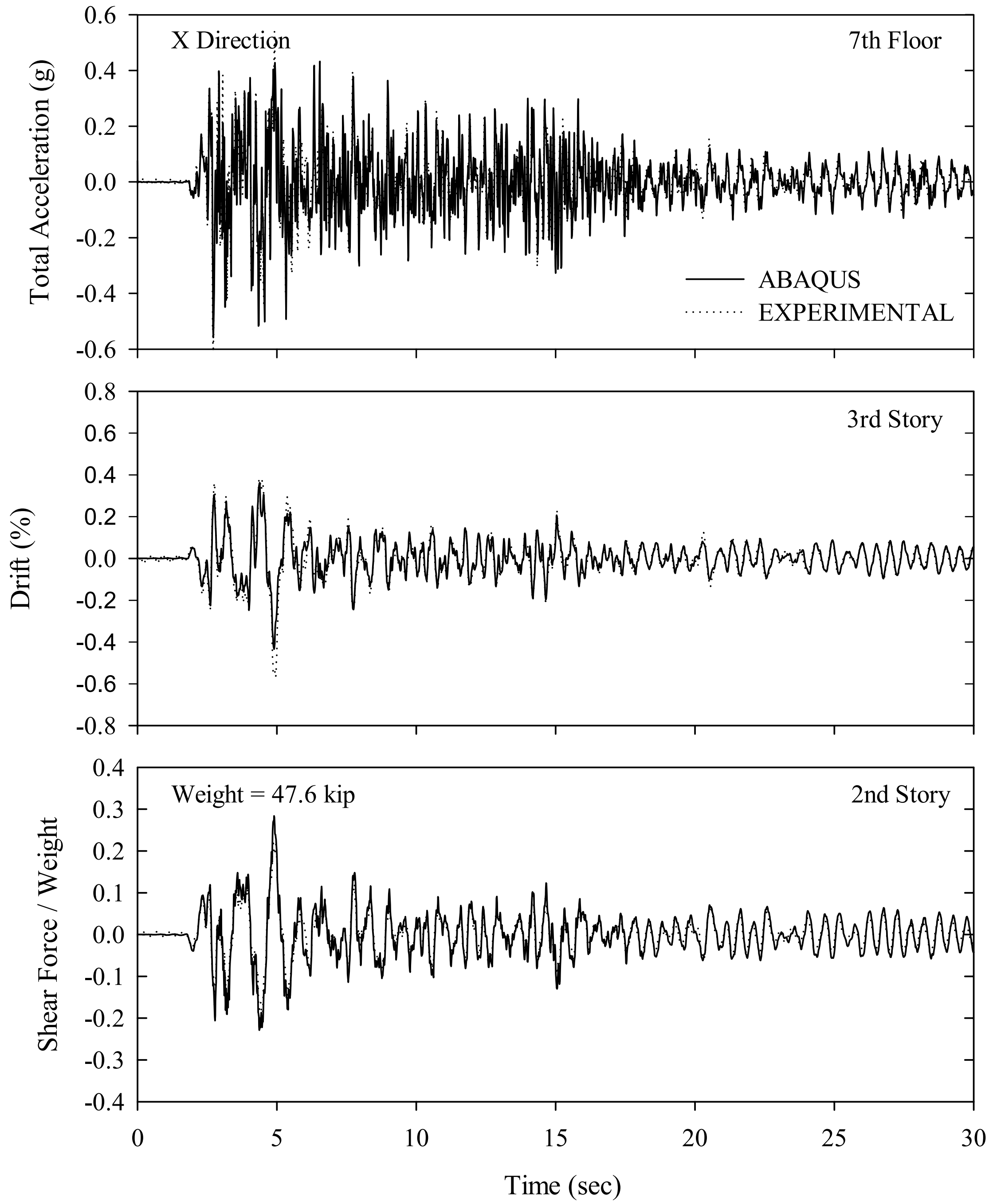

Isolation System Response: El Centro S00E 200%

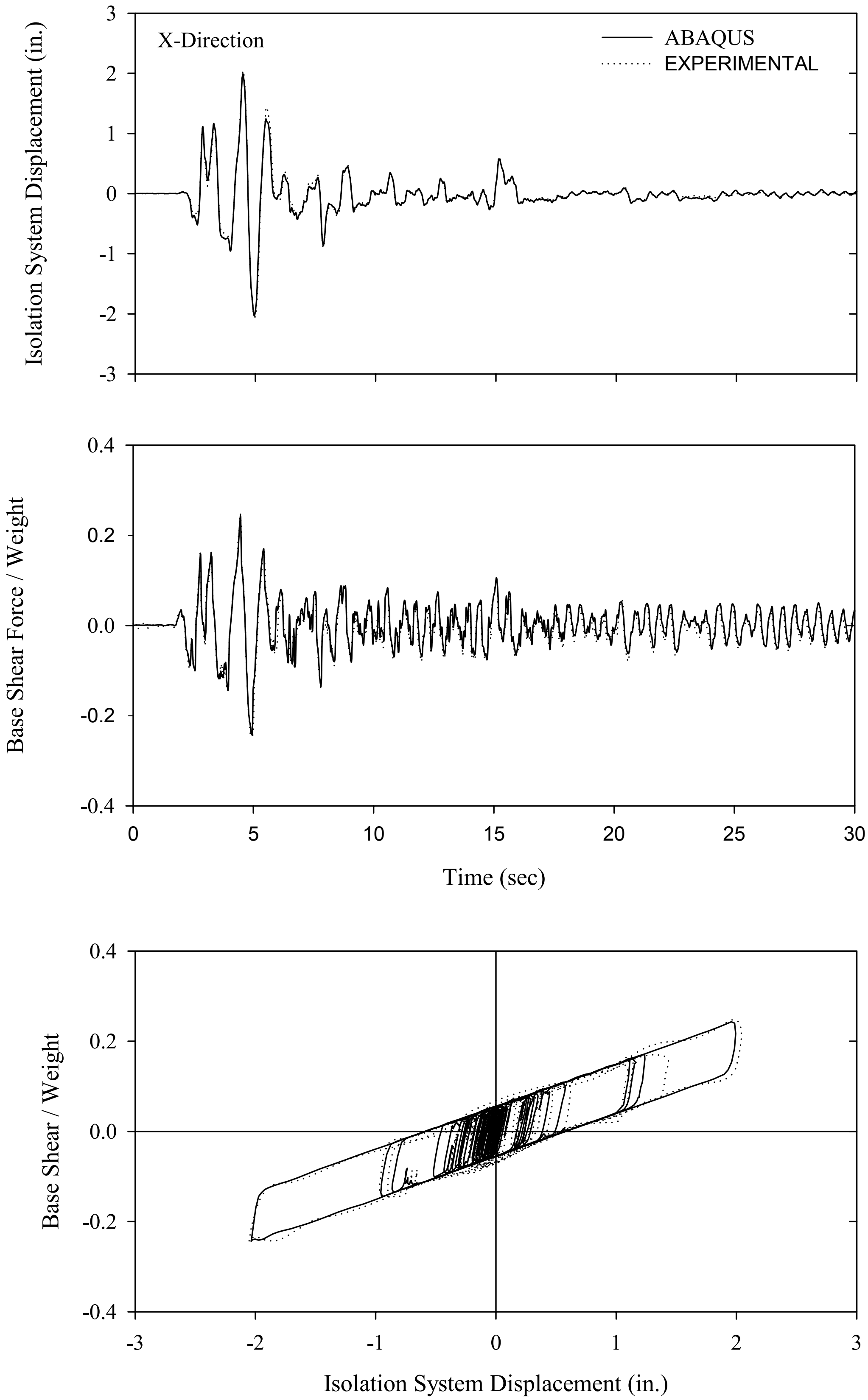

Individual Bearing Response: El Centro S00E 200%

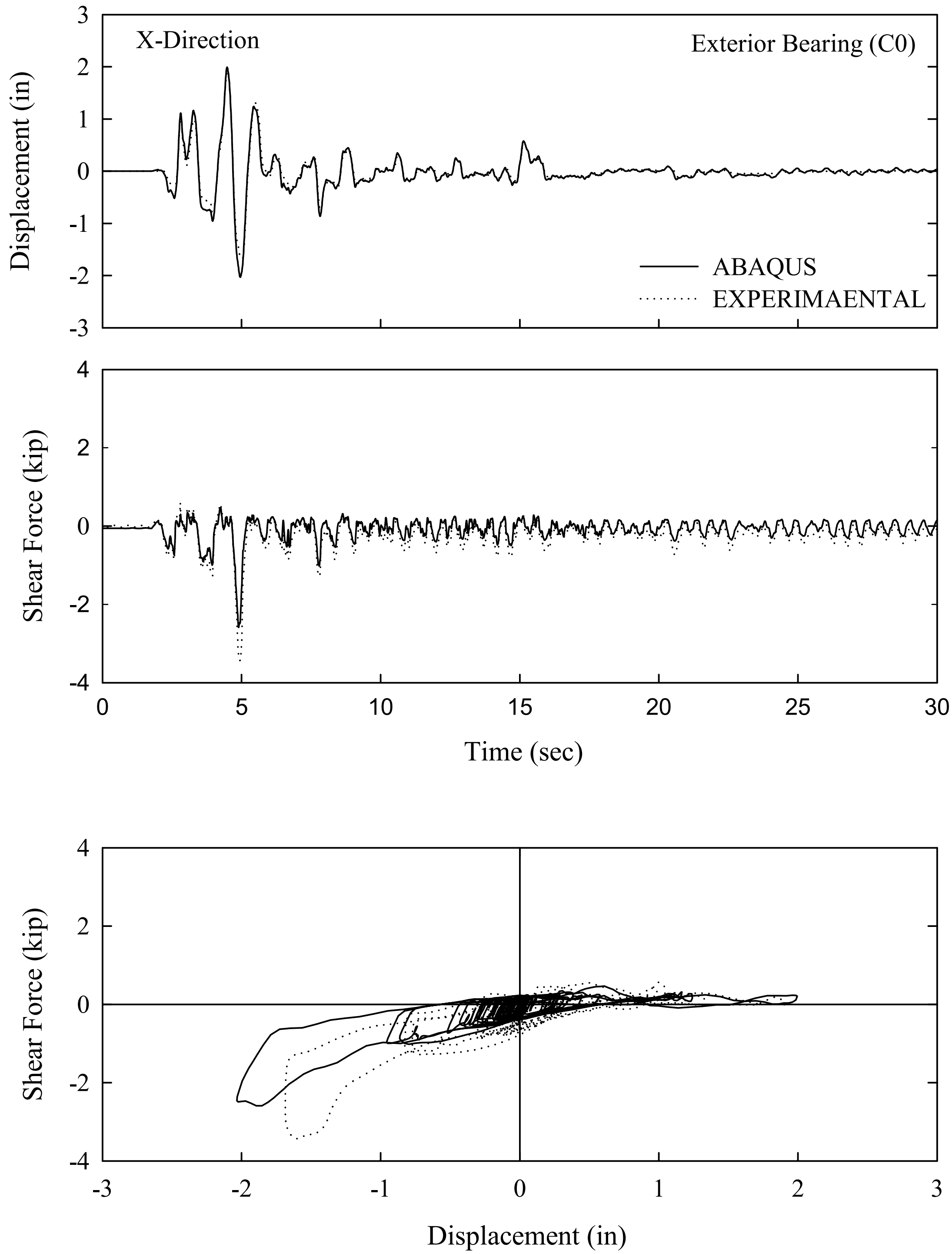

Individual Bearing Response: El Centro S00E 200%

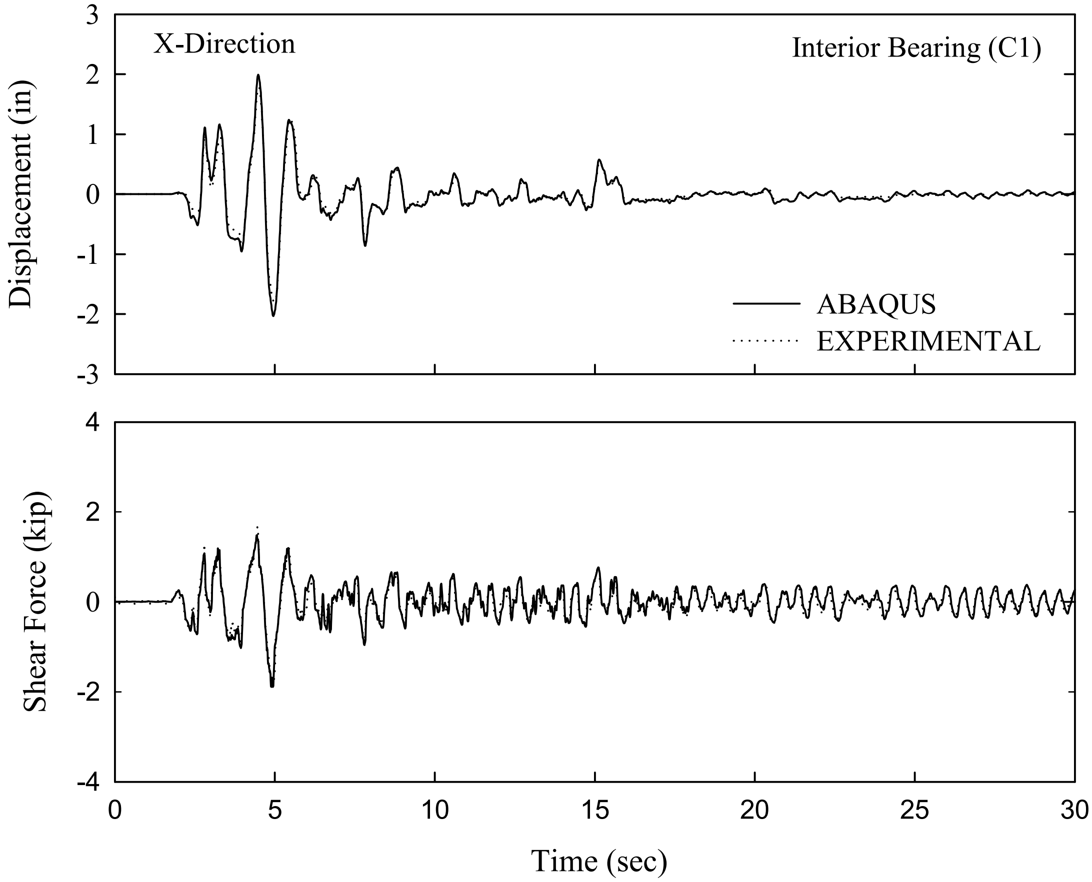

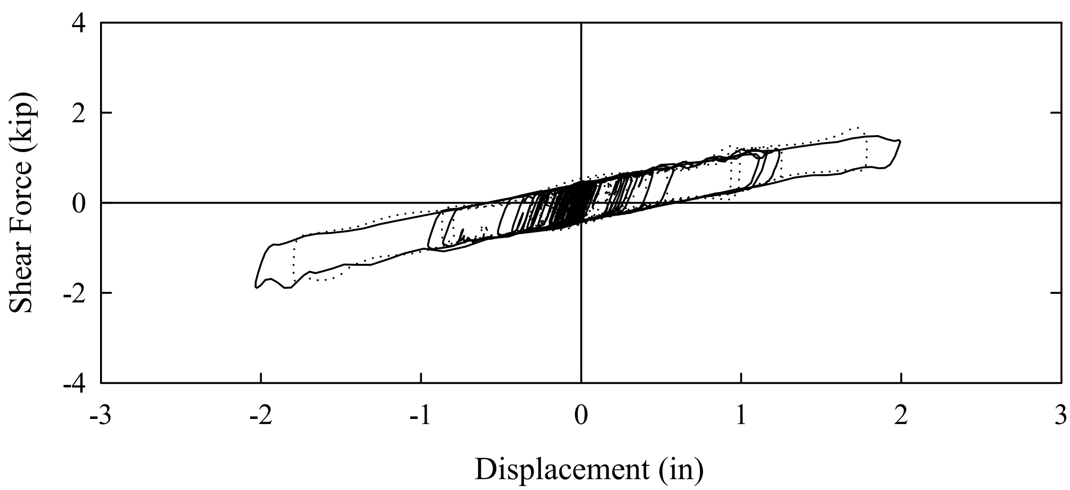

APPENDIX F

DESCRIPTION OF TWO-TOWER, SPLIT-ISOLATION LEVEL VERIFICATION MODEL

SECTION PROPERTIES

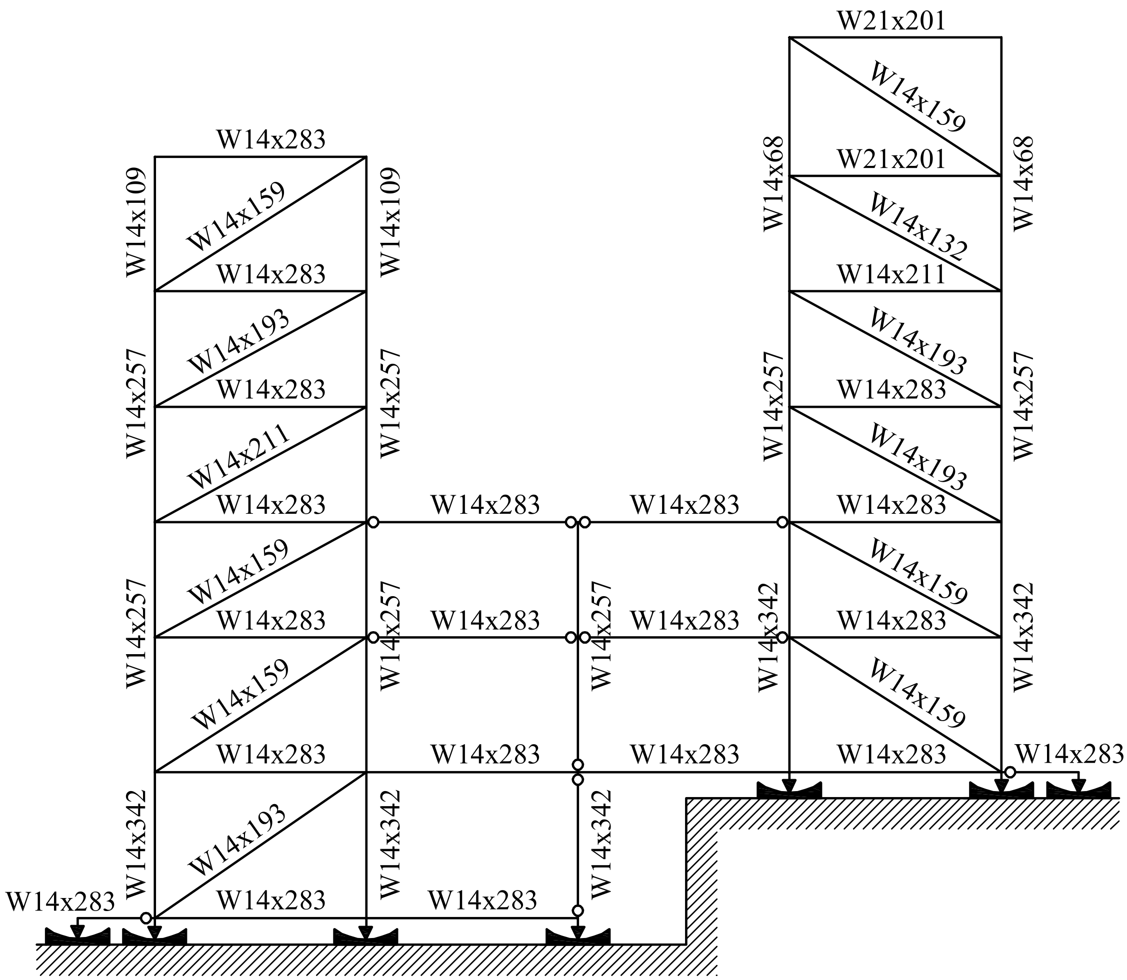

Section	A (in^2)	I (in^4)
W14x68	20.0	723
W14x109	32.0	1240
W14x159	46.7	1900
W14x193	56.8	2400
W14x257	75.6	3400
W14x283	83.3	3840
W14x342	101.0	4900
W21x201	59.2	5310
W14x211	62.0	2660
W14X132	38.8	1530

$E=E_{STEEL}=29{,}000$ ksi; $G=G_{STEEL}=11{,}000$ ksi; $A_{SHEAR}=A=AREA$

MODEL MASSES

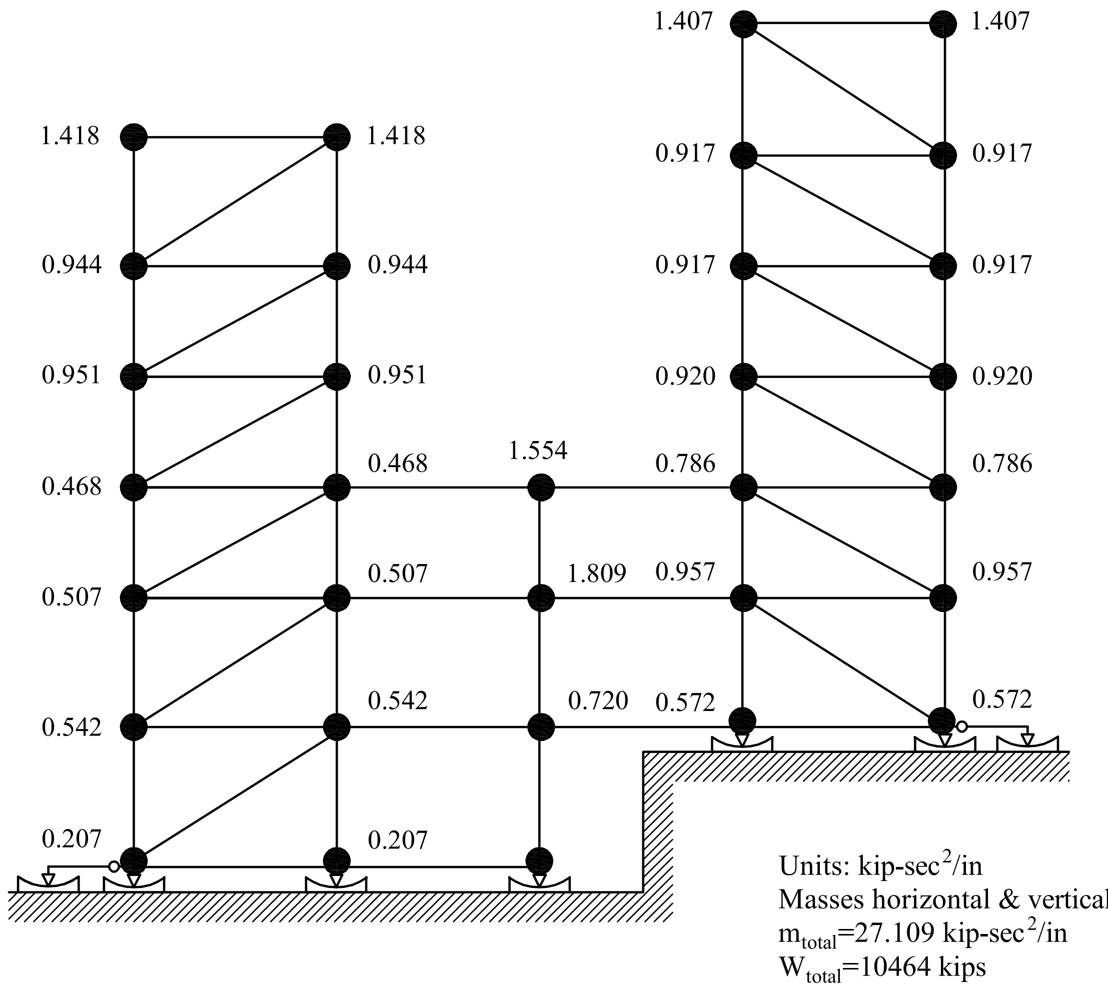

WEIGHT ON BEARINGS

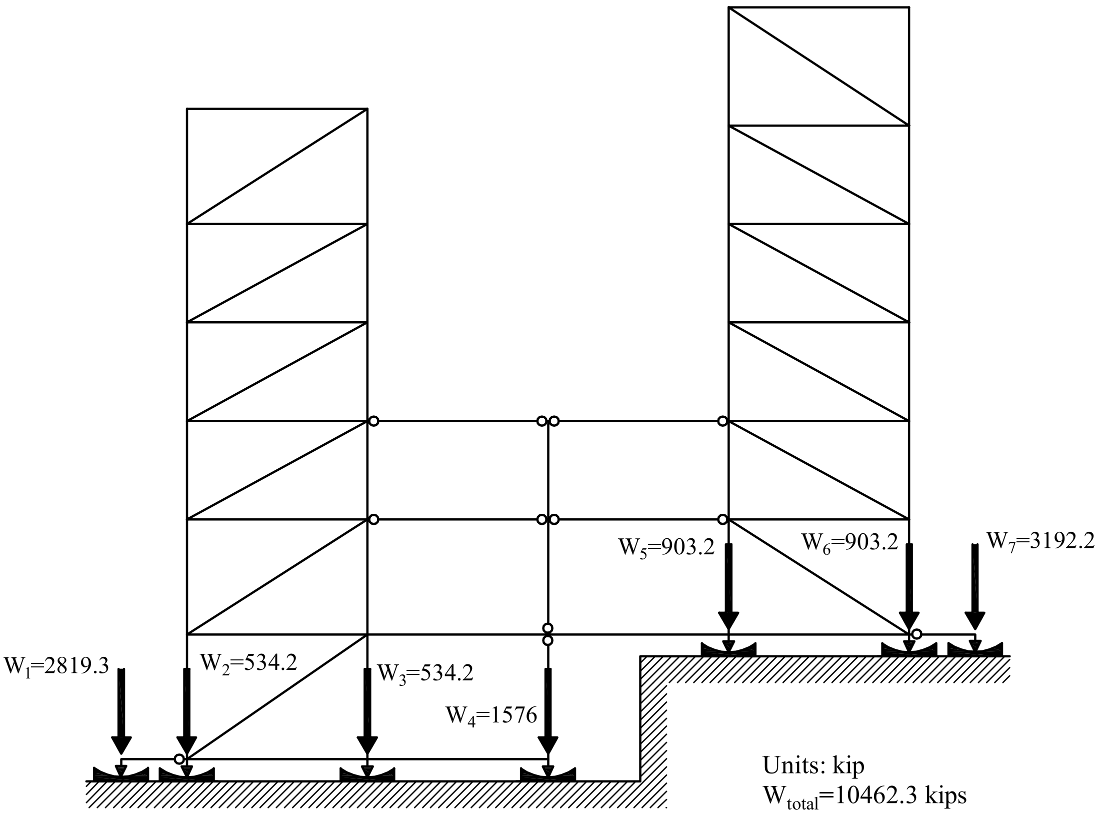

APPENDIX G

INPUT TO PROGRAM 3D-BASIS-ME-MB

FOR TWO-TOWER VERIFICATION MODEL

Input consists of the following (six) files:

- File **3DBMEMB.DAT** which contains the description of the structure to be analyzed. The content of the file for this structure is printed below.

```
2-Tower Hospital Model 2D  7-FPS ISOLATORS
in              Kip/in*sec^2        sec
GENERAL CONTROL INFORMATION
: comment line
2  2 4  7  7  2 386.22
SUPERSTRUCTURE CONTROL INFORMATION
3 3
4 4
INTEGRATION CONTROL PARAMETERS
0.001 0.0001 10000 1000 1
NEWMARK METHOD CONTROL PARAMETERS
:(DEFAULT VALUES: 0.50 AND 0.25)
0.5 0.25
EARTHQUAKE CONTROL PARAMETERS
: scale factor  386.22
1 0.005 8200 0 386.22
SUPERSTRUCTURE INFORMATION
BUILDING No#1
EIGENVALUES
:8.82  33.979  59.537
77.79 1154.57 3544.65
EIGENVECTORS
0.5079    0.0000    0.0000    0.3321    0.0000    0.0000    0.1779    0.0000    0.0000
0.2896    0.0000    0.0000 -0.4003    0.0000    0.0000    -0.4916   0.0000    0.0000
0.1036    0.0000    0.0000    -0.5091   0.0000    0.0000    0.5025    0.0000    0.0000
TRANSLATIONAL MASS OF FLOORS
2.846 1.888 1.902
ROTATIONAL MOMENT OF INERTIA OF FLOORS
1.E+6 1.E+6 1.E+6
MODAL DAMPING RATIO
0.02 0.02 0.02    0.02 0.02 0.02    0.02 0.02 0.02
X-Y COORDINATES OF C.M. OF FLOORS W.R.T. C.M. OF TOP/1ST BASE
0.0 0.0    0.0 0.0    0.0 0.0
HEIGHT OF FLOORS  of Building #1
 99.0   81.5  66.5
BUILDING No#2
EIGENVALUES
:6.863 23.937 43.542 60.439
47.10 572.98 1895.91 3652.87
EIGENVECTORS
0.4915    0.0000    0.0000    0.3432    0.0000    0.0000    0.2115    0.0000    0.0000  0.1098    0.0000    0.0000
0.2952    0.0000    0.0000 -0.2425    0.0000    0.0000    -0.4705   0.0000    0.0000 -0.3619    0.0000    0.0000
0.1606    0.0000    0.0000    -0.5625   0.0000    0.0000    0.1230    0.0000    0.0000  0.4167    0.0000    0.0000
0.0295    0.0000    0.0000 -0.2287    0.0000    0.0000    0.5138  0.0000    0.0000    -0.4763 0.0000    0.0000
TRANSLATIONAL MASS OF FLOORS
2.814 1.834 1.834 1.84
ROTATIONAL MOMENT OF INERTIA OF FLOORS
1.E+6 1.E+6 1.E+6 1.E+6
MODAL DAMPING RATIO
0.02 0.02 0.02    0.02 0.02 0.02    0.02 0.02 0.02    0.02 0.02 0.02
X-Y COORDINATES OF C.M. OF FLOORS W.R.T. C.M. OF TOP/1ST BASE
0.0 0.0    0.0 0.0    0.0 0.0    0.0 0.0
HEIGHT OF FLOORS  of Building #2
 114.5  96.5   81.5  66.5
```

```
HEIGHT OF BASES  FROM GROUND
 51.5   36.5  19.0  0.0
STIFFNESS DATA OF THE LINEAR ELASTIC ELENMENTS CONNECTING TWO SUBSEQUENT BASES
: ONLY BRACES CONTRIBUTE IN STIFFNESS
4586.   4586.    1.e+15   0.0  0.0     0.0  0.0
4775.   4775.    1.e+15   0.0  0.0     0.0  0.0
2307.   2307.    1.e+15   0.0  0.0     0.0  0.0
   0.0         0.0       0.0      0.0  0.0     0.0  0.0
TRANSLATIONAL AND ROTATIONAL MASS DATA OF THE BASES
4.062 1.E8
4.737 1.E8
2.948 1.E8
0.414 1.E8
DAMPER DATA OF THE LINEAR VISCOUS ELENMENTS CONNECTING TWO SUBSEQUENT BASES
 14.3  14.3 1.e4       0.0  0.0     0.0  0.0
 14.9  14.9 1.e4       0.0  0.0     0.0  0.0
  7.2   7.2 1.e4       0.0  0.0     0.0  0.0
  0.0   0.0 0.00       0.0  0.0     0.0  0.0
X-Y COORDINATES OF ISOLATORS
 -65.0 0.0
 -55.0 0.0
 -27.5 0.0
   0.0 0.0
  27.5 0.0
  55.0 0.0
  65.0 0.0
ISOLATOR DATA
4 1 6
169.0 0.07 0.02 0.5  0.004  2819.3
4 1 6
169.0 0.07 0.02 0.5  0.004  534.2
4 1 6
169.0 0.07 0.02 0.5  0.004  534.2
4 1 6
169.0 0.07 0.02 0.5  0.004 1576.0
3 1 6
169.0 0.07 0.02 0.5  0.004  903.2
3 1 6
169.0 0.07 0.02 0.5  0.004  903.2
3 1 6
169.0 0.07 0.02 0.5  0.004  3192.2
OUTPUT CONTROL PARAMETERS
1 10 1
ISOLATOR NUMBER WHICH OUTPUT IS DESIRED
1 2 3 4 5 6 7
COORDINATES OF DESIRED INTERSTORY DRIFT
BUILDING No 1
1
0.0 0.0
BUILDING No 2
1
0.0 0.0
INITIAL CONDITIONS OF EACH BASE
 0.0 0.0 0.0
 0.0 0.0 0.0
 0.0 0.0 0.0
 0.0 0.0 0.0
```

■ File **TMATRIX.DAT** which contains matrix [T]. The content of the file for this structure is printed below.

```
 0.0 0 0   0.0 0 0   0.0 0 0   0.0 0 0   0.0 0 0   0.0 0 0   0.0 0 0   0.0 0 0   0.0 0 0   0.0 0 0   0.0 0 0
-2.39 0 0 -1.85 0 0 -1.39 0 0 -0.97 0 0 -0.93 0 0  -0.90 0 0 -0.86 0 0 -0.87 0 0 -0.63 0 0 -0.32 0 0   0.37 0 0
 2.38 0 0   1.84 0 0   1.38 0 0  0.97 0 0   0.93 0 0   0.90 0 0   0.86 0 0  0.87 0 0   0.63 0 0   0.32 0 0  -0.37 0 0
 0.0 0 0   0.0 0 0   0.0 0 0   0.0 0 0   0.0 0 0   0.0 0 0   0.0 0 0   0.0 0 0   0.0 0 0   0.0 0 0   0.0 0 0
-0.91 0 0 -0.81 0 0 -0.73 0 0  -2.89 0 0 -2.27 0 0 -1.76 0 0 -1.25 0 0 -0.70 0 0 -0.39 0 0 -0.07 0 0 -0.08 0 0
 0.91 0 0  0.81 0 0 0.73 0 0   2.89 0 0  2.27 0 0  1.76 0 0   1.25 0 0 0.70 0 0 0.39 0 0 0.07 0 0 0.08 0 0
 0.0 0 0   0.0 0 0   0.0 0 0   0.0 0 0   0.0 0 0   0.0 0 0   0.0 0 0   0.0 0 0   0.0 0 0   0.0 0 0   0.0 0 0
```

■ File **TMATRIXUPLF.DAT** which contains matrix [A]. The content of the file for this structure is printed below.

```
 1.0  0.00   0.00   0.00   0.00  0.00  0.00
 0.0  1.00  -0.92   0.24  -0.92  0.98  0.00
 0.0 -1.03   1.00  -0.80   0.94 -0.98  0.00
 0.0  0.03  -0.10   1.00  -0.07  0.01  0.00
 0.0 -0.97   0.88  -0.52   1.00 -1.01  0.00
 0.0  0.97  -0.86   0.09  -0.95  1.00  0.00
 0.0  0.00   0.00   0.00   0.00  0.00  1.00
```

■ Files **WAVEX.DAT, WAVEY.DAT**, and **WAVEZ.DAT** which contain the seismic input (acceleration histories in horizontal longitudinal, horizontal transverse and vertical directions). Partial contents of these files are printed below.

WAVEX.DAT	**WAVEY.DAT**	**WAVEZ.DAT**
-0.004118458	0	0
-0.005039125	0	0
-0.005097430	0	0
-0.004822879	0	0
-0.004773737	0	0
etc.	etc.	etc.

APPENDIX H

CONSTRUCTION OF RELATION BETWEEN INERTIA FORCES AND AXIAL BEARING LOADS IN TWO-TOWER VERIFICATION MODEL

CONSTRUCTION OF RELATION BETWEEN INERTIA FORCES AND AXIAL BEARING LOADS IN EXAMPLE OF TWO-TOWER, FOUR-BASE MODEL

For the two-tower on a four-base model verification example described in Section 5, the coefficient matrices [T] and [A] were calculated as follows:

- Matrix [T], supplied in file **TMATRIX.DAT**, was calculated by static analysis in computer code STAAD considering a model with all bearings represented by pins and rollers and accounting for the distribution of horizontal reaction at the two levels. It should be noted that the two exterior bearings of the structure (see Appendix F for complete description) were not modeled since they do not carry additional axial load due to overturning moment effects. (Consider that these bearings carry the weight of part of the structure that is simply connected to the two towers so that there is no transfer of moment between this part of the structure and the towers. The mass of this part of the structure was distributed to the two towers for proper consideration of inertia effects). The procedure is illustrated in Figure H-1. The loads shown in Figure H-1 were distributed to the joints of the floor to which they acted in accordance with the distribution of mass. For example, in the case of unit loading at the first base level (calculation of reactions $T_{1,22}$, $T_{2,22}$, etc., the load was distributed to the five joints of the structure at that level as 0.115 kip, 0.115 kip, 0.382 kip, 0.194 kip and 0.194 kip from left to right, in proportion to the masses at these joints (see Appendix F for distribution of mass). The bearings were model as rollers with one pin at the lower isolation level. Moreover, a horizontal load (0.48 kip opposing the unit kip load) was applied at one of the rollers of the upper isolation level so that the horizontal components of reaction at the two isolation levels were in proportion to the weight carried by the bearings at that level. This is appropriate for FP isolators for which the lateral force is proportional to the vertical force acting on them. Referring to Appendix F, the axial gravity load carried by the bearings at the upper isolation level is 4998.6 kip, whereas the weight carried by all bearings is 10462.3 kip. Since for FP isolators the lateral force is proportional to axial load, the lateral force in the bearings of the upper isolation system is 4998.6/10462.3=0.48 times the total lateral load. This explains the application of the 0.48 kip load in deriving the coefficients of matrix T. It should be mentioned that the derivation of the 0.48 kip figure, it was assumed that the isolator displacements are equal at each instant of time (which is basically true). Moreover, it was assumed that the ratio of axial load at the upper isolators to the total weight remains constant at each instant of time. This is not always approximately true but rather depends on the analyzed structural system configuration. For the system analyzed herein, bearings 1 and 2, and bearings 4 and 5 act as pairs for which the sum of axial load remains nearly constant during seismic excitation. That is, the overturning moment created by the inertia forces of the left tower primarily affect the axial loads on bearing pair 1-2, whereas those of the right tower affect the axial loads on bearing pair 4-5. The result is that the ratio of lateral load in the upper isolators to the lateral load in all isolators remains practically constant (herein calculated as 0.48) even in the presence of bearing uplift.

- Matrix [A], supplied in file **TMATRIXUPLF.DAT**, was also calculated by static analysis in program STAAD considering a model with each support successively removed, a unit load applied at that location and the reactions at the remaining supports calculated. The supports were modeled as rollers with one pin. The procedure is illustrated in Figure H-2.

It should be noted that the model displayed in Figures H-1 and H-2 does not contain the two exterior bearings. These bearings (and the structure above them of which the bearings carry the weight) are connected to the structure by simple connections so that they do not carry additional axial as a result of horizontal inertia forces. That is, axial load on these bearings remains constant when horizontal seismic excitation is applied. Accordingly, these bearings were not included in the formulation of matrices [T] and [A].

Matrices [T] and [A] are presented below:

$$\left[T\right] =$$

$$\begin{bmatrix} -1.92 & 0 & 0 & -1.44 & 0 & 0 & -1.03 & 0 & 0 & -0.69 & 0 & 0 & -0.64 & 0 & 0 & -0.60 & 0 & 0 & -0.57 & 0 & 0 & -0.56 & 0 & 0 & -0.35 & 0 & 0 & -0.13 & 0 & 0 & 0.02 & 0 & 0 \\ 1.92 & 0 & 0 & 1.44 & 0 & 0 & 1.03 & 0 & 0 & 0.69 & 0 & 0 & 0.64 & 0 & 0 & 0.60 & 0 & 0 & 0.57 & 0 & 0 & 0.56 & 0 & 0 & 0.35 & 0 & 0 & 0.12 & 0 & 0 & -0.03 & 0 & 0 \\ 0 & 0 & 0 & 0 & 0 & 0 & 0 & 0 & 0 & 0 & 0 & 0 & 0 & 0 & 0 & 0 & 0 & 0 & 0 & 0 & 0 & 0 & 0 & 0 & 0 & 0 & 0 & 0 & 0 & 0 & 0.01 & 0 & 0 \\ -0.97 & 0 & 0 & -0.87 & 0 & 0 & -0.77 & 0 & 0 & -2.92 & 0 & 0 & -2.13 & 0 & 0 & -1.80 & 0 & 0 & -1.29 & 0 & 0 & -0.74 & 0 & 0 & -0.42 & 0 & 0 & -0.08 & 0 & 0 & -0.01 & 0 & 0 \\ 0.97 & 0 & 0 & 0.87 & 0 & 0 & 0.77 & 0 & 0 & 2.92 & 0 & 0 & 2.31 & 0 & 0 & 1.80 & 0 & 0 & 1.29 & 0 & 0 & 0.74 & 0 & 0 & 0.42 & 0 & 0 & 0.09 & 0 & 0 & 0.01 & 0 & 0 \end{bmatrix}$$

$$[A]=\begin{bmatrix} 1 & -0.97 & -0.05 & -1.12 & 1.21 \\ -1 & 1 & -0.55 & 1.13 & -1.21 \\ 0 & -0.03 & 1 & -0.06 & 0.02 \\ -0.44 & 0.43 & -0.48 & 1 & -1.02 \\ 0.44 & -0.43 & 0.08 & -0.95 & 1 \end{bmatrix}$$

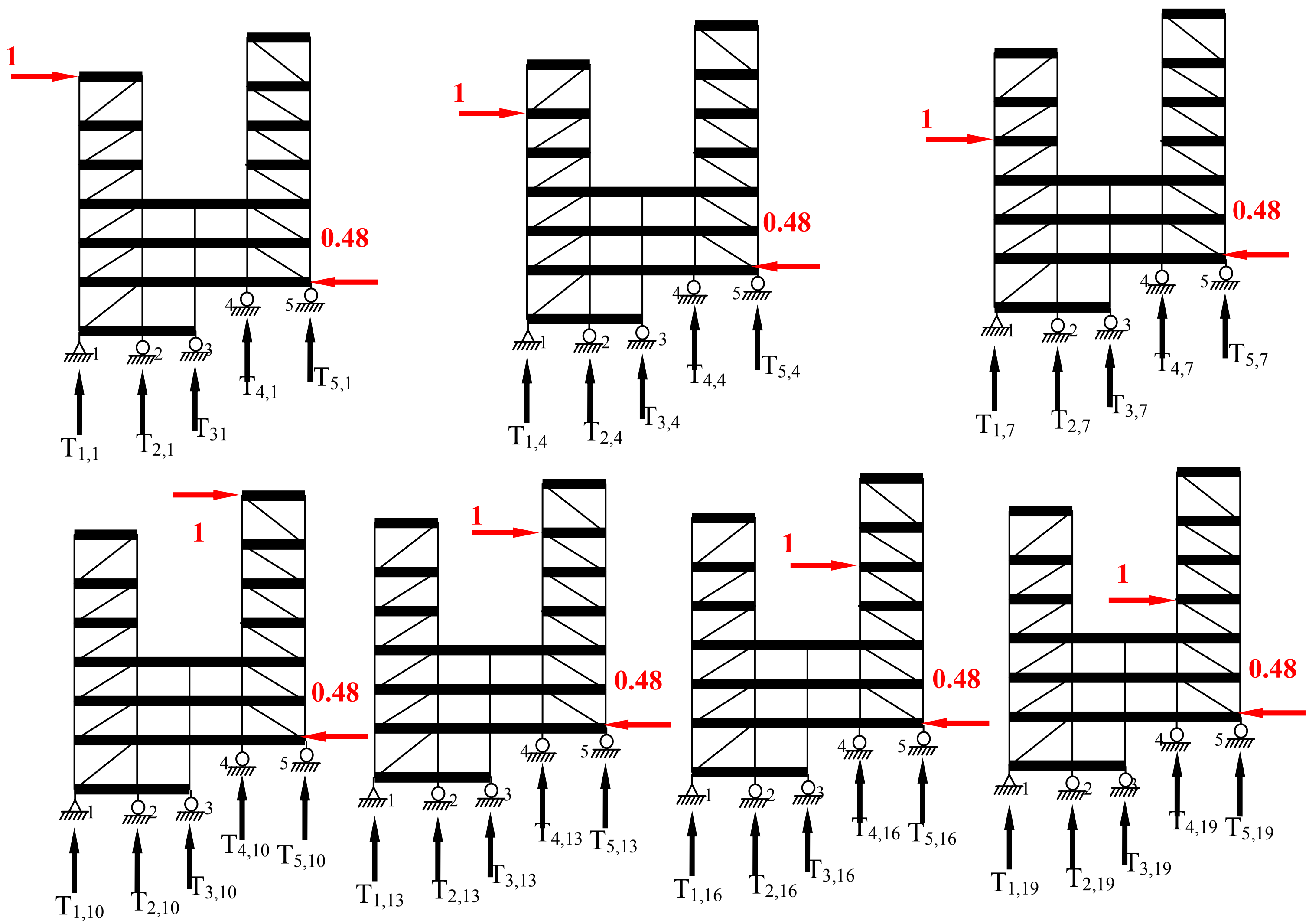

Figure H-1: Structural model used in construction of matrix $[T]$

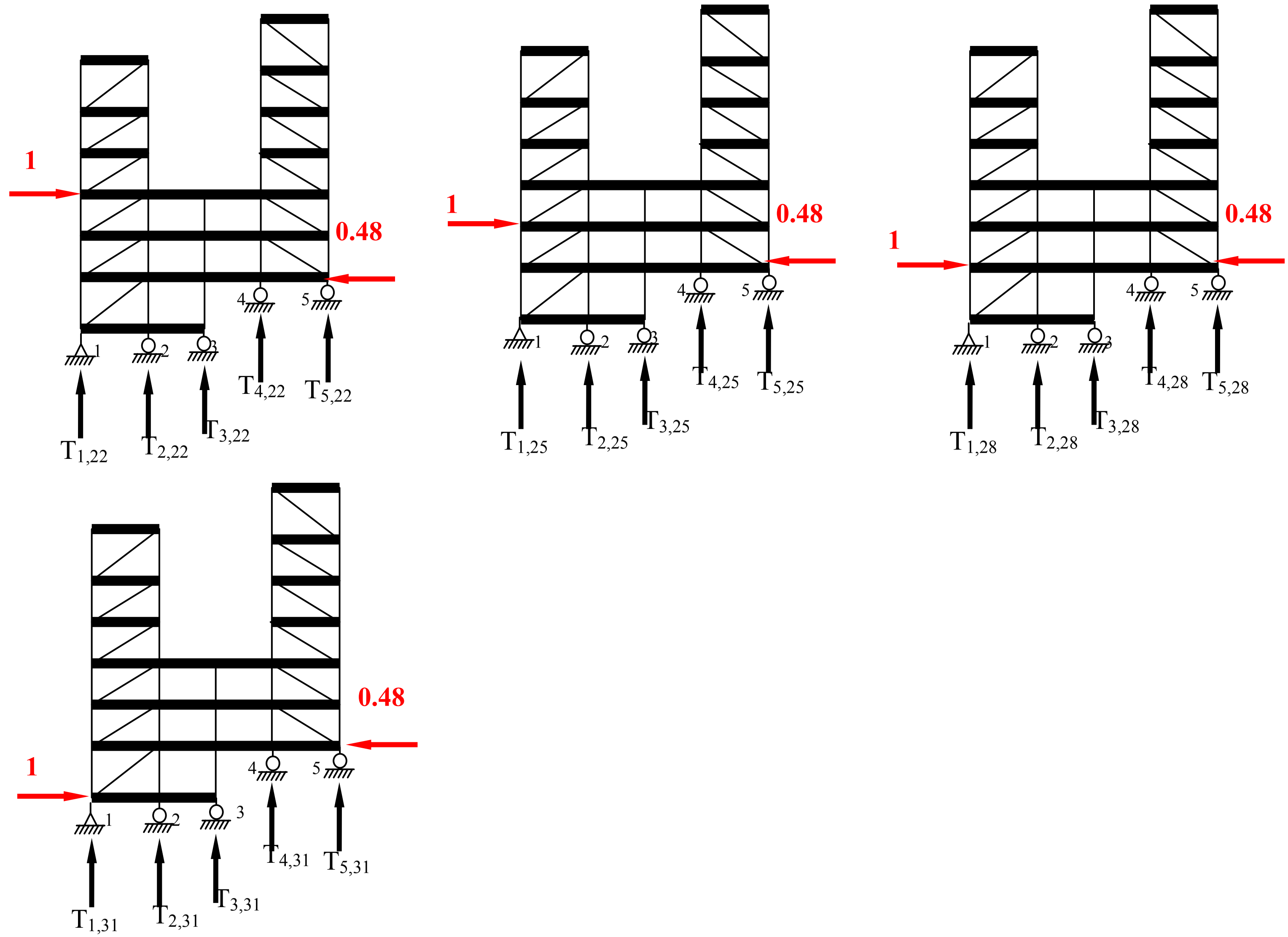

Figure H-1 Continued

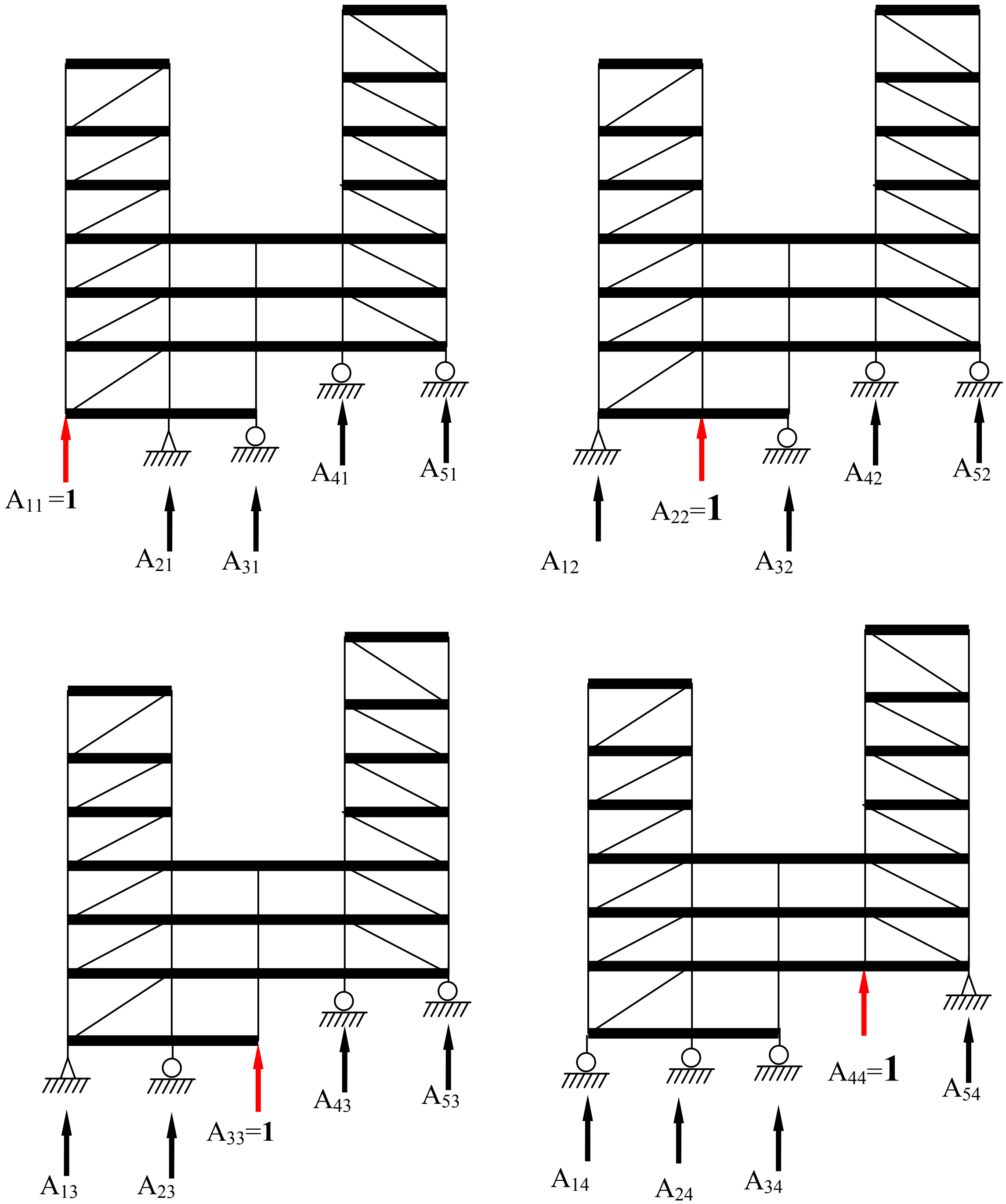

Figure H-2: Structural models used in construction of matrix [A]

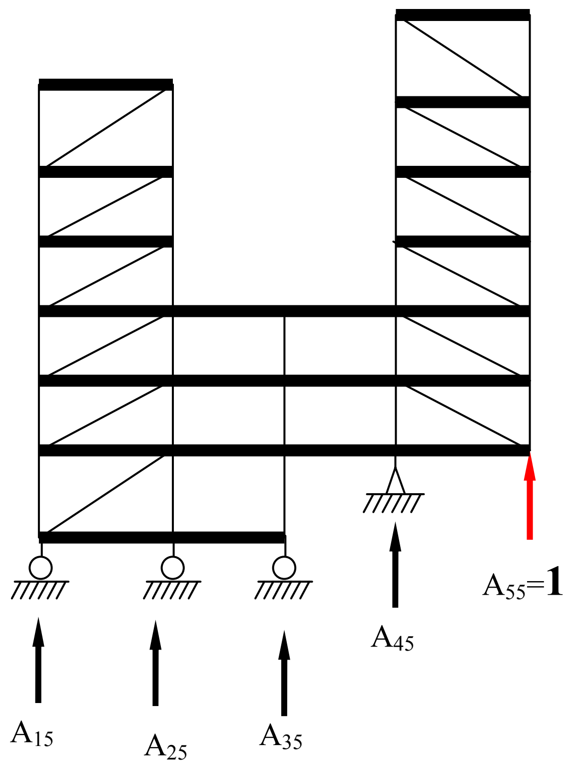

Figure H-2 Continued

APPENDIX I

CALCULATION OF INPUT PARAMETERS

FOR SUPERSTRUCTURE OF TWO-TOWER EXAMPLE

CALCULATION OF INPUT PARAMETERS FOR SUPERSTRUCTURE OF TWO-TOWER EXAMPLE

Input parameters for the description of the isolated superstructure in 3D-BASIS-ME-MB include the stiffness, mass and damping properties of each of the two towers (termed superstructures) and the stiffness, mass and damping properties of each of the stories below the two towers(termed the bases). In this example, there are two superstructures (left and right towers, respectively of 3 and 4 stories) and four bases. The bases are numbered 1, 2, 3 and 4 starting from the one at the top. Information on the two superstructures (towers) was input in the form of floor masses, mode shapes, frequencies and damping ratios (best way of describing properties). For the four bases (stories below the towers), the parameters were input as mass, shear stiffness and damping constant. For example, for base 1, the input consisted of the mass at the level of joints 4-11-18-21-28 (see Figure I-1) and the stiffness K_1 and damping constant C_1 for the story below the mass. (Note that the joint numbering mentioned above was not used in 3D-BASIS-ME-MB but rather used only in program STAAD in the model to calculate various stiffness parameters as described below).

The structure was modeled in computer program STAAD in order to calculate the stiffness parameters needed to input in program 3D-BASIS-ME-MB. Figure I-1 shows the model.

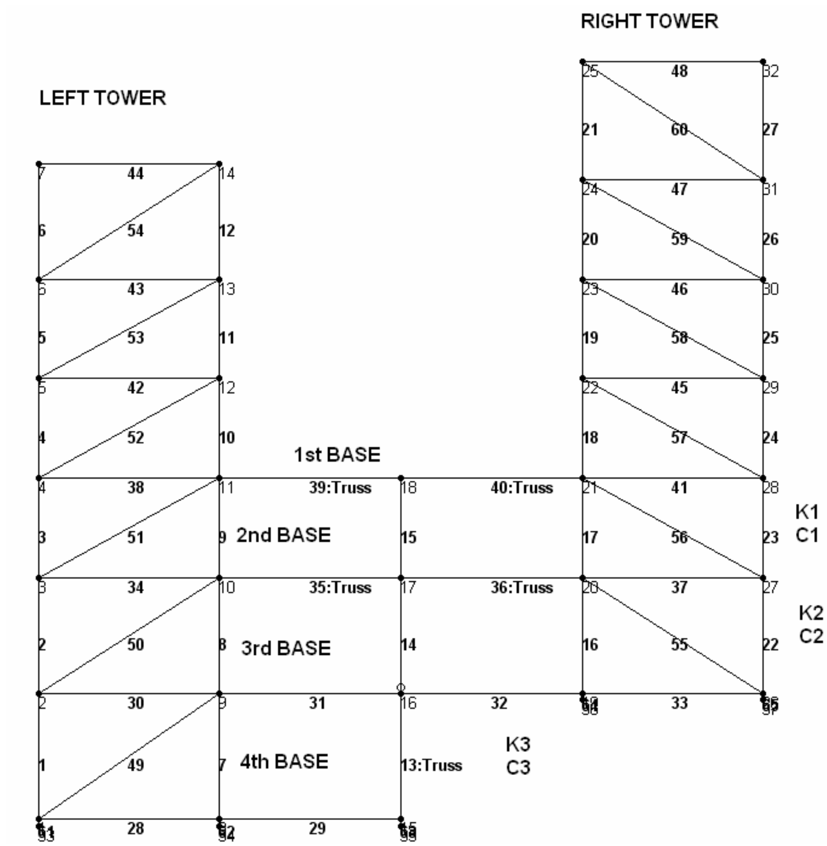

Figure I-1: Model of two-tower example structure in program STAAD.

<u>Right Tower</u>

To obtain the stiffness properties of the right tower (a similar approach was followed for the left tower), unit displacements of the four floors of the right tower were imposed and the forces needed to impose these displacements were calculated while all joints were restrained against lateral movement. The input file to program STAAD to achieve this is presented in Table I-1.

Table I-1: Input to program STAAD.

```
STAAD PLANE TWO-TOWER
*
INPUT WIDTH 79
PAGE LENGTH 50
UNITS FEET KIP
JOINT COORDINATES
1 0 0; 2 0 19; 3 0 36.5; 4 0 51.5; 5 0 66.5; 6 0 81.5;7 0 99;
8 27.5 0; 9 27.5 19; 10 27.5 36.5; 11 27.5 51.5; 12 27.5 66.5; 13 27.5 81.5;
14 27.5 99;
15 55 0; 16 55 19; 17 55 36.5; 18 55 51.5;
19 82.5 19; 20 82.5 36.5;21 82.5 51.5;22 82.5 66.5;23 82.5 81.5;24 82.5 96.5;
```

```
25 82.5 114.5;
26 110 19;27 110 36.5;28 110 51.5;29 110 66.5;30 110 81.5;31 110 96.5;
32 110 114.5
33 0 -1;34 27.5 -1;35 55 -1;36 82.5 18; 37 110 18
MEMBER INCIDENCES
1 1 2 6;
7 8 9 12;
13 15 16 15;
16 19 20 21;
22 26 27 27;
28 1 8; 29 8 15;
30 2 9;31 9 16;32 16 19;33 19 26;
34 3 10;35 10 17;36 17 20;37 20 27;
38 4 11;39 11 18;40 18 21;41 21 28
42 5 12;
43 6 13;
44 7 14;
45 22 29;
46 23 30;
47 24 31;
48 25 32;
49 1 9 54;
55 20 26 60
61 1 33;62 8 34;63 15 35;64 19 36;65 26 37
MEMBER PROPERTY AMERICAN
1 7 13 16 17 22 23 TABLE ST W14X342
2 TO 5 8 TO 11 14 15 18 19 24 25 TABLE ST W14X257
6 12 TABLE ST W14X109
20 21 26 27 TABLE ST W14X68
28 TO 45 TABLE ST W14X283
46 TABLE ST W14X211
47 48 TABLE ST W21X201
49 TABLE ST W14X193
50 51 54 55 56 60 TABLE ST W14X159
52 TABLE ST W14X211
53 57 58 TABLE ST W14X193
59 TABLE ST W14X132
*1 FOOT TALL BEARINGS
61 TO 65 TABLE ST W14X342
*
MEMBER TRUSS
13 35 36 39 40
MEMBER RELEASES
14 START MZ
CONSTANTS
E STEEL ALL
POISSON STEEL ALL
SUPPORTS
33 TO 37 PINNED
*
* CONSTRUCTION OF STIFFNESS MATRIX OF RIGHT TOWER
*
*FLOORS RESTRAINED AGAINST LATERAL MOVEMENT
16 17 18 FIXED BUT FY MZ
14 13 12 25 24 23 22 FIXED BUT FY MZ
*
UNITS INCH
*SUPPORT MOVEMENTS
LOAD 1
SUPPORT DISPL
25 FX 1
LOAD 2
```

```
SUPPORT DISPL
24 FX 1
LOAD 3
SUPPORT DISPL
23 FX 1.0
LOAD 4
SUPPORT DISPL
22 FX 1
PERFORM ANALYSIS
PRINT SUPPORT REACTIONS LIST 25 24 23 22
FINISH
```

The output of the program (reactions at the joints of the four floors of the right tower is presented in Table I-2. Moreover, Figure I-2 presents a view of the deformed structure when the unit displacement is imposed at the second floor of the right tower. Since joints 25, 24, 23 and 22 represent the four floors of the tower, top to bottom, the reactions calculated for each of the joints represent elements of the stiffness matrix of the tower. For example, the reactions listed below for joint 25 in the four loadings (1 is unit displacement at joint 25, 2 is unit displacement at joint 24, etc.) form the first column of the stiffness matrix. The complete stiffness matrix for the right tower (DOF, top to bottom, units kip/in) is

$$K_R = \begin{bmatrix} 898 & -1183 & 94 & 87 \\ -1183 & 2793 & -1654 & 19 \\ 94 & -1654 & 3774 & -2356 \\ 87 & 19 & -2356 & 4176 \end{bmatrix} \tag{H-1}$$

Note that the matrix is close in form to the matrix in a shear type representation of the tower (elements of the matrix with values of 19, 87 and 94 would have been zero). However, the values of shear stiffness for each story extracted from this matrix are much less than those calculated assuming shear type of deformation (inextensible columns- stiffness is shear stiffness of columns plus the contribution from axial deformation of the braces). This is due to joint rotations and change of length of columns accounted for in the detailed model used in representing the structure.

Table I-2: Output of program STAAD

JOINT	LOAD	FORCE-X	FORCE-Y	FORCE-Z	MOM-X	MOM-Y	MOM Z
25	1	898.44	0.00	0.00	0.00	0.00	0.00
	2	-1182.65	0.00	0.00	0.00	0.00	0.00
	3	94.02	0.00	0.00	0.00	0.00	0.00
	4	87.41	0.00	0.00	0.00	0.00	0.00
24	1	-1182.65	0.00	0.00	0.00	0.00	0.00
	2	2791.92	0.00	0.00	0.00	0.00	0.00
	3	-1653.97	0.00	0.00	0.00	0.00	0.00
	4	18.53	0.00	0.00	0.00	0.00	0.00
23	1	94.02	0.00	0.00	0.00	0.00	0.00
	2	-1653.97	0.00	0.00	0.00	0.00	0.00
	3	3774.19	0.00	0.00	0.00	0.00	0.00
	4	-2356.13	0.00	0.00	0.00	0.00	0.00
22	1	87.41	0.00	0.00	0.00	0.00	0.00
	2	18.53	0.00	0.00	0.00	0.00	0.00
	3	-2356.13	0.00	0.00	0.00	0.00	0.00
	4	4175.55	0.00	0.00	0.00	0.00	0.00

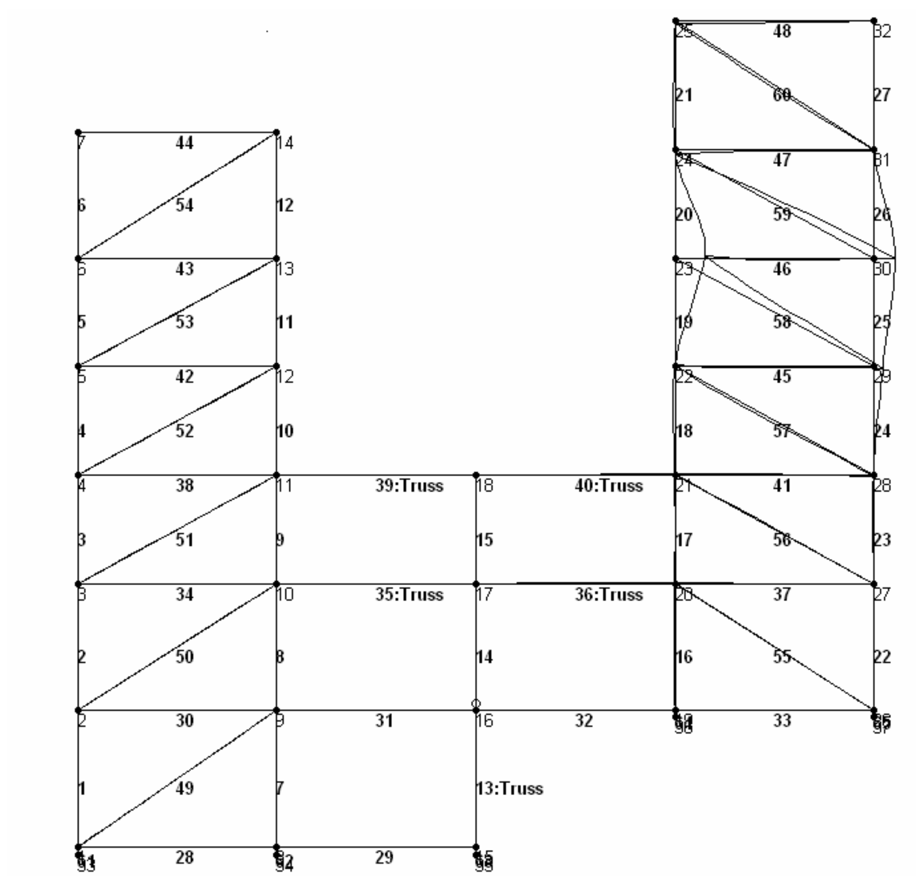

Figure I-2: Deformed structure when imposing unit displacement at second floor of right tower.

The mass matrix (units kip-sec^2/in) associated with the right tower is (see Appendix F for details on mass distribution)

$$M_R = \begin{bmatrix} 2.184 & 0 & 0 & 0 \\ 0 & 1.834 & 0 & 0 \\ 0 & 0 & 1.834 & 0 \\ 0 & 0 & 0 & 1.840 \end{bmatrix} \tag{H-2}$$

Solution of the eigenvalue problem using the stiffness and mass matrices for the right tower in program MATLAB yielded the information presented in Table I-3.

Table I-3: Dynamic characteristics of fixed-base right-tower model.

Mode	Frequency (rad/sec)	Damping Ratio	Mode Shape			
			Floor 4	Floor 3	Floor 2	Floor 1
1	6.863	0.02	1.0000	0.6983	0.4306	0.2235
2	23.937	0.02	1.0000	-0.8216	-1.5944	-1.2263
3	43.542	0.02	1.0000	-3.5023	0.7659	2.5953
4	60.439	0.02	1.0000	-7.7500	17.4150	-16.1450

Mode shapes and frequencies can be directly obtained from programs like STAAD, SAP2000 and ETABS. (Here it was more convenient to work outside these programs for obtaining information on frequencies and mode shapes.)

Note that the input to program 3D-BASIS-ME-MB for the right tower consists of the masses, frequencies, mode shapes, and damping ratio for each of the four modes. The damping ratio was specified as 2% in each mode of the tower.

<u>Left Tower</u>

In a similar way, the properties of the left tower (three degrees of freedom) were determined to be as follows.

The stiffness matrix for the left tower (DOF, top to bottom, units kip/in) is

$$K_L = \begin{bmatrix} 1246 & -1647 & 146 \\ -1647 & 3965 & -2424 \\ 146 & -2424 & 4256 \end{bmatrix} \tag{H-3}$$

The mass matrix (units kip-sec^2/in) associated with the left tower is

$$M_L = \begin{bmatrix} 2.836 & 0 & 0 \\ 0 & 1.888 & 0 \\ 0 & 0 & 1.902 \end{bmatrix} \tag{H-4}$$

Table I-4 lists the dynamic characteristics of the left tower in terms of natural frequencies, damping ratios, and mode shapes.

Table I-4: Dynamic characteristics of fixed-base left-tower model.

Mode	Frequency (rad/sec)	Damping Ratio	Mode Shape		
			Floor 3	Floor 2	Floor 1
1	8.820	0.02	1.0000	0.6537	0.3502
2	33.979	0.02	1.0000	-1.3819	-1.6971
3	59.537	0.02	1.0000	-4.9156	4.8514

Story Below First Base

The calculation of stiffness K_1 of the story below the first base (see Figure I-1) was based on restraining the lateral movement of all nodes below the first base, imposing a distributed (based on mass distribution) 1000-kip load at the first base level (joints 4, 11, 18, 21 and 28), and calculating the average displacement of these joints.

The input file to program STAAD is presented in Table I-5 and the deformed structure is shown in Figure I-3. The calculated displacements at the joints of the floor ranged from 0.2010 to 0.2333 in., with the average being 0.2180 in. The story stiffness was then calculated as K_1 = 1000 kip / 0.21807 in = 4586 kip/in.

Table I-5: Input to program STAAD.

```
STAAD PLANE TWO-TOWER
*
INPUT WIDTH 79
PAGE LENGTH 50
UNITS FEET KIP
JOINT COORDINATES
1 0 0; 2 0 19; 3 0 36.5; 4 0 51.5; 5 0 66.5; 6 0 81.5;7 0 99;
8 27.5 0; 9 27.5 19; 10 27.5 36.5; 11 27.5 51.5; 12 27.5 66.5; 13 27.5 81.5;
14 27.5 99;
15 55 0; 16 55 19; 17 55 36.5; 18 55 51.5;
19 82.5 19; 20 82.5 36.5;21 82.5 51.5;22 82.5 66.5;23 82.5 81.5;24 82.5 96.5;
25 82.5 114.5;
26 110 19;27 110 36.5;28 110 51.5;29 110 66.5;30 110 81.5;31 110 96.5;
32 110 114.5
33 0 -1;34 27.5 -1;35 55 -1;36 82.5 18; 37 110 18
MEMBER INCIDENCES
1 1 2 6;
7 8 9 12;
13 15 16 15;
16 19 20 21;
22 26 27 27;
28 1 8; 29 8 15;
30 2 9;31 9 16;32 16 19;33 19 26;
34 3 10;35 10 17;36 17 20;37 20 27;
38 4 11;39 11 18;40 18 21;41 21 28
42 5 12;
43 6 13;
44 7 14;
45 22 29;
46 23 30;
47 24 31;
48 25 32;
49 1 9 54;
55 20 26 60
61 1 33;62 8 34;63 15 35;64 19 36;65 26 37
MEMBER PROPERTY AMERICAN
1 7 13 16 17 22 23 TABLE ST W14X342
2 TO 5 8 TO 11 14 15 18 19 24 25 TABLE ST W14X257
6 12 TABLE ST W14X109
20 21 26 27 TABLE ST W14X68
28 TO 45 TABLE ST W14X283
46 TABLE ST W14X211
47 48 TABLE ST W21X201
49 TABLE ST W14X193
50 51 54 55 56 60 TABLE ST W14X159
52 TABLE ST W14X211
53 57 58 TABLE ST W14X193
59 TABLE ST W14X132
*1 FOOT TALL BEARINGS
61 TO 65 TABLE ST W14X342
*
MEMBER TRUSS
13 35 36 39 40
MEMBER RELEASES
14 START MZ
CONSTANTS
E STEEL ALL
POISSON STEEL ALL
SUPPORTS
33 TO 37 PINNED
```

```
*
* CONSTRUCTION OF STIFFNESS K1
*
*FLOORS RESTRAINED AGAINST LATERAL MOVEMENT
1 2 3 8 9 10 15 16 17 FIXED BUT FY MZ
19 20 26 27 FIXED BUT FY MZ
UNITS INCH
LOAD 1
JOINT LOAD
4 11 FX 115
21 28 FX 194
18 FX 382
PERFORM ANALYSIS
*PRINT SUPPORT REACTIONS LIST 25 24 23 22
*PRINT MEMBER PROPERTIES ALL
*PRINT MEMBERS FORCES
PRINT JOINT DISPLACEMENTS LIST 4 11 18 21 28
FINISH
```

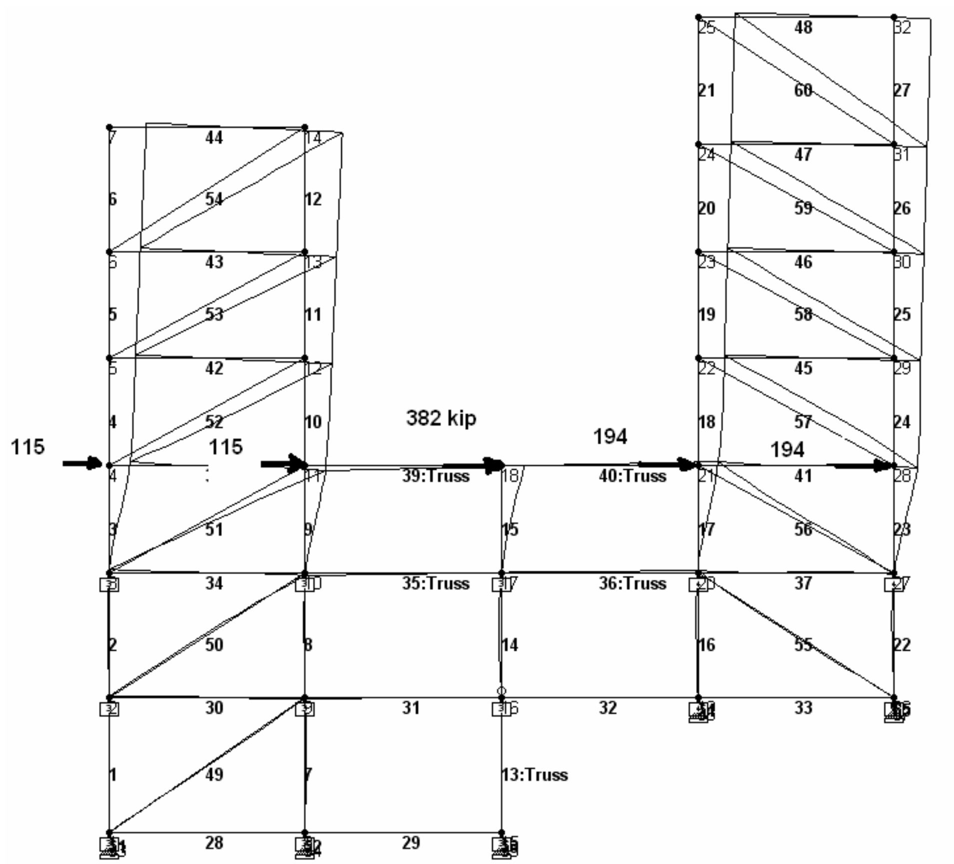

Figure I-3: Deformed two-tower structural model used for calculation of stiffness K_1.

Story Below Second Base

The calculation of stiffness K_2 of the story below the second base (see Figure I-1) was based on two different procedures:

(a) By restraining the lateral movement of all nodes below the second base, imposing a distributed (based on mass distribution) 1000-kip load at the second base level (joints 3, 10, 17, 20 and 27), and calculating the average displacement of these joints. The loads at these joints were 107, 107, 382, 202, and 202 kip, respectively.

The deformed structure is shown in Figure I-4. The calculated displacements at the joints of the floor ranged from 0.2133 to 0.2492 in., with the average being 0.23153 in. The story stiffness was then calculated as $K_2 = 1000$ kip / 0.23153 in = 4319 kip/in.

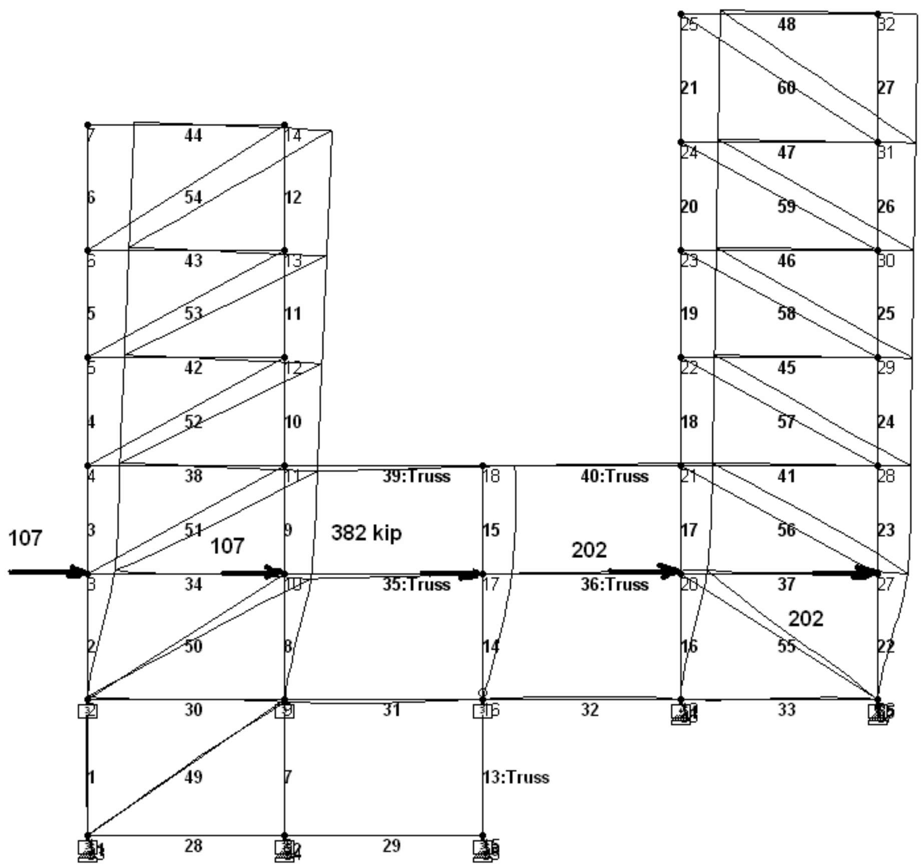

Figure I-4: Deformed two-tower structural model used for calculation of stiffness K_1.

(b) By restraining the lateral movement of all nodes below and above the second base (except those of the two towers), imposing a distributed (based on mass distribution) 1000-kip load at the second base level (joints 3, 10, 17, 20 and 27), and calculating the average displacement of these joints. The loads at these joints were 107, 107, 382, 202 and 202 kip, respectively. The resulting stiffness is the sum $K_1 + K_2$, from where K_2 can be calculated.

The deformed structure is shown in Figure I-5. The calculated displacements at the joints of the floor ranged from 0.0789 to 0.1270 in., with the average being 0.10187 in. The stiffness was then calculated as K_1+K_2 = 1000 kip / 0.10187 in = 9816 kip/in. Given that stiffness K_1 = 4586 kip/in, K_2 = 9816 – 4586 = 5230 kip/in.

That is, stiffness K_2 is in the range of 4319 to 5230 kip/in. The value used is the average value, K_2=4775kip/in, which is within 10% of the two limits.

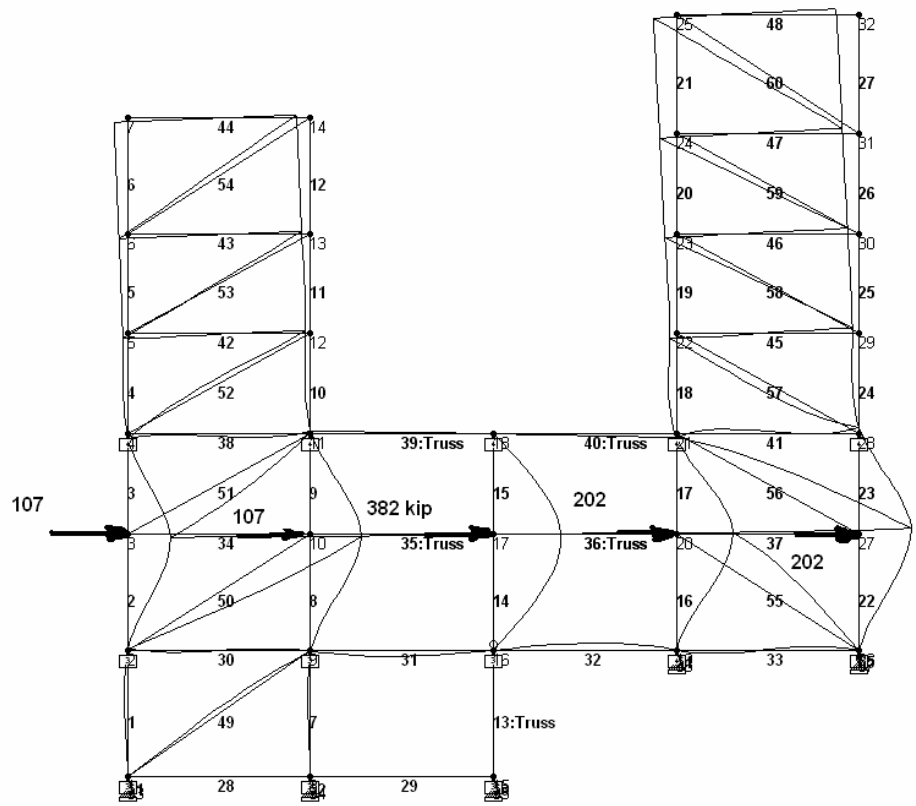

Figure I-5: Deformed two-tower structural model used for calculation of K_1+K_2.

Story Below Third Base

The stiffness of the story below the third base was calculated in a similar manner, using three different approaches, and resulting in three values of stiffness K_3: 2172, 2317 and 2431 kip/in. Again, the average value was used: K_3=2307 kip/in.

Calculation of Damping Constants C1, C2 and C3

Damping constants C_1, C_2 and C_3 should be calculated so that the global damping ratio of the structure attains specific values in specific modes. This is a difficult task to accomplish given the way damping is specified for the superstructures (towers) in program 3D-BASIS-ME-MB and the complex eigenvalue procedures required to calculate damping ratios.

The structure with all supports pinned was analyzed and the frequencies were calculated. It was chosen to construct the stiffness matrix of the structure using program STAAD and then perform the eigenvalue analysis in MATLAB. When the bearings are pinned, the structure has nine effective degrees of freedom, which are selected to be the lateral displacements of the floors, starting from the right tower, top to bottom(4 degrees), followed by the left tower, top to bottom (3 degrees) and then the first and second bases.

The global stiffness matrix, in units of kip/in, is

$$K = \begin{bmatrix}
898 & -1183 & 94 & 87 & 0 & 0 & 0 & 41 & 29 \\
-1183 & 2793 & -1654 & 19 & 0 & 0 & 0 & 11 & 7 \\
94 & -1654 & 3774 & -2356 & 0 & 0 & 0 & 63 & 38 \\
87 & 19 & -2356 & 4176 & 0 & 0 & 0 & -1587 & -279 \\
0 & 0 & 0 & 0 & 1246 & -1647 & 146 & 93 & 69 \\
0 & 0 & 0 & 0 & -1647 & 3965 & -2424 & 46 & 26 \\
0 & 0 & 0 & 0 & 146 & -2424 & 4259 & -1655 & -298 \\
41 & 11 & 63 & -1587 & 93 & 46 & -1655 & 5287 & -1894 \\
29 & 7 & 38 & -279 & 69 & 26 & -298 & -1894 & 4860 \\
4 & 1 & 6 & -11 & 43 & 16 & -34 & -155 & -1165 \\
898 & -1183 & 94 & 87 & 0 & 0 & 0 & 41 & 29 \\
-1183 & 2793 & -1654 & 19 & 0 & 0 & 0 & 11 & 7 \\
94 & -1654 & 3774 & -2356 & 0 & 0 & 0 & 63 & 38 \\
87 & 19 & -2356 & 4176 & 0 & 0 & 0 & -1587 & -279 \\
0 & 0 & 0 & 0 & 1246 & -1647 & 146 & 93 & 69 \\
0 & 0 & 0 & 0 & -1647 & 3965 & -2424 & 46 & 26 \\
0 & 0 & 0 & 0 & 146 & -2424 & 4259 & -1655 & -298 \\
41 & 11 & 63 & -1587 & 93 & 46 & -1655 & 5287 & -1894 \\
29 & 7 & 38 & -279 & 69 & 26 & -298 & -1894 & 4860
\end{bmatrix} \tag{H-5}$$

and the global mass matrix, in units of kip-sec^2/in, is

$$M=\begin{bmatrix} 2.814 & 0 & 0 & 0 & 0 & 0 & 0 & 0 & 0 \\ 0 & 1.834 & 0 & 0 & 0 & 0 & 0 & 0 & 0 \\ 0 & 0 & 1.834 & 0 & 0 & 0 & 0 & 0 & 0 \\ 0 & 0 & 0 & 1.840 & 0 & 0 & 0 & 0 & 0 \\ 0 & 0 & 0 & 0 & 2.836 & 0 & 0 & 0 & 0 \\ 0 & 0 & 0 & 0 & 0 & 1.888 & 0 & 0 & 0 \\ 0 & 0 & 0 & 0 & 0 & 0 & 1.902 & 0 & 0 \\ 0 & 0 & 0 & 0 & 0 & 0 & 0 & 4.062 & 0 \\ 0 & 0 & 0 & 0 & 0 & 0 & 0 & 0 & 4.737 \end{bmatrix} \quad \text{(H-6)}$$

Eigenvalue analysis resulted in the following frequencies in units of rad/sec: [5.495, 7.849, 17.661, 26.565, 34.164, 39.912, 45.429, 59.880, 61.291].

Constructing the damping matrix [C] based on the Rayleigh approach,

$$[C]=a_1[M]+a_2[K] \quad \text{(H-7)}$$

where [M] and [K] are the mass and stiffness matrices of (H-6) and (H-5), respectively. Parameters a_1 and a_2 were selected so that the damping ratio in the first two modes is matched, that is:

$$a_1=\frac{2\xi_1\omega_1\omega_2^2-2\xi_2\omega_2\omega_1^2}{\omega_2^2-\omega_1^2} \quad \text{(H-8)}$$

$$a_2=\frac{2\xi_2\omega_2-2\xi_1\omega_1}{\omega_2^2-\omega_1^2} \quad \text{(H-9)}$$

Using $\xi_1=\xi_2=0.02$, $\omega_1=5.45\ rad/\sec$ and $\omega_2=7.84\ rad/\sec$, we calculate $a_1=0.1286$ and $a_2=0.003$. The damping constants C_i, $i=1$ or 2 were calculated as

$$C_i=a_1M_i+a_2K_i \quad \text{(H-10)}$$

APPENDIX J

COMPARISON OF RESULTS OF PROGRAM 3D-BASIS-ME-MB TO RESULTS OF PROGRAM ABAQUS FOR TWO-TOWER VERIFICATION MODEL (CASE OF FRICTION COEFFICIENT $f_{\max} = 0.07$)

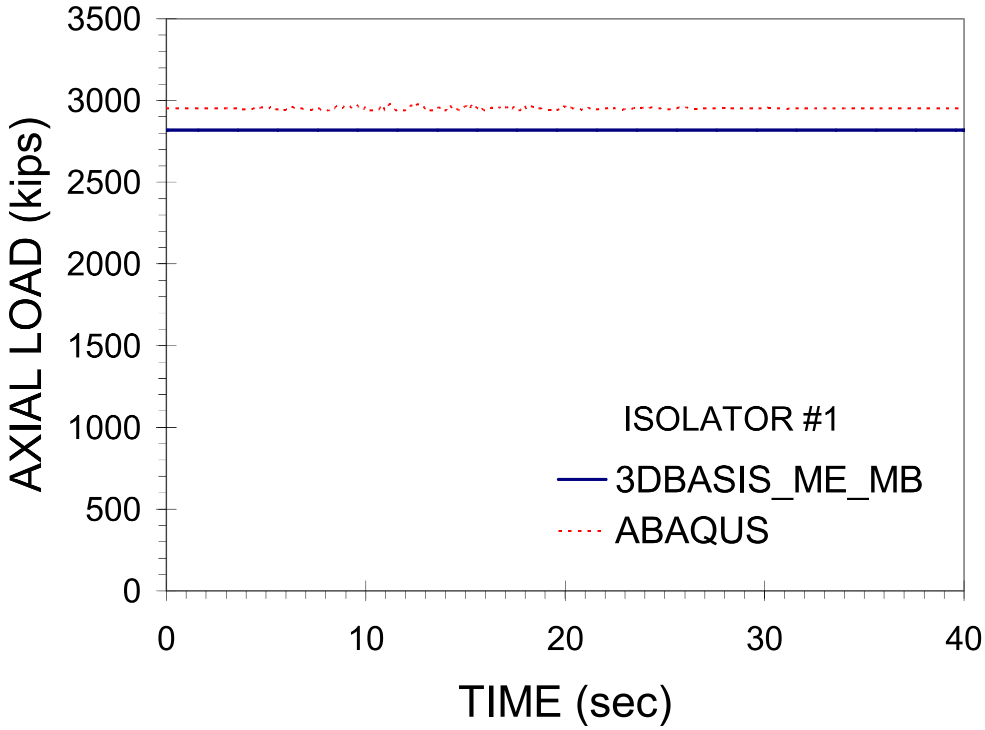
3500
3000
2500
2000
1500
1000
500
0
AXIAL LOAD (kips)
0
10
20
30
40
TIME (sec)
ISOLATOR #1
3DBASIS_ME_MB
ABAQUS

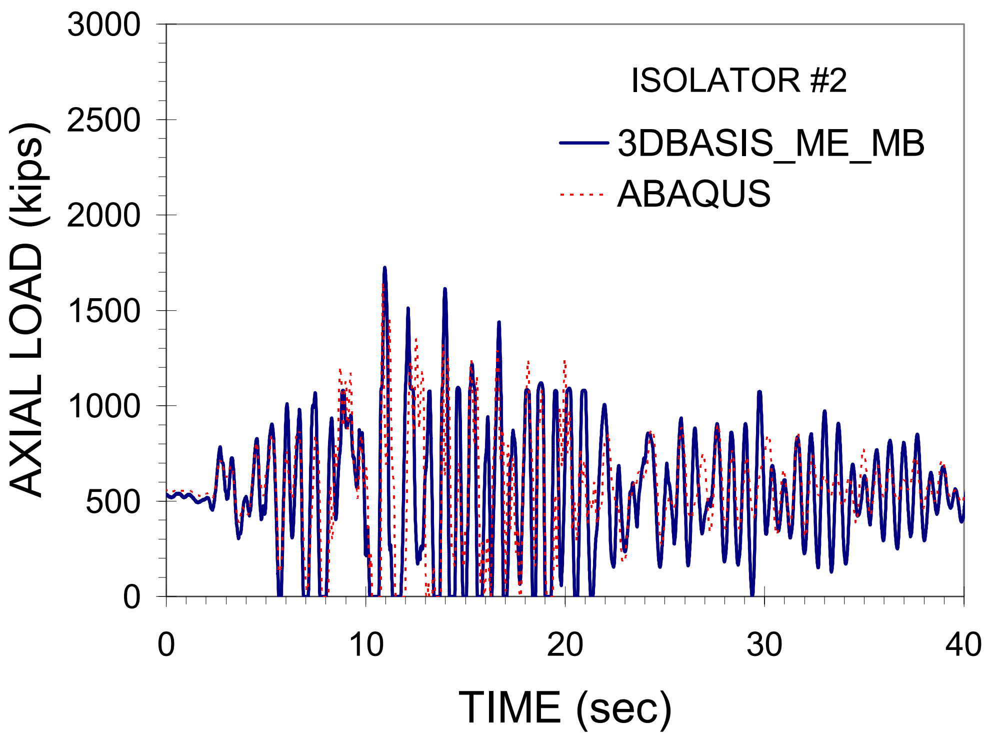
3000
2500
2000
1500
1000
500
0
AXIAL LOAD (kips)
0
10
20
30
40
TIME (sec)
ISOLATOR #2
3DBASIS_ME_MB
ABAQUS

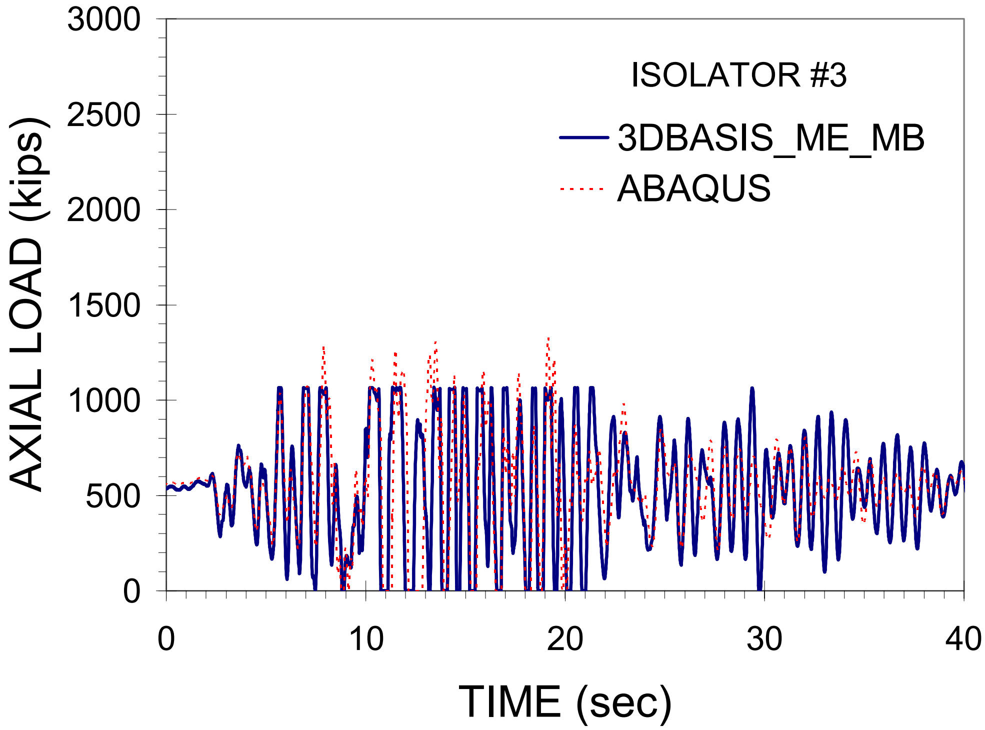
ISOLATOR #3
3DBASIS_ME_MB
ABAQUS
AXIAL LOAD (kips)
TIME (sec)
0
500
1000
1500
2000
2500
3000
0
10
20
30
40

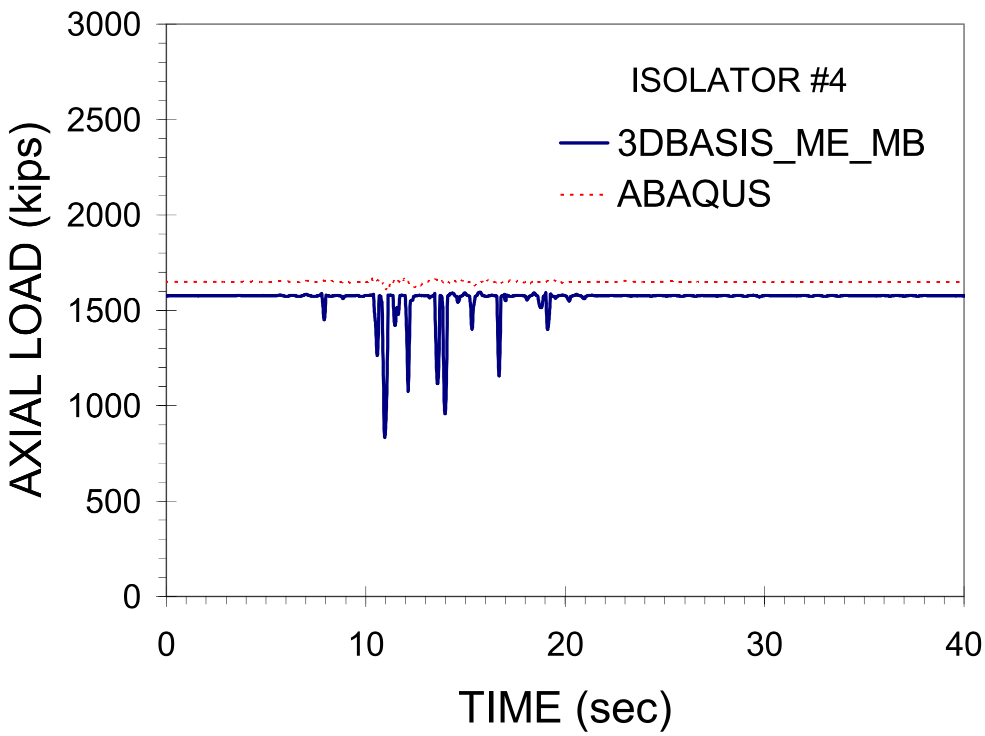
ISOLATOR #4
3DBASIS_ME_MB
ABAQUS
AXIAL LOAD (kips)
TIME (sec)
0
500
1000
1500
2000
2500
3000
0
10
20
30
40

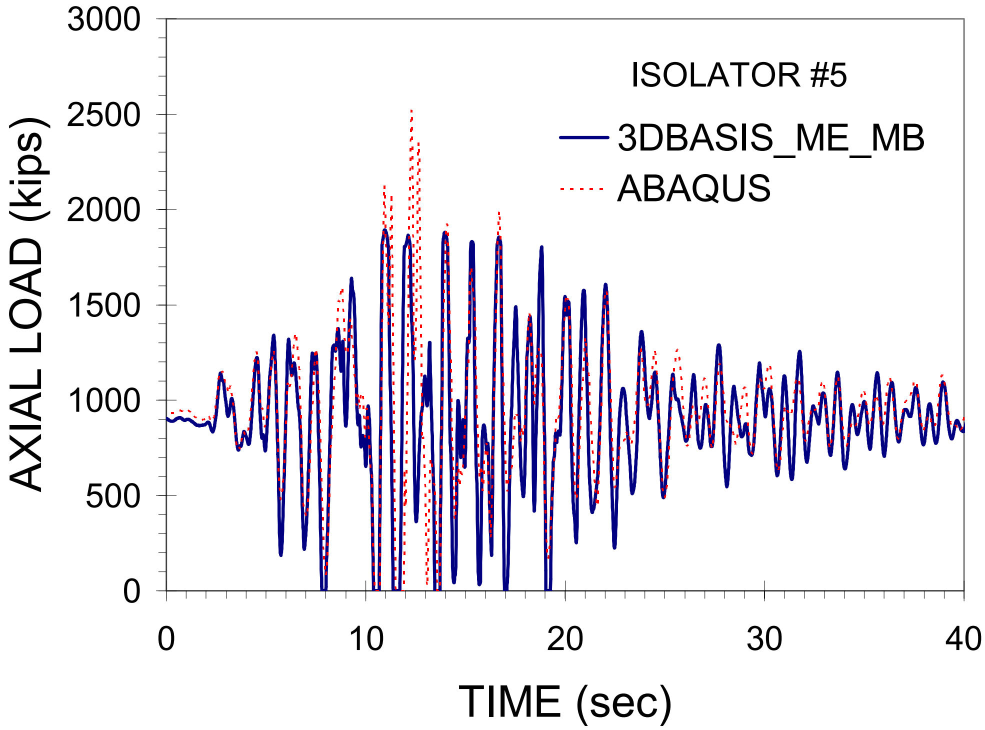

ISOLATOR #5
3DBASIS_ME_MB
ABAQUS
AXIAL LOAD (kips)
TIME (sec)

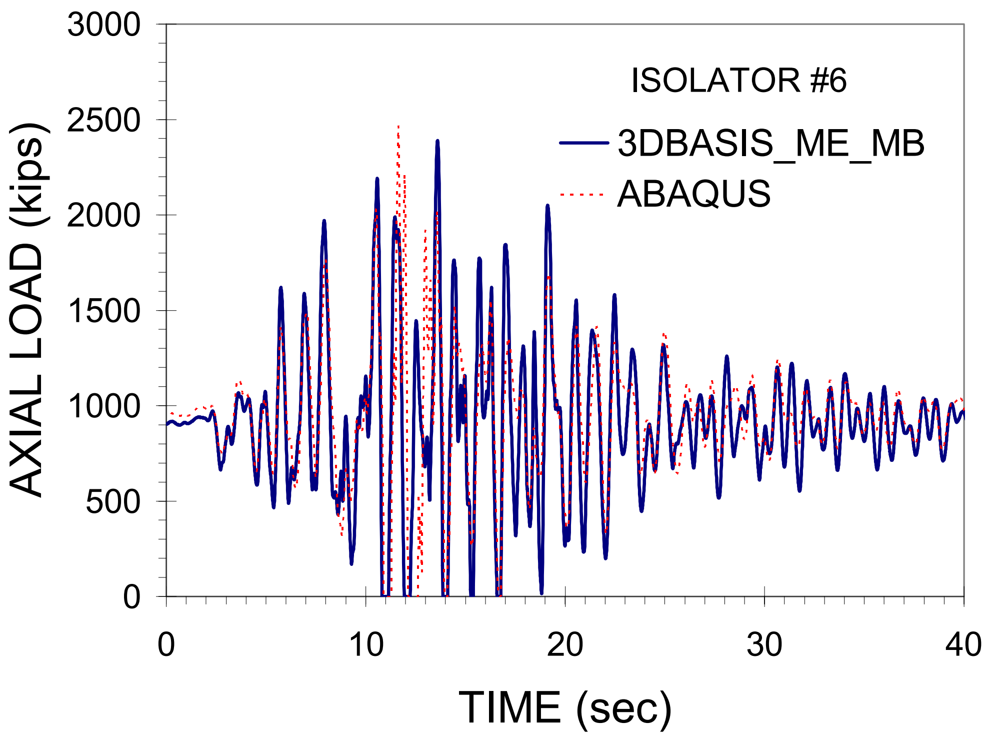

ISOLATOR #6
3DBASIS_ME_MB
ABAQUS
AXIAL LOAD (kips)
TIME (sec)

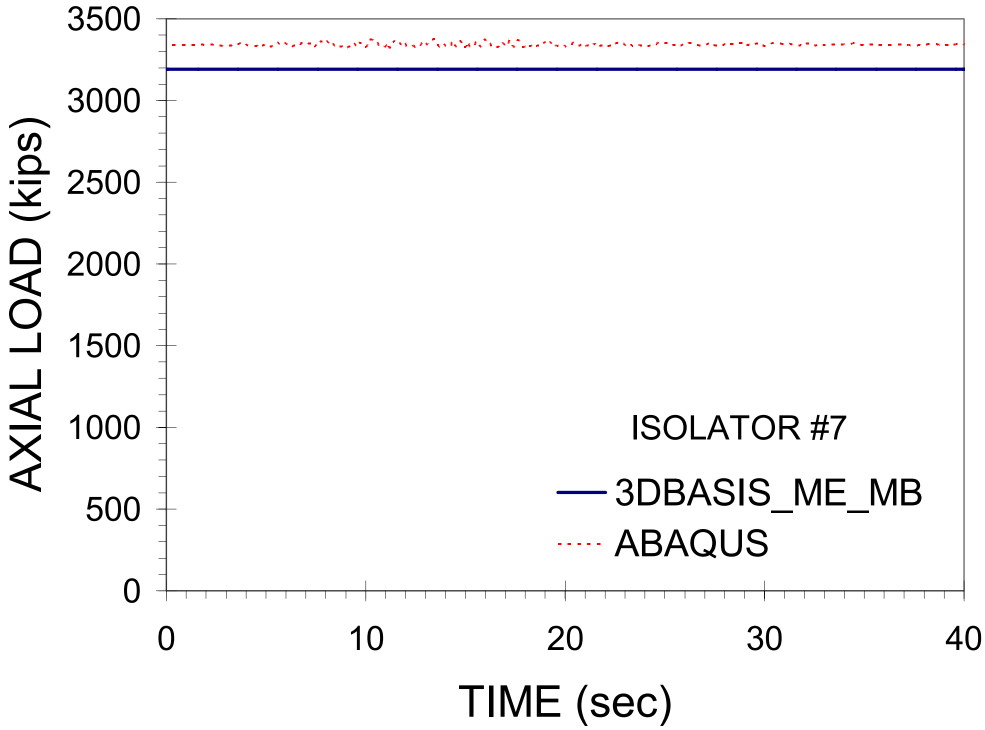

3500
3000
2500
2000
1500
1000
500
0
AXIAL LOAD (kips)
0
10
20
30
40
TIME (sec)
ISOLATOR #7
3DBASIS_ME_MB
ABAQUS

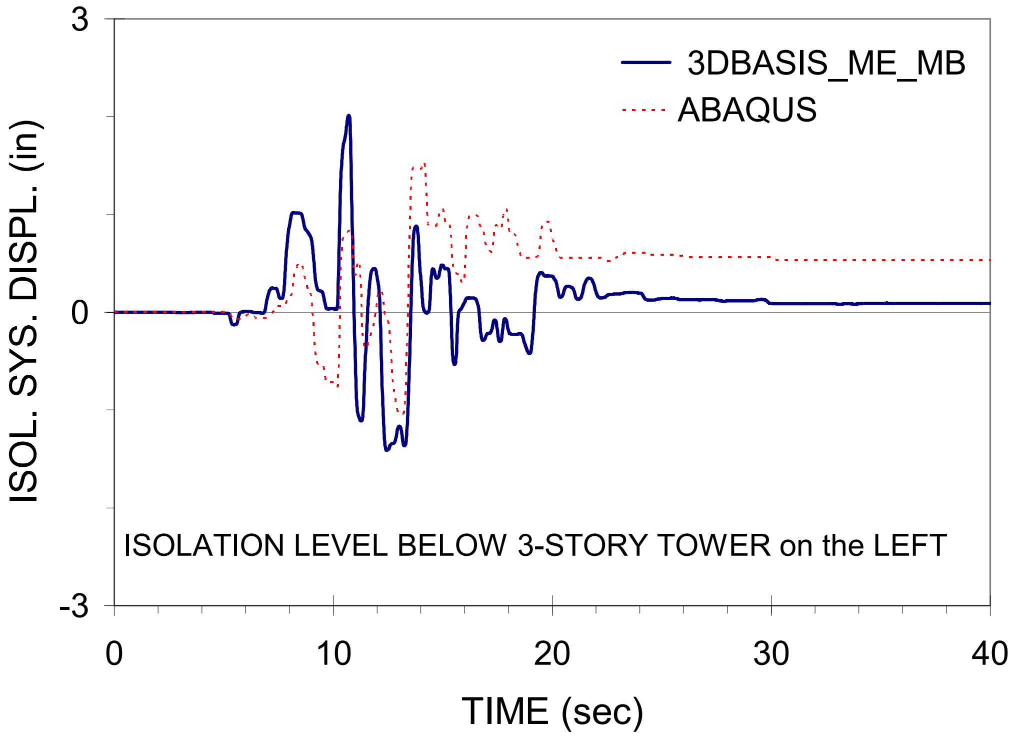
3DBASIS_ME_MB
ABAQUS
ISOLATION LEVEL BELOW 3-STORY TOWER on the LEFT
ISOL. SYS. DISPL. (in)
TIME (sec)
3
0
-3
0
10
20
30
40

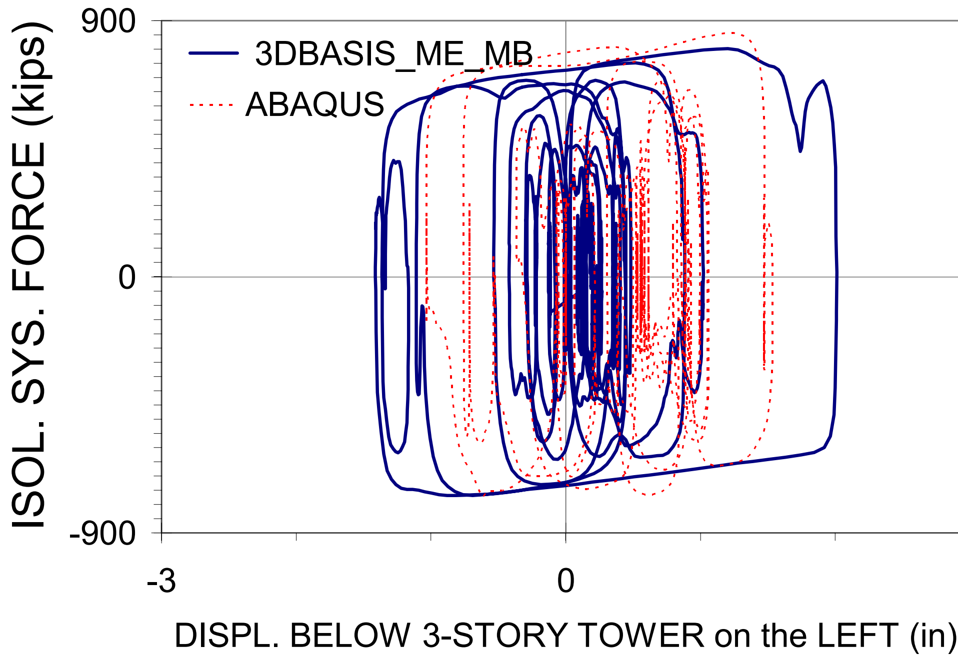
3DBASIS_ME_MB
ABAQUS
ISOL. SYS. FORCE (kips)
DISPL. BELOW 3-STORY TOWER on the LEFT (in)
900
0
-900
-3
0
3

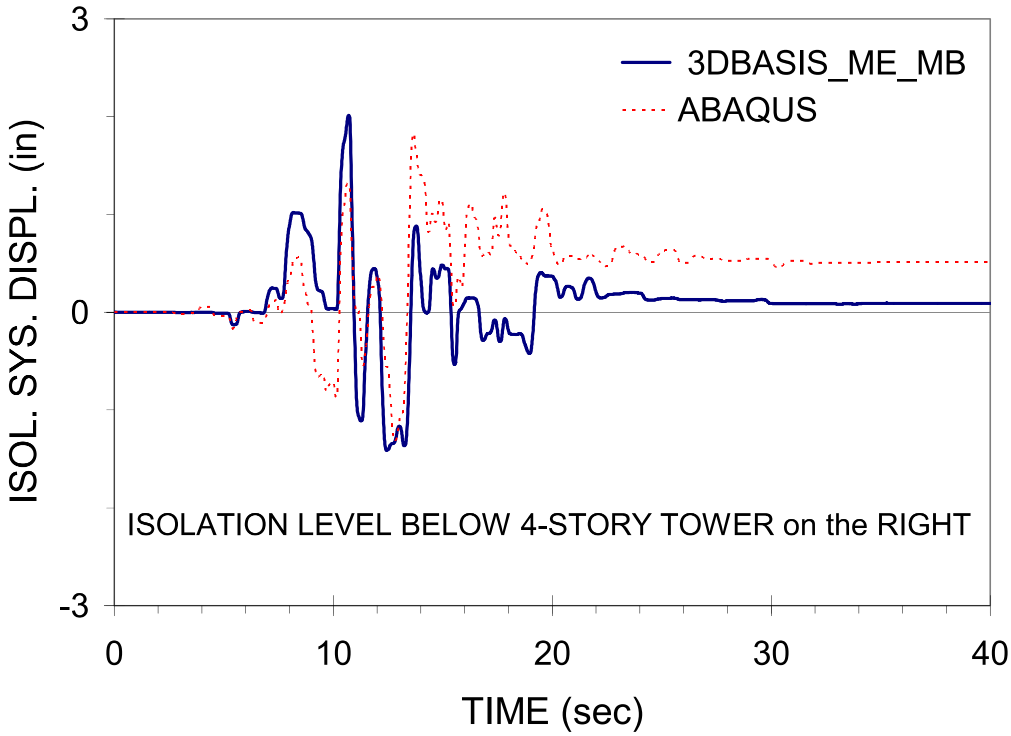

3DBASIS_ME_MB
ABAQUS
ISOLATION LEVEL BELOW 4-STORY TOWER on the RIGHT
ISOL. SYS. DISPL. (in)
TIME (sec)
3
0
-3
0
10
20
30
40

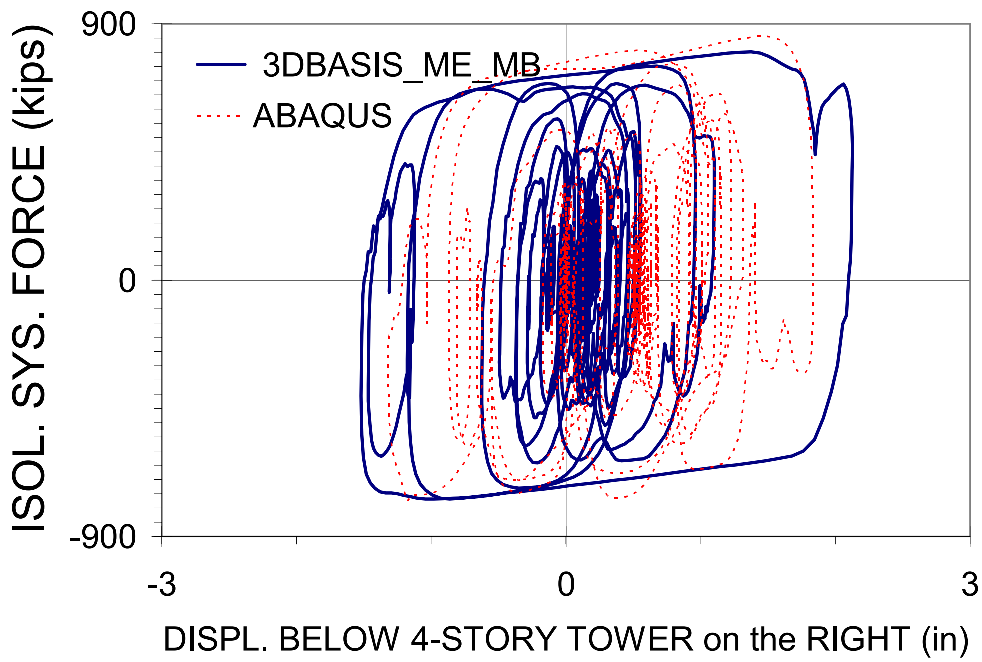

3DBASIS_ME_MB
ABAQUS
ISOL. SYS. FORCE (kips)
DISPL. BELOW 4-STORY TOWER on the RIGHT (in)
900
0
-900
-3
0
3

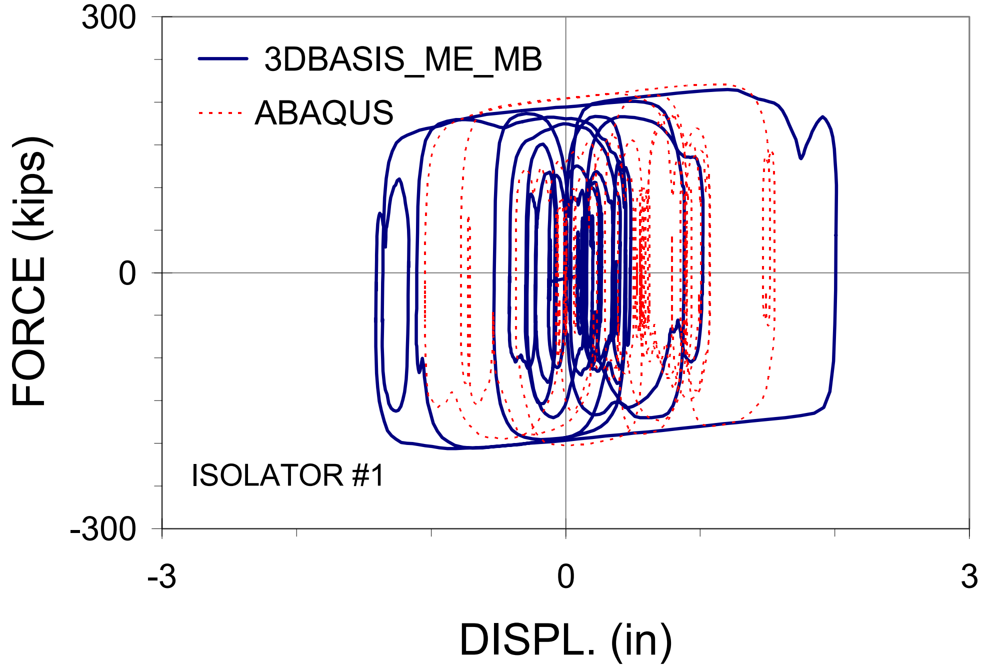

300
0
-300
FORCE (kips)
3DBASIS_ME_MB
ABAQUS
ISOLATOR #1
-3
0
3
DISPL. (in)

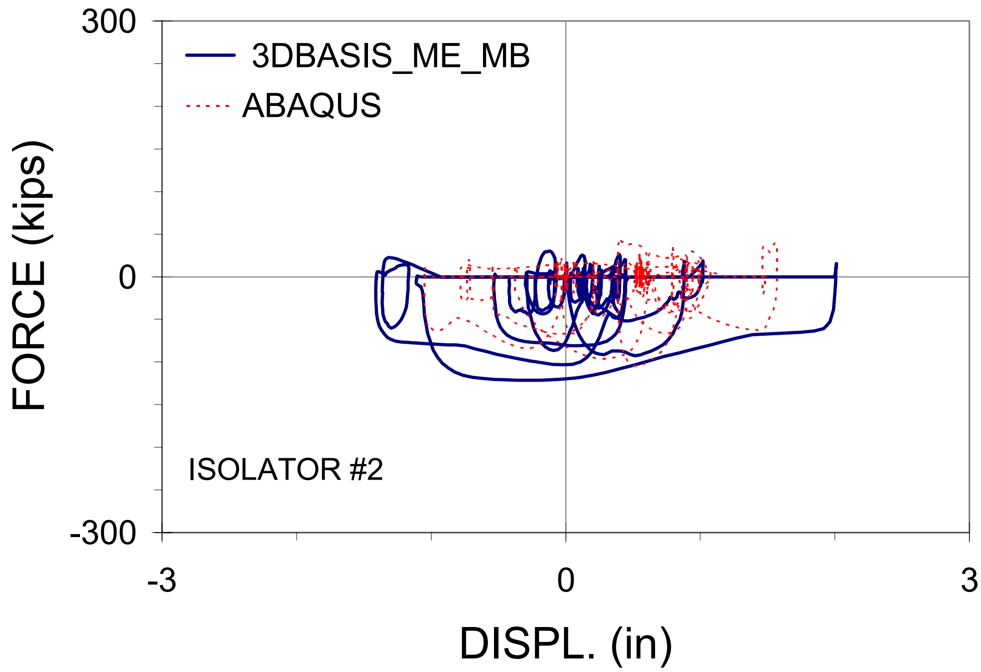

300
0
-300
FORCE (kips)
3DBASIS_ME_MB
ABAQUS
ISOLATOR #2
-3
0
3
DISPL. (in)

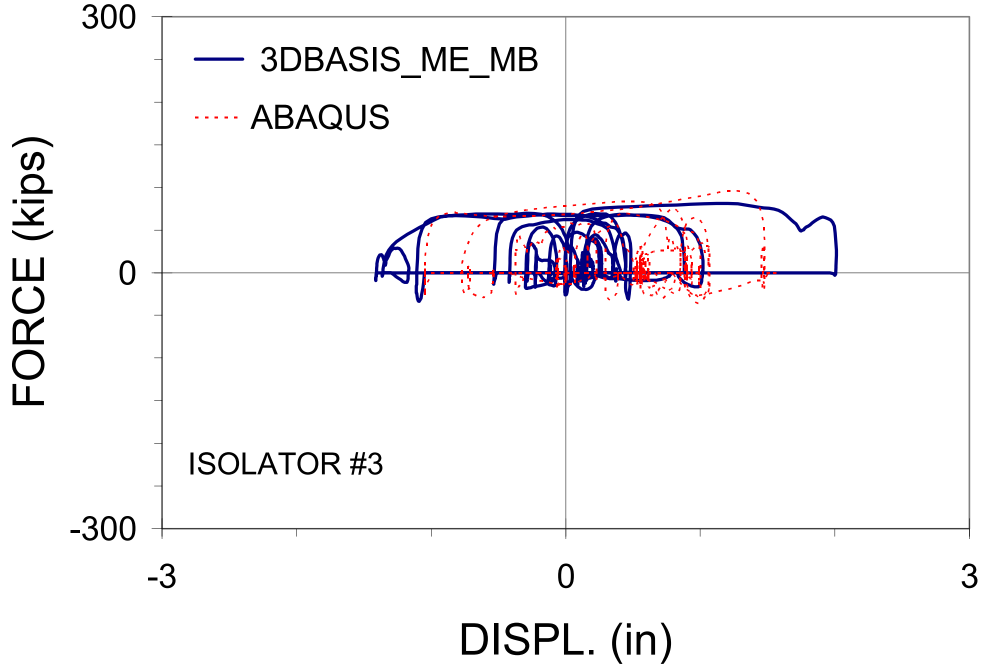
300
0
-300
-3
0
3
FORCE (kips)
DISPL. (in)
3DBASIS_ME_MB
ABAQUS
ISOLATOR #3

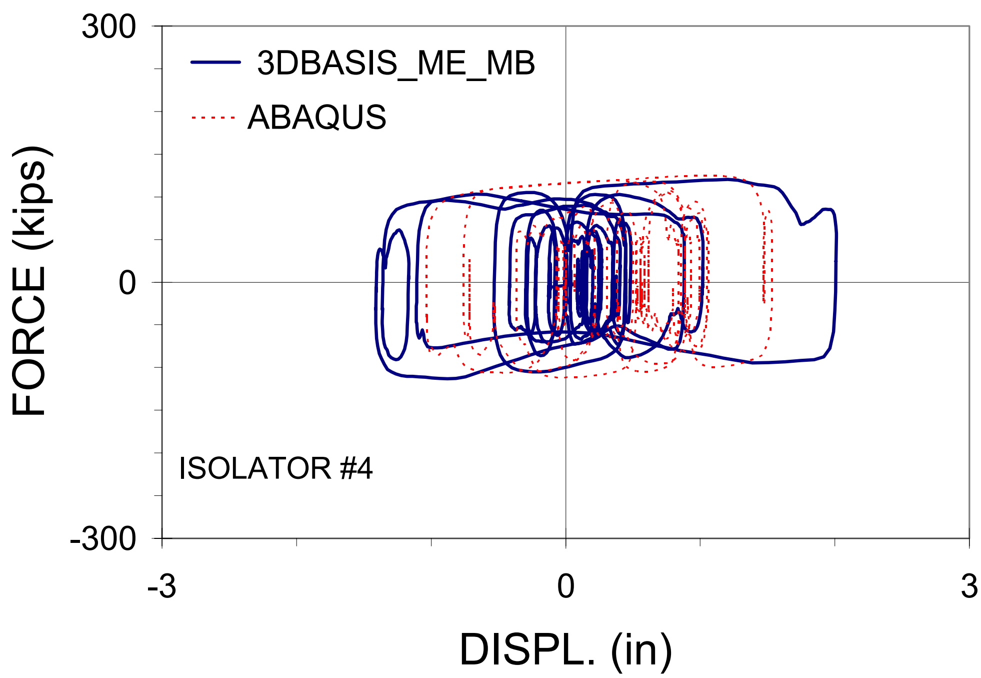
300
0
-300
-3
0
3
FORCE (kips)
DISPL. (in)
3DBASIS_ME_MB
ABAQUS
ISOLATOR #4

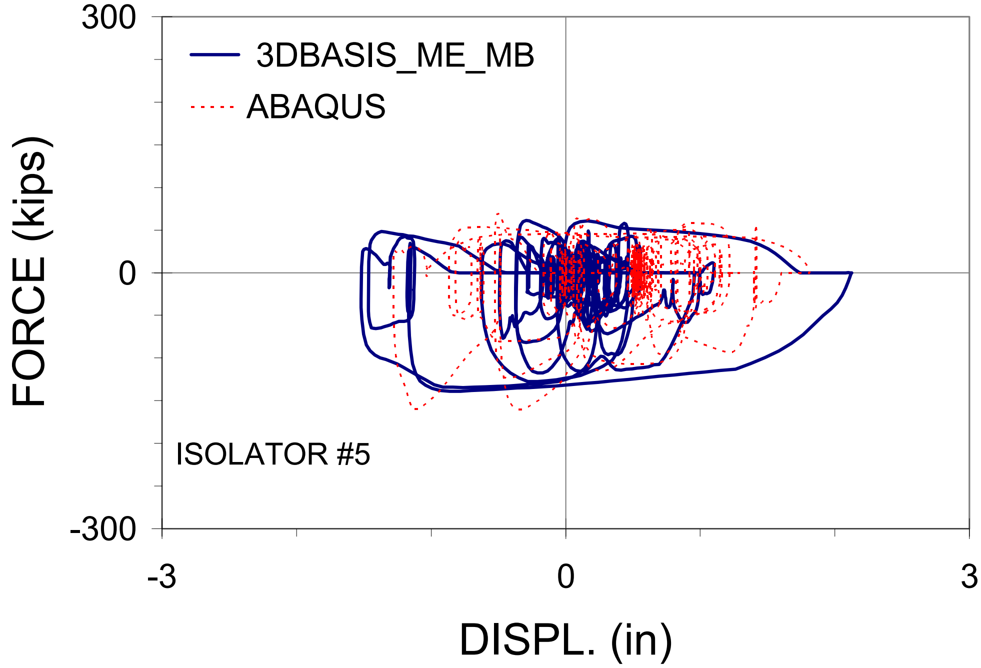
300
3DBASIS_ME_MB
ABAQUS
FORCE (kips)
0
ISOLATOR #5
-300
-3
0
3
DISPL. (in)

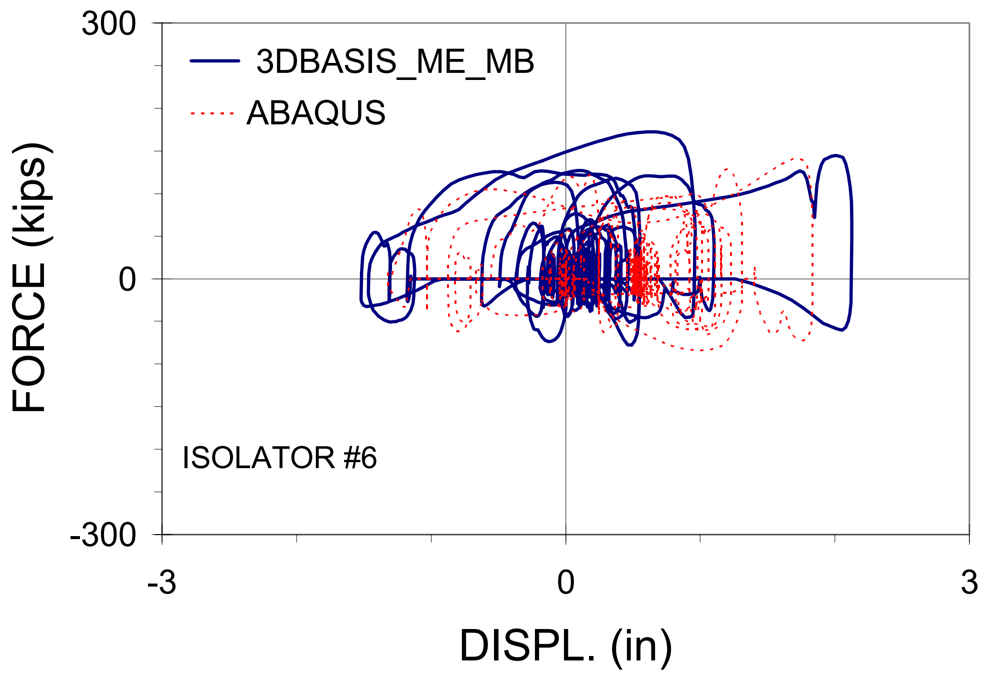
300
3DBASIS_ME_MB
ABAQUS
FORCE (kips)
0
ISOLATOR #6
-300
-3
0
3
DISPL. (in)

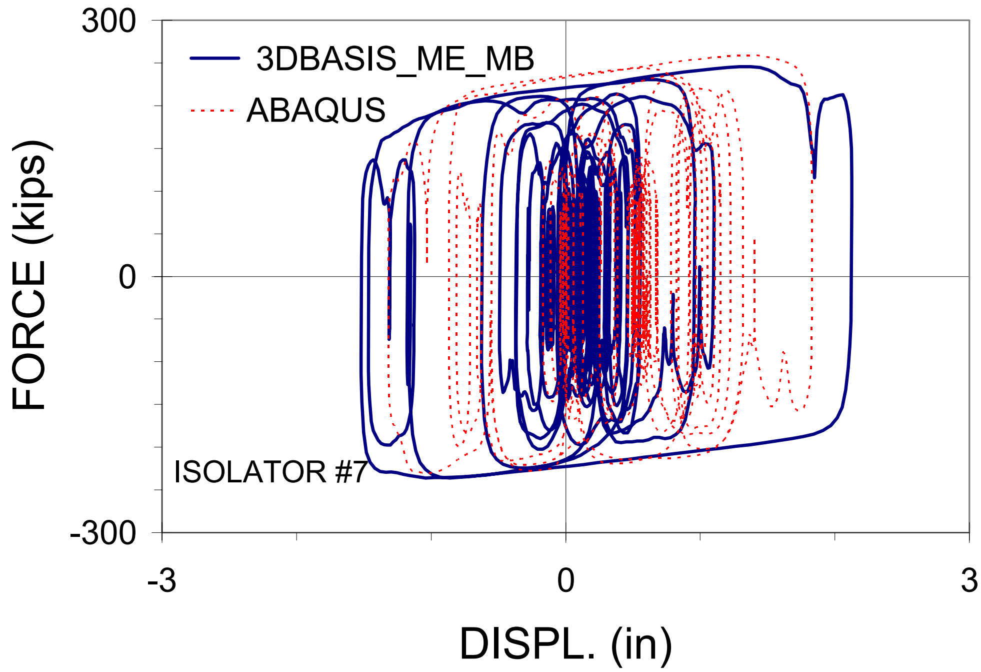
300
0
-300
-3
0
3
FORCE (kips)
DISPL. (in)
3DBASIS_ME_MB
ABAQUS
ISOLATOR #7

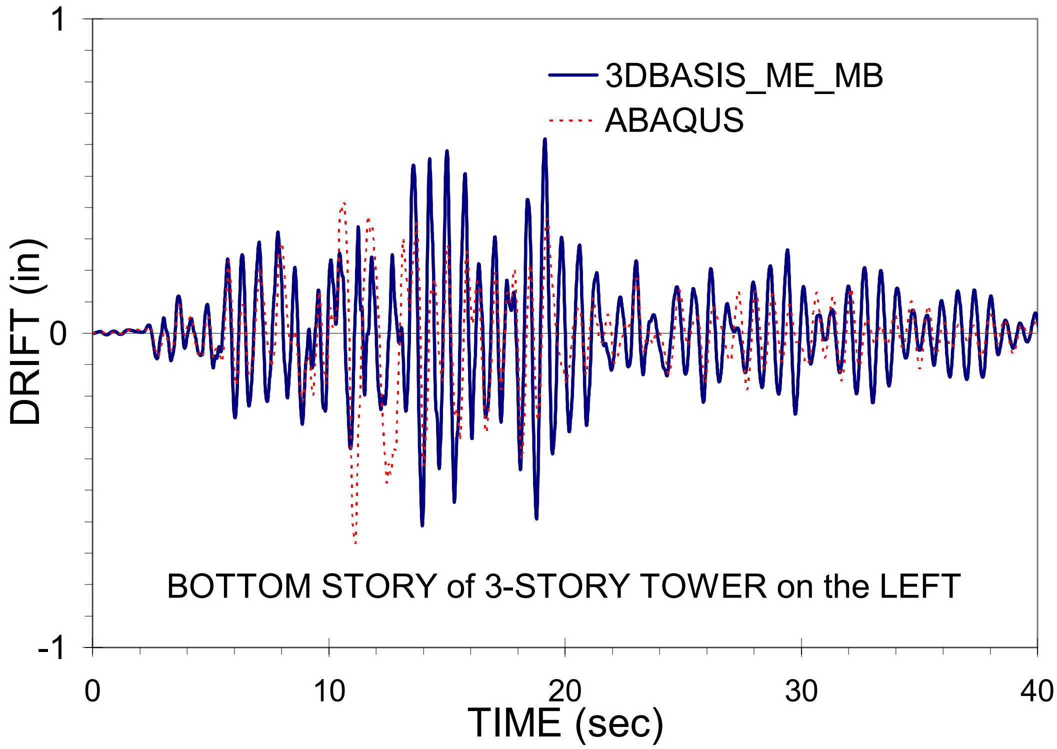
1
0
-1
DRIFT (in)
0
10
20
30
40
TIME (sec)
3DBASIS_ME_MB
ABAQUS
BOTTOM STORY of 3-STORY TOWER on the LEFT

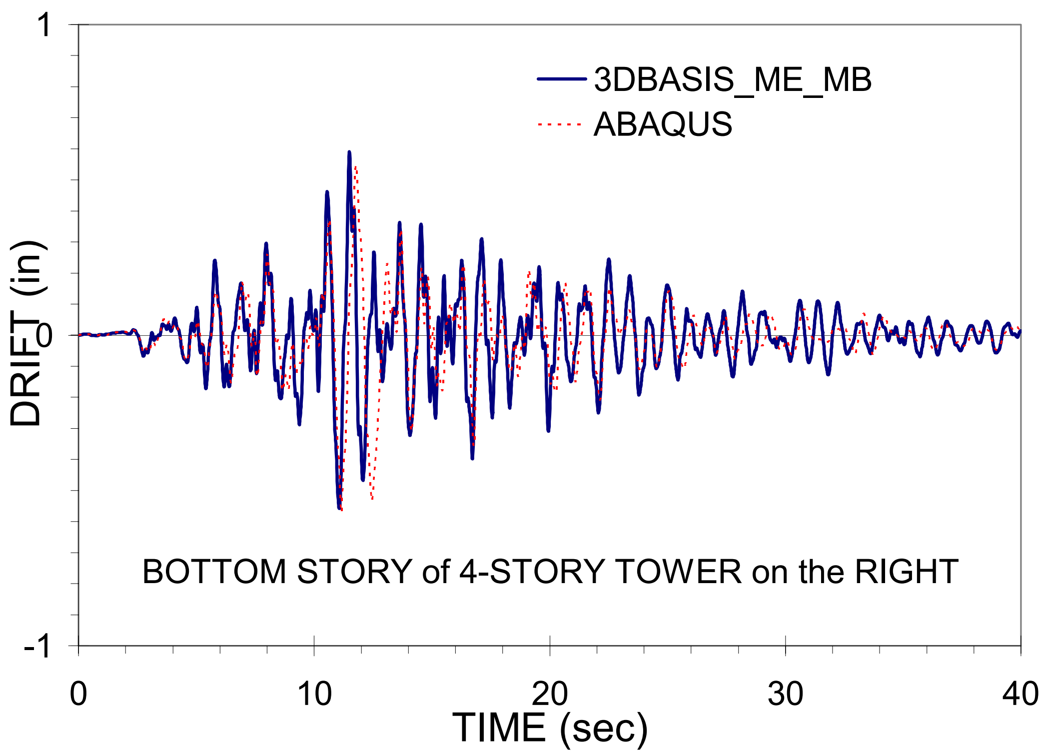
1
0
-1
DRIFT (in)
0
10
20
30
40
TIME (sec)
3DBASIS_ME_MB
ABAQUS
BOTTOM STORY of 4-STORY TOWER on the RIGHT

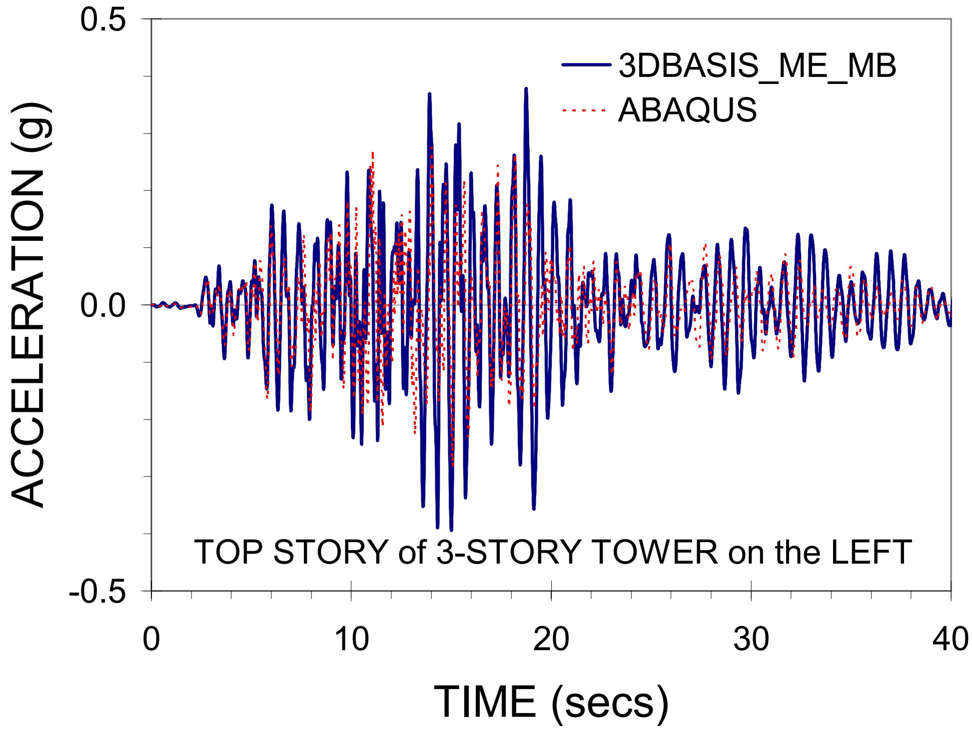

0.5
0.0
-0.5
ACCELERATION (g)
3DBASIS_ME_MB
ABAQUS
TOP STORY of 3-STORY TOWER on the LEFT
0
10
20
30
40
TIME (secs)

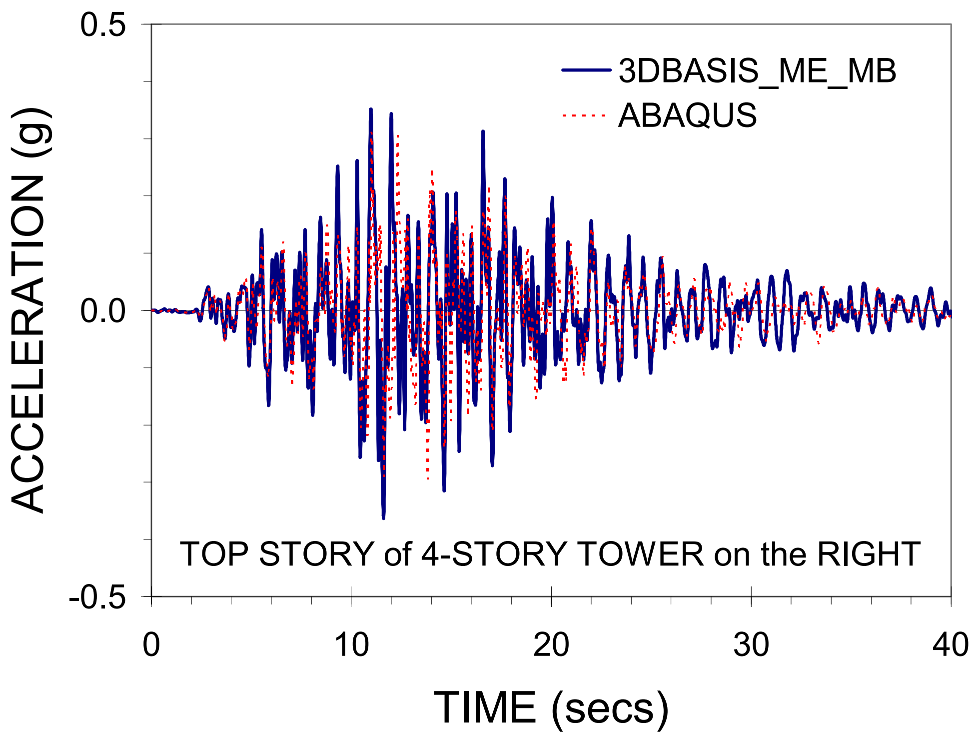

0.5
0.0
-0.5
ACCELERATION (g)
3DBASIS_ME_MB
ABAQUS
TOP STORY of 4-STORY TOWER on the RIGHT
0
10
20
30
40
TIME (secs)

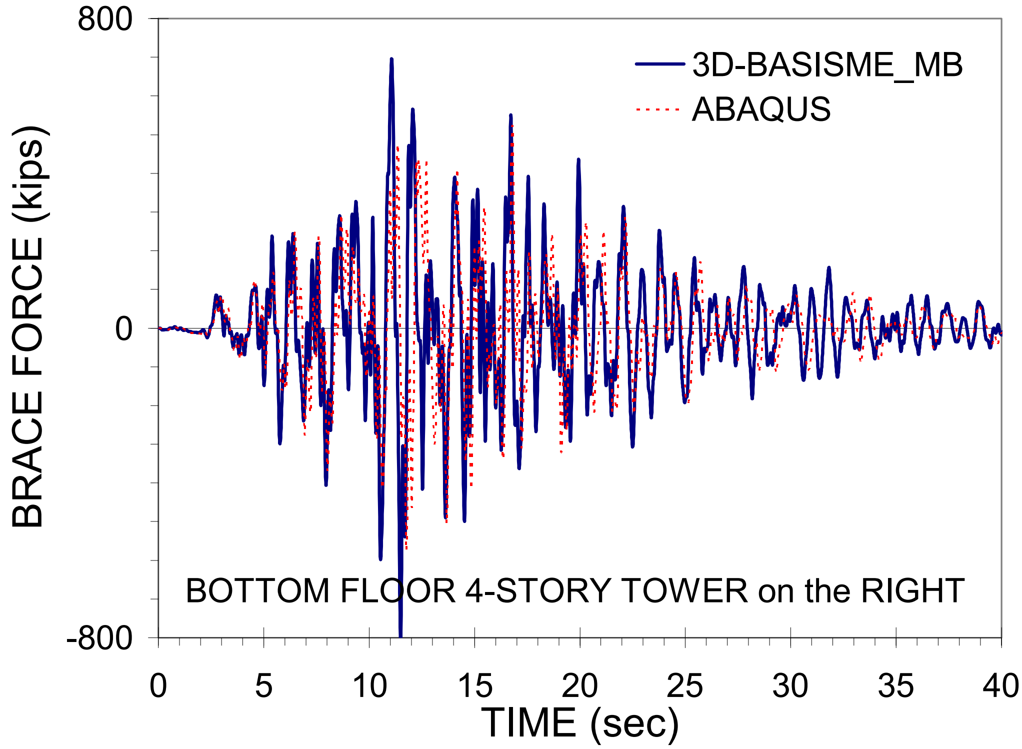
800
0
-800
BRACE FORCE (kips)
3D-BASISME_MB
ABAQUS
BOTTOM FLOOR 4-STORY TOWER on the RIGHT
0
5
10
15
20
25
30
35
40
TIME (sec)

APPENDIX K

COMPARISON OF RESULTS OF PROGRAM 3D-BASIS-ME-MB TO RESULTS OF PROGRAM ABAQUS FOR TWO-TOWER VERIFICATION MODEL

(CASE OF FRICTION COEFFICIENT $f_{\max} = 0.04$)

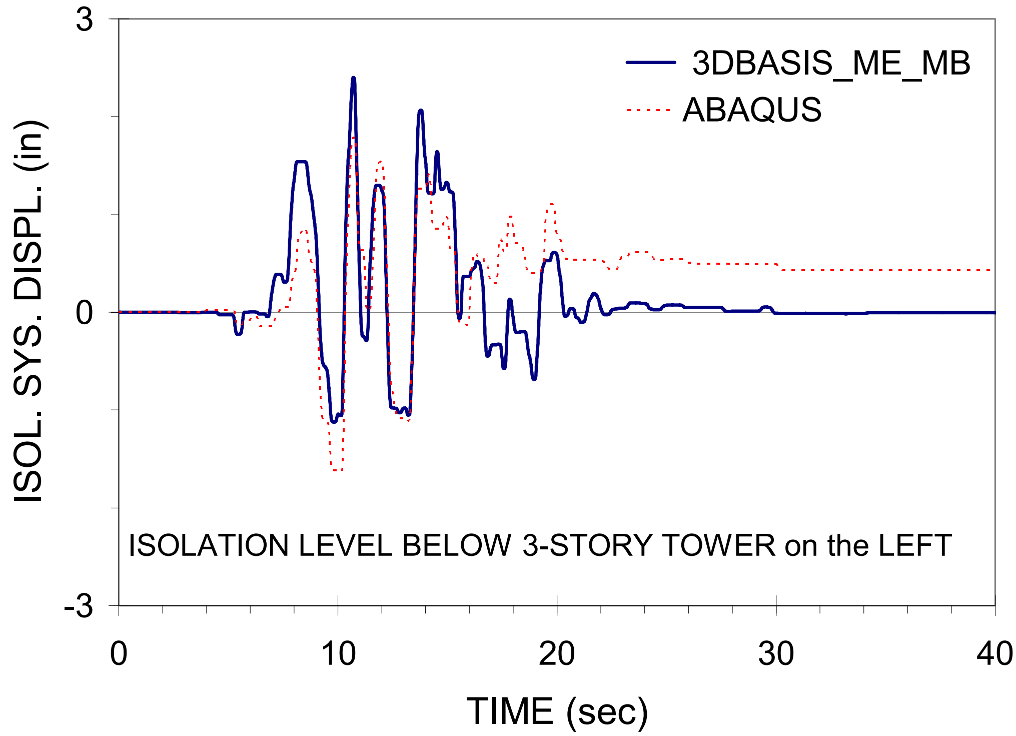
3
0
-3
ISOL. SYS. DISPL. (in)
3DBASIS_ME_MB
ABAQUS
ISOLATION LEVEL BELOW 3-STORY TOWER on the LEFT
0
10
20
30
40
TIME (sec)

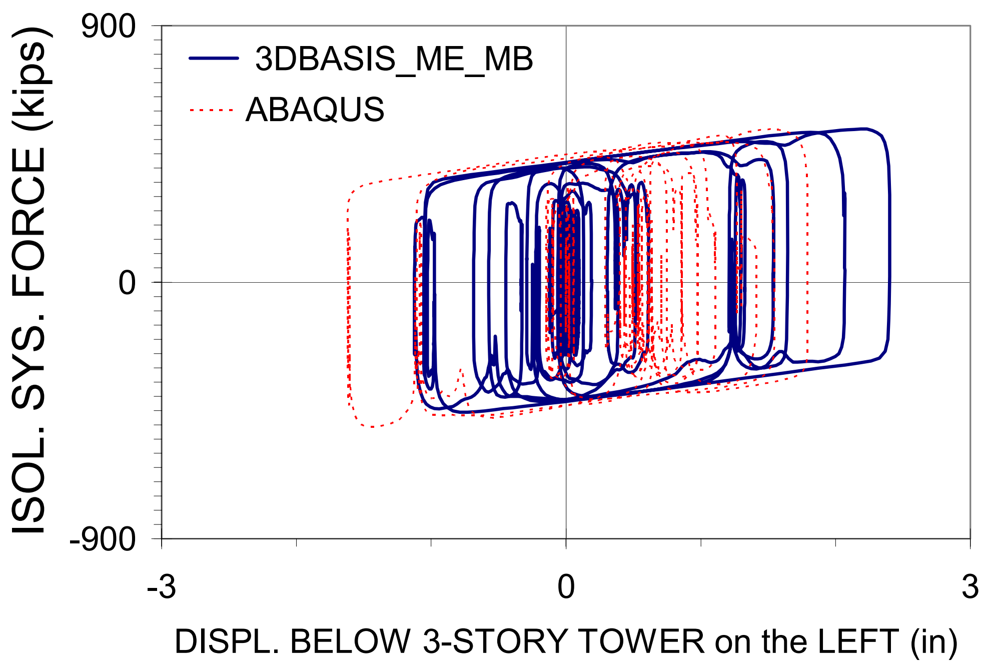
900
0
-900
ISOL. SYS. FORCE (kips)
3DBASIS_ME_MB
ABAQUS
-3
0
3
DISPL. BELOW 3-STORY TOWER on the LEFT (in)

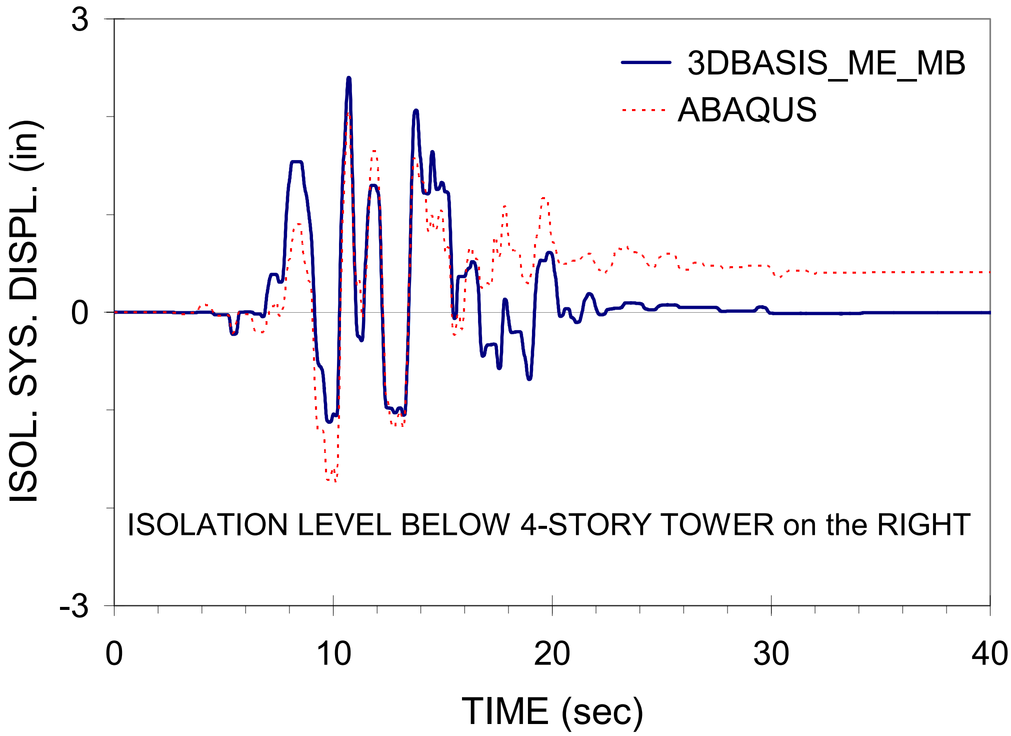

3DBASIS_ME_MB
ABAQUS
ISOLATION LEVEL BELOW 4-STORY TOWER on the RIGHT
ISOL. SYS. DISPL. (in)
TIME (sec)
3
0
-3
0
10
20
30
40

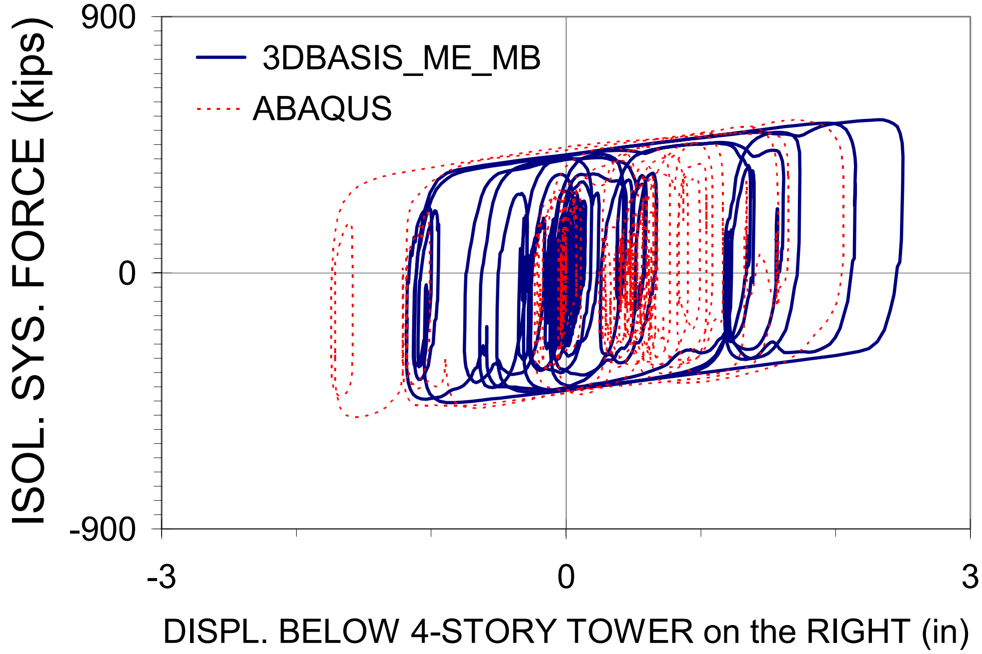

3DBASIS_ME_MB
ABAQUS
ISOL. SYS. FORCE (kips)
DISPL. BELOW 4-STORY TOWER on the RIGHT (in)
900
0
-900
-3
0
3

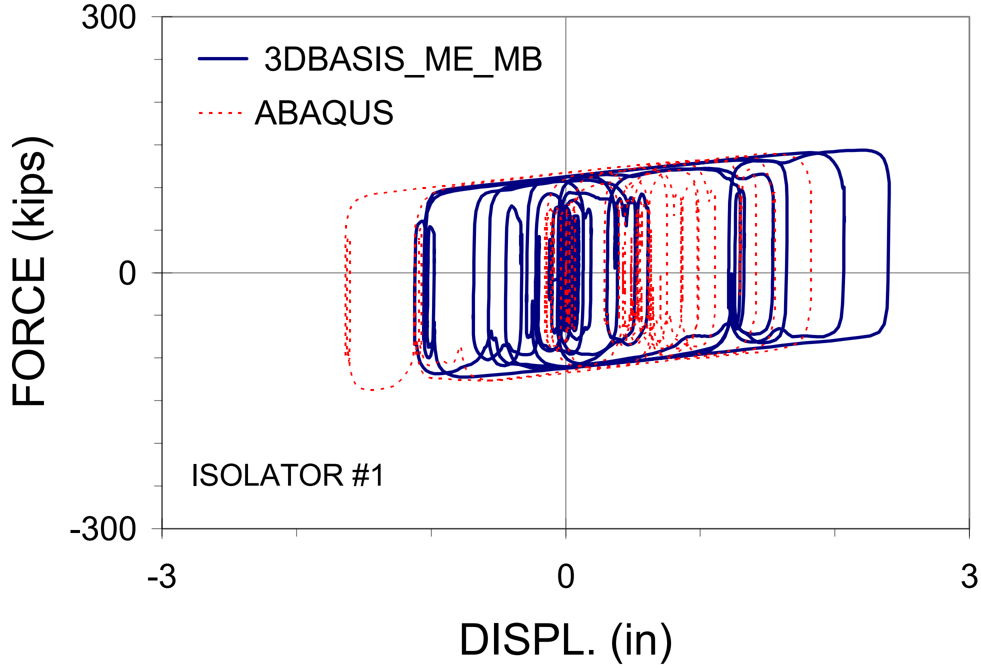
300
0
-300
-3
0
3
FORCE (kips)
DISPL. (in)
3DBASIS_ME_MB
ABAQUS
ISOLATOR #1

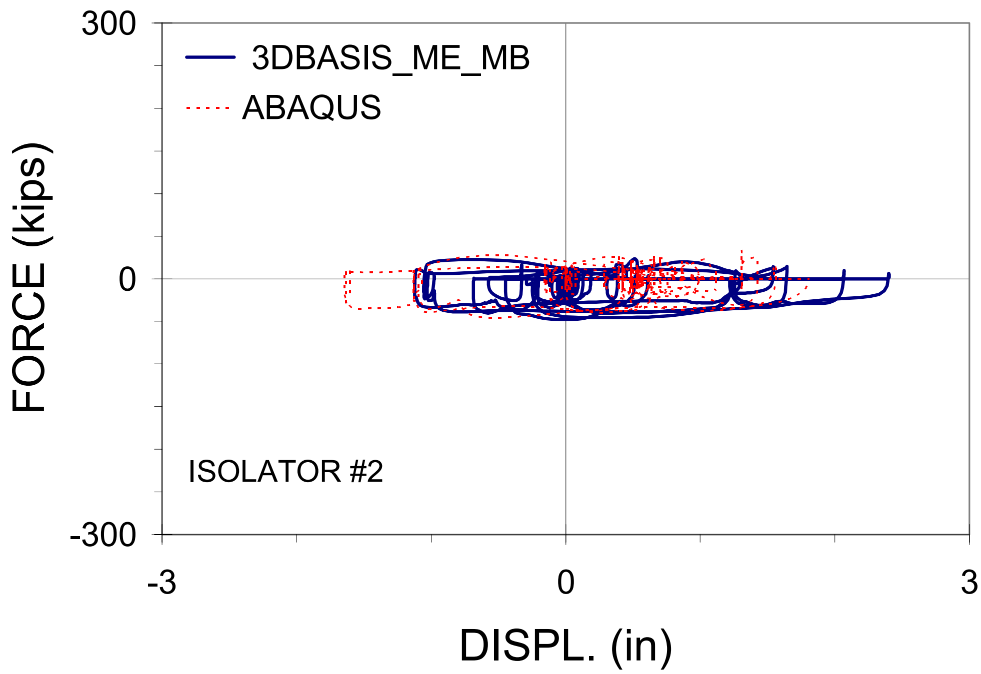
300
0
-300
-3
0
3
FORCE (kips)
DISPL. (in)
3DBASIS_ME_MB
ABAQUS
ISOLATOR #2

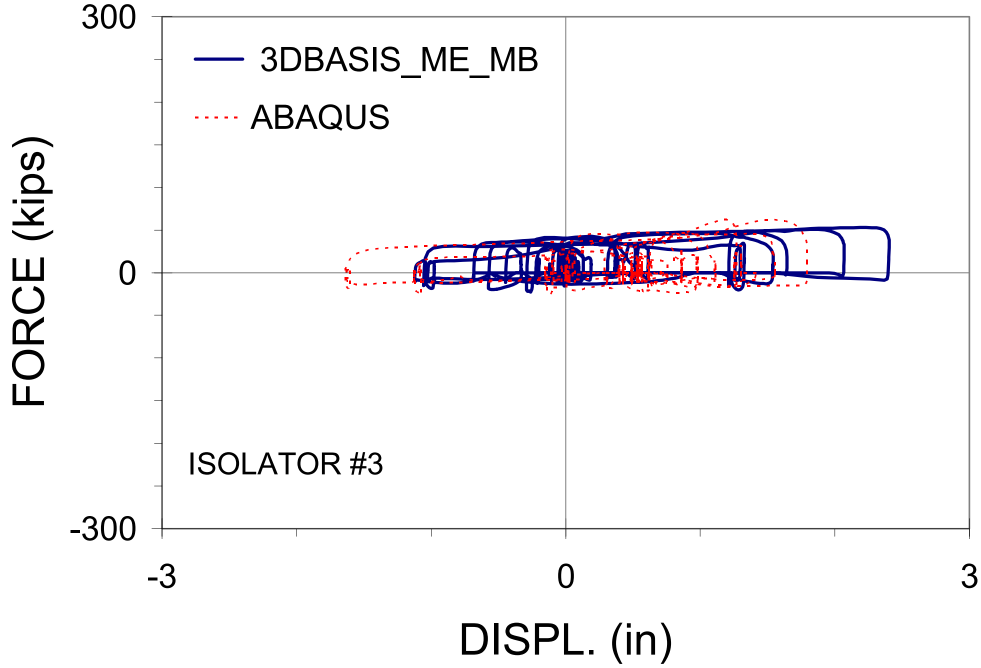
300
3DBASIS_ME_MB
ABAQUS
FORCE (kips)
0
ISOLATOR #3
-300
-3
0
3
DISPL. (in)

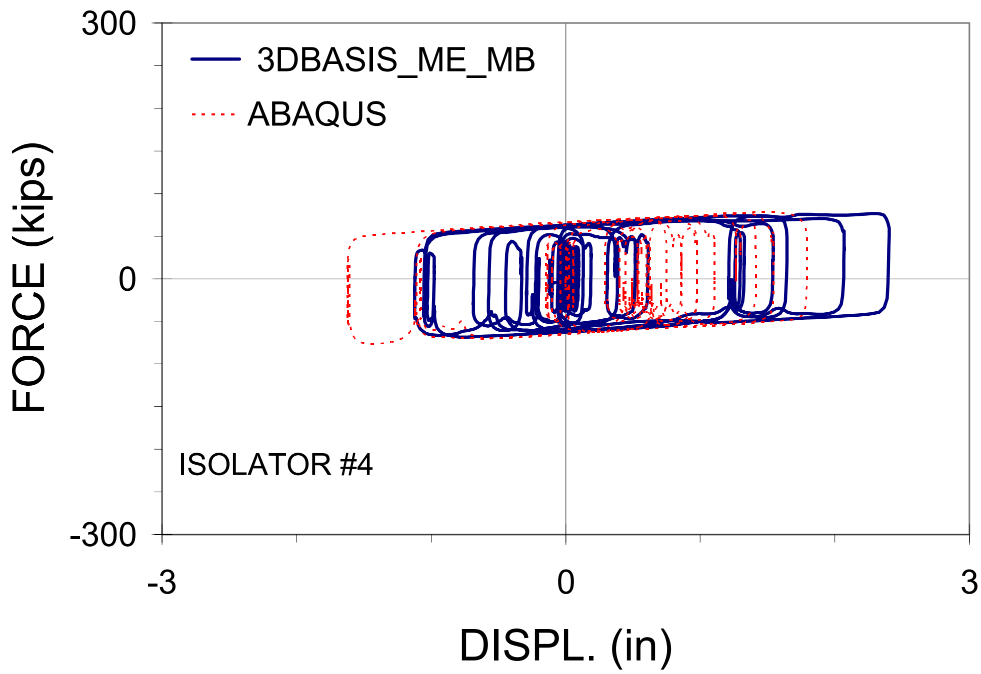
300
3DBASIS_ME_MB
ABAQUS
FORCE (kips)
0
ISOLATOR #4
-300
-3
0
3
DISPL. (in)

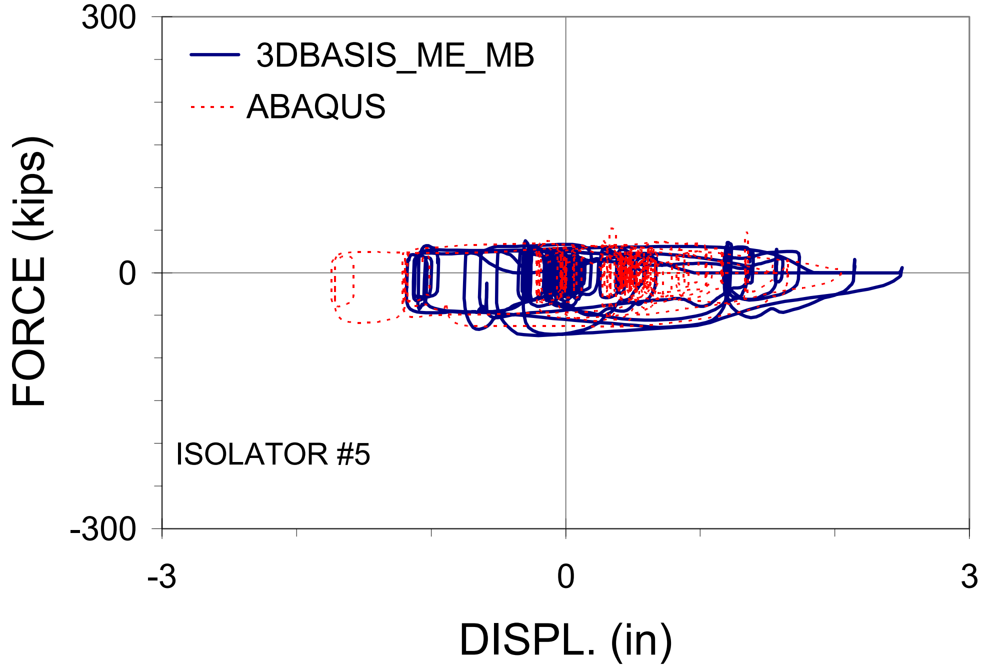

300
0
-300
-3
0
3
FORCE (kips)
DISPL. (in)
3DBASIS_ME_MB
ABAQUS
ISOLATOR #5

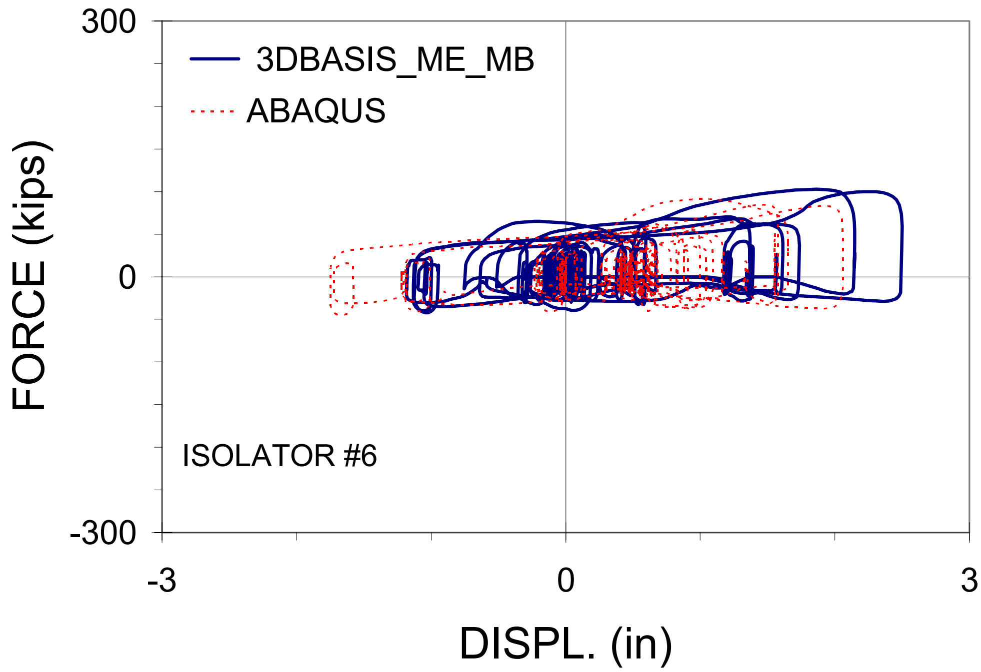

300
0
-300
-3
0
3
FORCE (kips)
DISPL. (in)
3DBASIS_ME_MB
ABAQUS
ISOLATOR #6

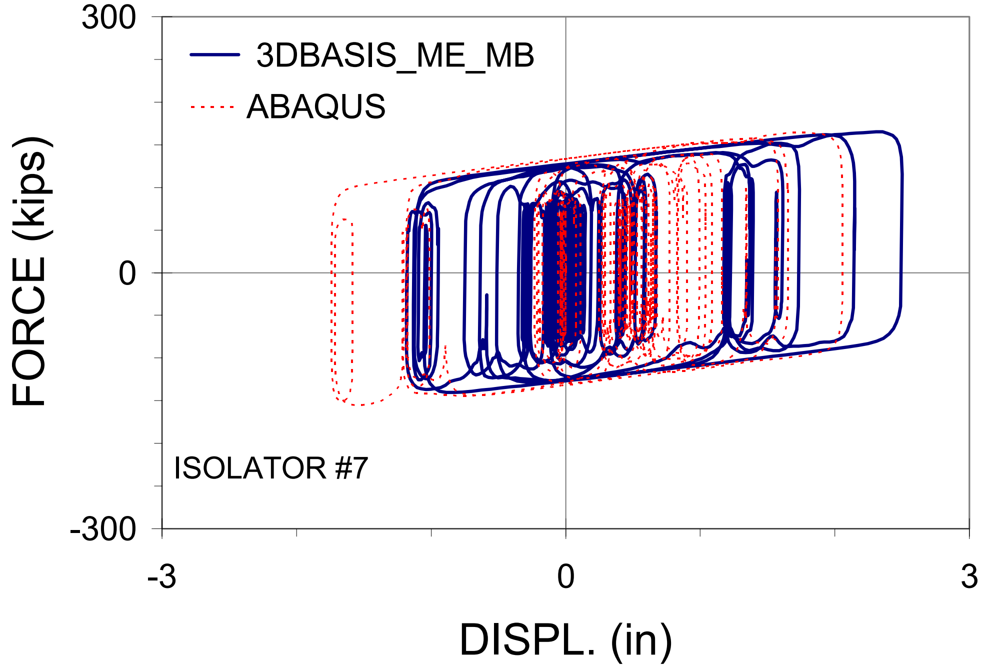

300
0
-300
FORCE (kips)
3DBASIS_ME_MB
ABAQUS
ISOLATOR #7
-3
0
3
DISPL. (in)

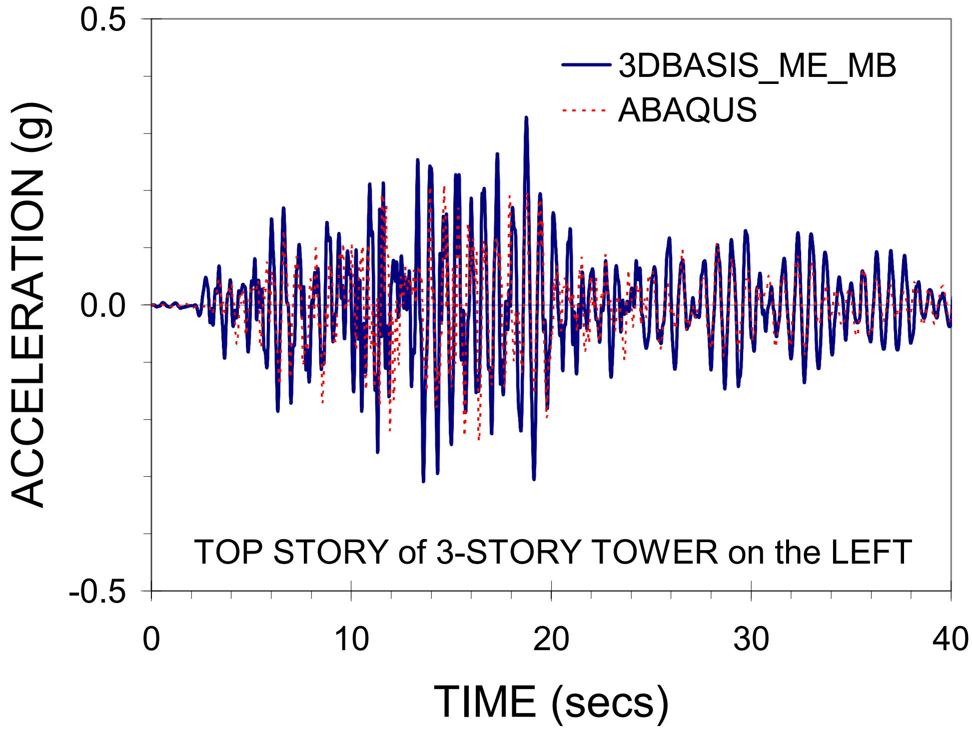
0.5
0.0
-0.5
ACCELERATION (g)
3DBASIS_ME_MB
ABAQUS
TOP STORY of 3-STORY TOWER on the LEFT
0
10
20
30
40
TIME (secs)

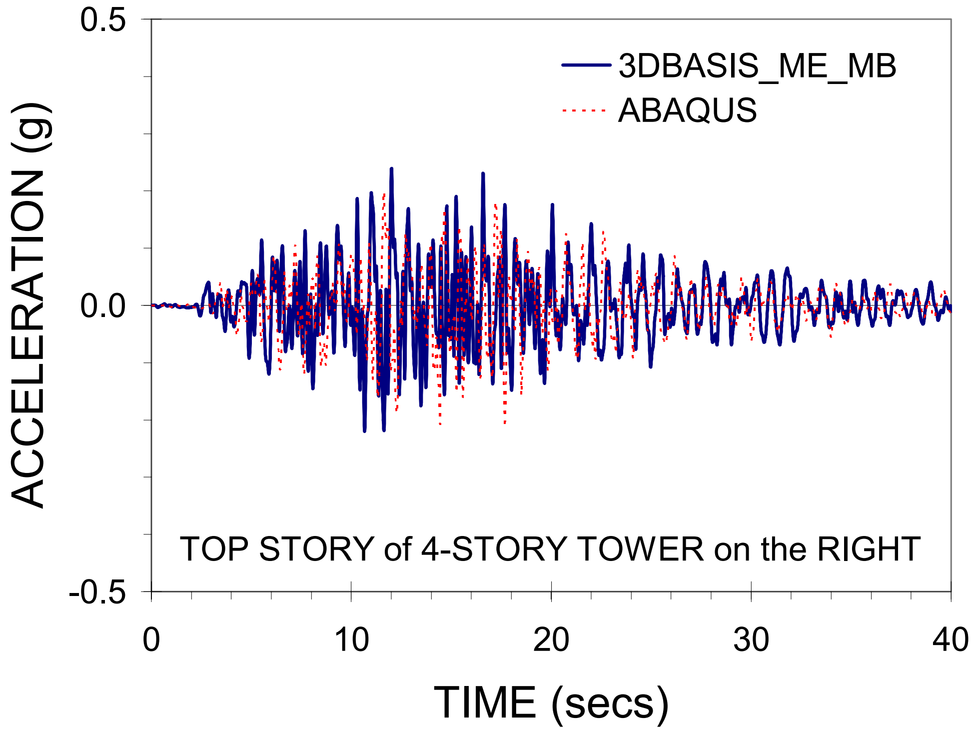
0.5
0.0
-0.5
ACCELERATION (g)
3DBASIS_ME_MB
ABAQUS
TOP STORY of 4-STORY TOWER on the RIGHT
0
10
20
30
40
TIME (secs)

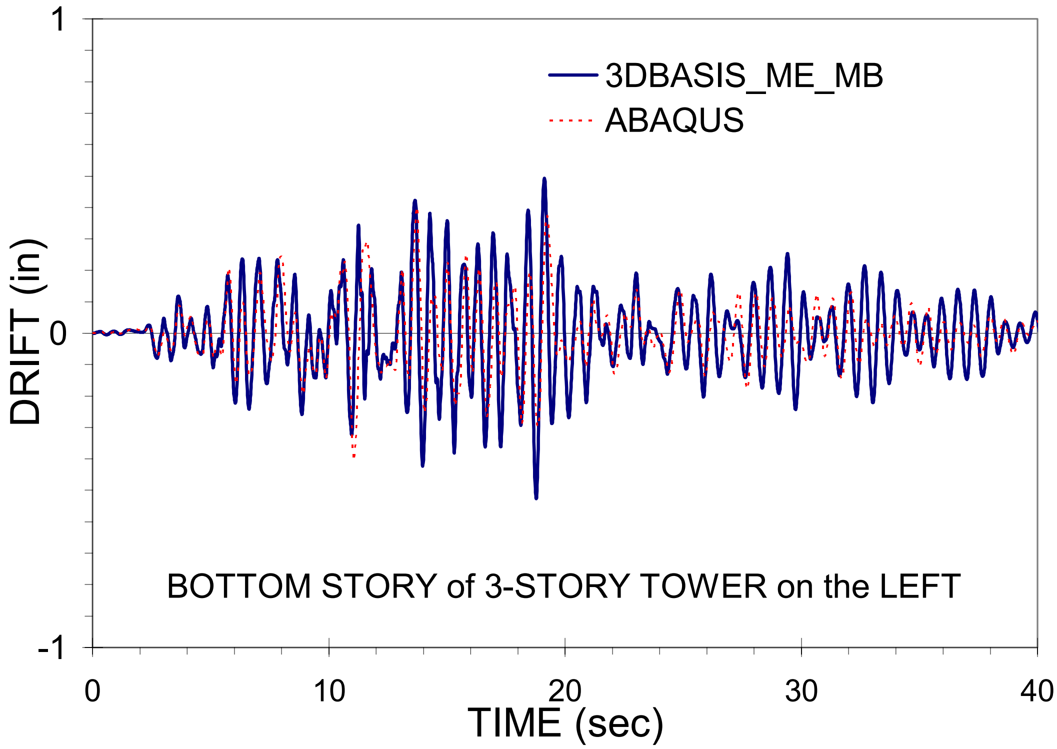
3DBASIS_ME_MB
ABAQUS
BOTTOM STORY of 3-STORY TOWER on the LEFT
DRIFT (in)
TIME (sec)
1
0
-1
0
10
20
30
40

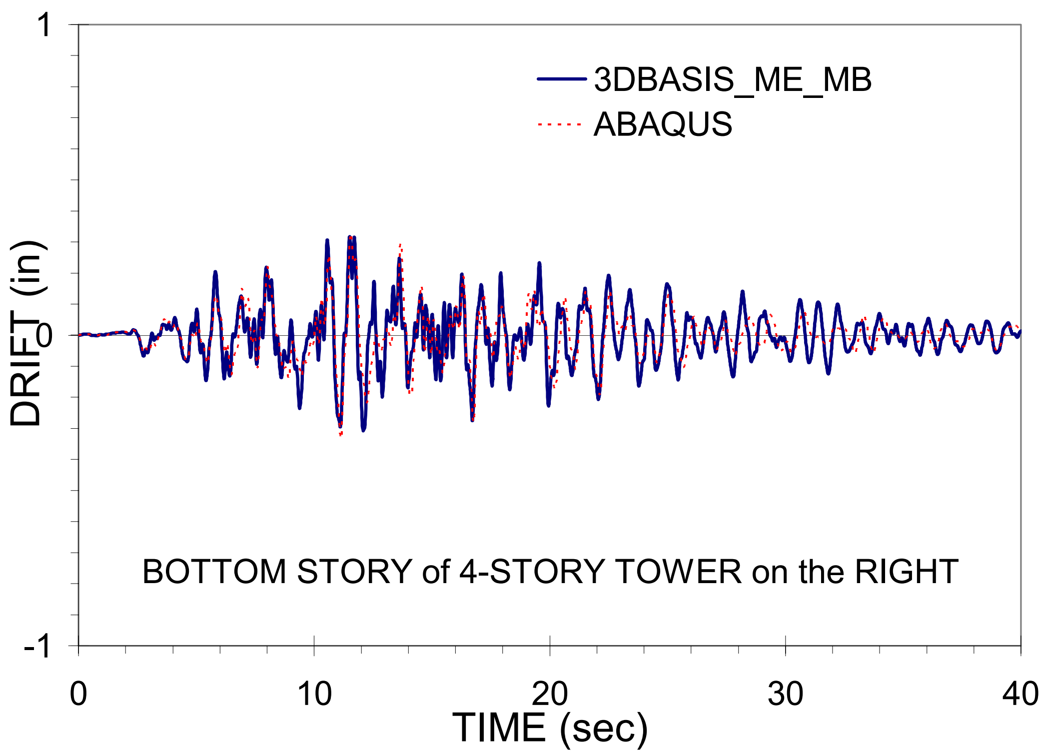
3DBASIS_ME_MB
ABAQUS
BOTTOM STORY of 4-STORY TOWER on the RIGHT
DRIFT (in)
TIME (sec)
1
0
-1
0
10
20
30
40

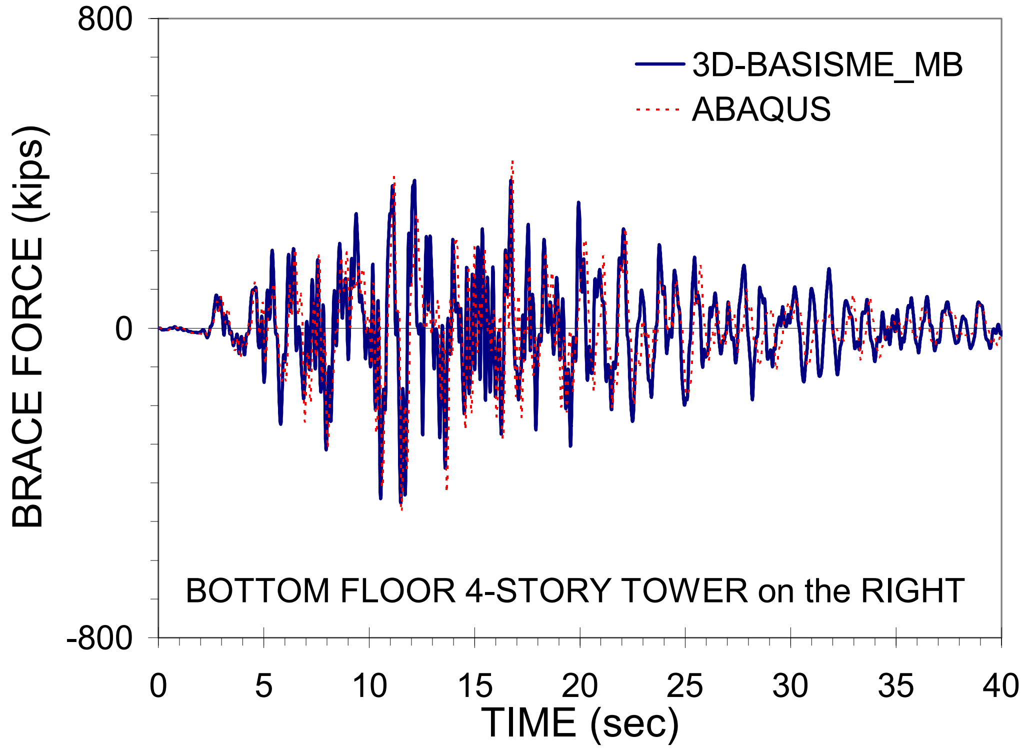

800
0
-800
BRACE FORCE (kips)
3D-BASISME_MB
ABAQUS
BOTTOM FLOOR 4-STORY TOWER on the RIGHT
0
5
10
15
20
25
30
35
40
TIME (sec)

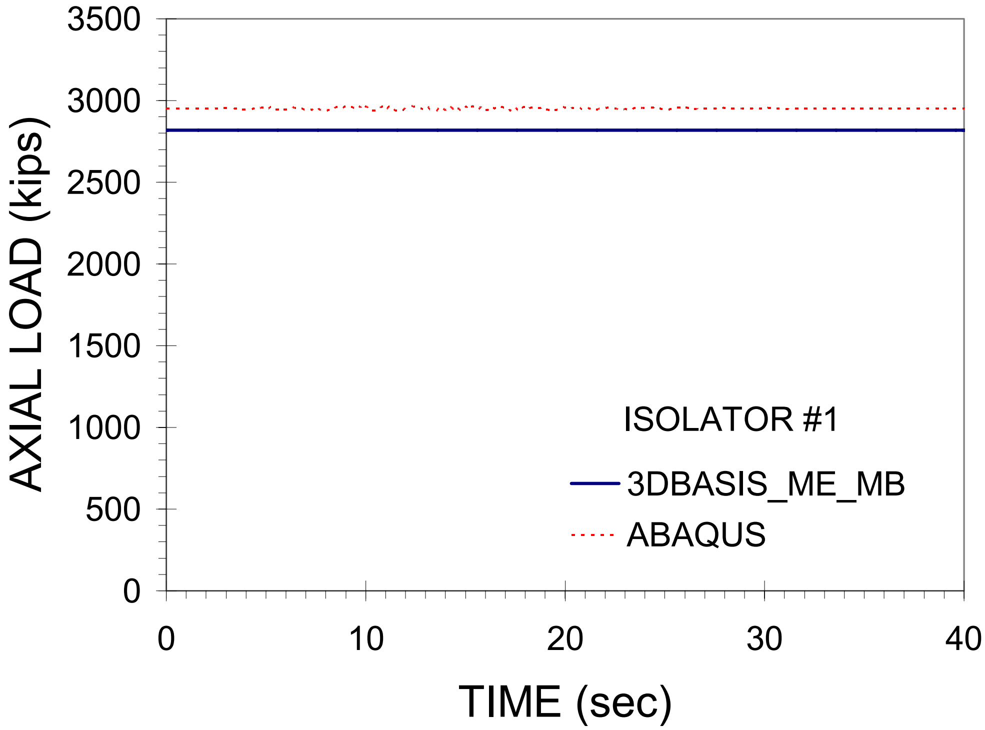

AXIAL LOAD (kips)
3500
3000
2500
2000
1500
1000
500
0
0
10
20
30
40
TIME (sec)
ISOLATOR #1
3DBASIS_ME_MB
ABAQUS

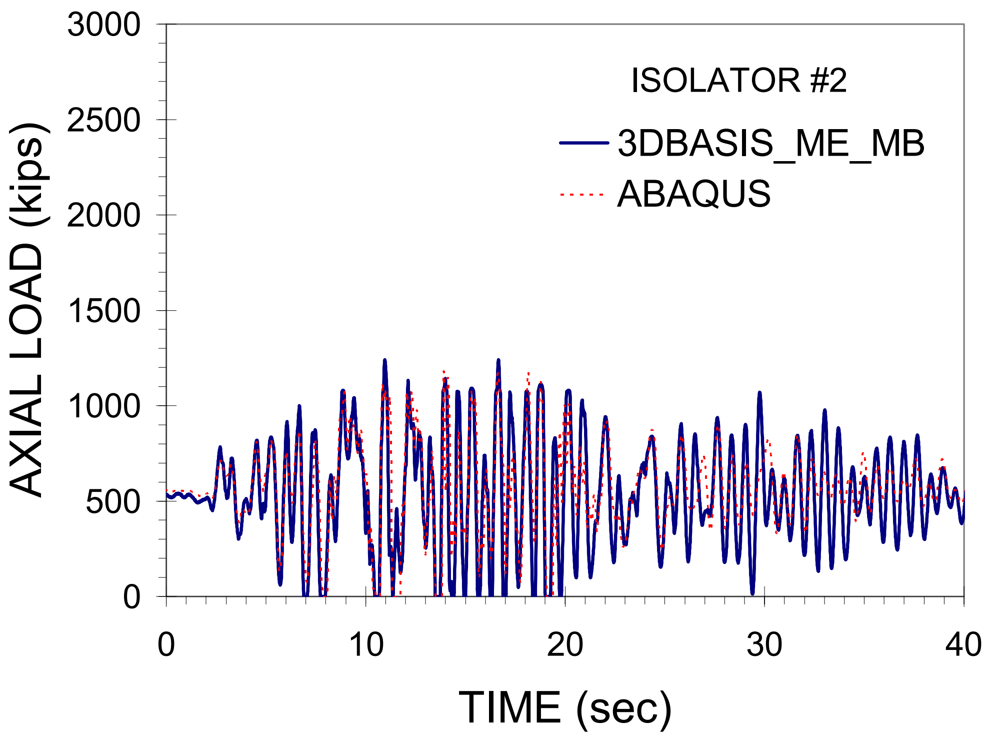

AXIAL LOAD (kips)
3000
2500
2000
1500
1000
500
0
0
10
20
30
40
TIME (sec)
ISOLATOR #2
3DBASIS_ME_MB
ABAQUS

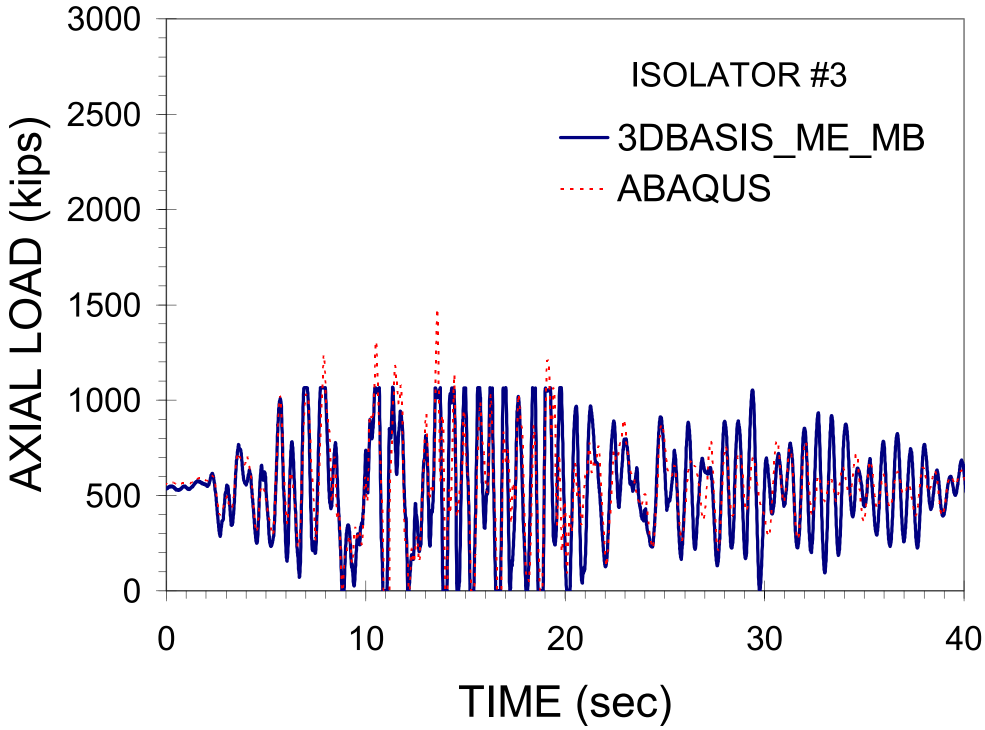
ISOLATOR #3
3DBASIS_ME_MB
ABAQUS
AXIAL LOAD (kips)
TIME (sec)
3000
2500
2000
1500
1000
500
0
0
10
20
30
40

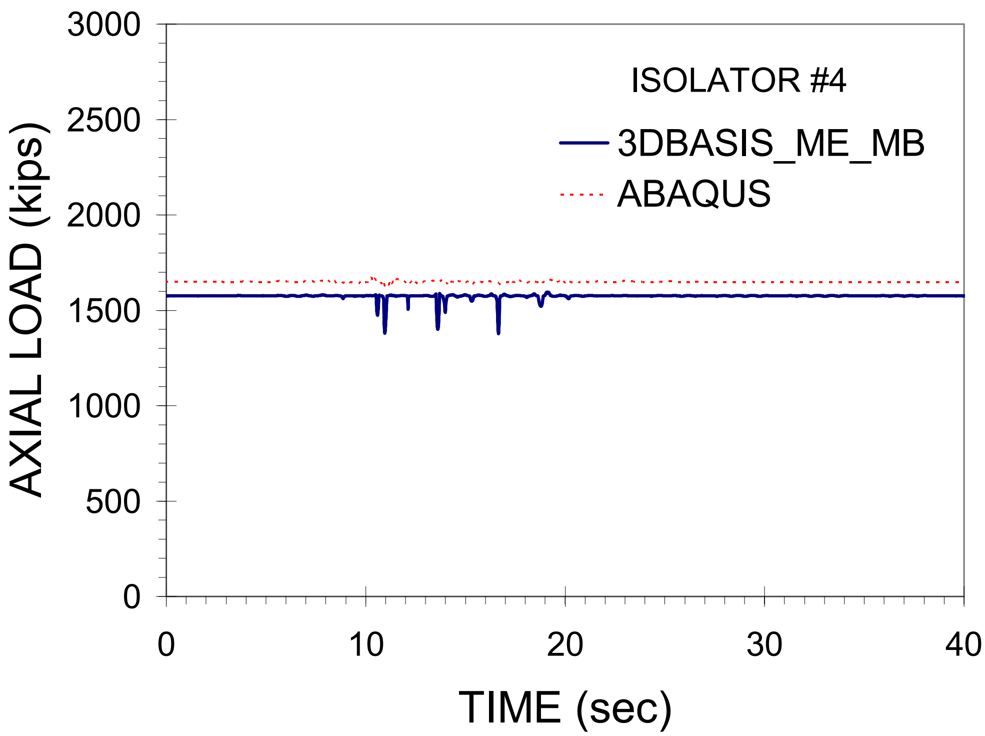
ISOLATOR #4
3DBASIS_ME_MB
ABAQUS
AXIAL LOAD (kips)
TIME (sec)
3000
2500
2000
1500
1000
500
0
0
10
20
30
40

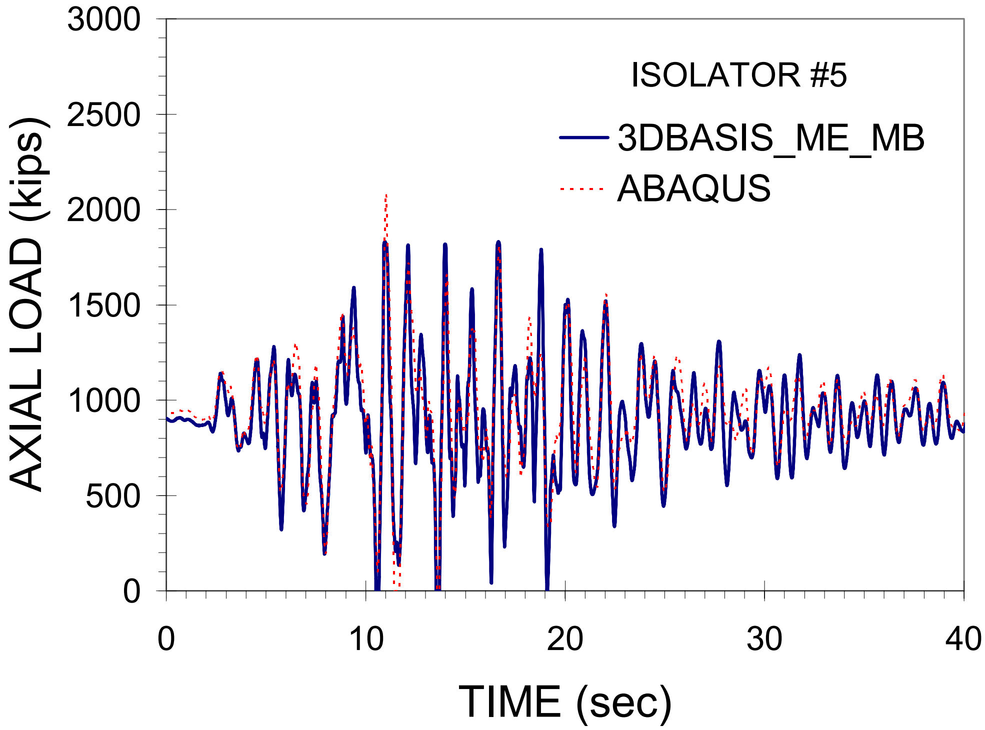

AXIAL LOAD (kips)
3000
2500
2000
1500
1000
500
0
ISOLATOR #5
3DBASIS_ME_MB
ABAQUS
0
10
20
30
40
TIME (sec)

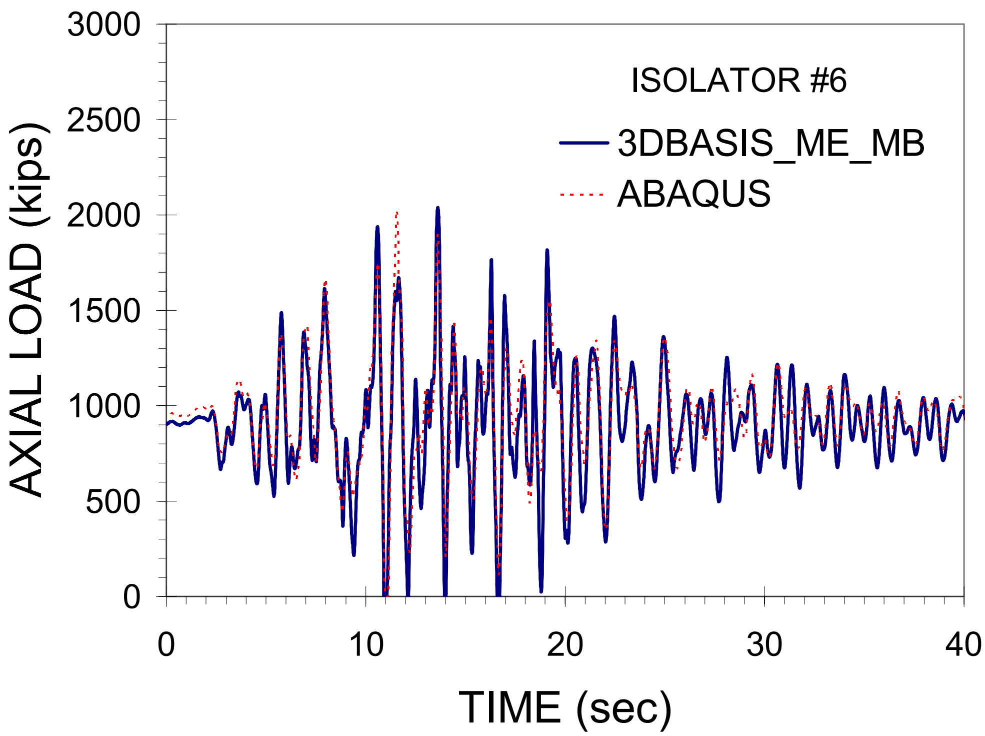

AXIAL LOAD (kips)
3000
2500
2000
1500
1000
500
0
ISOLATOR #6
3DBASIS_ME_MB
ABAQUS
0
10
20
30
40
TIME (sec)

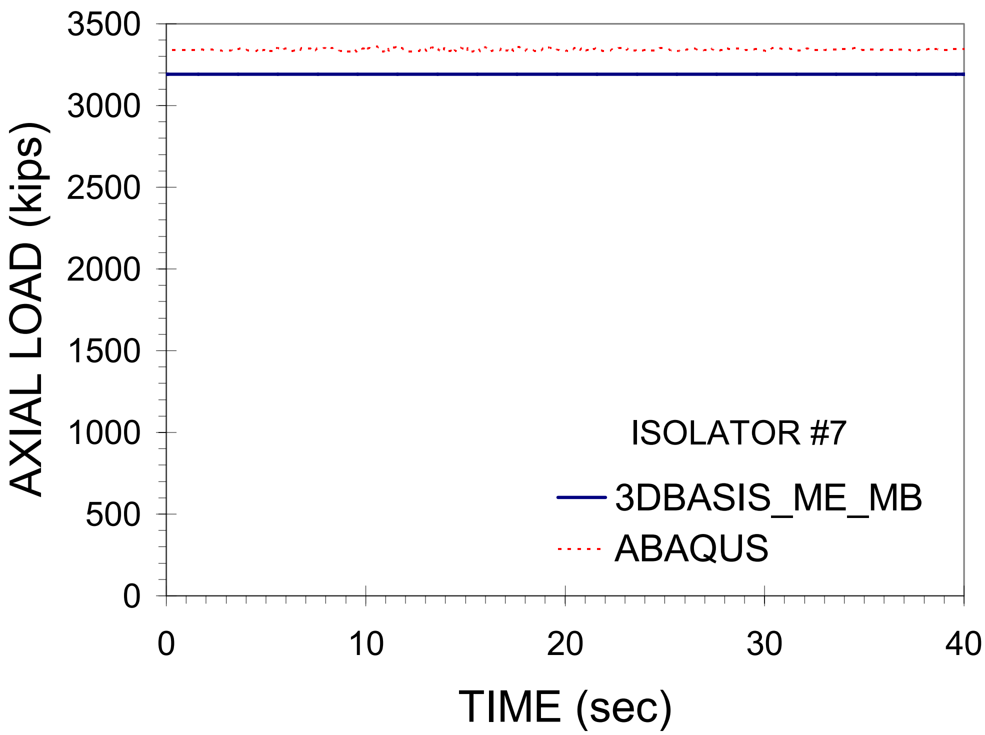
3500
3000
2500
2000
1500
1000
500
0
AXIAL LOAD (kips)
0
10
20
30
40
TIME (sec)
ISOLATOR #7
3DBASIS_ME_MB
ABAQUS

Multidisciplinary Center for Earthquake Engineering Research
List of Technical Reports

The Multidisciplinary Center for Earthquake Engineering Research (MCEER) publishes technical reports on a variety of subjects related to earthquake engineering written by authors funded through MCEER. These reports are available from both MCEER Publications and the National Technical Information Service (NTIS). Requests for reports should be directed to MCEER Publications, Multidisciplinary Center for Earthquake Engineering Research, State University of New York at Buffalo, Red Jacket Quadrangle, Buffalo, New York 14261. Reports can also be requested through NTIS, 5285 Port Royal Road, Springfield, Virginia 22161. NTIS accession numbers are shown in parenthesis, if available.

NCEER-87-0001 "First-Year Program in Research, Education and Technology Transfer," 3/5/87, (PB88-134275, A04, MF-A01).

NCEER-87-0002 "Experimental Evaluation of Instantaneous Optimal Algorithms for Structural Control," by R.C. Lin, T.T. Soong and A.M. Reinhorn, 4/20/87, (PB88-134341, A04, MF-A01).

NCEER-87-0003 "Experimentation Using the Earthquake Simulation Facilities at University at Buffalo," by A.M. Reinhorn and R.L. Ketter, to be published.

NCEER-87-0004 "The System Characteristics and Performance of a Shaking Table," by J.S. Hwang, K.C. Chang and G.C. Lee, 6/1/87, (PB88-134259, A03, MF-A01). This report is available only through NTIS (see address given above).

NCEER-87-0005 "A Finite Element Formulation for Nonlinear Viscoplastic Material Using a Q Model," by O. Gyebi and G. Dasgupta, 11/2/87, (PB88-213764, A08, MF-A01).

NCEER-87-0006 "Symbolic Manipulation Program (SMP) - Algebraic Codes for Two and Three Dimensional Finite Element Formulations," by X. Lee and G. Dasgupta, 11/9/87, (PB88-218522, A05, MF-A01).

NCEER-87-0007 "Instantaneous Optimal Control Laws for Tall Buildings Under Seismic Excitations," by J.N. Yang, A. Akbarpour and P. Ghaemmaghami, 6/10/87, (PB88-134333, A06, MF-A01). This report is only available through NTIS (see address given above).

NCEER-87-0008 "IDARC: Inelastic Damage Analysis of Reinforced Concrete Frame - Shear-Wall Structures," by Y.J. Park, A.M. Reinhorn and S.K. Kunnath, 7/20/87, (PB88-134325, A09, MF-A01). This report is only available through NTIS (see address given above).

NCEER-87-0009 "Liquefaction Potential for New York State: A Preliminary Report on Sites in Manhattan and Buffalo," by M. Budhu, V. Vijayakumar, R.F. Giese and L. Baumgras, 8/31/87, (PB88-163704, A03, MF-A01). This report is available only through NTIS (see address given above).

NCEER-87-0010 "Vertical and Torsional Vibration of Foundations in Inhomogeneous Media," by A.S. Veletsos and K.W. Dotson, 6/1/87, (PB88-134291, A03, MF-A01). This report is only available through NTIS (see address given above).

NCEER-87-0011 "Seismic Probabilistic Risk Assessment and Seismic Margins Studies for Nuclear Power Plants," by Howard H.M. Hwang, 6/15/87, (PB88-134267, A03, MF-A01). This report is only available through NTIS (see address given above).

NCEER-87-0012 "Parametric Studies of Frequency Response of Secondary Systems Under Ground-Acceleration Excitations," by Y. Yong and Y.K. Lin, 6/10/87, (PB88-134309, A03, MF-A01). This report is only available through NTIS (see address given above).

NCEER-87-0013 "Frequency Response of Secondary Systems Under Seismic Excitation," by J.A. HoLung, J. Cai and Y.K. Lin, 7/31/87, (PB88-134317, A05, MF-A01). This report is only available through NTIS (see address given above).

NCEER-87-0014 "Modelling Earthquake Ground Motions in Seismically Active Regions Using Parametric Time Series Methods," by G.W. Ellis and A.S. Cakmak, 8/25/87, (PB88-134283, A08, MF-A01). This report is only available through NTIS (see address given above).

NCEER-87-0015 "Detection and Assessment of Seismic Structural Damage," by E. DiPasquale and A.S. Cakmak, 8/25/87, (PB88-163712, A05, MF-A01). This report is only available through NTIS (see address given above).

NCEER-87-0016 "Pipeline Experiment at Parkfield, California," by J. Isenberg and E. Richardson, 9/15/87, (PB88-163720, A03, MF-A01). This report is available only through NTIS (see address given above).

NCEER-87-0017 "Digital Simulation of Seismic Ground Motion," by M. Shinozuka, G. Deodatis and T. Harada, 8/31/87, (PB88-155197, A04, MF-A01). This report is available only through NTIS (see address given above).

NCEER-87-0018 "Practical Considerations for Structural Control: System Uncertainty, System Time Delay and Truncation of Small Control Forces," J.N. Yang and A. Akbarpour, 8/10/87, (PB88-163738, A08, MF-A01). This report is only available through NTIS (see address given above).

NCEER-87-0019 "Modal Analysis of Nonclassically Damped Structural Systems Using Canonical Transformation," by J.N. Yang, S. Sarkani and F.X. Long, 9/27/87, (PB88-187851, A04, MF-A01).

NCEER-87-0020 "A Nonstationary Solution in Random Vibration Theory," by J.R. Red-Horse and P.D. Spanos, 11/3/87, (PB88-163746, A03, MF-A01).

NCEER-87-0021 "Horizontal Impedances for Radially Inhomogeneous Viscoelastic Soil Layers," by A.S. Veletsos and K.W. Dotson, 10/15/87, (PB88-150859, A04, MF-A01).

NCEER-87-0022 "Seismic Damage Assessment of Reinforced Concrete Members," by Y.S. Chung, C. Meyer and M. Shinozuka, 10/9/87, (PB88-150867, A05, MF-A01). This report is available only through NTIS (see address given above).

NCEER-87-0023 "Active Structural Control in Civil Engineering," by T.T. Soong, 11/11/87, (PB88-187778, A03, MF-A01).

NCEER-87-0024 "Vertical and Torsional Impedances for Radially Inhomogeneous Viscoelastic Soil Layers," by K.W. Dotson and A.S. Veletsos, 12/87, (PB88-187786, A03, MF-A01).

NCEER-87-0025 "Proceedings from the Symposium on Seismic Hazards, Ground Motions, Soil-Liquefaction and Engineering Practice in Eastern North America," October 20-22, 1987, edited by K.H. Jacob, 12/87, (PB88-188115, A23, MF-A01). This report is available only through NTIS (see address given above).

NCEER-87-0026 "Report on the Whittier-Narrows, California, Earthquake of October 1, 1987," by J. Pantelic and A. Reinhorn, 11/87, (PB88-187752, A03, MF-A01). This report is available only through NTIS (see address given above).

NCEER-87-0027 "Design of a Modular Program for Transient Nonlinear Analysis of Large 3-D Building Structures," by S. Srivastav and J.F. Abel, 12/30/87, (PB88-187950, A05, MF-A01). This report is only available through NTIS (see address given above).

NCEER-87-0028 "Second-Year Program in Research, Education and Technology Transfer," 3/8/88, (PB88-219480, A04, MF-A01).

NCEER-88-0001 "Workshop on Seismic Computer Analysis and Design of Buildings With Interactive Graphics," by W. McGuire, J.F. Abel and C.H. Conley, 1/18/88, (PB88-187760, A03, MF-A01). This report is only available through NTIS (see address given above).

NCEER-88-0002 "Optimal Control of Nonlinear Flexible Structures," by J.N. Yang, F.X. Long and D. Wong, 1/22/88, (PB88-213772, A06, MF-A01).

NCEER-88-0003 "Substructuring Techniques in the Time Domain for Primary-Secondary Structural Systems," by G.D. Manolis and G. Juhn, 2/10/88, (PB88-213780, A04, MF-A01).

NCEER-88-0004 "Iterative Seismic Analysis of Primary-Secondary Systems," by A. Singhal, L.D. Lutes and P.D. Spanos, 2/23/88, (PB88-213798, A04, MF-A01).

NCEER-88-0005 "Stochastic Finite Element Expansion for Random Media," by P.D. Spanos and R. Ghanem, 3/14/88, (PB88-213806, A03, MF-A01).

NCEER-88-0006 "Combining Structural Optimization and Structural Control," by F.Y. Cheng and C.P. Pantelides, 1/10/88, (PB88-213814, A05, MF-A01).

NCEER-88-0007 "Seismic Performance Assessment of Code-Designed Structures," by H.H-M. Hwang, J-W. Jaw and H-J. Shau, 3/20/88, (PB88-219423, A04, MF-A01). This report is only available through NTIS (see address given above).

NCEER-88-0008 "Reliability Analysis of Code-Designed Structures Under Natural Hazards," by H.H-M. Hwang, H. Ushiba and M. Shinozuka, 2/29/88, (PB88-229471, A07, MF-A01). This report is only available through NTIS (see address given above).

NCEER-88-0009 "Seismic Fragility Analysis of Shear Wall Structures," by J-W Jaw and H.H-M. Hwang, 4/30/88, (PB89-102867, A04, MF-A01).

NCEER-88-0010 "Base Isolation of a Multi-Story Building Under a Harmonic Ground Motion - A Comparison of Performances of Various Systems," by F-G Fan, G. Ahmadi and I.G. Tadjbakhsh, 5/18/88, (PB89-122238, A06, MF-A01). This report is only available through NTIS (see address given above).

NCEER-88-0011 "Seismic Floor Response Spectra for a Combined System by Green's Functions," by F.M. Lavelle, L.A. Bergman and P.D. Spanos, 5/1/88, (PB89-102875, A03, MF-A01).

NCEER-88-0012 "A New Solution Technique for Randomly Excited Hysteretic Structures," by G.Q. Cai and Y.K. Lin, 5/16/88, (PB89-102883, A03, MF-A01).

NCEER-88-0013 "A Study of Radiation Damping and Soil-Structure Interaction Effects in the Centrifuge," by K. Weissman, supervised by J.H. Prevost, 5/24/88, (PB89-144703, A06, MF-A01).

NCEER-88-0014 "Parameter Identification and Implementation of a Kinematic Plasticity Model for Frictional Soils," by J.H. Prevost and D.V. Griffiths, to be published.

NCEER-88-0015 "Two- and Three- Dimensional Dynamic Finite Element Analyses of the Long Valley Dam," by D.V. Griffiths and J.H. Prevost, 6/17/88, (PB89-144711, A04, MF-A01).

NCEER-88-0016 "Damage Assessment of Reinforced Concrete Structures in Eastern United States," by A.M. Reinhorn, M.J. Seidel, S.K. Kunnath and Y.J. Park, 6/15/88, (PB89-122220, A04, MF-A01). This report is only available through NTIS (see address given above).

NCEER-88-0017 "Dynamic Compliance of Vertically Loaded Strip Foundations in Multilayered Viscoelastic Soils," by S. Ahmad and A.S.M. Israil, 6/17/88, (PB89-102891, A04, MF-A01).

NCEER-88-0018 "An Experimental Study of Seismic Structural Response With Added Viscoelastic Dampers," by R.C. Lin, Z. Liang, T.T. Soong and R.H. Zhang, 6/30/88, (PB89-122212, A05, MF-A01). This report is available only through NTIS (see address given above).

NCEER-88-0019 "Experimental Investigation of Primary - Secondary System Interaction," by G.D. Manolis, G. Juhn and A.M. Reinhorn, 5/27/88, (PB89-122204, A04, MF-A01).

NCEER-88-0020 "A Response Spectrum Approach For Analysis of Nonclassically Damped Structures," by J.N. Yang, S. Sarkani and F.X. Long, 4/22/88, (PB89-102909, A04, MF-A01).

NCEER-88-0021 "Seismic Interaction of Structures and Soils: Stochastic Approach," by A.S. Veletsos and A.M. Prasad, 7/21/88, (PB89-122196, A04, MF-A01). This report is only available through NTIS (see address given above).

NCEER-88-0022 "Identification of the Serviceability Limit State and Detection of Seismic Structural Damage," by E. DiPasquale and A.S. Cakmak, 6/15/88, (PB89-122188, A05, MF-A01). This report is available only through NTIS (see address given above).

NCEER-88-0023 "Multi-Hazard Risk Analysis: Case of a Simple Offshore Structure," by B.K. Bhartia and E.H. Vanmarcke, 7/21/88, (PB89-145213, A05, MF-A01).

NCEER-88-0024 "Automated Seismic Design of Reinforced Concrete Buildings," by Y.S. Chung, C. Meyer and M. Shinozuka, 7/5/88, (PB89-122170, A06, MF-A01). This report is available only through NTIS (see address given above).

NCEER-88-0025 "Experimental Study of Active Control of MDOF Structures Under Seismic Excitations," by L.L. Chung, R.C. Lin, T.T. Soong and A.M. Reinhorn, 7/10/88, (PB89-122600, A04, MF-A01).

NCEER-88-0026 "Earthquake Simulation Tests of a Low-Rise Metal Structure," by J.S. Hwang, K.C. Chang, G.C. Lee and R.L. Ketter, 8/1/88, (PB89-102917, A04, MF-A01).

NCEER-88-0027 "Systems Study of Urban Response and Reconstruction Due to Catastrophic Earthquakes," by F. Kozin and H.K. Zhou, 9/22/88, (PB90-162348, A04, MF-A01).

NCEER-88-0028 "Seismic Fragility Analysis of Plane Frame Structures," by H.H-M. Hwang and Y.K. Low, 7/31/88, (PB89-131445, A06, MF-A01).

NCEER-88-0029 "Response Analysis of Stochastic Structures," by A. Kardara, C. Bucher and M. Shinozuka, 9/22/88, (PB89-174429, A04, MF-A01).

NCEER-88-0030 "Nonnormal Accelerations Due to Yielding in a Primary Structure," by D.C.K. Chen and L.D. Lutes, 9/19/88, (PB89-131437, A04, MF-A01).

NCEER-88-0031 "Design Approaches for Soil-Structure Interaction," by A.S. Veletsos, A.M. Prasad and Y. Tang, 12/30/88, (PB89-174437, A03, MF-A01). This report is available only through NTIS (see address given above).

NCEER-88-0032 "A Re-evaluation of Design Spectra for Seismic Damage Control," by C.J. Turkstra and A.G. Tallin, 11/7/88, (PB89-145221, A05, MF-A01).

NCEER-88-0033 "The Behavior and Design of Noncontact Lap Splices Subjected to Repeated Inelastic Tensile Loading," by V.E. Sagan, P. Gergely and R.N. White, 12/8/88, (PB89-163737, A08, MF-A01).

NCEER-88-0034 "Seismic Response of Pile Foundations," by S.M. Mamoon, P.K. Banerjee and S. Ahmad, 11/1/88, (PB89-145239, A04, MF-A01).

NCEER-88-0035 "Modeling of R/C Building Structures With Flexible Floor Diaphragms (IDARC2)," by A.M. Reinhorn, S.K. Kunnath and N. Panahshahi, 9/7/88, (PB89-207153, A07, MF-A01).

NCEER-88-0036 "Solution of the Dam-Reservoir Interaction Problem Using a Combination of FEM, BEM with Particular Integrals, Modal Analysis, and Substructuring," by C-S. Tsai, G.C. Lee and R.L. Ketter, 12/31/88, (PB89-207146, A04, MF-A01).

NCEER-88-0037 "Optimal Placement of Actuators for Structural Control," by F.Y. Cheng and C.P. Pantelides, 8/15/88, (PB89-162846, A05, MF-A01).

NCEER-88-0038 "Teflon Bearings in Aseismic Base Isolation: Experimental Studies and Mathematical Modeling," by A. Mokha, M.C. Constantinou and A.M. Reinhorn, 12/5/88, (PB89-218457, A10, MF-A01). This report is available only through NTIS (see address given above).

NCEER-88-0039 "Seismic Behavior of Flat Slab High-Rise Buildings in the New York City Area," by P. Weidlinger and M. Ettouney, 10/15/88, (PB90-145681, A04, MF-A01).

NCEER-88-0040 "Evaluation of the Earthquake Resistance of Existing Buildings in New York City," by P. Weidlinger and M. Ettouney, 10/15/88, to be published.

NCEER-88-0041 "Small-Scale Modeling Techniques for Reinforced Concrete Structures Subjected to Seismic Loads," by W. Kim, A. El-Attar and R.N. White, 11/22/88, (PB89-189625, A05, MF-A01).

NCEER-88-0042 "Modeling Strong Ground Motion from Multiple Event Earthquakes," by G.W. Ellis and A.S. Cakmak, 10/15/88, (PB89-174445, A03, MF-A01).

NCEER-88-0043 "Nonstationary Models of Seismic Ground Acceleration," by M. Grigoriu, S.E. Ruiz and E. Rosenblueth, 7/15/88, (PB89-189617, A04, MF-A01).

NCEER-88-0044 "SARCF User's Guide: Seismic Analysis of Reinforced Concrete Frames," by Y.S. Chung, C. Meyer and M. Shinozuka, 11/9/88, (PB89-174452, A08, MF-A01).

NCEER-88-0045 "First Expert Panel Meeting on Disaster Research and Planning," edited by J. Pantelic and J. Stoyle, 9/15/88, (PB89-174460, A05, MF-A01).

NCEER-88-0046 "Preliminary Studies of the Effect of Degrading Infill Walls on the Nonlinear Seismic Response of Steel Frames," by C.Z. Chrysostomou, P. Gergely and J.F. Abel, 12/19/88, (PB89-208383, A05, MF-A01).

NCEER-88-0047 "Reinforced Concrete Frame Component Testing Facility - Design, Construction, Instrumentation and Operation," by S.P. Pessiki, C. Conley, T. Bond, P. Gergely and R.N. White, 12/16/88, (PB89-174478, A04, MF-A01).

NCEER-89-0001 "Effects of Protective Cushion and Soil Compliancy on the Response of Equipment Within a Seismically Excited Building," by J.A. HoLung, 2/16/89, (PB89-207179, A04, MF-A01).

NCEER-89-0002 "Statistical Evaluation of Response Modification Factors for Reinforced Concrete Structures," by H.H-M. Hwang and J-W. Jaw, 2/17/89, (PB89-207187, A05, MF-A01).

NCEER-89-0003 "Hysteretic Columns Under Random Excitation," by G-Q. Cai and Y.K. Lin, 1/9/89, (PB89-196513, A03, MF-A01).

NCEER-89-0004 "Experimental Study of `Elephant Foot Bulge' Instability of Thin-Walled Metal Tanks," by Z-H. Jia and R.L. Ketter, 2/22/89, (PB89-207195, A03, MF-A01).

NCEER-89-0005 "Experiment on Performance of Buried Pipelines Across San Andreas Fault," by J. Isenberg, E. Richardson and T.D. O'Rourke, 3/10/89, (PB89-218440, A04, MF-A01). This report is available only through NTIS (see address given above).

NCEER-89-0006 "A Knowledge-Based Approach to Structural Design of Earthquake-Resistant Buildings," by M. Subramani, P. Gergely, C.H. Conley, J.F. Abel and A.H. Zaghw, 1/15/89, (PB89-218465, A06, MF-A01).

NCEER-89-0007 "Liquefaction Hazards and Their Effects on Buried Pipelines," by T.D. O'Rourke and P.A. Lane, 2/1/89, (PB89-218481, A09, MF-A01).

NCEER-89-0008 "Fundamentals of System Identification in Structural Dynamics," by H. Imai, C-B. Yun, O. Maruyama and M. Shinozuka, 1/26/89, (PB89-207211, A04, MF-A01).

NCEER-89-0009 "Effects of the 1985 Michoacan Earthquake on Water Systems and Other Buried Lifelines in Mexico," by A.G. Ayala and M.J. O'Rourke, 3/8/89, (PB89-207229, A06, MF-A01).

NCEER-89-R010 "NCEER Bibliography of Earthquake Education Materials," by K.E.K. Ross, Second Revision, 9/1/89, (PB90-125352, A05, MF-A01). This report is replaced by NCEER-92-0018.

NCEER-89-0011 "Inelastic Three-Dimensional Response Analysis of Reinforced Concrete Building Structures (IDARC-3D), Part I - Modeling," by S.K. Kunnath and A.M. Reinhorn, 4/17/89, (PB90-114612, A07, MF-A01). This report is available only through NTIS (see address given above).

NCEER-89-0012 "Recommended Modifications to ATC-14," by C.D. Poland and J.O. Malley, 4/12/89, (PB90-108648, A15, MF-A01).

NCEER-89-0013 "Repair and Strengthening of Beam-to-Column Connections Subjected to Earthquake Loading," by M. Corazao and A.J. Durrani, 2/28/89, (PB90-109885, A06, MF-A01).

NCEER-89-0014 "Program EXKAL2 for Identification of Structural Dynamic Systems," by O. Maruyama, C-B. Yun, M. Hoshiya and M. Shinozuka, 5/19/89, (PB90-109877, A09, MF-A01).

NCEER-89-0015 "Response of Frames With Bolted Semi-Rigid Connections, Part I - Experimental Study and Analytical Predictions," by P.J. DiCorso, A.M. Reinhorn, J.R. Dickerson, J.B. Radziminski and W.L. Harper, 6/1/89, to be published.

NCEER-89-0016 "ARMA Monte Carlo Simulation in Probabilistic Structural Analysis," by P.D. Spanos and M.P. Mignolet, 7/10/89, (PB90-109893, A03, MF-A01).

NCEER-89-P017 "Preliminary Proceedings from the Conference on Disaster Preparedness - The Place of Earthquake Education in Our Schools," Edited by K.E.K. Ross, 6/23/89, (PB90-108606, A03, MF-A01).

NCEER-89-0017 "Proceedings from the Conference on Disaster Preparedness - The Place of Earthquake Education in Our Schools," Edited by K.E.K. Ross, 12/31/89, (PB90-207895, A012, MF-A02). This report is available only through NTIS (see address given above).

NCEER-89-0018 "Multidimensional Models of Hysteretic Material Behavior for Vibration Analysis of Shape Memory Energy Absorbing Devices, by E.J. Graesser and F.A. Cozzarelli, 6/7/89, (PB90-164146, A04, MF-A01).

NCEER-89-0019 "Nonlinear Dynamic Analysis of Three-Dimensional Base Isolated Structures (3D-BASIS)," by S. Nagarajaiah, A.M. Reinhorn and M.C. Constantinou, 8/3/89, (PB90-161936, A06, MF-A01). This report has been replaced by NCEER-93-0011.

NCEER-89-0020 "Structural Control Considering Time-Rate of Control Forces and Control Rate Constraints," by F.Y. Cheng and C.P. Pantelides, 8/3/89, (PB90-120445, A04, MF-A01).

NCEER-89-0021 "Subsurface Conditions of Memphis and Shelby County," by K.W. Ng, T-S. Chang and H-H.M. Hwang, 7/26/89, (PB90-120437, A03, MF-A01).

NCEER-89-0022 "Seismic Wave Propagation Effects on Straight Jointed Buried Pipelines," by K. Elhmadi and M.J. O'Rourke, 8/24/89, (PB90-162322, A10, MF-A02).

NCEER-89-0023 "Workshop on Serviceability Analysis of Water Delivery Systems," edited by M. Grigoriu, 3/6/89, (PB90-127424, A03, MF-A01).

NCEER-89-0024 "Shaking Table Study of a 1/5 Scale Steel Frame Composed of Tapered Members," by K.C. Chang, J.S. Hwang and G.C. Lee, 9/18/89, (PB90-160169, A04, MF-A01).

NCEER-89-0025 "DYNA1D: A Computer Program for Nonlinear Seismic Site Response Analysis - Technical Documentation," by Jean H. Prevost, 9/14/89, (PB90-161944, A07, MF-A01). This report is available only through NTIS (see address given above).

NCEER-89-0026 "1:4 Scale Model Studies of Active Tendon Systems and Active Mass Dampers for Aseismic Protection," by A.M. Reinhorn, T.T. Soong, R.C. Lin, Y.P. Yang, Y. Fukao, H. Abe and M. Nakai, 9/15/89, (PB90-173246, A10, MF-A02). This report is available only through NTIS (see address given above).

NCEER-89-0027 "Scattering of Waves by Inclusions in a Nonhomogeneous Elastic Half Space Solved by Boundary Element Methods," by P.K. Hadley, A. Askar and A.S. Cakmak, 6/15/89, (PB90-145699, A07, MF-A01).

NCEER-89-0028 "Statistical Evaluation of Deflection Amplification Factors for Reinforced Concrete Structures," by H.H.M. Hwang, J-W. Jaw and A.L. Ch'ng, 8/31/89, (PB90-164633, A05, MF-A01).

NCEER-89-0029 "Bedrock Accelerations in Memphis Area Due to Large New Madrid Earthquakes," by H.H.M. Hwang, C.H.S. Chen and G. Yu, 11/7/89, (PB90-162330, A04, MF-A01).

NCEER-89-0030 "Seismic Behavior and Response Sensitivity of Secondary Structural Systems," by Y.Q. Chen and T.T. Soong, 10/23/89, (PB90-164658, A08, MF-A01).

NCEER-89-0031 "Random Vibration and Reliability Analysis of Primary-Secondary Structural Systems," by Y. Ibrahim, M. Grigoriu and T.T. Soong, 11/10/89, (PB90-161951, A04, MF-A01).

NCEER-89-0032 "Proceedings from the Second U.S. - Japan Workshop on Liquefaction, Large Ground Deformation and Their Effects on Lifelines, September 26-29, 1989," Edited by T.D. O'Rourke and M. Hamada, 12/1/89, (PB90-209388, A22, MF-A03).

NCEER-89-0033 "Deterministic Model for Seismic Damage Evaluation of Reinforced Concrete Structures," by J.M. Bracci, A.M. Reinhorn, J.B. Mander and S.K. Kunnath, 9/27/89, (PB91-108803, A06, MF-A01).

NCEER-89-0034 "On the Relation Between Local and Global Damage Indices," by E. DiPasquale and A.S. Cakmak, 8/15/89, (PB90-173865, A05, MF-A01).

NCEER-89-0035 "Cyclic Undrained Behavior of Nonplastic and Low Plasticity Silts," by A.J. Walker and H.E. Stewart, 7/26/89, (PB90-183518, A10, MF-A01).

NCEER-89-0036 "Liquefaction Potential of Surficial Deposits in the City of Buffalo, New York," by M. Budhu, R. Giese and L. Baumgrass, 1/17/89, (PB90-208455, A04, MF-A01).

NCEER-89-0037 "A Deterministic Assessment of Effects of Ground Motion Incoherence," by A.S. Veletsos and Y. Tang, 7/15/89, (PB90-164294, A03, MF-A01).

NCEER-89-0038 "Workshop on Ground Motion Parameters for Seismic Hazard Mapping," July 17-18, 1989, edited by R.V. Whitman, 12/1/89, (PB90-173923, A04, MF-A01).

NCEER-89-0039 "Seismic Effects on Elevated Transit Lines of the New York City Transit Authority," by C.J. Costantino, C.A. Miller and E. Heymsfield, 12/26/89, (PB90-207887, A06, MF-A01).

NCEER-89-0040 "Centrifugal Modeling of Dynamic Soil-Structure Interaction," by K. Weissman, Supervised by J.H. Prevost, 5/10/89, (PB90-207879, A07, MF-A01).

NCEER-89-0041 "Linearized Identification of Buildings With Cores for Seismic Vulnerability Assessment," by I-K. Ho and A.E. Aktan, 11/1/89, (PB90-251943, A07, MF-A01).

NCEER-90-0001 "Geotechnical and Lifeline Aspects of the October 17, 1989 Loma Prieta Earthquake in San Francisco," by T.D. O'Rourke, H.E. Stewart, F.T. Blackburn and T.S. Dickerman, 1/90, (PB90-208596, A05, MF-A01).

NCEER-90-0002 "Nonnormal Secondary Response Due to Yielding in a Primary Structure," by D.C.K. Chen and L.D. Lutes, 2/28/90, (PB90-251976, A07, MF-A01).

NCEER-90-0003 "Earthquake Education Materials for Grades K-12," by K.E.K. Ross, 4/16/90, (PB91-251984, A05, MF-A05). This report has been replaced by NCEER-92-0018.

NCEER-90-0004 "Catalog of Strong Motion Stations in Eastern North America," by R.W. Busby, 4/3/90, (PB90-251984, A05, MF-A01).

NCEER-90-0005 "NCEER Strong-Motion Data Base: A User Manual for the GeoBase Release (Version 1.0 for the Sun3)," by P. Friberg and K. Jacob, 3/31/90 (PB90-258062, A04, MF-A01).

NCEER-90-0006 "Seismic Hazard Along a Crude Oil Pipeline in the Event of an 1811-1812 Type New Madrid Earthquake," by H.H.M. Hwang and C-H.S. Chen, 4/16/90, (PB90-258054, A04, MF-A01).

NCEER-90-0007 "Site-Specific Response Spectra for Memphis Sheahan Pumping Station," by H.H.M. Hwang and C.S. Lee, 5/15/90, (PB91-108811, A05, MF-A01).

NCEER-90-0008 "Pilot Study on Seismic Vulnerability of Crude Oil Transmission Systems," by T. Ariman, R. Dobry, M. Grigoriu, F. Kozin, M. O'Rourke, T. O'Rourke and M. Shinozuka, 5/25/90, (PB91-108837, A06, MF-A01).

NCEER-90-0009 "A Program to Generate Site Dependent Time Histories: EQGEN," by G.W. Ellis, M. Srinivasan and A.S. Cakmak, 1/30/90, (PB91-108829, A04, MF-A01).

NCEER-90-0010 "Active Isolation for Seismic Protection of Operating Rooms," by M.E. Talbott, Supervised by M. Shinozuka, 6/8/9, (PB91-110205, A05, MF-A01).

NCEER-90-0011 "Program LINEARID for Identification of Linear Structural Dynamic Systems," by C-B. Yun and M. Shinozuka, 6/25/90, (PB91-110312, A08, MF-A01).

NCEER-90-0012 "Two-Dimensional Two-Phase Elasto-Plastic Seismic Response of Earth Dams," by A.N. Yiagos, Supervised by J.H. Prevost, 6/20/90, (PB91-110197, A13, MF-A02).

NCEER-90-0013 "Secondary Systems in Base-Isolated Structures: Experimental Investigation, Stochastic Response and Stochastic Sensitivity," by G.D. Manolis, G. Juhn, M.C. Constantinou and A.M. Reinhorn, 7/1/90, (PB91-110320, A08, MF-A01).

NCEER-90-0014 "Seismic Behavior of Lightly-Reinforced Concrete Column and Beam-Column Joint Details," by S.P. Pessiki, C.H. Conley, P. Gergely and R.N. White, 8/22/90, (PB91-108795, A11, MF-A02).

NCEER-90-0015 "Two Hybrid Control Systems for Building Structures Under Strong Earthquakes," by J.N. Yang and A. Danielians, 6/29/90, (PB91-125393, A04, MF-A01).

NCEER-90-0016 "Instantaneous Optimal Control with Acceleration and Velocity Feedback," by J.N. Yang and Z. Li, 6/29/90, (PB91-125401, A03, MF-A01).

NCEER-90-0017 "Reconnaissance Report on the Northern Iran Earthquake of June 21, 1990," by M. Mehrain, 10/4/90, (PB91-125377, A03, MF-A01).

NCEER-90-0018 "Evaluation of Liquefaction Potential in Memphis and Shelby County," by T.S. Chang, P.S. Tang, C.S. Lee and H. Hwang, 8/10/90, (PB91-125427, A09, MF-A01).

NCEER-90-0019 "Experimental and Analytical Study of a Combined Sliding Disc Bearing and Helical Steel Spring Isolation System," by M.C. Constantinou, A.S. Mokha and A.M. Reinhorn, 10/4/90, (PB91-125385, A06, MF-A01). This report is available only through NTIS (see address given above).

NCEER-90-0020 "Experimental Study and Analytical Prediction of Earthquake Response of a Sliding Isolation System with a Spherical Surface," by A.S. Mokha, M.C. Constantinou and A.M. Reinhorn, 10/11/90, (PB91-125419, A05, MF-A01).

NCEER-90-0021 "Dynamic Interaction Factors for Floating Pile Groups," by G. Gazetas, K. Fan, A. Kaynia and E. Kausel, 9/10/90, (PB91-170381, A05, MF-A01).

NCEER-90-0022 "Evaluation of Seismic Damage Indices for Reinforced Concrete Structures," by S. Rodriguez-Gomez and A.S. Cakmak, 9/30/90, PB91-171322, A06, MF-A01).

NCEER-90-0023 "Study of Site Response at a Selected Memphis Site," by H. Desai, S. Ahmad, E.S. Gazetas and M.R. Oh, 10/11/90, (PB91-196857, A03, MF-A01).

NCEER-90-0024 "A User's Guide to Strongmo: Version 1.0 of NCEER's Strong-Motion Data Access Tool for PCs and Terminals," by P.A. Friberg and C.A.T. Susch, 11/15/90, (PB91-171272, A03, MF-A01).

NCEER-90-0025 "A Three-Dimensional Analytical Study of Spatial Variability of Seismic Ground Motions," by L-L. Hong and A.H.-S. Ang, 10/30/90, (PB91-170399, A09, MF-A01).

NCEER-90-0026 "MUMOID User's Guide - A Program for the Identification of Modal Parameters," by S. Rodriguez-Gomez and E. DiPasquale, 9/30/90, (PB91-171298, A04, MF-A01).

NCEER-90-0027 "SARCF-II User's Guide - Seismic Analysis of Reinforced Concrete Frames," by S. Rodriguez-Gomez, Y.S. Chung and C. Meyer, 9/30/90, (PB91-171280, A05, MF-A01).

NCEER-90-0028 "Viscous Dampers: Testing, Modeling and Application in Vibration and Seismic Isolation," by N. Makris and M.C. Constantinou, 12/20/90 (PB91-190561, A06, MF-A01).

NCEER-90-0029 "Soil Effects on Earthquake Ground Motions in the Memphis Area," by H. Hwang, C.S. Lee, K.W. Ng and T.S. Chang, 8/2/90, (PB91-190751, A05, MF-A01).

NCEER-91-0001 "Proceedings from the Third Japan-U.S. Workshop on Earthquake Resistant Design of Lifeline Facilities and Countermeasures for Soil Liquefaction, December 17-19, 1990," edited by T.D. O'Rourke and M. Hamada, 2/1/91, (PB91-179259, A99, MF-A04).

NCEER-91-0002 "Physical Space Solutions of Non-Proportionally Damped Systems," by M. Tong, Z. Liang and G.C. Lee, 1/15/91, (PB91-179242, A04, MF-A01).

NCEER-91-0003 "Seismic Response of Single Piles and Pile Groups," by K. Fan and G. Gazetas, 1/10/91, (PB92-174994, A04, MF-A01).

NCEER-91-0004 "Damping of Structures: Part 1 - Theory of Complex Damping," by Z. Liang and G. Lee, 10/10/91, (PB92-197235, A12, MF-A03).

NCEER-91-0005 "3D-BASIS - Nonlinear Dynamic Analysis of Three Dimensional Base Isolated Structures: Part II," by S. Nagarajaiah, A.M. Reinhorn and M.C. Constantinou, 2/28/91, (PB91-190553, A07, MF-A01). This report has been replaced by NCEER-93-0011.

NCEER-91-0006 "A Multidimensional Hysteretic Model for Plasticity Deforming Metals in Energy Absorbing Devices," by E.J. Graesser and F.A. Cozzarelli, 4/9/91, (PB92-108364, A04, MF-A01).

NCEER-91-0007 "A Framework for Customizable Knowledge-Based Expert Systems with an Application to a KBES for Evaluating the Seismic Resistance of Existing Buildings," by E.G. Ibarra-Anaya and S.J. Fenves, 4/9/91, (PB91-210930, A08, MF-A01).

NCEER-91-0008 "Nonlinear Analysis of Steel Frames with Semi-Rigid Connections Using the Capacity Spectrum Method," by G.G. Deierlein, S-H. Hsieh, Y-J. Shen and J.F. Abel, 7/2/91, (PB92-113828, A05, MF-A01).

NCEER-91-0009 "Earthquake Education Materials for Grades K-12," by K.E.K. Ross, 4/30/91, (PB91-212142, A06, MF-A01). This report has been replaced by NCEER-92-0018.

NCEER-91-0010 "Phase Wave Velocities and Displacement Phase Differences in a Harmonically Oscillating Pile," by N. Makris and G. Gazetas, 7/8/91, (PB92-108356, A04, MF-A01).

NCEER-91-0011 "Dynamic Characteristics of a Full-Size Five-Story Steel Structure and a 2/5 Scale Model," by K.C. Chang, G.C. Yao, G.C. Lee, D.S. Hao and Y.C. Yeh," 7/2/91, (PB93-116648, A06, MF-A02).

NCEER-91-0012 "Seismic Response of a 2/5 Scale Steel Structure with Added Viscoelastic Dampers," by K.C. Chang, T.T. Soong, S-T. Oh and M.L. Lai, 5/17/91, (PB92-110816, A05, MF-A01).

NCEER-91-0013 "Earthquake Response of Retaining Walls; Full-Scale Testing and Computational Modeling," by S. Alampalli and A-W.M. Elgamal, 6/20/91, to be published.

NCEER-91-0014 "3D-BASIS-M: Nonlinear Dynamic Analysis of Multiple Building Base Isolated Structures," by P.C. Tsopelas, S. Nagarajaiah, M.C. Constantinou and A.M. Reinhorn, 5/28/91, (PB92-113885, A09, MF-A02).

NCEER-91-0015 "Evaluation of SEAOC Design Requirements for Sliding Isolated Structures," by D. Theodossiou and M.C. Constantinou, 6/10/91, (PB92-114602, A11, MF-A03).

NCEER-91-0016 "Closed-Loop Modal Testing of a 27-Story Reinforced Concrete Flat Plate-Core Building," by H.R. Somaprasad, T. Toksoy, H. Yoshiyuki and A.E. Aktan, 7/15/91, (PB92-129980, A07, MF-A02).

NCEER-91-0017 "Shake Table Test of a 1/6 Scale Two-Story Lightly Reinforced Concrete Building," by A.G. El-Attar, R.N. White and P. Gergely, 2/28/91, (PB92-222447, A06, MF-A02).

NCEER-91-0018 "Shake Table Test of a 1/8 Scale Three-Story Lightly Reinforced Concrete Building," by A.G. El-Attar, R.N. White and P. Gergely, 2/28/91, (PB93-116630, A08, MF-A02).

NCEER-91-0019 "Transfer Functions for Rigid Rectangular Foundations," by A.S. Veletsos, A.M. Prasad and W.H. Wu, 7/31/91, to be published.

NCEER-91-0020 "Hybrid Control of Seismic-Excited Nonlinear and Inelastic Structural Systems," by J.N. Yang, Z. Li and A. Danielians, 8/1/91, (PB92-143171, A06, MF-A02).

NCEER-91-0021 "The NCEER-91 Earthquake Catalog: Improved Intensity-Based Magnitudes and Recurrence Relations for U.S. Earthquakes East of New Madrid," by L. Seeber and J.G. Armbruster, 8/28/91, (PB92-176742, A06, MF-A02).

NCEER-91-0022 "Proceedings from the Implementation of Earthquake Planning and Education in Schools: The Need for Change - The Roles of the Changemakers," by K.E.K. Ross and F. Winslow, 7/23/91, (PB92-129998, A12, MF-A03).

NCEER-91-0023 "A Study of Reliability-Based Criteria for Seismic Design of Reinforced Concrete Frame Buildings," by H.H.M. Hwang and H-M. Hsu, 8/10/91, (PB92-140235, A09, MF-A02).

NCEER-91-0024 "Experimental Verification of a Number of Structural System Identification Algorithms," by R.G. Ghanem, H. Gavin and M. Shinozuka, 9/18/91, (PB92-176577, A18, MF-A04).

NCEER-91-0025 "Probabilistic Evaluation of Liquefaction Potential," by H.H.M. Hwang and C.S. Lee," 11/25/91, (PB92-143429, A05, MF-A01).

NCEER-91-0026 "Instantaneous Optimal Control for Linear, Nonlinear and Hysteretic Structures - Stable Controllers," by J.N. Yang and Z. Li, 11/15/91, (PB92-163807, A04, MF-A01).

NCEER-91-0027 "Experimental and Theoretical Study of a Sliding Isolation System for Bridges," by M.C. Constantinou, A. Kartoum, A.M. Reinhorn and P. Bradford, 11/15/91, (PB92-176973, A10, MF-A03).

NCEER-92-0001 "Case Studies of Liquefaction and Lifeline Performance During Past Earthquakes, Volume 1: Japanese Case Studies," Edited by M. Hamada and T. O'Rourke, 2/17/92, (PB92-197243, A18, MF-A04).

NCEER-92-0002 "Case Studies of Liquefaction and Lifeline Performance During Past Earthquakes, Volume 2: United States Case Studies," Edited by T. O'Rourke and M. Hamada, 2/17/92, (PB92-197250, A20, MF-A04).

NCEER-92-0003 "Issues in Earthquake Education," Edited by K. Ross, 2/3/92, (PB92-222389, A07, MF-A02).

NCEER-92-0004 "Proceedings from the First U.S. - Japan Workshop on Earthquake Protective Systems for Bridges," Edited by I.G. Buckle, 2/4/92, (PB94-142239, A99, MF-A06).

NCEER-92-0005 "Seismic Ground Motion from a Haskell-Type Source in a Multiple-Layered Half-Space," A.P. Theoharis, G. Deodatis and M. Shinozuka, 1/2/92, to be published.

NCEER-92-0006 "Proceedings from the Site Effects Workshop," Edited by R. Whitman, 2/29/92, (PB92-197201, A04, MF-A01).

NCEER-92-0007 "Engineering Evaluation of Permanent Ground Deformations Due to Seismically-Induced Liquefaction," by M.H. Baziar, R. Dobry and A-W.M. Elgamal, 3/24/92, (PB92-222421, A13, MF-A03).

NCEER-92-0008 "A Procedure for the Seismic Evaluation of Buildings in the Central and Eastern United States," by C.D. Poland and J.O. Malley, 4/2/92, (PB92-222439, A20, MF-A04).

NCEER-92-0009 "Experimental and Analytical Study of a Hybrid Isolation System Using Friction Controllable Sliding Bearings," by M.Q. Feng, S. Fujii and M. Shinozuka, 5/15/92, (PB93-150282, A06, MF-A02).

NCEER-92-0010 "Seismic Resistance of Slab-Column Connections in Existing Non-Ductile Flat-Plate Buildings," by A.J. Durrani and Y. Du, 5/18/92, (PB93-116812, A06, MF-A02).

NCEER-92-0011 "The Hysteretic and Dynamic Behavior of Brick Masonry Walls Upgraded by Ferrocement Coatings Under Cyclic Loading and Strong Simulated Ground Motion," by H. Lee and S.P. Prawel, 5/11/92, to be published.

NCEER-92-0012 "Study of Wire Rope Systems for Seismic Protection of Equipment in Buildings," by G.F. Demetriades, M.C. Constantinou and A.M. Reinhorn, 5/20/92, (PB93-116655, A08, MF-A02).

NCEER-92-0013 "Shape Memory Structural Dampers: Material Properties, Design and Seismic Testing," by P.R. Witting and F.A. Cozzarelli, 5/26/92, (PB93-116663, A05, MF-A01).

NCEER-92-0014 "Longitudinal Permanent Ground Deformation Effects on Buried Continuous Pipelines," by M.J. O'Rourke, and C. Nordberg, 6/15/92, (PB93-116671, A08, MF-A02).

NCEER-92-0015 "A Simulation Method for Stationary Gaussian Random Functions Based on the Sampling Theorem," by M. Grigoriu and S. Balopoulou, 6/11/92, (PB93-127496, A05, MF-A01).

NCEER-92-0016 "Gravity-Load-Designed Reinforced Concrete Buildings: Seismic Evaluation of Existing Construction and Detailing Strategies for Improved Seismic Resistance," by G.W. Hoffmann, S.K. Kunnath, A.M. Reinhorn and J.B. Mander, 7/15/92, (PB94-142007, A08, MF-A02).

NCEER-92-0017 "Observations on Water System and Pipeline Performance in the Limón Area of Costa Rica Due to the April 22, 1991 Earthquake," by M. O'Rourke and D. Ballantyne, 6/30/92, (PB93-126811, A06, MF-A02).

NCEER-92-0018 "Fourth Edition of Earthquake Education Materials for Grades K-12," Edited by K.E.K. Ross, 8/10/92, (PB93-114023, A07, MF-A02).

NCEER-92-0019 "Proceedings from the Fourth Japan-U.S. Workshop on Earthquake Resistant Design of Lifeline Facilities and Countermeasures for Soil Liquefaction," Edited by M. Hamada and T.D. O'Rourke, 8/12/92, (PB93-163939, A99, MF-E11).

NCEER-92-0020 "Active Bracing System: A Full Scale Implementation of Active Control," by A.M. Reinhorn, T.T. Soong, R.C. Lin, M.A. Riley, Y.P. Wang, S. Aizawa and M. Higashino, 8/14/92, (PB93-127512, A06, MF-A02).

NCEER-92-0021 "Empirical Analysis of Horizontal Ground Displacement Generated by Liquefaction-Induced Lateral Spreads," by S.F. Bartlett and T.L. Youd, 8/17/92, (PB93-188241, A06, MF-A02).

NCEER-92-0022 "IDARC Version 3.0: Inelastic Damage Analysis of Reinforced Concrete Structures," by S.K. Kunnath, A.M. Reinhorn and R.F. Lobo, 8/31/92, (PB93-227502, A07, MF-A02).

NCEER-92-0023 "A Semi-Empirical Analysis of Strong-Motion Peaks in Terms of Seismic Source, Propagation Path and Local Site Conditions, by M. Kamiyama, M.J. O'Rourke and R. Flores-Berrones, 9/9/92, (PB93-150266, A08, MF-A02).

NCEER-92-0024 "Seismic Behavior of Reinforced Concrete Frame Structures with Nonductile Details, Part I: Summary of Experimental Findings of Full Scale Beam-Column Joint Tests," by A. Beres, R.N. White and P. Gergely, 9/30/92, (PB93-227783, A05, MF-A01).

NCEER-92-0025 "Experimental Results of Repaired and Retrofitted Beam-Column Joint Tests in Lightly Reinforced Concrete Frame Buildings," by A. Beres, S. El-Borgi, R.N. White and P. Gergely, 10/29/92, (PB93-227791, A05, MF-A01).

NCEER-92-0026 "A Generalization of Optimal Control Theory: Linear and Nonlinear Structures," by J.N. Yang, Z. Li and S. Vongchavalitkul, 11/2/92, (PB93-188621, A05, MF-A01).

NCEER-92-0027 "Seismic Resistance of Reinforced Concrete Frame Structures Designed Only for Gravity Loads: Part I - Design and Properties of a One-Third Scale Model Structure," by J.M. Bracci, A.M. Reinhorn and J.B. Mander, 12/1/92, (PB94-104502, A08, MF-A02).

NCEER-92-0028 "Seismic Resistance of Reinforced Concrete Frame Structures Designed Only for Gravity Loads: Part II - Experimental Performance of Subassemblages," by L.E. Aycardi, J.B. Mander and A.M. Reinhorn, 12/1/92, (PB94-104510, A08, MF-A02).

NCEER-92-0029 "Seismic Resistance of Reinforced Concrete Frame Structures Designed Only for Gravity Loads: Part III - Experimental Performance and Analytical Study of a Structural Model," by J.M. Bracci, A.M. Reinhorn and J.B. Mander, 12/1/92, (PB93-227528, A09, MF-A01).

NCEER-92-0030 "Evaluation of Seismic Retrofit of Reinforced Concrete Frame Structures: Part I - Experimental Performance of Retrofitted Subassemblages," by D. Choudhuri, J.B. Mander and A.M. Reinhorn, 12/8/92, (PB93-198307, A07, MF-A02).

NCEER-92-0031 "Evaluation of Seismic Retrofit of Reinforced Concrete Frame Structures: Part II - Experimental Performance and Analytical Study of a Retrofitted Structural Model," by J.M. Bracci, A.M. Reinhorn and J.B. Mander, 12/8/92, (PB93-198315, A09, MF-A03).

NCEER-92-0032 "Experimental and Analytical Investigation of Seismic Response of Structures with Supplemental Fluid Viscous Dampers," by M.C. Constantinou and M.D. Symans, 12/21/92, (PB93-191435, A10, MF-A03). This report is available only through NTIS (see address given above).

NCEER-92-0033 "Reconnaissance Report on the Cairo, Egypt Earthquake of October 12, 1992," by M. Khater, 12/23/92, (PB93-188621, A03, MF-A01).

NCEER-92-0034 "Low-Level Dynamic Characteristics of Four Tall Flat-Plate Buildings in New York City," by H. Gavin, S. Yuan, J. Grossman, E. Pekelis and K. Jacob, 12/28/92, (PB93-188217, A07, MF-A02).

NCEER-93-0001 "An Experimental Study on the Seismic Performance of Brick-Infilled Steel Frames With and Without Retrofit," by J.B. Mander, B. Nair, K. Wojtkowski and J. Ma, 1/29/93, (PB93-227510, A07, MF-A02).

NCEER-93-0002 "Social Accounting for Disaster Preparedness and Recovery Planning," by S. Cole, E. Pantoja and V. Razak, 2/22/93, (PB94-142114, A12, MF-A03).

NCEER-93-0003 "Assessment of 1991 NEHRP Provisions for Nonstructural Components and Recommended Revisions," by T.T. Soong, G. Chen, Z. Wu, R-H. Zhang and M. Grigoriu, 3/1/93, (PB93-188639, A06, MF-A02).

NCEER-93-0004 "Evaluation of Static and Response Spectrum Analysis Procedures of SEAOC/UBC for Seismic Isolated Structures," by C.W. Winters and M.C. Constantinou, 3/23/93, (PB93-198299, A10, MF-A03).

NCEER-93-0005 "Earthquakes in the Northeast - Are We Ignoring the Hazard? A Workshop on Earthquake Science and Safety for Educators," edited by K.E.K. Ross, 4/2/93, (PB94-103066, A09, MF-A02).

NCEER-93-0006 "Inelastic Response of Reinforced Concrete Structures with Viscoelastic Braces," by R.F. Lobo, J.M. Bracci, K.L. Shen, A.M. Reinhorn and T.T. Soong, 4/5/93, (PB93-227486, A05, MF-A02).

NCEER-93-0007 "Seismic Testing of Installation Methods for Computers and Data Processing Equipment," by K. Kosar, T.T. Soong, K.L. Shen, J.A. HoLung and Y.K. Lin, 4/12/93, (PB93-198299, A07, MF-A02).

NCEER-93-0008 "Retrofit of Reinforced Concrete Frames Using Added Dampers," by A. Reinhorn, M. Constantinou and C. Li, to be published.

NCEER-93-0009 "Seismic Behavior and Design Guidelines for Steel Frame Structures with Added Viscoelastic Dampers," by K.C. Chang, M.L. Lai, T.T. Soong, D.S. Hao and Y.C. Yeh, 5/1/93, (PB94-141959, A07, MF-A02).

NCEER-93-0010 "Seismic Performance of Shear-Critical Reinforced Concrete Bridge Piers," by J.B. Mander, S.M. Waheed, M.T.A. Chaudhary and S.S. Chen, 5/12/93, (PB93-227494, A08, MF-A02).

NCEER-93-0011 "3D-BASIS-TABS: Computer Program for Nonlinear Dynamic Analysis of Three Dimensional Base Isolated Structures," by S. Nagarajaiah, C. Li, A.M. Reinhorn and M.C. Constantinou, 8/2/93, (PB94-141819, A09, MF-A02).

NCEER-93-0012 "Effects of Hydrocarbon Spills from an Oil Pipeline Break on Ground Water," by O.J. Helweg and H.H.M. Hwang, 8/3/93, (PB94-141942, A06, MF-A02).

NCEER-93-0013 "Simplified Procedures for Seismic Design of Nonstructural Components and Assessment of Current Code Provisions," by M.P. Singh, L.E. Suarez, E.E. Matheu and G.O. Maldonado, 8/4/93, (PB94-141827, A09, MF-A02).

NCEER-93-0014 "An Energy Approach to Seismic Analysis and Design of Secondary Systems," by G. Chen and T.T. Soong, 8/6/93, (PB94-142767, A11, MF-A03).

NCEER-93-0015 "Proceedings from School Sites: Becoming Prepared for Earthquakes - Commemorating the Third Anniversary of the Loma Prieta Earthquake," Edited by F.E. Winslow and K.E.K. Ross, 8/16/93, (PB94-154275, A16, MF-A02).

NCEER-93-0016 "Reconnaissance Report of Damage to Historic Monuments in Cairo, Egypt Following the October 12, 1992 Dahshur Earthquake," by D. Sykora, D. Look, G. Croci, E. Karaesmen and E. Karaesmen, 8/19/93, (PB94-142221, A08, MF-A02).

NCEER-93-0017 "The Island of Guam Earthquake of August 8, 1993," by S.W. Swan and S.K. Harris, 9/30/93, (PB94-141843, A04, MF-A01).

NCEER-93-0018 "Engineering Aspects of the October 12, 1992 Egyptian Earthquake," by A.W. Elgamal, M. Amer, K. Adalier and A. Abul-Fadl, 10/7/93, (PB94-141983, A05, MF-A01).

NCEER-93-0019 "Development of an Earthquake Motion Simulator and its Application in Dynamic Centrifuge Testing," by I. Krstelj, Supervised by J.H. Prevost, 10/23/93, (PB94-181773, A-10, MF-A03).

NCEER-93-0020 "NCEER-Taisei Corporation Research Program on Sliding Seismic Isolation Systems for Bridges: Experimental and Analytical Study of a Friction Pendulum System (FPS)," by M.C. Constantinou, P. Tsopelas, Y-S. Kim and S. Okamoto, 11/1/93, (PB94-142775, A08, MF-A02).

NCEER-93-0021 "Finite Element Modeling of Elastomeric Seismic Isolation Bearings," by L.J. Billings, Supervised by R. Shepherd, 11/8/93, to be published.

NCEER-93-0022 "Seismic Vulnerability of Equipment in Critical Facilities: Life-Safety and Operational Consequences," by K. Porter, G.S. Johnson, M.M. Zadeh, C. Scawthorn and S. Eder, 11/24/93, (PB94-181765, A16, MF-A03).

NCEER-93-0023 "Hokkaido Nansei-oki, Japan Earthquake of July 12, 1993, by P.I. Yanev and C.R. Scawthorn, 12/23/93, (PB94-181500, A07, MF-A01).

NCEER-94-0001 "An Evaluation of Seismic Serviceability of Water Supply Networks with Application to the San Francisco Auxiliary Water Supply System," by I. Markov, Supervised by M. Grigoriu and T. O'Rourke, 1/21/94, (PB94-204013, A07, MF-A02).

NCEER-94-0002 "NCEER-Taisei Corporation Research Program on Sliding Seismic Isolation Systems for Bridges: Experimental and Analytical Study of Systems Consisting of Sliding Bearings, Rubber Restoring Force Devices and Fluid Dampers," Volumes I and II, by P. Tsopelas, S. Okamoto, M.C. Constantinou, D. Ozaki and S. Fujii, 2/4/94, (PB94-181740, A09, MF-A02 and PB94-181757, A12, MF-A03).

NCEER-94-0003 "A Markov Model for Local and Global Damage Indices in Seismic Analysis," by S. Rahman and M. Grigoriu, 2/18/94, (PB94-206000, A12, MF-A03).

NCEER-94-0004 "Proceedings from the NCEER Workshop on Seismic Response of Masonry Infills," edited by D.P. Abrams, 3/1/94, (PB94-180783, A07, MF-A02).

NCEER-94-0005 "The Northridge, California Earthquake of January 17, 1994: General Reconnaissance Report," edited by J.D. Goltz, 3/11/94, (PB94-193943, A10, MF-A03).

NCEER-94-0006 "Seismic Energy Based Fatigue Damage Analysis of Bridge Columns: Part I - Evaluation of Seismic Capacity," by G.A. Chang and J.B. Mander, 3/14/94, (PB94-219185, A11, MF-A03).

NCEER-94-0007 "Seismic Isolation of Multi-Story Frame Structures Using Spherical Sliding Isolation Systems," by T.M. Al-Hussaini, V.A. Zayas and M.C. Constantinou, 3/17/94, (PB94-193745, A09, MF-A02).

NCEER-94-0008 "The Northridge, California Earthquake of January 17, 1994: Performance of Highway Bridges," edited by I.G. Buckle, 3/24/94, (PB94-193851, A06, MF-A02).

NCEER-94-0009 "Proceedings of the Third U.S.-Japan Workshop on Earthquake Protective Systems for Bridges," edited by I.G. Buckle and I. Friedland, 3/31/94, (PB94-195815, A99, MF-A06).

NCEER-94-0010 "3D-BASIS-ME: Computer Program for Nonlinear Dynamic Analysis of Seismically Isolated Single and Multiple Structures and Liquid Storage Tanks," by P.C. Tsopelas, M.C. Constantinou and A.M. Reinhorn, 4/12/94, (PB94-204922, A09, MF-A02).

NCEER-94-0011 "The Northridge, California Earthquake of January 17, 1994: Performance of Gas Transmission Pipelines," by T.D. O'Rourke and M.C. Palmer, 5/16/94, (PB94-204989, A05, MF-A01).

NCEER-94-0012 "Feasibility Study of Replacement Procedures and Earthquake Performance Related to Gas Transmission Pipelines," by T.D. O'Rourke and M.C. Palmer, 5/25/94, (PB94-206638, A09, MF-A02).

NCEER-94-0013 "Seismic Energy Based Fatigue Damage Analysis of Bridge Columns: Part II - Evaluation of Seismic Demand," by G.A. Chang and J.B. Mander, 6/1/94, (PB95-18106, A08, MF-A02).

NCEER-94-0014 "NCEER-Taisei Corporation Research Program on Sliding Seismic Isolation Systems for Bridges: Experimental and Analytical Study of a System Consisting of Sliding Bearings and Fluid Restoring Force/Damping Devices," by P. Tsopelas and M.C. Constantinou, 6/13/94, (PB94-219144, A10, MF-A03).

NCEER-94-0015 "Generation of Hazard-Consistent Fragility Curves for Seismic Loss Estimation Studies," by H. Hwang and J-R. Huo, 6/14/94, (PB95-181996, A09, MF-A02).

NCEER-94-0016 "Seismic Study of Building Frames with Added Energy-Absorbing Devices," by W.S. Pong, C.S. Tsai and G.C. Lee, 6/20/94, (PB94-219136, A10, A03).

NCEER-94-0017 "Sliding Mode Control for Seismic-Excited Linear and Nonlinear Civil Engineering Structures," by J. Yang, J. Wu, A. Agrawal and Z. Li, 6/21/94, (PB95-138483, A06, MF-A02).

NCEER-94-0018 "3D-BASIS-TABS Version 2.0: Computer Program for Nonlinear Dynamic Analysis of Three Dimensional Base Isolated Structures," by A.M. Reinhorn, S. Nagarajaiah, M.C. Constantinou, P. Tsopelas and R. Li, 6/22/94, (PB95-182176, A08, MF-A02).

NCEER-94-0019 "Proceedings of the International Workshop on Civil Infrastructure Systems: Application of Intelligent Systems and Advanced Materials on Bridge Systems," Edited by G.C. Lee and K.C. Chang, 7/18/94, (PB95-252474, A20, MF-A04).

NCEER-94-0020 "Study of Seismic Isolation Systems for Computer Floors," by V. Lambrou and M.C. Constantinou, 7/19/94, (PB95-138533, A10, MF-A03).

NCEER-94-0021 "Proceedings of the U.S.-Italian Workshop on Guidelines for Seismic Evaluation and Rehabilitation of Unreinforced Masonry Buildings," Edited by D.P. Abrams and G.M. Calvi, 7/20/94, (PB95-138749, A13, MF-A03).

NCEER-94-0022 "NCEER-Taisei Corporation Research Program on Sliding Seismic Isolation Systems for Bridges: Experimental and Analytical Study of a System Consisting of Lubricated PTFE Sliding Bearings and Mild Steel Dampers," by P. Tsopelas and M.C. Constantinou, 7/22/94, (PB95-182184, A08, MF-A02).

NCEER-94-0023 “Development of Reliability-Based Design Criteria for Buildings Under Seismic Load,” by Y.K. Wen, H. Hwang and M. Shinozuka, 8/1/94, (PB95-211934, A08, MF-A02).

NCEER-94-0024 “Experimental Verification of Acceleration Feedback Control Strategies for an Active Tendon System,” by S.J. Dyke, B.F. Spencer, Jr., P. Quast, M.K. Sain, D.C. Kaspari, Jr. and T.T. Soong, 8/29/94, (PB95-212320, A05, MF-A01).

NCEER-94-0025 “Seismic Retrofitting Manual for Highway Bridges,” Edited by I.G. Buckle and I.F. Friedland, published by the Federal Highway Administration (PB95-212676, A15, MF-A03).

NCEER-94-0026 “Proceedings from the Fifth U.S.-Japan Workshop on Earthquake Resistant Design of Lifeline Facilities and Countermeasures Against Soil Liquefaction,” Edited by T.D. O’Rourke and M. Hamada, 11/7/94, (PB95-220802, A99, MF-E08).

NCEER-95-0001 "Experimental and Analytical Investigation of Seismic Retrofit of Structures with Supplemental Damping: Part 1 - Fluid Viscous Damping Devices," by A.M. Reinhorn, C. Li and M.C. Constantinou, 1/3/95, (PB95-266599, A09, MF-A02).

NCEER-95-0002 "Experimental and Analytical Study of Low-Cycle Fatigue Behavior of Semi-Rigid Top-And-Seat Angle Connections," by G. Pekcan, J.B. Mander and S.S. Chen, 1/5/95, (PB95-220042, A07, MF-A02).

NCEER-95-0003 "NCEER-ATC Joint Study on Fragility of Buildings," by T. Anagnos, C. Rojahn and A.S. Kiremidjian, 1/20/95, (PB95-220026, A06, MF-A02).

NCEER-95-0004 "Nonlinear Control Algorithms for Peak Response Reduction," by Z. Wu, T.T. Soong, V. Gattulli and R.C. Lin, 2/16/95, (PB95-220349, A05, MF-A01).

NCEER-95-0005 "Pipeline Replacement Feasibility Study: A Methodology for Minimizing Seismic and Corrosion Risks to Underground Natural Gas Pipelines," by R.T. Eguchi, H.A. Seligson and D.G. Honegger, 3/2/95, (PB95-252326, A06, MF-A02).

NCEER-95-0006 "Evaluation of Seismic Performance of an 11-Story Frame Building During the 1994 Northridge Earthquake," by F. Naeim, R. DiSulio, K. Benuska, A. Reinhorn and C. Li, to be published.

NCEER-95-0007 "Prioritization of Bridges for Seismic Retrofitting," by N. Basöz and A.S. Kiremidjian, 4/24/95, (PB95-252300, A08, MF-A02).

NCEER-95-0008 "Method for Developing Motion Damage Relationships for Reinforced Concrete Frames," by A. Singhal and A.S. Kiremidjian, 5/11/95, (PB95-266607, A06, MF-A02).

NCEER-95-0009 "Experimental and Analytical Investigation of Seismic Retrofit of Structures with Supplemental Damping: Part II - Friction Devices," by C. Li and A.M. Reinhorn, 7/6/95, (PB96-128087, A11, MF-A03).

NCEER-95-0010 "Experimental Performance and Analytical Study of a Non-Ductile Reinforced Concrete Frame Structure Retrofitted with Elastomeric Spring Dampers," by G. Pekcan, J.B. Mander and S.S. Chen, 7/14/95, (PB96-137161, A08, MF-A02).

NCEER-95-0011 "Development and Experimental Study of Semi-Active Fluid Damping Devices for Seismic Protection of Structures," by M.D. Symans and M.C. Constantinou, 8/3/95, (PB96-136940, A23, MF-A04).

NCEER-95-0012 "Real-Time Structural Parameter Modification (RSPM): Development of Innervated Structures," by Z. Liang, M. Tong and G.C. Lee, 4/11/95, (PB96-137153, A06, MF-A01).

NCEER-95-0013 "Experimental and Analytical Investigation of Seismic Retrofit of Structures with Supplemental Damping: Part III - Viscous Damping Walls," by A.M. Reinhorn and C. Li, 10/1/95, (PB96-176409, A11, MF-A03).

NCEER-95-0014 "Seismic Fragility Analysis of Equipment and Structures in a Memphis Electric Substation," by J-R. Huo and H.H.M. Hwang, 8/10/95, (PB96-128087, A09, MF-A02).

NCEER-95-0015 "The Hanshin-Awaji Earthquake of January 17, 1995: Performance of Lifelines," Edited by M. Shinozuka, 11/3/95, (PB96-176383, A15, MF-A03).

NCEER-95-0016 "Highway Culvert Performance During Earthquakes," by T.L. Youd and C.J. Beckman, available as NCEER-96-0015.

NCEER-95-0017 "The Hanshin-Awaji Earthquake of January 17, 1995: Performance of Highway Bridges," Edited by I.G. Buckle, 12/1/95, to be published.

NCEER-95-0018 "Modeling of Masonry Infill Panels for Structural Analysis," by A.M. Reinhorn, A. Madan, R.E. Valles, Y. Reichmann and J.B. Mander, 12/8/95, (PB97-110886, MF-A01, A06).

NCEER-95-0019 "Optimal Polynomial Control for Linear and Nonlinear Structures," by A.K. Agrawal and J.N. Yang, 12/11/95, (PB96-168737, A07, MF-A02).

NCEER-95-0020 "Retrofit of Non-Ductile Reinforced Concrete Frames Using Friction Dampers," by R.S. Rao, P. Gergely and R.N. White, 12/22/95, (PB97-133508, A10, MF-A02).

NCEER-95-0021 "Parametric Results for Seismic Response of Pile-Supported Bridge Bents," by G. Mylonakis, A. Nikolaou and G. Gazetas, 12/22/95, (PB97-100242, A12, MF-A03).

NCEER-95-0022 "Kinematic Bending Moments in Seismically Stressed Piles," by A. Nikolaou, G. Mylonakis and G. Gazetas, 12/23/95, (PB97-113914, MF-A03, A13).

NCEER-96-0001 "Dynamic Response of Unreinforced Masonry Buildings with Flexible Diaphragms," by A.C. Costley and D.P. Abrams," 10/10/96, (PB97-133573, MF-A03, A15).

NCEER-96-0002 "State of the Art Review: Foundations and Retaining Structures," by I. Po Lam, to be published.

NCEER-96-0003 "Ductility of Rectangular Reinforced Concrete Bridge Columns with Moderate Confinement," by N. Wehbe, M. Saiidi, D. Sanders and B. Douglas, 11/7/96, (PB97-133557, A06, MF-A02).

NCEER-96-0004 "Proceedings of the Long-Span Bridge Seismic Research Workshop," edited by I.G. Buckle and I.M. Friedland, to be published.

NCEER-96-0005 "Establish Representative Pier Types for Comprehensive Study: Eastern United States," by J. Kulicki and Z. Prucz, 5/28/96, (PB98-119217, A07, MF-A02).

NCEER-96-0006 "Establish Representative Pier Types for Comprehensive Study: Western United States," by R. Imbsen, R.A. Schamber and T.A. Osterkamp, 5/28/96, (PB98-118607, A07, MF-A02).

NCEER-96-0007 "Nonlinear Control Techniques for Dynamical Systems with Uncertain Parameters," by R.G. Ghanem and M.I. Bujakov, 5/27/96, (PB97-100259, A17, MF-A03).

NCEER-96-0008 "Seismic Evaluation of a 30-Year Old Non-Ductile Highway Bridge Pier and Its Retrofit," by J.B. Mander, B. Mahmoodzadegan, S. Bhadra and S.S. Chen, 5/31/96, (PB97-110902, MF-A03, A10).

NCEER-96-0009 "Seismic Performance of a Model Reinforced Concrete Bridge Pier Before and After Retrofit," by J.B. Mander, J.H. Kim and C.A. Ligozio, 5/31/96, (PB97-110910, MF-A02, A10).

NCEER-96-0010 "IDARC2D Version 4.0: A Computer Program for the Inelastic Damage Analysis of Buildings," by R.E. Valles, A.M. Reinhorn, S.K. Kunnath, C. Li and A. Madan, 6/3/96, (PB97-100234, A17, MF-A03).

NCEER-96-0011 "Estimation of the Economic Impact of Multiple Lifeline Disruption: Memphis Light, Gas and Water Division Case Study," by S.E. Chang, H.A. Seligson and R.T. Eguchi, 8/16/96, (PB97-133490, A11, MF-A03).

NCEER-96-0012 "Proceedings from the Sixth Japan-U.S. Workshop on Earthquake Resistant Design of Lifeline Facilities and Countermeasures Against Soil Liquefaction, Edited by M. Hamada and T. O'Rourke, 9/11/96, (PB97-133581, A99, MF-A06).

NCEER-96-0013 "Chemical Hazards, Mitigation and Preparedness in Areas of High Seismic Risk: A Methodology for Estimating the Risk of Post-Earthquake Hazardous Materials Release," by H.A. Seligson, R.T. Eguchi, K.J. Tierney and K. Richmond, 11/7/96, (PB97-133565, MF-A02, A08).

NCEER-96-0014 "Response of Steel Bridge Bearings to Reversed Cyclic Loading," by J.B. Mander, D-K. Kim, S.S. Chen and G.J. Premus, 11/13/96, (PB97-140735, A12, MF-A03).

NCEER-96-0015 "Highway Culvert Performance During Past Earthquakes," by T.L. Youd and C.J. Beckman, 11/25/96, (PB97-133532, A06, MF-A01).

NCEER-97-0001 "Evaluation, Prevention and Mitigation of Pounding Effects in Building Structures," by R.E. Valles and A.M. Reinhorn, 2/20/97, (PB97-159552, A14, MF-A03).

NCEER-97-0002 "Seismic Design Criteria for Bridges and Other Highway Structures," by C. Rojahn, R. Mayes, D.G. Anderson, J. Clark, J.H. Hom, R.V. Nutt and M.J. O'Rourke, 4/30/97, (PB97-194658, A06, MF-A03).

NCEER-97-0003 "Proceedings of the U.S.-Italian Workshop on Seismic Evaluation and Retrofit," Edited by D.P. Abrams and G.M. Calvi, 3/19/97, (PB97-194666, A13, MF-A03).

NCEER-97-0004 "Investigation of Seismic Response of Buildings with Linear and Nonlinear Fluid Viscous Dampers," by A.A. Seleemah and M.C. Constantinou, 5/21/97, (PB98-109002, A15, MF-A03).

NCEER-97-0005 "Proceedings of the Workshop on Earthquake Engineering Frontiers in Transportation Facilities," edited by G.C. Lee and I.M. Friedland, 8/29/97, (PB98-128911, A25, MR-A04).

NCEER-97-0006 "Cumulative Seismic Damage of Reinforced Concrete Bridge Piers," by S.K. Kunnath, A. El-Bahy, A. Taylor and W. Stone, 9/2/97, (PB98-108814, A11, MF-A03).

NCEER-97-0007 "Structural Details to Accommodate Seismic Movements of Highway Bridges and Retaining Walls," by R.A. Imbsen, R.A. Schamber, E. Thorkildsen, A. Kartoum, B.T. Martin, T.N. Rosser and J.M. Kulicki, 9/3/97, (PB98-108996, A09, MF-A02).

NCEER-97-0008 "A Method for Earthquake Motion-Damage Relationships with Application to Reinforced Concrete Frames," by A. Singhal and A.S. Kiremidjian, 9/10/97, (PB98-108988, A13, MF-A03).

NCEER-97-0009 "Seismic Analysis and Design of Bridge Abutments Considering Sliding and Rotation," by K. Fishman and R. Richards, Jr., 9/15/97, (PB98-108897, A06, MF-A02).

NCEER-97-0010 "Proceedings of the FHWA/NCEER Workshop on the National Representation of Seismic Ground Motion for New and Existing Highway Facilities," edited by I.M. Friedland, M.S. Power and R.L. Mayes, 9/22/97, (PB98-128903, A21, MF-A04).

NCEER-97-0011 "Seismic Analysis for Design or Retrofit of Gravity Bridge Abutments," by K.L. Fishman, R. Richards, Jr. and R.C. Divito, 10/2/97, (PB98-128937, A08, MF-A02).

NCEER-97-0012 "Evaluation of Simplified Methods of Analysis for Yielding Structures," by P. Tsopelas, M.C. Constantinou, C.A. Kircher and A.S. Whittaker, 10/31/97, (PB98-128929, A10, MF-A03).

NCEER-97-0013 "Seismic Design of Bridge Columns Based on Control and Repairability of Damage," by C-T. Cheng and J.B. Mander, 12/8/97, (PB98-144249, A11, MF-A03).

NCEER-97-0014 "Seismic Resistance of Bridge Piers Based on Damage Avoidance Design," by J.B. Mander and C-T. Cheng, 12/10/97, (PB98-144223, A09, MF-A02).

NCEER-97-0015 "Seismic Response of Nominally Symmetric Systems with Strength Uncertainty," by S. Balopoulou and M. Grigoriu, 12/23/97, (PB98-153422, A11, MF-A03).

NCEER-97-0016 "Evaluation of Seismic Retrofit Methods for Reinforced Concrete Bridge Columns," by T.J. Wipf, F.W. Klaiber and F.M. Russo, 12/28/97, (PB98-144215, A12, MF-A03).

NCEER-97-0017 "Seismic Fragility of Existing Conventional Reinforced Concrete Highway Bridges," by C.L. Mullen and A.S. Cakmak, 12/30/97, (PB98-153406, A08, MF-A02).

NCEER-97-0018 "Loss Asssessment of Memphis Buildings," edited by D.P. Abrams and M. Shinozuka, 12/31/97, (PB98-144231, A13, MF-A03).

NCEER-97-0019 "Seismic Evaluation of Frames with Infill Walls Using Quasi-static Experiments," by K.M. Mosalam, R.N. White and P. Gergely, 12/31/97, (PB98-153455, A07, MF-A02).

NCEER-97-0020 "Seismic Evaluation of Frames with Infill Walls Using Pseudo-dynamic Experiments," by K.M. Mosalam, R.N. White and P. Gergely, 12/31/97, (PB98-153430, A07, MF-A02).

NCEER-97-0021 "Computational Strategies for Frames with Infill Walls: Discrete and Smeared Crack Analyses and Seismic Fragility," by K.M. Mosalam, R.N. White and P. Gergely, 12/31/97, (PB98-153414, A10, MF-A02).

NCEER-97-0022 "Proceedings of the NCEER Workshop on Evaluation of Liquefaction Resistance of Soils," edited by T.L. Youd and I.M. Idriss, 12/31/97, (PB98-155617, A15, MF-A03).

MCEER-98-0001 "Extraction of Nonlinear Hysteretic Properties of Seismically Isolated Bridges from Quick-Release Field Tests," by Q. Chen, B.M. Douglas, E.M. Maragakis and I.G. Buckle, 5/26/98, (PB99-118838, A06, MF-A01).

MCEER-98-0002 "Methodologies for Evaluating the Importance of Highway Bridges," by A. Thomas, S. Eshenaur and J. Kulicki, 5/29/98, (PB99-118846, A10, MF-A02).

MCEER-98-0003 "Capacity Design of Bridge Piers and the Analysis of Overstrength," by J.B. Mander, A. Dutta and P. Goel, 6/1/98, (PB99-118853, A09, MF-A02).

MCEER-98-0004 "Evaluation of Bridge Damage Data from the Loma Prieta and Northridge, California Earthquakes," by N. Basoz and A. Kiremidjian, 6/2/98, (PB99-118861, A15, MF-A03).

MCEER-98-0005 "Screening Guide for Rapid Assessment of Liquefaction Hazard at Highway Bridge Sites," by T. L. Youd, 6/16/98, (PB99-118879, A06, not available on microfiche).

MCEER-98-0006 "Structural Steel and Steel/Concrete Interface Details for Bridges," by P. Ritchie, N. Kauhl and J. Kulicki, 7/13/98, (PB99-118945, A06, MF-A01).

MCEER-98-0007 "Capacity Design and Fatigue Analysis of Confined Concrete Columns," by A. Dutta and J.B. Mander, 7/14/98, (PB99-118960, A14, MF-A03).

MCEER-98-0008 "Proceedings of the Workshop on Performance Criteria for Telecommunication Services Under Earthquake Conditions," edited by A.J. Schiff, 7/15/98, (PB99-118952, A08, MF-A02).

MCEER-98-0009 "Fatigue Analysis of Unconfined Concrete Columns," by J.B. Mander, A. Dutta and J.H. Kim, 9/12/98, (PB99-123655, A10, MF-A02).

MCEER-98-0010 "Centrifuge Modeling of Cyclic Lateral Response of Pile-Cap Systems and Seat-Type Abutments in Dry Sands," by A.D. Gadre and R. Dobry, 10/2/98, (PB99-123606, A13, MF-A03).

MCEER-98-0011 "IDARC-BRIDGE: A Computational Platform for Seismic Damage Assessment of Bridge Structures," by A.M. Reinhorn, V. Simeonov, G. Mylonakis and Y. Reichman, 10/2/98, (PB99-162919, A15, MF-A03).

MCEER-98-0012 "Experimental Investigation of the Dynamic Response of Two Bridges Before and After Retrofitting with Elastomeric Bearings," by D.A. Wendichansky, S.S. Chen and J.B. Mander, 10/2/98, (PB99-162927, A15, MF-A03).

MCEER-98-0013 "Design Procedures for Hinge Restrainers and Hinge Sear Width for Multiple-Frame Bridges," by R. Des Roches and G.L. Fenves, 11/3/98, (PB99-140477, A13, MF-A03).

MCEER-98-0014 "Response Modification Factors for Seismically Isolated Bridges," by M.C. Constantinou and J.K. Quarshie, 11/3/98, (PB99-140485, A14, MF-A03).

MCEER-98-0015 "Proceedings of the U.S.-Italy Workshop on Seismic Protective Systems for Bridges," edited by I.M. Friedland and M.C. Constantinou, 11/3/98, (PB2000-101711, A22, MF-A04).

MCEER-98-0016 "Appropriate Seismic Reliability for Critical Equipment Systems: Recommendations Based on Regional Analysis of Financial and Life Loss," by K. Porter, C. Scawthorn, C. Taylor and N. Blais, 11/10/98, (PB99-157265, A08, MF-A02).

MCEER-98-0017 "Proceedings of the U.S. Japan Joint Seminar on Civil Infrastructure Systems Research," edited by M. Shinozuka and A. Rose, 11/12/98, (PB99-156713, A16, MF-A03).

MCEER-98-0018 "Modeling of Pile Footings and Drilled Shafts for Seismic Design," by I. PoLam, M. Kapuskar and D. Chaudhuri, 12/21/98, (PB99-157257, A09, MF-A02).

MCEER-99-0001 "Seismic Evaluation of a Masonry Infilled Reinforced Concrete Frame by Pseudodynamic Testing," by S.G. Buonopane and R.N. White, 2/16/99, (PB99-162851, A09, MF-A02).

MCEER-99-0002 "Response History Analysis of Structures with Seismic Isolation and Energy Dissipation Systems: Verification Examples for Program SAP2000," by J. Scheller and M.C. Constantinou, 2/22/99, (PB99-162869, A08, MF-A02).

MCEER-99-0003 "Experimental Study on the Seismic Design and Retrofit of Bridge Columns Including Axial Load Effects," by A. Dutta, T. Kokorina and J.B. Mander, 2/22/99, (PB99-162877, A09, MF-A02).

MCEER-99-0004 "Experimental Study of Bridge Elastomeric and Other Isolation and Energy Dissipation Systems with Emphasis on Uplift Prevention and High Velocity Near-source Seismic Excitation," by A. Kasalanati and M. C. Constantinou, 2/26/99, (PB99-162885, A12, MF-A03).

MCEER-99-0005 "Truss Modeling of Reinforced Concrete Shear-flexure Behavior," by J.H. Kim and J.B. Mander, 3/8/99, (PB99-163693, A12, MF-A03).

MCEER-99-0006 "Experimental Investigation and Computational Modeling of Seismic Response of a 1:4 Scale Model Steel Structure with a Load Balancing Supplemental Damping System," by G. Pekcan, J.B. Mander and S.S. Chen, 4/2/99, (PB99-162893, A11, MF-A03).

MCEER-99-0007 "Effect of Vertical Ground Motions on the Structural Response of Highway Bridges," by M.R. Button, C.J. Cronin and R.L. Mayes, 4/10/99, (PB2000-101411, A10, MF-A03).

MCEER-99-0008 "Seismic Reliability Assessment of Critical Facilities: A Handbook, Supporting Documentation, and Model Code Provisions," by G.S. Johnson, R.E. Sheppard, M.D. Quilici, S.J. Eder and C.R. Scawthorn, 4/12/99, (PB2000-101701, A18, MF-A04).

MCEER-99-0009 "Impact Assessment of Selected MCEER Highway Project Research on the Seismic Design of Highway Structures," by C. Rojahn, R. Mayes, D.G. Anderson, J.H. Clark, D'Appolonia Engineering, S. Gloyd and R.V. Nutt, 4/14/99, (PB99-162901, A10, MF-A02).

MCEER-99-0010 "Site Factors and Site Categories in Seismic Codes," by R. Dobry, R. Ramos and M.S. Power, 7/19/99, (PB2000-101705, A08, MF-A02).

MCEER-99-0011 "Restrainer Design Procedures for Multi-Span Simply-Supported Bridges," by M.J. Randall, M. Saiidi, E. Maragakis and T. Isakovic, 7/20/99, (PB2000-101702, A10, MF-A02).

MCEER-99-0012 "Property Modification Factors for Seismic Isolation Bearings," by M.C. Constantinou, P. Tsopelas, A. Kasalanati and E. Wolff, 7/20/99, (PB2000-103387, A11, MF-A03).

MCEER-99-0013 "Critical Seismic Issues for Existing Steel Bridges," by P. Ritchie, N. Kauhl and J. Kulicki, 7/20/99, (PB2000-101697, A09, MF-A02).

MCEER-99-0014 "Nonstructural Damage Database," by A. Kao, T.T. Soong and A. Vender, 7/24/99, (PB2000-101407, A06, MF-A01).

MCEER-99-0015 "Guide to Remedial Measures for Liquefaction Mitigation at Existing Highway Bridge Sites," by H.G. Cooke and J. K. Mitchell, 7/26/99, (PB2000-101703, A11, MF-A03).

MCEER-99-0016 "Proceedings of the MCEER Workshop on Ground Motion Methodologies for the Eastern United States," edited by N. Abrahamson and A. Becker, 8/11/99, (PB2000-103385, A07, MF-A02).

MCEER-99-0017 "Quindío, Colombia Earthquake of January 25, 1999: Reconnaissance Report," by A.P. Asfura and P.J. Flores, 10/4/99, (PB2000-106893, A06, MF-A01).

MCEER-99-0018 "Hysteretic Models for Cyclic Behavior of Deteriorating Inelastic Structures," by M.V. Sivaselvan and A.M. Reinhorn, 11/5/99, (PB2000-103386, A08, MF-A02).

MCEER-99-0019 "Proceedings of the 7th U.S.- Japan Workshop on Earthquake Resistant Design of Lifeline Facilities and Countermeasures Against Soil Liquefaction," edited by T.D. O'Rourke, J.P. Bardet and M. Hamada, 11/19/99, (PB2000-103354, A99, MF-A06).

MCEER-99-0020 "Development of Measurement Capability for Micro-Vibration Evaluations with Application to Chip Fabrication Facilities," by G.C. Lee, Z. Liang, J.W. Song, J.D. Shen and W.C. Liu, 12/1/99, (PB2000-105993, A08, MF-A02).

MCEER-99-0021 "Design and Retrofit Methodology for Building Structures with Supplemental Energy Dissipating Systems," by G. Pekcan, J.B. Mander and S.S. Chen, 12/31/99, (PB2000-105994, A11, MF-A03).

MCEER-00-0001 "The Marmara, Turkey Earthquake of August 17, 1999: Reconnaissance Report," edited by C. Scawthorn; with major contributions by M. Bruneau, R. Eguchi, T. Holzer, G. Johnson, J. Mander, J. Mitchell, W. Mitchell, A. Papageorgiou, C. Scaethorn, and G. Webb, 3/23/00, (PB2000-106200, A11, MF-A03).

MCEER-00-0002 "Proceedings of the MCEER Workshop for Seismic Hazard Mitigation of Health Care Facilities," edited by G.C. Lee, M. Ettouney, M. Grigoriu, J. Hauer and J. Nigg, 3/29/00, (PB2000-106892, A08, MF-A02).

MCEER-00-0003 "The Chi-Chi, Taiwan Earthquake of September 21, 1999: Reconnaissance Report," edited by G.C. Lee and C.H. Loh, with major contributions by G.C. Lee, M. Bruneau, I.G. Buckle, S.E. Chang, P.J. Flores, T.D. O'Rourke, M. Shinozuka, T.T. Soong, C-H. Loh, K-C. Chang, Z-J. Chen, J-S. Hwang, M-L. Lin, G-Y. Liu, K-C. Tsai, G.C. Yao and C-L. Yen, 4/30/00, (PB2001-100980, A10, MF-A02).

MCEER-00-0004 "Seismic Retrofit of End-Sway Frames of Steel Deck-Truss Bridges with a Supplemental Tendon System: Experimental and Analytical Investigation," by G. Pekcan, J.B. Mander and S.S. Chen, 7/1/00, (PB2001-100982, A10, MF-A02).

MCEER-00-0005 "Sliding Fragility of Unrestrained Equipment in Critical Facilities," by W.H. Chong and T.T. Soong, 7/5/00, (PB2001-100983, A08, MF-A02).

MCEER-00-0006 "Seismic Response of Reinforced Concrete Bridge Pier Walls in the Weak Direction," by N. Abo-Shadi, M. Saiidi and D. Sanders, 7/17/00, (PB2001-100981, A17, MF-A03).

MCEER-00-0007 "Low-Cycle Fatigue Behavior of Longitudinal Reinforcement in Reinforced Concrete Bridge Columns," by J. Brown and S.K. Kunnath, 7/23/00, (PB2001-104392, A08, MF-A02).

MCEER-00-0008 "Soil Structure Interaction of Bridges for Seismic Analysis," I. PoLam and H. Law, 9/25/00, (PB2001-105397, A08, MF-A02).

MCEER-00-0009 "Proceedings of the First MCEER Workshop on Mitigation of Earthquake Disaster by Advanced Technologies (MEDAT-1), edited by M. Shinozuka, D.J. Inman and T.D. O'Rourke, 11/10/00, (PB2001-105399, A14, MF-A03).

MCEER-00-0010 "Development and Evaluation of Simplified Procedures for Analysis and Design of Buildings with Passive Energy Dissipation Systems," by O.M. Ramirez, M.C. Constantinou, C.A. Kircher, A.S. Whittaker, M.W. Johnson, J.D. Gomez and C. Chrysostomou, 11/16/01, (PB2001-105523, A23, MF-A04).

MCEER-00-0011 "Dynamic Soil-Foundation-Structure Interaction Analyses of Large Caissons," by C-Y. Chang, C-M. Mok, Z-L. Wang, R. Settgast, F. Waggoner, M.A. Ketchum, H.M. Gonnermann and C-C. Chin, 12/30/00, (PB2001-104373, A07, MF-A02).

MCEER-00-0012 "Experimental Evaluation of Seismic Performance of Bridge Restrainers," by A.G. Vlassis, E.M. Maragakis and M. Saiid Saiidi, 12/30/00, (PB2001-104354, A09, MF-A02).

MCEER-00-0013 "Effect of Spatial Variation of Ground Motion on Highway Structures," by M. Shinozuka, V. Saxena and G. Deodatis, 12/31/00, (PB2001-108755, A13, MF-A03).

MCEER-00-0014 "A Risk-Based Methodology for Assessing the Seismic Performance of Highway Systems," by S.D. Werner, C.E. Taylor, J.E. Moore, II, J.S. Walton and S. Cho, 12/31/00, (PB2001-108756, A14, MF-A03).

MCEER-01-0001 "Experimental Investigation of P-Delta Effects to Collapse During Earthquakes," by D. Vian and M. Bruneau, 6/25/01, (PB2002-100534, A17, MF-A03).

MCEER-01-0002 "Proceedings of the Second MCEER Workshop on Mitigation of Earthquake Disaster by Advanced Technologies (MEDAT-2)," edited by M. Bruneau and D.J. Inman, 7/23/01, (PB2002-100434, A16, MF-A03).

MCEER-01-0003 "Sensitivity Analysis of Dynamic Systems Subjected to Seismic Loads," by C. Roth and M. Grigoriu, 9/18/01, (PB2003-100884, A12, MF-A03).

MCEER-01-0004 "Overcoming Obstacles to Implementing Earthquake Hazard Mitigation Policies: Stage 1 Report," by D.J. Alesch and W.J. Petak, 12/17/01, (PB2002-107949, A07, MF-A02).

MCEER-01-0005 "Updating Real-Time Earthquake Loss Estimates: Methods, Problems and Insights," by C.E. Taylor, S.E. Chang and R.T. Eguchi, 12/17/01, (PB2002-107948, A05, MF-A01).

MCEER-01-0006 "Experimental Investigation and Retrofit of Steel Pile Foundations and Pile Bents Under Cyclic Lateral Loadings," by A. Shama, J. Mander, B. Blabac and S. Chen, 12/31/01, (PB2002-107950, A13, MF-A03).

MCEER-02-0001 "Assessment of Performance of Bolu Viaduct in the 1999 Duzce Earthquake in Turkey" by P.C. Roussis, M.C. Constantinou, M. Erdik, E. Durukal and M. Dicleli, 5/8/02, (PB2003-100883, A08, MF-A02).

MCEER-02-0002 "Seismic Behavior of Rail Counterweight Systems of Elevators in Buildings," by M.P. Singh, Rildova and L.E. Suarez, 5/27/02. (PB2003-100882, A11, MF-A03).

MCEER-02-0003 "Development of Analysis and Design Procedures for Spread Footings," by G. Mylonakis, G. Gazetas, S. Nikolaou and A. Chauncey, 10/02/02, (PB2004-101636, A13, MF-A03, CD-A13).

MCEER-02-0004 "Bare-Earth Algorithms for Use with SAR and LIDAR Digital Elevation Models," by C.K. Huyck, R.T. Eguchi and B. Houshmand, 10/16/02, (PB2004-101637, A07, CD-A07).

MCEER-02-0005 "Review of Energy Dissipation of Compression Members in Concentrically Braced Frames," by K.Lee and M. Bruneau, 10/18/02, (PB2004-101638, A10, CD-A10).

MCEER-03-0001 "Experimental Investigation of Light-Gauge Steel Plate Shear Walls for the Seismic Retrofit of Buildings" by J. Berman and M. Bruneau, 5/2/03, (PB2004-101622, A10, MF-A03, CD-A10).

MCEER-03-0002 "Statistical Analysis of Fragility Curves," by M. Shinozuka, M.Q. Feng, H. Kim, T. Uzawa and T. Ueda, 6/16/03, (PB2004-101849, A09, CD-A09).

MCEER-03-0003 "Proceedings of the Eighth U.S.-Japan Workshop on Earthquake Resistant Design f Lifeline Facilities and Countermeasures Against Liquefaction," edited by M. Hamada, J.P. Bardet and T.D. O'Rourke, 6/30/03, (PB2004-104386, A99, CD-A99).

MCEER-03-0004 "Proceedings of the PRC-US Workshop on Seismic Analysis and Design of Special Bridges," edited by L.C. Fan and G.C. Lee, 7/15/03, (PB2004-104387, A14, CD-A14).

MCEER-03-0005 "Urban Disaster Recovery: A Framework and Simulation Model," by S.B. Miles and S.E. Chang, 7/25/03, (PB2004-104388, A07, CD-A07).

MCEER-03-0006 "Behavior of Underground Piping Joints Due to Static and Dynamic Loading," by R.D. Meis, M. Maragakis and R. Siddharthan, 11/17/03, (PB2005-102194, A13, MF-A03, CD-A00).

MCEER-03-0007 "Seismic Vulnerability of Timber Bridges and Timber Substructures," by A.A. Shama, J.B. Mander, I.M. Friedland and D.R. Allicock, 12/15/03.

MCEER-04-0001 "Experimental Study of Seismic Isolation Systems with Emphasis on Secondary System Response and Verification of Accuracy of Dynamic Response History Analysis Methods," by E. Wolff and M. Constantinou, 1/16/04 (PB2005-102195, A99, MF-E08, CD-A00).

MCEER-04-0002 "Tension, Compression and Cyclic Testing of Engineered Cementitious Composite Materials," by K. Kesner and S.L. Billington, 3/1/04, (PB2005-102196, A08, CD-A08).

MCEER-04-0003 "Cyclic Testing of Braces Laterally Restrained by Steel Studs to Enhance Performance During Earthquakes," by O.C. Celik, J.W. Berman and M. Bruneau, 3/16/04, (PB2005-102197, A13, MF-A03, CD-A00).

MCEER-04-0004 "Methodologies for Post Earthquake Building Damage Detection Using SAR and Optical Remote Sensing: Application to the August 17, 1999 Marmara, Turkey Earthquake," by C.K. Huyck, B.J. Adams, S. Cho, R.T. Eguchi, B. Mansouri and B. Houshmand, 6/15/04, (PB2005-104888, A10, CD-A00).

MCEER-04-0005 "Nonlinear Structural Analysis Towards Collapse Simulation: A Dynamical Systems Approach," by M.V. Sivaselvan and A.M. Reinhorn, 6/16/04, (PB2005-104889, A11, MF-A03, CD-A00).

MCEER-04-0006 "Proceedings of the Second PRC-US Workshop on Seismic Analysis and Design of Special Bridges," edited by G.C. Lee and L.C. Fan, 6/25/04, (PB2005-104890, A16, CD-A00).

MCEER-04-0007 "Seismic Vulnerability Evaluation of Axially Loaded Steel Built-up Laced Members," by K. Lee and M. Bruneau, 6/30/04, (PB2005-104891, A16, CD-A00).

MCEER-04-0008 "Evaluation of Accuracy of Simplified Methods of Analysis and Design of Buildings with Damping Systems for Near-Fault and for Soft-Soil Seismic Motions," by E.A. Pavlou and M.C. Constantinou, 8/16/04, (PB2005-104892, A08, MF-A02, CD-A00).

MCEER-04-0009 "Assessment of Geotechnical Issues in Acute Care Facilities in California," by M. Lew, T.D. O'Rourke, R. Dobry and M. Koch, 9/15/04, (PB2005-104893, A08, CD-A00).

MCEER-04-0010 "Scissor-Jack-Damper Energy Dissipation System," by A.N. Sigaher-Boyle and M.C. Constantinou, 12/1/04.

MCEER-04-0011 "Seismic Retrofit of Bridge Steel Truss Piers Using a Controlled Rocking Approach," by M. Pollino and M. Bruneau, 12/20/04.

MCEER-05-0001 "Experimental and Analytical Studies of Structures Seismically Isolated with an Uplift-Restraint Isolation System," by P.C. Roussis and M.C. Constantinou, 1/10/05.

MCEER-05-0002 "A Versatile Experimentation Model for Study of Structures Near Collapse Applied to Seismic Evaluation of Irregular Structures," by D. Kusumastuti, A.M. Reinhorn and A. Rutenberg, 3/31/05.

MCEER-05-0003 "Proceedings of the Third PRC-US Workshop on Seismic Analysis and Design of Special Bridges," edited by L.C. Fan and G.C. Lee, 4/20/05.

MCEER-05-0004 "Approaches for the Seismic Retrofit of Braced Steel Bridge Piers and Proof-of-Concept Testing of an Eccentrically Braced Frame with Tubular Link," by J.W. Berman and M. Bruneau, 4/21/05.

MCEER-05-0005 "Simulation of Strong Ground Motions for Seismic Fragility Evaluation of Nonstructural Components in Hospitals," by A. Wanitkorkul and A. Filiatrault, 5/26/05.

MCEER-05-0006 "Seismic Safety in California Hospitals: Assessing an Attempt to Accelerate the Replacement or Seismic Retrofit of Older Hospital Facilities," by D.J. Alesch, L.A. Arendt and W.J. Petak, 6/6/05.

MCEER-05-0007 "Development of Seismic Strengthening and Retrofit Strategies for Critical Facilities Using Engineered Cementitious Composite Materials," by K. Kesner and S.L. Billington, 8/29/05.

MCEER-05-0008 "Experimental and Analytical Studies of Base Isolation Systems for Seismic Protection of Power Transformers," by N. Murota, M.Q. Feng and G-Y. Liu, 9/30/05.

MCEER-05-0009 "3D-BASIS-ME-MB: Computer Program for Nonlinear Dynamic Analysis of Seismically Isolated Structures," by P.C. Tsopelas, P.C. Roussis, M.C. Constantinou, R. Buchanan and A.M. Reinhorn, 10/3/05.

MCEER

University at Buffalo, State University of New York
Red Jacket Quadrangle ■ Buffalo, New York 14261
Phone: (716) 645-3391 ■ Fax: (716) 645-3399
E-mail: *mceer@mceermail.buffalo.edu* ■ WWW Site *http://mceer.buffalo.edu*

University at Buffalo *The State University of New York*

ISSN 1520-295X